



ENHANCED OIL RECOVERY INSTITUTE

Tensleep Formation Fracture Study Compendium



Scott P. Cooper and John C. Lorenz



 UNIVERSITY OF WYOMING

DISCLAIMER

THIS MATERIAL WAS PREPARED AS AN ACCOUNT OF WORK PRODUCED BY AN AGENCY OF THE STATE OF WYOMING. NEITHER THE STATE OF WYOMING, NOR THE UNIVERSITY OF WYOMING, NOR THE ENHANCED OIL RECOVERY INSTITUTE (EORI), NOR ANY OF THEIR EMPLOYEES, MAKES ANY WARRANTY, EXPRESS OR IMPLIED, OR ASSUMES ANY LEGAL LIABILITY OR RESPONSIBILITY FOR THE ACCURACY, COMPLETENESS, OR USEFULNESS OF ANY INFORMATION, APPARATUS, PRODUCT, OR PROCESS DISCLOSED, OR REPRESENTS THAT ITS USE WOULD NOT INFRINGE PRIVATELY OWNED RIGHTS. THE EORI RESERVES THE RIGHT TO CHANGE, AMEND, ALTER, ADDEND OR REMOVE THE CONTENTS OF THIS REPORT IN FUTURE EDITIONS BOTH IN PART OR IN ITS ENTIRETY.

THIS DISCLAIMER IS MADE WITH RESPECT TO THE DOCUMENT AS WELL AS THE ASSOCIATED DATA.

CONFIDENTIALITY NOTICE:

THIS REPORT CONTAINS INFORMATION BELONGING TO THE AUTHORS AND THE ENHANCED OIL RECOVERY INSTITUTE WHICH MAY BE PRIVILEGED, CONFIDENTIAL AND/OR PROTECTED FROM DISCLOSURE.

Executive Summary

This Tensleep Formation Fracture Study compendium contains the field studies, core analyses and literature reviews conducted over the 2007-2010 period in effort to understand the characteristics and distributions of fractures and their influence on fluid flow within Tensleep Formation reservoirs. The studies reported here are the results of a large-scale project on fractures in the Tensleep Formation in Wyoming initiated by the Enhanced Oil Recovery Institute (EORI) at the University of Wyoming. Additional copies of this compilation report can be requested directly from the EORI at The University of Wyoming or from their website at www.eori.uwyo.edu. The supporting data are also available through EORI and can be utilized in a variety of modeling software.

Table of Contents

INDEX

Introduction	6
Acknowledgements	6
Summary of Published Information on Tensleep Fractures	7
Subsurface Studies	
Hatfield	44
Assessment of Fractures in Core from the Nadel and Gussman Hatfield 16-35 Well	
Analysis of Fractures in Cores from the Tensleep Sandstones in the Hatfield Oil Field, Carbon County, Wyoming	
Mahoney Dome	95
Report on Fractures in core from the Mahoney Dome #12 and #20 wells	
Natural Fracture Characteristics in Core from the Mahoney Dome #24 Well, Wyoming, and Comparisons with Fractures from the MD #12 and #20 cores	
Teapot Dome	125
Fracture interpretations of the Tensleep core taken from well # 45-4-X-21	
Fracture interpretations of the Tensleep core taken from well # 48-X-28	
Outcrop studies	
Flat Top Anticline	142
Fractures and Strain Accommodation in the Tensleep Formation at Flat Top Anticline, Carbon County Wyoming: Implications for Analog Reservoir Systems	
Beer Mug Anticline	224
Natural Fracture Patterns and Strain Accommodation in the Tensleep Formation within a Tightly-Folded Laramide Anticline, Beer Mug Anticline, Carbon County Wyoming: Implications and Data Sets for Analog Reservoirs	
Wyoming Geological Association 2010 Field guidebook paper	358
Fracture Variability within the Tensleep Formation, Southeastern Wyoming	

Appendix	386
Abstracts	386
2008 - Natural hydraulic Injection Fractures, Lorenz and Yin	
Natural Hydraulic Injection Fractures: Examples from the Tensleep Formation, Wyoming	386
2008 - Tensleep Reservoir fractures, AAPG RMS, Lorenz	
Fracture Characteristics in Core from Tensleep Reservoirs across Wyoming	387
2008 - Casper Sandstone WGA, Lorenz	
Fractures and Faults in an Eolian Sandstone in a Non-Structural Setting: the Casper Sandstone	388
2010 - Alcova AAPG RMS, Lorenz and Cooper	
Thrust faults in the Alcova Limestone: Nature's Sand-Table Experiment	389
2010 - Beer Mug AAPG Annual Meeting, Cooper and Lorenz	
Fracture Patterns Associated with Tightly Folded Laramide Structures: The Example of Beer Mug Anticline, Wyoming	390
2010 - GSA Rocky Mtn Section Meeting, Cooper and Lorenz	
Fracture Patterns Associated with Laramide Anticlines	391
2010 – WGA Annual Meeting, Cooper and Lorenz	
Fracture Variability within the Tensleep Formation	392
Presentations and/or/posters associated with the above abstracts are available through EORI	
Field Trips - Flat Top Mountain Field Trip Handout	393
Tensleep Bibliography	400

TENSLEEP FORMATION FRACTURE STUDY COMPENDIUM

John C. Lorenz

Fracture Studies, Geoflight LLC, 61 Blanco Drive, Edgewood, NM 87015, Phone (505) 231-6235, john@fracturestudies.com, Enhanced Oil Recovery Institute, University of Wyoming, 1000 E. University Ave., Dept. 4068, Laramie, WY 8207, Phone: (307) 766-2791

Scott P. Cooper

Enhanced Oil Recovery Institute, University of Wyoming, 1000 E. University Ave., Dept. 4068, Laramie, WY 8207, Phone: (307) 766-2791, sccoopel3@uwyo.edu
Fracture Studies, Cooper Geological Consulting, 76 Raven Road, Tijeras, NM 87059, Phone (505) 286-1462, scott@fracturestudies.com

INTRODUCTION

This Tensleep Formation Fracture Study compendium contains the field studies, core analyses and literature reviews conducted over the 2007-2010 period in an effort to understand the characteristics and distributions of fractures and their influence on fluid flow within Tensleep Formation reservoirs. The studies reported here are the results of a large-scale project on fractures in the Tensleep Formation in Wyoming initiated by the Enhanced Oil Recovery Institute (EORI) at the University of Wyoming. The supporting data are also available through EORI and can be utilized in a variety of modeling software.

ACKNOWLEDGEMENTS

The authors would like to thank the landowners; without their help, support and interest none of this work could have been accomplished. The authors would also like to acknowledge Dr. Jim Steidtmann, who initiated this project while director of the University of Wyoming's Enhanced Oil Recovery Institute (EORI). We greatly benefited from interactions with the entire staff and contractors at EORI, including Lon Whitman, Juliann Hamilton, Carolyn Coolidge, Glen Murrell, Laura Rehmeier, Brian Reyes, Geoff Thyne, Mark Tomasso, and Shaochang Wo. Dr. Peigui Yin at EORI made the thin sections and photomicrographs presented here and helped formulate their interpretations. This study was funded by and conducted for the Enhanced Oil Recovery Institute, with thanks to David Mohrbacher, Director.

Summary of Published Information on Tensleep Fractures

John Lorenz, April, 2007

SUMMARY

Fracture data from the Tensleep Formation have been published for seven reservoirs (Oregon Basin, Byron field, Little Buffalo Basin, Teapot Dome, South Casper Creek field, Circle Ridge field in Wyoming, and Rangely Dome in Colorado) and three outcropping anticlines (Zeisman Dome and Sheep Mountain Anticline in Wyoming, and Skull Creek Anticline near Rangely Dome in Colorado). These studies range from sophisticated mechanical/kinematic interpretations of anticlines formation based on detailed fracture characterizations, to brief collateral descriptions of fractures made during sedimentological studies, to inferences about fractures based on reservoir performance. This report attempts to synthesize the known fracture data from these locations, and to derive generalizations that may be useful in reservoir modeling and production.

Subsurface Studies

In the subsurface, most of the fractures that have been described from Tensleep core are vertical, and fracture distributions are strongly influenced by bedding and lithology. Several authors report qualitatively that sandstones are more fractured where heavily cemented with dolomite, and that the poorly cemented, crossbedded dune deposits are the least fractured facies (but fractured nevertheless). Most authors report that dolomites are more intensely fractured than sandstones, although the highly fractured inter-reservoir dolomites at Oregon basin apparently do not create enough permeability to allow pressure communication between vertically stacked Tensleep reservoirs. Average reported fracture height is on the order of 30 cm (1 ft.), but fractures extending up to 1.5 m (5 ft.) along the vertical axis of cores have been reported. The few reported in situ fracture spacing measurements, from horizontal core, range from 1-4 m (4-12 ft.).

Reported fracture widths range from 0.1-1.0 mm: although larger fracture widths are common, their widths cannot be measured accurately because the rock is not intact. All fractures cored from the Wyoming reservoirs contain mineral filling, commonly anhydrite, quartz, or dolomite, and locally bitumen: the fractures at Rangely Dome are reported to be unmineralized.

Where mineralized, reported fracture filling ranges from total occlusion to partial mineralization with significant remnant aperture. The more open fractures should 1) enhance permeability over matrix values, and 2) provide significant horizontal permeability anisotropy.

Several authors have described fracture planes in core as being filled with sand or silt, but these are probably misidentifications of a specific type of shear fracture called a deformation band. Deformation bands provide no fracture-parallel permeability enhancement and in fact they reduce the local permeability to well below matrix values. Both deformation bands and bitumen-lined fractures should compartmentalize reservoirs.

The reported subsurface fracture distributions suggest that fractures are more common on the hinges than on the limbs of anticlines, with strikes most commonly being reported to be approximately parallel and normal to the anticlinal hinge. Other local orientations have been reported, both in addition to and instead of the two basic orientations. In the few instances where it can be determined, fractures that strike normal to the hinge of an anticline and parallel to the maximum horizontal in situ stress have the most influence on interwell communication patterns. The in situ stress anisotropy, though rarely reported, is an important control on fracture permeability.

Outcrop Studies

Outcrop data that have been taken specifically for providing inputs into reservoir models come only from Rangely and Zeisman domes. Fracture attributes such as spacings (2 m median spacing), lengths (up to 100 m) and distributions (log normal) come from the former, while the later supplied information such as distributions with respect to lithology and the relative intensities of different fracture sets: as in the subsurface, dolomites are the most intensely fractured. Sandstone fracture facies have been divided into parallel-bedded interdune facies having intermediate fracture intensities and crossbedded dune facies that are the least fractured of all facies.

Fracture strikes at Zeisman Dome vary by who reports them. One author recorded a hinge-parallel fracture set that isn't developed everywhere, and a more pervasive hinge-normal set, whereas another author reported only two nearly hinge-normal sets. However, the former author indicates that where developed, the hinge-parallel set is more closely spaced by a factor of four than the more widespread hinge-normal set. Both authors report locally-developed fracture

corridors with spacings of about 500 ft., which would form permeability streaks in a reservoir. Their orientations relative to structure are unspecified.

The reported fracture patterns at Sheep Mountain Anticline, where two groups of authors were focused on interpreting the mechanisms of folding and ultimately Laramide tectonics, have even less consistency. One paper reports the widespread development around the anticline of an idealized, dynamically compatible, Stearns-and-Friedman type of fracture suite, consisting of two fracture families with three related strikes each (a conjugate pair with an acute-angle bisector); another author group suggests that five unrelated, basic fracture sets are developed variably in domains that are demarcated by structural position on the anticline. Both sets of investigators agree that the bed-normal fractures formed prior to or during the initial stages of folding. However, some fractures were reactivated during folding according to one paper; the other authors did not note these features. The other authors did however describe small-scale, bed-parallel thrust faults that were not noted by the former authors. No deformation bands have been reported in these outcrops.

INTRODUCTION

Although relatively few in number, published descriptions of the characteristics, distributions, and effects of fractures in the Tensleep Formation vary from short after-thought descriptions of fractures to detailed analyses of fracture patterns as indicators of structural development. The following summary synthesizes the published Tensleep fracture data, from both outcrop and subsurface studies. This report serves as an introduction to and a foundation block for the outcrop and subsurface studies that will be undertaken during the course of the Tensleep fracture characterization project. It is intended to be both a progress report and the draft of the “previous work” chapter for a final report on this Tensleep fractures project. It is likely that other published data sources, including various student theses that are rumored to be available, will be uncovered in the course of this study. Such references will be included in the final version of this report.

Fractures in seven reservoirs and at three outcrop locations have been described by various authors, several locations by more than one author. It is interesting and cautionary to note the significantly different fracture characteristic and types have sometimes been reported by different authors for the same field or outcrop where more than one study has been published.

Part of this may be due to the evolving knowledge of fractures, i.e., fracture types that were poorly understood and therefore ignored were finally deciphered and therefore were described once their significance became appreciated. Some of this difference is related to the differing objectives the various authors had for their studies.

Not all authors described the same features when characterizing Tensleep fractures and their distributions, and the ability to make comparisons between the different structural settings and lithologies suffers accordingly. Nevertheless, these descriptions highlight the variability of fracturing in the Tensleep Formation, and provide a foundation for constructing more complete descriptions that will allow more robust comparisons between reservoirs, between outcrops, and between reservoirs and outcrops.

SUBSURFACE DATA

Introduction

Subsurface data come primarily from cores and wellbore image logs. Tensleep fracture data from six different fields in Wyoming and one in nearby Colorado (Rangely Dome) have been published, and are assessed below. Three of the Wyoming fields (Oregon Basin, Byron Field, and Little Buffalo Basin) are within the Bighorn Basin, while the other three (Teapot Dome, South Casper Creek, and Circle Ridge) are from the Powder River and Wind River basins. The attempt is made here to find the commonalities among fractures in the different fields. Ultimately the hope is to be able to explain the reasons for the differences. The Teapot Dome report, although technically unpublished, is available on the RMOTC website (www.rmotc.com). Data from that preliminary report are used here; the core and its fractures will be described more fully at a later date as another element of this study.

Geophysical data, mostly seismic, are increasingly being used to infer fracture orientations and subsurface characteristics. However, the few brief published Tensleep geophysical fracture-characterization summaries (e.g., Gray and Todorovic-Marinic, 2004) have not been included here. Geophysical techniques read a signal, but it is usually not clear what subsurface feature or combination of features has produced that signal. Preferentially oriented fractures is the usual interpretation for observed seismic anisotropy, but such signals can also result from intersecting fractures where one set produces a better signal than the other (due to

better development, less mineralization, more ideal orientation with respect to the in situ stresses, etc.), by an anisotropic in situ stress, and by sedimentary anisotropy. Since seismic studies of Tensleep reservoirs have not been calibrated with core, it is not always clear what they are measuring.

Fracture Geometry, Intensity, and Mineralization

Geometry

Most of the fractures described from image logs and cores taken from Tensleep reservoirs appear to be vertical extension fractures. Inclined fractures are mentioned only at Teapot Dome, where they comprise a small population confined to a narrow interval of the core. Inclined fractures cannot be numerous in the subsurface or they would have been intersected more frequently by the vertical cores: inclined fractures have a much higher probability of being intersected by a vertical core than do vertical fractures, yet only vertical fractures are reported. Conversely, vertical fractures must be common to have been cored as frequently as they have been. The fact that many sedimentology, stratigraphy, and diagenesis studies of Tensleep cores mention fractures when they were only peripheral to such studies also suggests that fractures are pervasive in the subsurface.

Vertical extension fractures have been mentioned, shown in photographs, and even briefly described at South Casper Creek field (Cole and Mullen, 1992), Little Buffalo Basin (Emmett et al., 1971), and Oregon Basin (Morgan et al., 1978). Some of the fractures at Oregon Basin appear to be multistranded in the photographs presented by Morgan et al. Shebl (1996) also briefly described extension fractures in Tensleep cores from unspecified locations in the Bighorn Basin. Fractures were not the main focus of these studies, thus descriptions of the fractures are brief and sketchy. The most complete descriptions of Tensleep fractures in core come from Teapot Dome (based on 197 ft. of core: Lorenz and Cooper, 2004) and for the Tensleep-equivalent Weber Sandstone at Rangely Dome (based on 12 cores, two of them oriented: Narr, 1998).

At Teapot Dome, most of the fractures are vertical to near vertical (FIG); only one four-ft. thick zone containing inclined shear fractures is present. The vertical fractures extend up to 2.1 m (7 ft.) along the axis of the core, averaging about 30 cm (1 ft.) in height. The fractures

commonly terminate vertically at sedimentary discontinuities, but also terminate for no apparent reason within a lithology. The same types of vertical limitations are apparently present at Oregon Basin, where Morgan et al. (1978) describe high-angle fractures that commonly “terminate at contacts (even at faint bedding planes)”. Fractures from this field are “rarely as long as several feet” and terminate at the “softer” lithologies. In contrast, the vertical, planar fractures at Rangely Dome described by Narr (1998) have a median fracture height of 20 cm (8 in), but most terminate blindly within a lithology since few lithologic/mechanical breaks are present in the 300-meter/1000 ft. thick, well-indurated sandstone sequence.



Vertical extension fracture from the Tensleep Formation at Teapot Dome that terminates top and bottom within a lithology for no apparent reason.

The available descriptions suggest that most Tensleep reservoirs contain numerous vertical fractures which average a foot to a few feet in vertical extent. Where the lithologic contacts are present, fractures terminate vertically at these mechanical barriers. Inclined fractures are rare.

Intensity

Quantitative estimates and measurements of fracture spacing or intensity rare because of the problem of limited sampling presented by vertical cores and vertical fractures, and because spacing is a lateral dimension whereas cores are one-dimensional vertically. Qualitative estimates of fracture intensity can be obtained from some of the published data, and Narr (1996) has described a quantitative technique for determining fracture spacing from vertical core, but few of the published descriptions provide enough data to use this technique for estimating fracture intensity.

The types of fracture intensity data vary. Vertical data at Teapot Dome suggest that there is an average of one natural fracture present for each five feet of core examined. The ratio diminishes to one fracture per ten feet of core when only the reservoir sandstones are considered, and in fact the ratio varies by an order of magnitude as a function of lithology (see the lithology discussion below). The abundant data from 12 cores allowed Narr (1998) to calculate that fracture spacing at Rangely Dome ranges from 0.3 m (1 ft.) to infinity using his 1996 technique, a wide range of spacings that would be difficult to put into a reservoir model. The foregoing are inferences about intensity from indirect sources: the only direct measurements, from horizontal cores, were reported by Aviantara (1996), who measured average fracture spacings at Byron field as 4.3 ft. (1.3 m) for a NW-SE striking fracture set, and 11.6 ft. (3.5 m) for an ENE-WSW striking set.

The published data do not allow definitive comparisons between the different cored reservoirs: fractures per vertical foot of core do not equate to fracture spacing in horizontal core, and horizontal fracture spacing calculated from vertical core does not always equate to actual spacing. However, the available data suggest that fractures in the subsurface are closely spaced relative to most reservoir engineering models, and that Tensleep sandstones should behave as a fractured reservoir if the permeability along the fractures is greater than matrix permeability.

Apertures and Mineralization

The reported degree and type of mineralization in subsurface Tensleep fractures vary significantly, and fracture apertures, which are critical to creating permeability, vary by fracture width as well as the degree of occlusion of that width by mineralization. Some of the exotic

types of fractures described in print have been misidentified due to an author's lack of familiarity with fracture types, as noted below.

Garden-variety mineralization

Quartz, anhydrite, and dolomite have been reported as mineralization phases in subsurface fractures, but fracture widths and apertures are rarely reported. Peigui Yin (personal communication, March 2007) indicates that anhydrite is by far the most common phase of mineralization in cored Tensleep fractures. Several types of mineralization (sand and silt) have also been reported, but as discussed below these are more plausibly interpreted as micro-gouge in deformation bands, which are actually small shear fractures. These fractures described as sand and silt-filled may also be similar to micrite and sand filled fractures documented in outcrops at Flatop and Beer Mug anticlines and proposed to be natural hydraulic injection structures. Bitumen is also present in many of the Tensleep fractures.

On the other hand, Narr reports that fractures at Rangely Dome are “generally unmineralized” and have an average width of 0.1 mm. The fractures at Teapot Dome are wider, with total widths (the distance between fracture walls, including both void space and mineralization) in intact core averaging about a millimeter. Many of the Teapot fractures are actually wider than this, but the core was broken along larger fracture planes so that widest fracture apertures, which include the unmineralized void space, were not measurable and not reported. The widest fractures in this core probably have in situ apertures of several mm. The original fracture apertures at Teapot Dome are partially mineralized with anhydrite and dolomite: between 10-80% of the original aperture widths remain as remnant porosity that forms potential permeability pathways between patches of amorphous to crystalline of mineralization.



Partially mineralized vertical extension fracture face in Tensleep sandstone, Teapot Dome.

Open fractures with the potential to control fluid flow are present in other reservoirs: Cole and Mullen (1992, p. 135) seem to suggest that the fractures at South Casper Creek field comprise two mutually exclusive classes: —both distained (open) and mineralized (dolomite) types”. Morgan et al. (1978) show photos of what appear to be unmineralized hairline fractures with remnant porosity from the Oregon Basin, but note that some of the fractures are cemented (mineral unspecified).

Deformation Bands

Both Emmett et al. (1971) and Shebl (1966) describe fractures that are —filled by fine-grained sand, fine silt” (Emmett et al., their figures 7 and 10) and —Gauge [sic: _gouge_] fracture fillings of silt and clay” (Shebl, his figure 3.15B). These features are probably not fractures filled with implausible injections of silt and clay, but rather are deformation bands as described by Jamison and Stearns (1982) and Aydin (XXX), where minor amounts of shear offset (a few

millimeters, commonly much less) crush sand grains into a localized cataclasite or gouge within the narrow region of shear, giving it the appearance of silt and clay in thin section. Shebl reports that ~~most~~ [of these features] were later filled with anhydrite or late-stage calcite”, which suggests that they were later reactivated in extension, with minerals precipitating in the resulting aperture.

Stylofracture

Another reactivated feature was reported by Emmett et al. (1971, their figure 4), who show the photo of a core taken from a carbonate in Little Buffalo Basin that contains what they describe as a ~~vertical~~ fracture that has been widened by secondary deposition of anhydrite after the margins of the fracture were lined with shale.” The fracture plane is highly irregular, and in fact it is a vertical stylolite (thus the irregularity and the shale ~~lining~~”). However, it has been reactivated in extension allowing secondary mineralization by anhydrite in the resulting aperture. Such compound features can be called ~~stylofractures~~” and although not common, they are not rare in carbonate reservoirs such as the Aneth field. They indicate high magnitudes of horizontal compression (necessary to form vertical stylolites), and later re-adjustments in the stress regime which open a new fracture *against* the previous direction of compression along the plane of weakness presented by the stylolite.

Organic Material

Several authors have noted ~~asphalt residue~~” (Little Buffalo Basin; Emmett et al, 1971), ~~residual oil~~” (Bighorn Basin; Shebl, 1996), ~~oil stain~~” (South Casper Creek field; Cole and Mullen, 1992), and bitumen (Teapot Dome; Lorenz and Cooper, 2004) within fractures in Tensleep cores. The oil may be dispersed within the intercrystalline porosity of the fracture mineralization, or may actually line the fractures, behaving like a mineralization phase itself. At Teapot Dome, the bitumen-lined fractures form a network of sub-parallel planes within a 1.5 m (5 ft.) thick white dolomite that overlies an oil-stained sandstone interval, suggesting that the fractures may be a form of hydraulic escape feature.

Tensleep fractures may be unmineralized, partially mineralized, or completely occluded by quartz, anhydrite, or dolomite. Most fractures seem to have only one mineralization phase, and to retain some remnant porosity despite mineralization. This porosity would contribute to

reservoir system permeability. Reported fracture apertures range from 0.1-1.0 mm. Some fractures were obviously wider in situ but are now broken open such that the apertures cannot be measured.

Fracture-filling mineralization reduces the fracture-system permeability, as would the oil residue in the form of asphalt and bitumen that is common in the fractures. One example of a vertical stylofracture has been reported, recording a compound stress history. Micro-gouge –filled” deformation bands have been reported in several reservoirs, and these will severely degrade permeability normal the fracture plane. It is likely that deformation bands are common but not widely recognized in Tensleep reservoirs, since deformation bands form readily in poorly consolidated, high-porosity sandstones such as the Tensleep.

Fracture Distributions with respect to Lithology

Fractures are best developed in strata that are mechanically the most susceptible to fracturing, typically the more brittle strata. Therefore fracture spacings and intensities vary with lithology. Unfortunately, the published subsurface data rarely support a quantitative analysis of fracture distributions, partly because insufficient vertical core is taken to adequately sample vertical fractures and partly because fractures have not been the focus of most authors’ studies. Rather, attention to fractures seems often to have been forced on an author merely because fractures are too numerous to ignore despite the sampling bias against them. Nevertheless, empirical observations have been offered in various reports, and some semi-quantitative data are available.

Narr (1998) indicates that fractures are more frequent at the top of the 300-meter thick –well indurated” Weber Sandstone at Rangely Dome. Although he does not suggest why, it is possible that this is due to better cementation, leading to more brittle rock properties near the top of the unit. At South Casper Creek field, image logs suggest that the best fracturing occurs in the dolomitic sandstones (Montgomery, 1996). At the same field, Cole and Mullen (1992) record that, based on image logs and cores, both sandstones and carbonates are fractured and that some units have more fractures than others although they don’t specify which. At Oregon Basin, Morgan et al. (1978) indicate that closely spaced fractures are present in both dolomites and sandstones, but that –Fractures are rare in the reservoir parts of the sandstone, but are somewhat more common in cemented (harder) zones.”

At Teapot Dome, fracture data that were collected in a systematic way provide a measure of the variation in fracture intensity by lithology (Lorenz and Cooper, 2004). Intensity is defined as the ratio of the cumulative feet of fracture height that were found in a given lithology to the cumulative feet of core from that lithology, so that a larger number indicates more intense fracturing.

These data show that high-porosity sandstones, whether oil stained or not, have a fracture intensity of only about 0.12 feet of fracture height per foot of core. Based on experience, this 1:10 ratio is common in other fractured U.S. reservoirs. An increase in cement changes the fracture ratio, and dolomitic sandstones have a fracture intensity of 0.32. The ratio increases to 0.71 when a sandstone is heavily cemented. Interestingly, the interbedded micritic dolomites have only an intermediate fracture intensity of 0.23, although one anomalous five-foot thick dolomite, not included in this ratio, was intensely fractured with numerous, parallel, bitumen-lined fractures (FIG). These fracture ratios are based on a relatively small sampling of each lithology (i.e., the 0.71 ratio derives from only 3 m/10 ft. of core XXX), and it is likely that they would drift towards the anticipated trend where dolomites are more fractured than sandstones if larger a sampling was available.



Tensleep dolomite with several parallel, bitumen-lined fractures, Teapot Dome. Arrow points to a patch of additional mineralization, probably anhydrite, along one bitumen-coated fracture.

These data and observations indicate a variability in fracture spacings may vary systematically by lithology, all other factors such as structural deformation being equal. Most reports suggest that dolomites are more heavily fractured than the reservoir sandstones, as would be expected given the ductility and relative fracture susceptibility of the two lithologies. The fracture intensity numbers suggest that fracture development is generally proportional to the degree of sandstone induration, but that the presence or absence of oil had no effect.

Fracture Orientations and Distributions across Structures

Orienting a vertical core or cutting a horizontal core so that fractures can be oriented in the subsurface adds significantly to the cost of drilling a well. Nevertheless, the costs are usually justified because:

1. the orientation of a fracture set relative to the structural configuration of a reservoir is useful in determining the origin of the structure

2. fracture strikes relative to the in situ stresses indicate which fracture sets are most likely to be permeable
3. the behavior of fractures during pressure drawdown caused by production depends on their orientations within the stress field
4. fracture strikes relative to north are useful in designing optimum azimuths for horizontal wells.

Therefore a significant amount of subsurface fracture orientation data has been collected and published. The fracture-orientation data are summarized for each structure individually because the context for fracture orientations is important. Locations outside of the Bighorn Basin are included in order to expand the data base, since only three locations within the basin have been described.

Locations within of the Bighorn Basin

Oregon Basin

Oregon Basin field, in the west-central Bighorn Basin, consists of two aligned, slightly asymmetric (west-vergent) anticlines along a north-south axis, with a maximum of about 340 m (1100 ft.) of relief over a maximum width of about 4 km (2.5 miles). Maximum structural dip (estimated from Morgan et al.'s structure-contour map, their figure 2) is about 20°, and is found on the west flank of the structure. Northeast and east-northeast trending faults cut across both anticlines. Morgan et al. (1978) report that two fracture sets strike approximately N-S and E-W (across and parallel to the hinge), and that more fractures were observed in cores taken from the anticlinal crest than from the flanks. However they do not provide data to support the orientation or fracture-distribution observations.

Little Buffalo Basin

Little Buffalo Basin is also another north-south trending, slightly asymmetric anticline on west-central side of the Bighorn Basin. It has about 200 m (600 ft.) of relief over a width of nearly two kilometers (slightly over a mile). The steepest mapped dips (inferred from Emmett et al.'s structure contour map, their figure 2), are on the west flank and are less than 10°. Emmett et al. (1971) report that two vertical, oriented cores show near-vertical fractures on the gently-dipping northern nose of the structure, and that the fractures have consistent strikes oblique to the

hinge, trending NNE-SSW (30°) at this location, where the structural dip is to the N and NE. Data from other cores, alluded to but not presented, apparently show that the highest degree of fracturing occurs along the anticline axis at ~~the~~ "maximum flexure".

Byron Field

Byron Field, located on the other side of the Bighorn basin, in the northeastern part, and is a northwesterly trending anticline. An abstract published by Aviantara (1996) indicates that one set of fractures in horizontal core taken from the local Tensleep reservoirs strikes NW-SE (312°) parallel to the axis of the anticline, and that a less numerous set of fractures strikes ENE-WSW (59°) across it. The number of fractures measured from each set and the location of the well on the anticline are not specified.

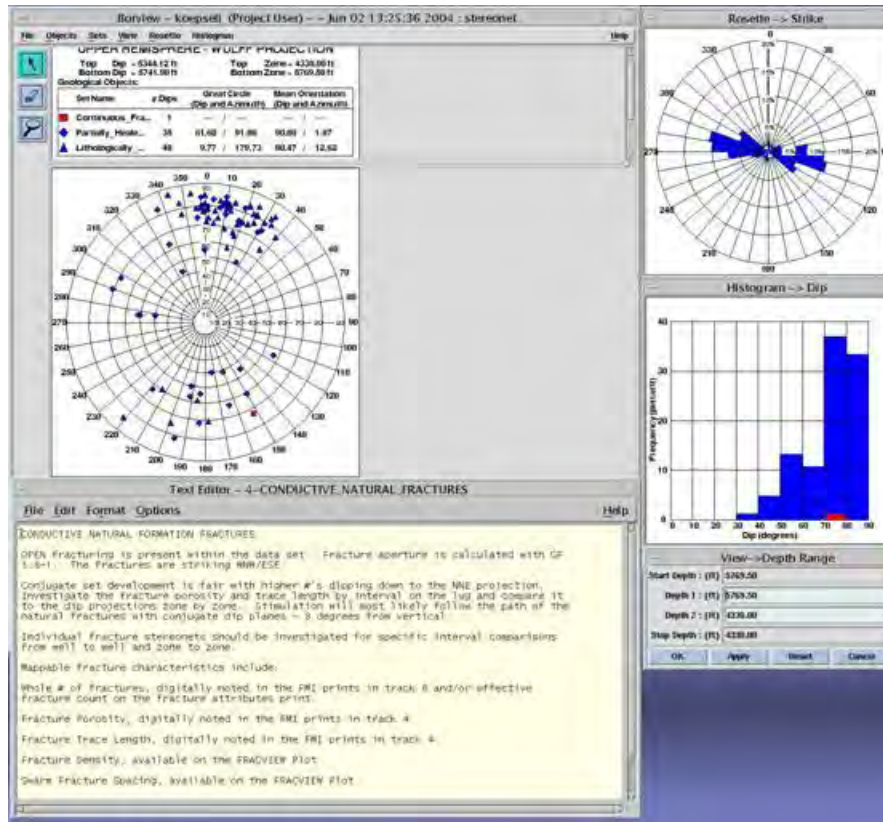
These observations suggest that in two out of three examples in the Bighorn Basin, fractures strike parallel and normal to the hinges of an anticline, compatible with extension in those directions during anticline development. The example of an oblique relationship between an anticline axis and fracture strike at Little Buffalo Basin may be due to sampling of the fractures near the nose of the anticline. The authors report enhanced fracturing along the crest of the anticlines, though no data are provided to demonstrate it and thus it is unclear what the factor of enhancement is or even whether it is real or just an expected outcome from concepts about where the highest strain should occur in a flexure.

Locations outside of the Bighorn Basin

Teapot Dome

The orientations of Tensleep fractures at Teapot Dome in the southwestern Powder River Basin have been determined by wellbore-image logs (FIG XXX), which indicate that most of the natural fractures strike E-W to WNW-ESE at depth, 30-40° oblique to the axes of the NNW-SSE striking, west-vergent anticline. The image logs suggest that this is also the orientation of the maximum horizontal compressive stress, and since most fractures in the core strike parallel to the coring-induced petal fractures that are controlled by the in situ stress orientation, a case can be made, with only modestly circular reasoning, that the core data corroborate the image-log data.

However, some core fractures are oriented at angles to the petal fractures, and the image logs and cores seem to agree that variability exists in the strikes and dips of this fracture set.



Wellbore image log data from the Tensleep Formation at Teapot Dome, showing WNW-ESE striking fractures. This data set suggests that most fractures have significantly more dip than observed in the core from the equivalent depth, most dipping towards the NNE.

South Casper Creek field

Located in the easternmost extent of Wind River Basin, South Casper Creek field is mapped as a northwesterly trending anticline with two aligned highs (Cole and Mullen, 1992; Montgomery, 1996). The anticline is slightly asymmetric, with steeper dips (up to 20° as reconstructed from the structure-contour maps) on the northeastern limb, and with about 120 m (400 ft.) of relief across nearly two kilometers (a mile) of maximum width. Stevenson and Mullen (1991) map an east-west fault system with offsets of 3-7 m (10-20 ft.) that cuts across the north plunging nose of the south dome, whereas Montgomery's (1996) map shows, in addition, several crest-parallel thrust faults near the hinge. Montgomery also provides a cross section of

the basement structure showing that the South Casper Creek field is a back-thrust-faulted anticline in the hanging wall of a northeast-dipping, basement thrust fault.

Cole and Mullen's data come from core and image logs (the latter measuring what they termed "fracture-like features") in the area of steep dip on the northeast flank of the southern anticline. These data show that the reservoir dune-sandstone facies contains three fracture sets: a NE-SW striking set that dips to the SE, and two sets that form an apparent conjugate pair, both striking E-W but dipping either south or north, the last being most common. In contrast, Montgomery (1996), based on six wellbore-image logs from unspecified locations on the dome, indicates that three fracture populations consist of a hinge-parallel fracture set (330°-340°, found mostly along the hinge), a hinge-normal fracture set (80°) that is dominant, and a hinge-oblique fracture set (20°-30°).

There seems to be minimal overlap between the fracture populations described in these two papers except possibly for the E-W striking sets. Although both papers mention that the most intense fracturing is associated with a fault or with fault intersections, neither provides data to support this.

Circle Ridge field

Located at the opposite, northwestern end of the Wind River basin, Circle Ridge field has been described by LaPointe et al. (2002). Although most of that report consists of data analysis rather than data, the authors suggest that the magnitude of fracture strain (intensity) and orientation vary, both across the field and by depth. Fractures strike generally ESE-WNW and NNW-SSE, segregated within relatively small domains. Although the subsurface fractures are not well documented, the importance of including this field in the discussion will become apparent when tracer tests are discussed below.

Rangely Dome

Rangely Dome consists of a large asymmetric anticline with the steepest dips on the south side. It is elongated east-west, with a slightly curved axis. The main reservoir is a 300 meter (1000 ft.) thick section of the Tensleep-equivalent Weber Sandstone. Narr (1998) analyzed 12 cores (two of them oriented) and showed that the most numerous fractures consistently strike ESE-WNW, nearly parallel to the local hinge axis at the eastern and western

ends of anticline. However, the data (Narr's figure 1) also show several minor fracture populations with hinge-oblique strikes, primarily NNW-SSE but also N-S in one well.

There seems to be little commonality between the different fractured anticlines for which fracture orientations exist, except for the common though not universal hinge-parallel fracture set. Either fracturing was not related to the formation of the anticlines except for those fractures caused by extension as the strata flexed at the crest of the anticlines, or the full range of fracture variability has not been assessed by the limited data available from wellbores. Between one and three sets of fractures have been reported in the subsurface, although authors describing the same field do not always agree on what the orientations of those sets are. It is probable that the authors of many of these reports did not intend or were not able to make full use of the available data, were more concerned with other aspects of the reservoirs, or were not allowed to publish the full data sets for proprietary reasons.

Fracture Effects on Reservoirs

One way to assess the orientations and permeability of subsurface fractures is to analyze the effects of the conduits and baffles they create in a reservoir. This can be done by assessing the performance, testing, and interference patterns of wells. This type of data reflects the full three-dimensional flow system within the reservoir, and it is up to the engineer and geologist to correctly interpret the data in light of what is known of the geology.

It is common practice, followed in several papers that discuss Tensleep fractures only in passing, to look at hand samples or thin sections and infer generalized permeability characteristics without actually measuring permeability in a laboratory. For example, Shebl (1996) speculates that the gouge-filled deformation bands are probably barriers to flow, Stevenson and Mullen (1991) suggest that "Fractures will create avenues of rapid transport of fluids within the reservoir" without providing documentation, and Morgan et al. (1978) "presume" a strong fracture-dependent permeability anisotropy.

Although speculation about the effects of natural fractures in a reservoir is common and perhaps justifiable in the absence of data (and is in fact indulged in within parts of this report), it is not quantitative. With that in mind, specific fluid-flow patterns that have been reported are examined below with the hope that they indicate something about the fracture orientations, distributions, and permeability in the subsurface at specific fields. As always, there is never as

much data as would be useful, and the different approaches and data sets of different authors leaves one largely comparing apples to oranges when trying to draw general conclusions.

Rangely Dome

At Rangely Dome, Narr (1998) notes that “actual reservoir productivity is significantly greater than can be explained by matrix flow”, and attributes the difference, unquantified, to a fracture-enhanced reservoir permeability system. At the east end of the Rangely anticline, Narr’s map (his figure 1) shows that the dominant E-W fracture trend is aligned with the three nearby examples of rapid interwell communication, but oblique to the nearby measurement of the maximum horizontal stress orientation. Near the western end of the anticline, measured fracture trends are oblique to *both* the alignment of communicating wells and to the local indications of the maximum compressive stress.

Byron field

At Byron field, Aviantara (1996, abstract), reports that fractures in horizontal core from the Tensleep strike NW-SE (312°), parallel to the axis of the anticline, and that a three-times more widely spaced set of fractures strikes ENE-WSW (59°) across it. Haws and Hurley (1992) report that the direction of maximum permeability within this anticline, as measured by pressure-interference tests, trends 60°, parallel to the less numerous fracture set. Significantly, the maximum horizontal stress as measured by image logs also has a ENE-WSW trend, so that if all other factors (aperture, mineralization, length, intensity, etc.) are equal, the ENE-WSW fractures would be preferentially open in this stress regime and would contribute more to the reservoir system permeability even though they are fewer.

Another important effect of fractures at Byron field is that, as measured in a horizontal wellbore (probably the same cored well described by Aviantara), the oil-water contact is several hundred feet higher in the fractures than in the adjacent matrix (Hurley et al., 2001, abstract). This would be a consideration for completions and for estimating reserves, and suggests that fracture apertures are significantly wider than matrix pore throats. Capillary forces would not be effective in wide fractures, allowing water invasion above the levels where invasion is blocked by capillary forces in the matrix.

Little Buffalo Basin

Engineering data are also published for Little Buffalo Basin, where Emmett et al. (1971) apparently conducted laboratory permeability tests on fractured core. The authors report that the tests show that —small closed fractures do not contribute significantly to permeability”. Moreover, when the permeability was measured in the direction *across* small fractures —the reduction in permeability is consistently in the range of 10 to 30 percent”, presumably relative to matrix values.

This is consistent with the low-permeability —silt-filled fractures” (deformation bands) described by the authors, and would seem to suggest that Tensleep fractures in the Little Buffalo field are more likely to be baffles than permeability conduits. However, the authors also indicate that many wells water out prematurely due to coning through enhanced fracture permeability, implying similarities to the elevated water levels seen in open fractures in Byron field by Hurley et al. Emmett et al. also report that gas-injection breakthroughs are typically parallel to the measured fracture strikes. These observations suggest that some segment of the fracture population does in fact create fracture-parallel permeability zones despite their low-permeability laboratory results.

The two, apparently mutually-exclusive observations may be explained by the existence of a fracture population consisting of parallel fractures but having a full range of sizes: many of the small-scale fractures are probably completely occluded by mineralization whereas the larger fractures are open and enhance permeability. Alternatively, there may be a population of small deformation-bands that inhibit permeability and that were measured in the laboratory, and a different population of larger, open, permeable fractures.

This implies a caution: inferences about fracture permeability based on thin sections and hand samples should be used carefully. In many reservoirs, only the largest fractures are significant to reservoir permeability, and they are rarely sampled because they tend to be widely spaced. Even when intersected by a wellbore, such fractures tend to break up when being cored and thus to be recovered only as rubble intervals. Moreover, even when recovered from a wellbore intact, the permeabilities of most larger fractures cannot be tested in the laboratory because they fall apart when plugged.

Oregon Basin

Another field where fractures are suggested to inhibit flow and to be barriers rather than conduits is Oregon Basin. At this field, Morgan et al. (1978) indicate that although closely spaced fractures are present in both dolomites and sandstones, they observed no communication through these fractured dolomites to connect the sandstone reservoir units. These authors suggest that the different sandstone layers in fact perform as discrete, pressure-isolated reservoirs. Morgan et al. (1978) report that two fracture sets strike approximately N-S and E-W, which is oblique to the 42° maximum-permeability trend reported by Haws and Hurley based on pressure-interference data for this field. Even though the fractures in Morgan et al.'s photos seem to have remnant porosity, the well tests described by the authors suggest that fractures have minimal effect on permeability at Oregon Basin.

Haws and Hurley 1992 reported maximum permeability trends derived from pressure-interference data for several Wyoming reservoirs, finding that maximum permeability follows the direction of maximum horizontal stress in all three Tensleep cases examined as well as for several non-Tensleep reservoirs. They noted that in all examples this direction was approximately normal to the axis of the anticline: as discussed above, at Oregon Basin field the maximum permeability trends 42° where the hinge axis strikes NNW-SSE, and at Byron field maximum permeability trends 60° while the hinge axis trends NW-SE. In addition, maximum permeability trends 45° in the Tensleep reservoirs at Garland field, which has a NW-SE hinge axis (but for which there are no published core fracture data).

Circle Ridge field

Few data are available from Circle Ridge field. However, LaPointe et al. (2002) mapped the breakthrough sequence for a nitrogen tracer near the middle of this field and found that although the paths taken by the tracer gas were approximately parallel to the inferred subsurface fracture strikes, the gas in fact by-passed many on-trend wells. The route that had to be reconstructed for the gas to travel between injection and observation wells without being detected in some of the intermediate wells is rather tortuous and suggests, as inferred by LaPointe et al. from other data, and as the composite data from the other fields described above are beginning to suggest, that different fracture domains may be present in the subsurface, and

that generalizing permeability enhancement and anisotropy from a few data points within a field covering hundreds to thousands of acres may be difficult to do accurately.

Discussion

Engineering well-test and laboratory data suggest that some fractures enhance permeability whereas others, especially deformation bands, may have no effect or may even degrade permeability. The effect of fractures is a relative one in that if the reservoir has a high matrix permeability, only the largest fractures will have an obvious effect. The same fractures that would have significant effects on a tight reservoir may be transparent in a reservoir with higher matrix permeability. Most fracture populations have a range of sizes, typically with a log-normal distribution (i.e., many small fractures, fewer larger fractures) and there is no reason to believe that the Tensleep fractures are any different. In fact, Narr (1998) reports that the distributions for fracture spacings, heights, apertures, and lengths in the Weber Sandstone at Rangely Dome are all log-normal. The numerous small fractures may have little effect on a reservoir, especially if they turn out to be deformation bands. Conversely, larger open fractures may dominate permeability even though they are less numerous and direct evidence for them in core is lacking. Although it's often the only option, inferences about fracture permeability based on thin sections and hand samples should be used carefully.

Although still rare in publication, more data are continually being acquired on the in situ maximum horizontal compressive stress orientations in a field, and estimates of stress magnitudes are even being calculated. The in situ stress system is an important part of the fracture-permeability puzzle as stress helps control fracture aperture and dynamics. Fractures that are closely aligned with the maximum horizontal stress will be preferentially open compared to similar fractures striking oblique or normal to the stress axes in the subsurface.

Conclusions from the subsurface data

Most of the fractures that have been described from Tensleep core are vertical and without apparent offset, and are probably extension fractures. Inclined fractures in core have only been described from one well, but this may in part be a lack of data and in part a lack of recognition in other fields: wellbore image logs suggest they are more common. Where strong bedding exists, fractures are commonly bounded by stylolites, shale partings, and other changes

in lithology. Average fracture height is on the order of 30 cm (1 ft.) and most are shorter, although fractures extending for up to 1.5 m (5 ft.) along the vertical core axis have been recorded. In the few places where such data exist, subsurface fracture spacing is on the order of 1-4 m (4-12 ft.). In most cases, but depending on matrix permeabilities, these fractures with this type of height distribution and these ranges of spacings should have important effects on reservoirs, as at Rangely Dome where production rates are reported to be greater than can be explained by the matrix permeability alone. Permeability would be enhanced in the horizontal plane but not vertically across bedding.

Most authors report qualitatively that dolomites are more intensely fractured than sandstones, and that sandstones are more fractured where heavily cemented with dolomite. Nevertheless, the highly fractured inter-reservoir dolomites at Oregon basin apparently do not create enough permeability to allow pressure communication between reservoirs.

Reported fracture widths range from 0.1-1.0 mm, though larger, broken fractures where widths cannot be measured are common. Fractures in the Weber sandstone at Rangely Dome are apparently smaller and unmineralized, but all fractures cored from the Wyoming reservoirs contain mineralization of some sort, including anhydrite, quartz, dolomite, and bitumen. Multiphase mineralization has not been reported. Where mineralized, fractures range from being completely occluded to having up to 80% remnant aperture despite mineralization. Fractures with these types of remnant apertures should enhance permeability over matrix values, and should provide significant horizontal permeability anisotropy.

Many fractures are lined with bitumen, which degrades fracture permeability. The fractures described by several authors as being filled with sand or silt are probably deformation bands where grains of the matrix rock have been reduced in size by minor shear offsets. Deformation bands provide no fracture-parallel permeability enhancement and in fact significantly reduce permeability in the direction across the fracture planes. Both deformation bands and bitumen-lined fractures may compartmentalize reservoirs. If they are unidirectional they may provide horizontal permeability anisotropy by channeling flow between fractures, although maximum permeability will be the matrix values.

What little data and verbal descriptions are available suggest that fractures are more common along the hinges than on the limbs of anticlines. Fractures trending parallel and normal to an anticlinal hinge are reported in several fields. Fractures that strike normal to the hinge and

parallel to the maximum horizontal in situ stress commonly have the most influence on well interference tests and interwell communication patterns, even where they are the least numerous of several in situ fracture sets (e.g., Bryon field). The in situ stress anisotropy is an important part of the equation, and at Bryon field authors report the puzzling observation that the maximum permeability direction is parallel to the maximum horizontal in situ stress rather than to either of the reported fracture sets. Additional, oblique fracture sets are present locally, although most subsurface data sets do not include enough information of fracture strikes to determine the number of sets present. As at Circle Ridge Field, relatively small fracture domains where fractures have slightly different orientations may be present in the subsurface. Inferring permeability enhancement and anisotropy from a few data points within a field covering hundreds to thousands of acres may be misleading.

Most of the fractures samples in wellbores and especially those plugged from cores and tested for permeability are relatively small. Such fractures may not have as much impact on a reservoir as less common larger fractures, explaining the observations that plug-sized fractures tested in the laboratory did not seem to enhance permeability whereas the production patterns could most easily be explained by the effects of permeability-enhancing fractures. Such larger fractures are hypothetical in the absence of evidence, but most fracture populations in fact have the same type of log-normal distribution reported for Rangely Dome, consisting of myriad small fractures with fewer fractures as the fracture size (height, length, aperture) increases. Large fractures in the subsurface are not improbable.

OUTCROP DATA

Introduction

Detailed Tensleep fracture studies have been published for only two locations (Zeisman Dome and Sheep Mountain Anticline), although a brief description was also published of the fractures that crop out on Skull Creek Anticline near Rangely Dome. Nevertheless, the amount and precision of three-dimensional data available at any specific outcrop far exceed that available from one-dimensional cores and image logs at any field, since the latter are pinprick data sources no matter how many wells have been cored or logged.

Extrapolating fracture patterns from outcrop into the subsurface can be a tricky business. Some phases of matrix cement and fracture mineralization, especially anhydrite, are not stable near the surface, so that rock properties and fracture apertures measured at the surface must be used carefully. Some types of fractures form during erosion and denudation, which allow the release of locked-in stresses, and some fractures form simply due to the uplift strains that cause the strata to be exposed in outcrop: such fractures should not be extrapolated into the subsurface. Surface data provide most of the information needed to reconstruct the stress systems that folded anticlines to create traps for oil, and some of the studies summarized here have been undertaken specifically to determine this mechanism. Although that is not the purpose of this study, data from such studies can be applied to reservoir permeability systems. However, it can be disconcerting to read the different fracture descriptions published by various authors for the same outcrops: as in the subsurface at Casper Creek Field, different geologists found or saw different features in some of the well-studied outcrops, particularly those at Sheep Mountain Anticline. As demonstrated by the literature, ample room also exists for variations in interpretation of the kinematics recorded by different fracture patterns.

Nevertheless, many surface fractures *are* analogous to reservoir patterns, and outcrops provide the opportunity to study fractures in full three-dimensional form over areas much broader than the span of a four-inch core, affording the ability to create models of the fracture networks that are important to reservoir permeability. Measuring fracture spacing and intensity is much easier in outcrop than in the subsurface, and outcrop studies can be tremendously useful if the surficial fractures can be filtered out. Even if they can't, outcrop studies can be useful just in determining the relative susceptibility of different types of strata to fracturing.

Whereas most of the subsurface fractures are reported to be vertical extension fractures, outcrop fractures seem to have more variety. In addition to tilted extension fractures, fractures that are vertical despite tilted bedding, bedding-parallel to low-angle thrust fractures (faults), and zones of fractures (fracture "corridors" or "swarms") have been reported. The nearly infinitely larger exposures that allow better sampling from outcrops is a contributing factor to this variety. Another is that most of the extension fractures are oriented normal to bedding, having formed when the strata were minimally deformed and nearly flat-lying. Most of the outcropping strata reported on here continued to deform and are now tilted fairly steeply, and the fractures now dip accordingly. In contrast, most of the sampled subsurface strata are on relatively gently-dipping

anticlines, with structural dips of less than 20°. This argues that some of the less deformed outcrops such as Flat Top and Alcova anticlines are probably more analogous to the producing reservoirs than are the more steeply deformed anticlines such as Sheep Mountain Anticline. The following discussion describes each location separately, then tries to draw conclusions and generalities from the descriptions.

Rangely Dome

Narr (1998) and Narr et al. (2006) published just enough fracture data from outcrops of strata equivalent to the reservoir at Rangely Dome to whet but not satisfy one's appetite. According to the pavement outcrop study, median fracture spacing is 2 m, and fracture lengths to can be in excess of 100 m. The distribution of the population of spacings and lengths is log-normal, compatible to Narr's subsurface data at Rangely Dome.

Zeisman Dome

Outcrop fracture data from Zeisman Dome, a northwest-southeast trending structure in the southeastern part of the Bighorn basin, have been published in semi-formal form, including a PhD dissertation and an abstract, by geologists from the University of Tulsa. This was a Marathon-sponsored study, and an unpublished field guide has been referenced in these papers, but to date I have been unable to locate a copy. The PhD study (McGinty, 2002) focused on applying fracture data to the "Fracman" computer model, while the other student study (Aviantara, 1996) apparently morphed into a sed-strat dissertation so that a full suite of fracture data was never published. Following are nuggets of fracture data mined in these papers.

Information on the Zeisman Dome fracture distributions is largely qualitative: McGinty (2002) reports that the fracture intensity in dolostones is the highest, that it is intermediate in the parallel laminated interdune sandstones, and that the dune sandstones are the least fractured of the three facies. The fractures (of all sets in all lithologies?) have a reported average spacing of 2 m (6 ft.). Information on fracture strikes is more quantitative, but the two studies are somewhat contradictory: Aviantara (1996) described two fracture sets, striking 59° on southern flank of the dome and 76° on northwest flank, whereas McGinty, without specifying locations, suggests that the two main fracture strikes are 65° and 150°.

The ENE-WSW strikes reported by the two studies (59° and 65°) are compatible and are approximately hinge-normal, while the 76° strike is not much different and may be a local forelimb-backlimb variation within this set. The NNW-SSE (150°) set, reported only by McGinty, would conform to an expected hinge-parallel fracture strike, and its absence from Aviantara's data set is puzzling although Aviantara only published an abstract. However, McGinty specifically notes that this set is also absent from Brokenback Mountain, the next aligned anticline to the southeast, where only the hinge-normal fracture set is present, striking 60°. McGinty also reports that where present, the hinge-parallel fractures are about four times more frequent than the hinge-normal fractures, average spacing being 0.6 m (2 ft.) and 2 m (6.6 ft.) respectively.

Both authors note that fracture "clusters" are present on Zeissman Dome, but neither indicate the orientations of the clusters. Aviantara notes that the clusters are spaced about 500 ft. (150 m) apart and are located "at the highest rate of fold axis plunge and dislocation". McGinty indicates that clusters occur where the both sets of fractures are present, and are not found at nearby Brokenback Anticline where only one set of fractures developed.

In summary, Zeissman Dome displays the expected hinge-parallel and hinge-normal fracture sets, with local variations, and all are probably bed-normal extension fractures. Directional permeability anisotropy in any analogous reservoir should depend on whether one or both fracture sets are developed. Fractures trending parallel to the hinge are more closely spaced of the two sets and subsurface permeability should be greatest parallel to the hinge except where the in situ stress anisotropy is a major factor as it seems to be in some of the reservoirs described above. Lithology controls fracture development, with eolian dune deposits being the least fractured reservoir facies and the interdune dolomites being the most heavily fractured. However, the reported average fracture spacing, probably an average of the different facies, is small enough to enhance fluid flow in a reservoir if they are conduits, or to seriously compartmentalize a reservoir if they are baffles or barriers. Fractures occur locally in closely spaced clusters, possibly incipient faults, that would create local high-permeability streaks in a reservoir.

Sheep Mountain Anticline

The most extensively studied Tensleep fractures in outcrop are at Sheep Mountain Anticline, a northwest-southeast trending structure in the east-central Bighorn Basin. Bellahsen et al. (2006b, their fig 2) suggest that this large fold is located in the hanging wall of basement-involved thrust fault, formed as a drape over a subsidiary, blind back thrust. These authors recognized five distinct fracture sets which are variably developed in five structural domains on and around the anticline.

Domain 1, off structure: the background pattern of fractures, Set I, is present off structure as well as being variably developed on structure. It strikes 110° and is the oldest set.

Domain 2, the backlimb: Four fracture sets are present in the southwest-dipping backlimb of the anticline,

Set I, striking 110° : bed-normal, 10-20 m long, a few meters high, with 1-3 meter spacing, and formed in extension and/or shear

Set II, striking 45° : bed-normal, 2-5 meters long, 1 meter spacing, formed in extension, and mineralized with crystalline calcite

Set III, striking 135° : bed-normal, spacing unspecified, a few meters long, mineralized with coarse calcite crystals, and formed in extension

Set IV, striking 110° : vertical and oblique to bedding, mineralized with a younger phase of calcite, and with a two-phase origin: shear followed by extension

Domain 3, the forelimb: Only the bed-normal Set I (110°) fractures are present in the forelimb, but they are less well developed here than on the backlimb, being shorter, typically only several meters long, and more widely spaced, a few tens of meters. Locally they have been reactivated as “~~bed-normal~~ reverse faults”, which constitute the authors’ Set V fractures.

Domain 4, the hinge: Three fracture sets occur in the hinge area, Set I, 110° (with a wider spacing than on the limbs, and evidence for shear only), Set II, and Set III, (best developed here where it is parallel to and coincides with the hinge)

Domain 5, the plunging nose: only fracture sets II and III are present here, where some fracture data came from other formations due to the minimal exposure of the Tensleep Formation.

This is a slightly different data set and interpretation than presented in an earlier abstract (Bellahsen et al. 2003), and probably represents an evolution of ideas with acquired data.

However, it is significantly different from the data set reported by Hennier and Spang (1983), who suggested that the Sheep Mountain Anticline fracture pattern, undifferentiated by domains, is consistent with “two orthogonal sets” in the generalized pattern suggested by Sterns and Friedman (1972). In this system, each “set” consists of three dynamically compatible fracture orientations: an intersecting strike-slip conjugate fracture pair with extension fractures oriented to bisect the acute conjugate angle. The two three-fracture sets are oriented such that the extension fractures strike normal and parallel to the Sheep Mountain hinge axis.

Based only on strike, four of Hennier and Spang’s suggested six orientations correlate reasonably well with four of Bellahsen et al.’s five fracture sets, but Hennier and Spang do not present data such as fracture-strike rose diagrams to document the inferred fracture system. It is possible that field data were applied to a preconceived pattern, with two of the six described orientations being assumed.

Perhaps more significantly, however, Hennier and Spang documented numerous and pervasive slickensided bedding-plane slip features, with the slicks trending normal to the anticlinal axis. These features are small thrust faults that locally break up and across bedding at low angles. They were not mentioned by Bellahsen et al. Such features would be significant in a reservoir because they would tie together bed-normal fractures in the third plane to create a highly interconnected reservoir plumbing system.

Vertical stylolites, also formed by high horizontal compressive stresses, are another feature mentioned by Hennier and Spang but not in the papers by Bellahsen et al. Relatively rare, and possibly found in the underlying Madison rather than in the Tensleep Formation (it is not clear from the description), such features would form baffles in a reservoir. Since they describe significantly different fracture systems, it is not surprising that Bellahsen et al. interpret the details of the formation of Sheep Mountain Anticline differently than Hennier and Spang. That discussion is not pertinent to the question of fracture effects on Tensleep reservoir permeability and will not be presented here. However, all authors at least seem to agree that most of the fractures, particularly those that are normal to bedding, pre-date or are contemporaneous with the early stages of folding, and all seem to agree that the anticline is located in the hanging wall of a basement thrust fault.

There is a significant difference in the system permeability that would be inferred for an analog reservoir from the two dissonant fracture descriptions. Hennier and Spang’s fracture

model, having six separate orientations, would provide nearly radial permeability in a reservoir provided that anisotropic stresses and/or mineralization do not preferentially close some of the sets. Moreover, these authors do not recognize the crestal extension that Bellahsen et al. document in the hinge-parallel (Set III) fractures, that are best developed along the hinge of the anticline, and where two other fracture sets intersect to form an interconnected system: either there would be or there wouldn't be enhanced permeability along and parallel to the crest of an analogous reservoir depending on which model is used.

Bellahsen et al. (2006a) have a more geographically discriminating data set that suggests higher, fracture-enhanced system permeability would be found on the backlimb, where four sets of intersecting fractures formed. The forelimb, containing only a single, widely-spaced fracture set, would have the least enhancement of permeability due to fracturing. Application of a stress anisotropy at different angles to any of these fracture patterns would significantly alter the permeability system.

Conclusions from outcrop data

Outcrop data that were taken with an eye towards developing reservoir models were taken only from Rangely and Zeisman domes. Fracture attributes such as spacings (2 m/6 ft. median), lengths (up to 100 m/300 ft.) and distributions (log normal) come from the former. An overall average 2 m/6 ft. spacing is also reported from Zeisman Dome, which supplies information such as distributions with lithology and relative intensities of fractures in different orientations: as in the subsurface, dolomites are the most intensely fractured, while the sandstones are divided into parallel-bedded interdune facies (with intermediate intensities) and crossbedded dune facies (least fractured).

The reported fracture strikes at Zeisman Dome varied by author: one recorded a hinge-parallel set that isn't developed everywhere and a hinge-normal set that is, whereas another reported only two nearly hinge-normal sets with slightly different orientations on the forelimb and backlimb. However, the former author indicates that where developed, the hinge-parallel set is more closely spaced, by a factor of four, than the other set. Both authors report locally-developed fracture corridors with spacings of about 150 m (500 ft.), which would form permeability streaks in a reservoir. Their orientations are unspecified.

The reported fracture patterns at Sheep Mountain Anticline have even less consistency: one paper reports an idealized Stearns-and-Friedman fracture suite consisting of two families of conjugate shear and extension fractures widespread across the structure, whereas another suggests that five basic sets of fractures are developed variably in distinguishable domains in different structural settings of the anticline. Both sets of investigators agree that the bed-normal fractures formed prior to or during the initial stages of folding, except for those fractures that were reactivated during folding and the small-scale bed-parallel thrust faults.

This is an interesting degree of inconsistency, but provides background for what to expect in the outcrop. The outcrop anticlines studied are larger than many of the anticline reservoirs in the subsurface, and it may be that the gentler structures such as Alcova and Flat Top anticlines are more analogous to the subsurface reservoirs.

Another consideration is that that part of an anticline which has usually been reported to be most intensely fractured in the subsurface, the crest or hinge, and that would also be theoretically the most intensely fractured due to highest strains, is commonly missing in outcrop due to erosion. Only those parts of the hinge located at the steeply plunging noses are typically preserved. Thus geologists have often taken fracture patterns from the underlying formations as a proxy for fracture patterns in the Tensleep along the hinges, even though this raises the possibility that different lithologies with different mechanical properties fractured in different ways.

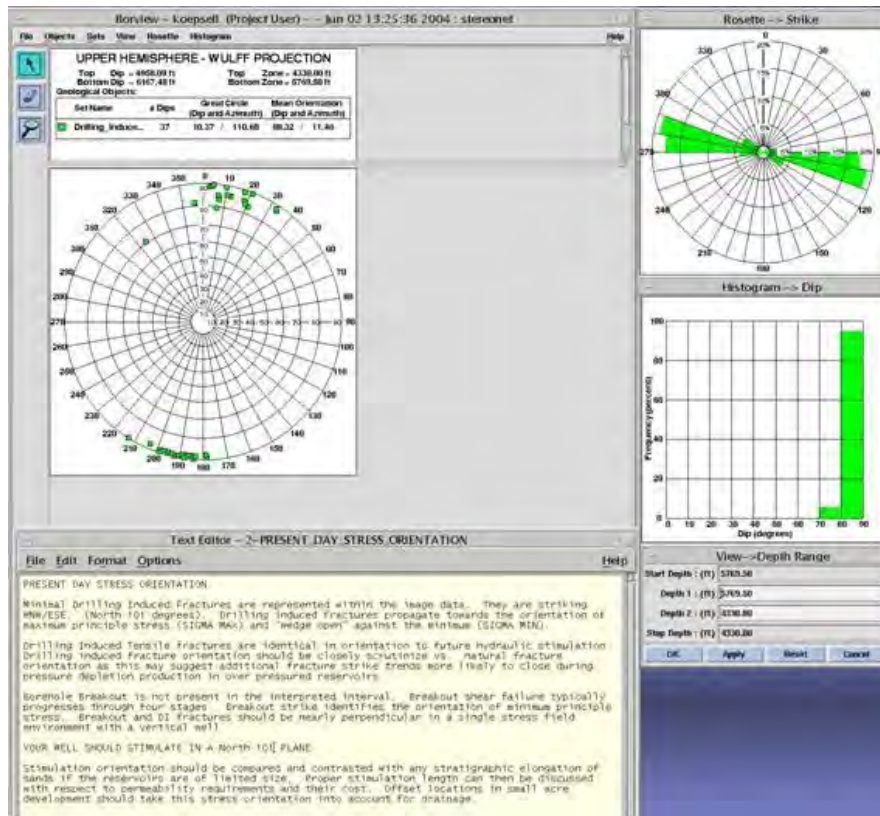
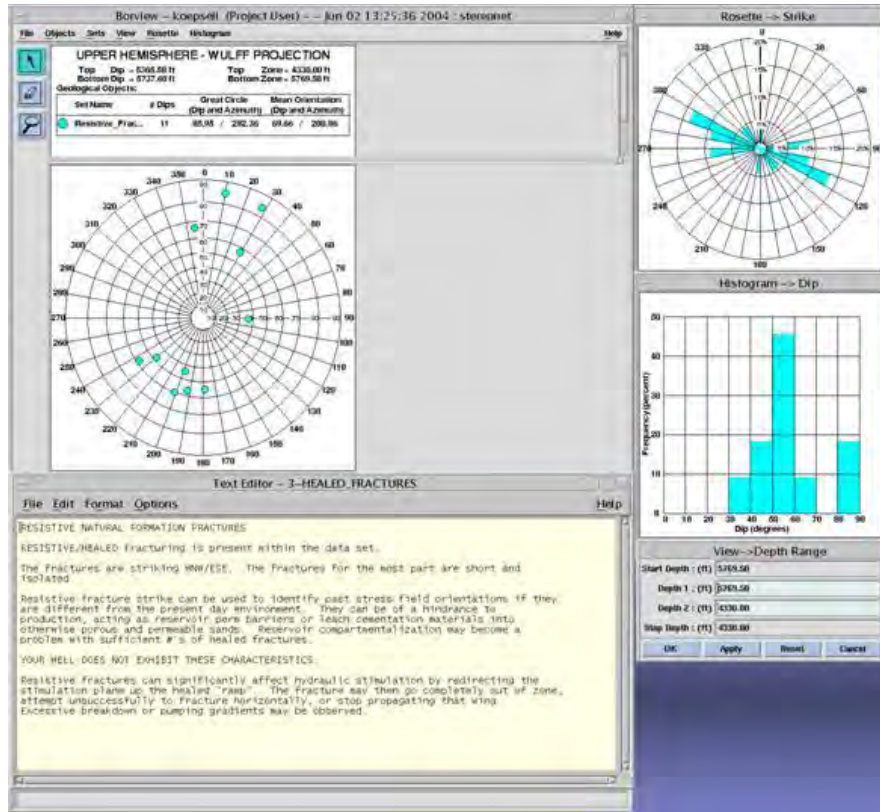
Interestingly, published reports of deformation bands in outcrop are rare, even though the poorly consolidated Tensleep sandstones should have been prone to the development of these features, and even though they are common at the Flat Top Mountain anticline.

REFERENCES

- Aviantara, Arya, 1996, Facies and fracture architecture of the Tensleep sandstone, Bighorn Basin, Wyoming: preliminary result of outcrop and subsurface study (abstract): American Association of Petroleum Geologists Bulletin.
- Bellahasen, Nicholas, Patricia Fiore, and David D. Pollard, 2003, Fold-fracture relationships in the Sheep Mountain Anticline, Bighorn Basin, Wyoming (abstract): Geological Society of America, Abstracts with Programs, v. 35, no. 6, p. 177.
- Bellahasen, Nicholas, Patricia Fiore, and David D. Pollard, 2006, From spatial variation of fracture patterns to fold kinematics: a geomechanical approach: Geophysical Research Letters, v. 33, p. L02301, 4 p.
- Bellahasen, Nicholas, Patricia Fiore, and David D. Pollard, 2006, The role of fractures in the structural interpretation of Sheep Mountain Anticline, Wyoming: Journal of Structural Geology, v. 28, p. 850-867.
- Cole, R.D., and C.E. Mullen, 1992, Sedimentologic reservoir characterization of Tensleep Sandstone, South Casper Creek Field, Wyoming: Wyoming Geological Association, 43rd Annual Field Conference Guidebook, p. 121-137.
- Emmett, W.R., K.W. Beaver, and J.A. McCaleb, 1971, Little Buffalo Basin Tensleep heterogeneity—its influence on drilling and secondary recovery: Journal of Petroleum Technology, February, 1971, p. 161-168.
- Gray, David, and Dragana Todorovic-Marinic, 2004, Fracture detection using 3D azimuthal AVO: CESG Recorder, December 2004, p. 5-8.
- Hennier, Jeff, and John H. Spang, 1983, Mechanisms for deformation of sedimentary strata at Sheep Mountain Anticline, Bighorn Basin, Wyoming: 34th Annual Field Conference, Wyoming Geological Association guidebook, p 97-111.
- Hurley, N.F., 2001, Structural and stratigraphic compartments determined from horizontal drilling in an eolian reservoir, Tensleep Sandstone, Wyoming (abstract): AAPG Bulletin (supplement), v. 85, p.
- Hurley, N.F., 2001, Alex Aviantara, and Dennis Kerr, 2001, Structural and stratigraphic compartments determined from horizontal drilling in an eolian reservoir, Tensleep Sandstone, Wyoming (abstract): American Association of Petroleum Geologists, Annual Meeting, June 3-6, Denver, Colorado.
- LaPointe, P.R., Robert Parney, Thorsten Eiben, Mike Dunleavy, John Whitney, and Darrel Eubanks, 2002, 3-D reservoir and stochastic fracture network modeling for enhanced oil recovery, Circle Ridge Phosphoria/Tensleep reservoir, Wind River Reservation, Arapaho and Shoshone tribes, Wyoming: National Energy Technology Laboratory, National Petroleum Technology Office, U.S. Department of Energy, Tulsa, Oklahoma, DOE/BC/15190-3 (OSTI ID: 800797), 63 p.
- McGinty, Sheila R., 2002, Fracture architecture of the Tensleep Sandstone at Zeisman Dome and Brokenback Anticline, Wyoming: PhD dissertation for the University of Tulsa, 170 pages plus appendices.
- McGinty, Sheila R., 2003, Fracture architecture of the Tensleep Sandstone at Zeisman Dome and Brokenback Anticline, Wyoming (abstract): American Association of Petroleum Geologists, Annual Meeting, June 3-6, Denver, Colorado.

- Montgomery, Scott L., 1996, South Casper Creek Field: a study in reservoir heterogeneity: American Association of Petroleum Geologists Bulletin, v. 80, p. 1161-1176.
- Morgan, J.T., F.S. Cordiner, and A.R. Livingston, 1978, Tensleep reservoir, Oregon Basin Field, Wyoming: American Association of Petroleum Geologists Bulletin, v. 62, p. 609-632.
- Narr, Wayne, 1998, Quantifying subsurface fracture sets: collecting and analyzing data with simulation in mind: (abstract), EXTIP 98 conference, Mexico City, 8 pages.
- Narr, Wayne, D. W. Schechter and L.B. Thompson, 2006, Naturally fractured reservoir characterization: Society of Petroleum Engineers, 112 p.
- Stevenson, V.M., and C.E. Mullen, 1991, Evolution of a successful steam drive in a geologically complex steeply dipping reservoir at South Casper Creek Field, Wyoming: Society of Petroleum Engineers, paper number SPE 21528, International Thermal Operations Symposium, Bakersfield, California, Feb 7-8, 1991, p. 61-72.

Appendix









SUBSURFACE STUDIES

HATFIELD

ASSESSMENT OF FRACTURES IN CORE FROM THE NADEL AND GUSSMAN HATFIELD 16-35 WELL

John Lorenz, April 17, 2008

INTRODUCTION

Fractures in 39 feet of core from the Nadel and Gussman Hatfield 16-35 well were logged on April 14, 2008. The logging was part of an ongoing study of core from the Hatfield field south of Rawlins. Most of the older cores taken from this field by the Ohio Company back in the late 1940's have been logged, and all cores from this field will be logged and the subject of a report by the end of this study. The report on this specific well is being written and distributed now since it comprises a better data set, as the core is largely intact, recent, and is associated with a wellbore-image log.

The Hatfield 16-35 core consists of the slabs and butts of slabbed, four-inch diameter core. The un-oriented core had been sampled and plugged, but was relatively intact or easily pieced together at the time of logging. Most of the core was taken from the formations overlying the Tensleep Formation, with only the bottom few feet being from the Tensleep Formation proper and none from the typical Tensleep dune-sandstone reservoir facies. However, some of the fracture types, and their orientations as derived from the associated wellbore image log, can be extrapolated to the deeper Tensleep Formation with a reasonable degree of reliability.

FRACTURES

Several types of lithologies were cored. The most regularly and intensely fractured lithology is the tan to pink, microcrystalline, massive dolomite beds. Fractures in this lithology are closely spaced, on the order of a centimeter or less in many beds, but they are typically occluded by dolomite cement.



Closely spaced, narrow, mineralized fractures in dolomite, looking end-on (uphole) to the core. Two fracture events are recorded, an older one striking top to bottom of the page, and a younger one trending upper right to lower left, sometimes originating from the ends of fractures from the older set. Fractures are occluded and should not enhance permeability. Similar dolomite interbeds in the Tensleep may be intensely fractured in similar fashion, but fracturing will be irrelevant to fluid flow if they are likewise mineralized.



Strata-bound, closely spaced fractures in tan microcrystalline dolomite. The fractures do not extend into the overlying anhydrite and muddy carbonate beds.

A different dolomite facies consists of relatively high porosity (7-12%) gray-brown, oil-stained rock with local anhydrite nodules. Although small, irregular, syn-sedimentary fractures are scattered locally within this facies, for the most part it is not fractured. Fluorescence indicates that the matrix contains oil. Several stylolites with vertical amplitudes of nearly half a foot occur in this facies, being marked by clay and bitumen residue. The bitumen residue does not fluoresce.

The interbeds and nodules of anhydrite, and the muddy shale intervals, are not fractured.

The lower ten feet of the core consists of an irregularly bedded limestone-dolomite-chert facies that contains a pervasive system of syn-sedimentary faults that are irregularly mineralized with a highly fluorescent calcite. Mineralization is incomplete, with numerous remnant millimeter- to centimeter-scale voids that are lined with euhedral calcite crystals.

The faults are marked by centimeter-scale bedding offsets, minor fault breccias, and locally by drag that suggests incomplete lithification at the time of faulting. The last few feet of core consist entirely of rubble and fault breccia, suggesting that the fault system becomes better developed downhole.

These faults created weakness planes in the rock that were later exploited by injections of hydrocarbons. Remnants of the hydrocarbon are found as bitumen layers within and cutting across some of the calcite-lined fault planes, as well as within the fault-breccia rubble at the bottom of the core. Bitumen is also present as a coating overlying crystalline calcite within some of the open voids along the faults.



Upper part of fault system, showing irregular calcite thicknesses and deformation of the overlying muddy strata, both suggesting poor lithification at the time of faulting.



Calcite-mineralized fault system near the bottom of the core. Note the rotated bedding between the two main fault planes, the connecting fault splays, and the thin black layers of bitumen (looking like pencil lines) that loosely follow the faults.



Close-up of the irregular, vuggy fault mineralization, and several dark layers of bitumen near the bottom of the photo, suggesting several injections of bitumen.



Calcite-mineralized fault plane (upper right to lower left), and truncated bed of fractured chert (dark gray horizontal layer in middle of the photo).



Syn-sedimentary fault breccia, displacement of bedding, and open void space along planes of a fault.



Euohedral calcite crystals line a fault, recording open porosity along the fault at depth.



Black bitumen coating calcite crystals in a void along one of the faults.

PLUG PERMEABILITY

Only one plug, taken from the depth of 5679.65, has anomalously high permeability, over ten times the permeability of the other samples. The rock around the hole from which this plug was taken does not appear to be fractured but does seem to be well bedded, and splits along the bedding may account for the high perm. No plugs were deliberately taken to test for fracture permeability, so the fracture permeability cannot be compared to matrix permeability.

COMPARISON BETWEEN CORE AND IMAGE LOG

One fault was picked on the image log, between 5696-5698 ft. Using a depth shift based on the core gamma compared to the downhole gamma, this fault does not seem to correlate to a discrete fault in the core. In fact, no discrete faults are present in the core. The multi-branched, irregular fault system in the basal ten feet of the core correlates in part to a chaotic pattern in the image log between 5702 and 5725 ft. If the core-log depth correction is not exact but allowed to shift a foot or two with depth, two irregularly faulted zones (5697-5700, and 5702-5707 ft.) bounding an unfaulted interval in the core may correlate to similar faulted and unfaulted intervals in the image log. If so, the sys-sedimentary fault system extends at least 25 ft. vertically, well into the top of the Tensleep proper.

All of the open (natural?) fractures picked in the image log are below the cored interval so no core-log comparison is possible. None of the vertical fractures that are so abundant in the microcrystalline dolomites was detected by the image log, probably because they are so tightly cemented with material of a similar dolomitic composition.

The open, natural fractures picked from the image log have a consistent NE-SW strike. There is no basis for checking this based on the numerous fractures found in the core.

IN SITU STRESSES

No petal fractures are present in the core, and only one drilling-induced fracture was picked on the image log found (below the cored interval) in the deeper intervals of the hole. One interpretation is that the present-day stress anisotropy is low, such that induced fractures, in core and in the wellbore, did not form readily. Other induced fractures are present higher in the hole, and are consistently NE-SW, lending credence to the interpretation that that is the orientation of the maximum horizontal compressive stress.

CONCLUSIONS

Although the core in this hole does not cut much of the Tensleep Formation, the fracturing it exhibits can be extrapolated to the deeper Tensleep. Fractures are well developed but totally mineralized and occluded in the microcrystalline dolomitic beds. Fractures less well or undeveloped in the higher porosity, oil-stained dolomites, and are not present in the anhydrites and shales. Fractures and the maximum horizontal in situ compressive stress probably strike dominantly NE-SW based on orientations picked in the image log, but there is no basis for quality checking this with the core. Where there core and logs cover the same interval, there is poor correlation between the structural features in the two data sets. A pervasive, irregular, branching, probably syn-sedimentary fault system is present at the top of the Tensleep Formation, and extends 25 ft. down into the reservoir. The irregularity of the system does not lend itself to image-log interpretation. Hydrocarbons were later injected along the fault system, possibly during charging of the Tensleep reservoir.

ANALYSIS OF FRACTURES IN CORES FROM THE TENSLEEP SANDSTONES IN THE HATFIELD OIL FIELD, CARBON COUNTY, WYOMING

John Lorenz, January 9, 2008

SUMMARY

The natural fractures in eight cores taken from the Tensleep Formation at the Hatfield oil field were logged and analyzed to assess their development across the field and their effects on production. The study suggests that although fractures are intensely developed, but no one fracture parameter controls fluid flow. Rather, interrelated fracture characteristics are necessary to create good production. Fractures and faults are best developed on the steep forelimb of the anticline where they would be expected, but wells located there are not the best producers. Fractures are variably developed on the backlimb: good development is correlated with good production, and poor fracture intensity correlates to a dry hole. Intersecting fracture sets are perhaps the most important control on production. The presence or absence of faults however is largely irrelevant to enhancing production, though they may provide pathways for water invasion.

INTRODUCTION

Fractures in cores taken from nine wells drilled into the Tensleep reservoirs at the Hatfield oil field, Carbon County Wyoming (about 10 miles south of Rawlins) were logged and analyzed. Eight of the cores, those drilled in 1948-1948, are housed at the USGS core library in Lakewood, Colorado. These older wells were probably only cored because the technology of the 1940's was such that it was easier to cut through the well-cemented Tensleep sandstones in this area with a diamond core bit than to drill through it with the standard tri-cone rotary bit. A more recent core was cut by Nadel and Gussman, the present owners of the field, in 2007 and was the subject of an earlier memo.

The Hatfield cores range from three and a half to four inches in diameter. Except for the recent core, they have not been slabbed or plugged. Although some of the cores had been partly washed, for the most part they were still coated with 1948 drilling mud. Drilling mud had to be completely washed off each piece of core in order to determine the presence/absence and

characteristics of the fractures. The older cores are stored in their original, heavy, nailed-together wooden boxes.



Calcite-mineralized fracture in core from the Union Pacific #5 well: the lower piece of core has been washed and details of the splaying fracture can be seen; the top piece has not been washed.

Although unslabbed core is commonly ideal for fracture studies since it presents a significantly larger volume of core than do slabs, the Hatfield fracture data set has been seriously degraded by the absence of anywhere from 20% to 90% of the core, the short missing pieces being scattered evenly along the core. The missing pieces were probably removed back in 1948-49, and probably discarded since the core was merely a by-product rather than the objective of the drilling process. It appears that it was a deliberate decision to preserve only representative samples of the cores. In many intervals, only three- to six- inch core segments were kept out of every one or two feet of core; in other intervals only an eight- to ten-inch piece for every four feet of core was put into the boxes. For example, only 56% of the 268 ft. of core that was cut in the Ohio UPR #3 well is in the boxes, and no boxes are missing from the sequentially numbered set. No plugs or samples appear to have been taken, and since they were not washed, the cores were apparently not logged at the time they were cut. The missing core pieces are probably buried in the 1948 mud pits or scattered on the ground somewhere near the drill pads.



Short samples were taken from each foot of core, and the remainder was probably tossed. The cores are stored in heavy wooden boxes. Ohio Government #5.

Because only short, non-continuous pieces of core were preserved, much of the detailed fracture information that was originally available in the whole core has been destroyed. Statistical analyses of the existing fractures (i.e., fracture heights, number of fractures per foot, etc.) are therefore skewed. The general fracture characteristics can still be observed, but data such as vertical terminations, bearing on whether fracture permeability extended across heterogeneities, bedding breaks and stylolites, are gone.

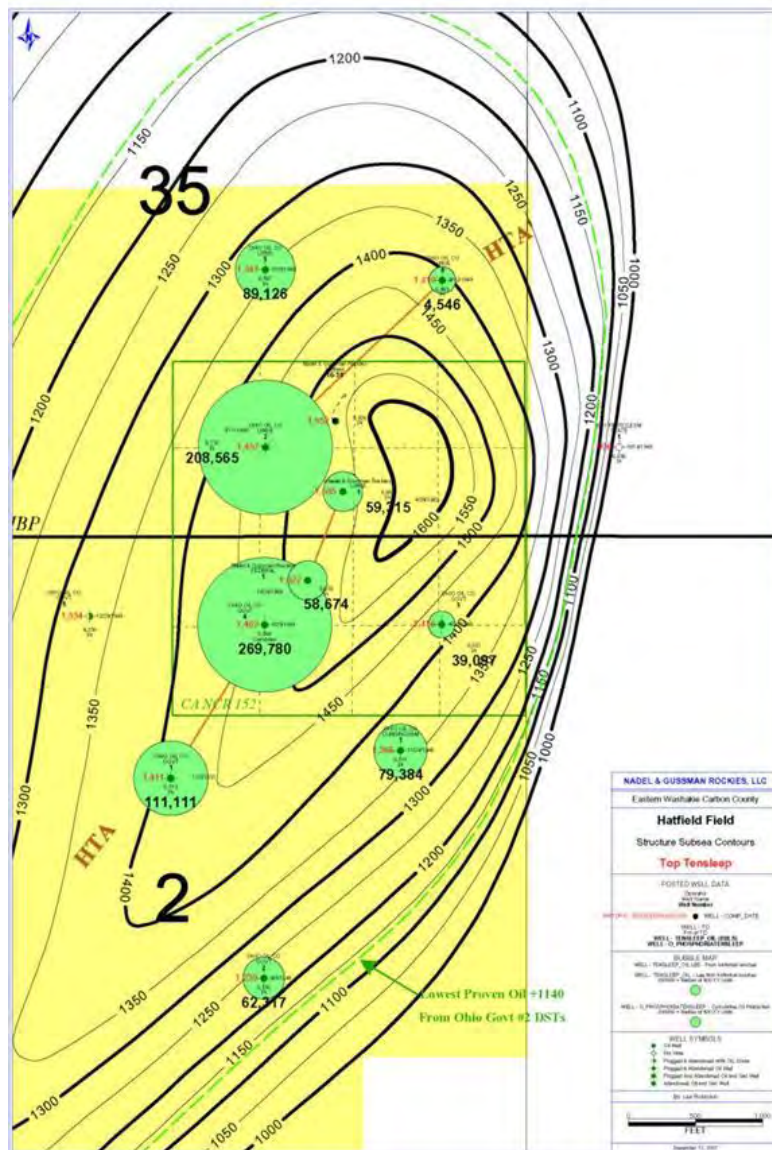
A more significant loss is the relative orientation data, i.e., the ability to relate the different fracture strikes to each other and to the in situ stress indicators (petal fractures) along the length of the cores. Adding to this problem is the fact that the core pieces are not usually marked for depth and are never marked for up-down orientation, thus there is no confidence in the locations or relative positioning of the different core pieces. For these reasons, only qualitative estimates could be obtained for important parameters such as fracture orientations, distributions, and spacings. The assessment and characterizations offered here are based on frustratingly incomplete data.

Nevertheless, the remaining core does support a semi-quantitative, holistic fracture study because the reservoir is so heavily fractured that even the incomplete cores contain numerous fractures. Enough core has been preserved that generalizations can be made about fracture characteristics and distributions. Fracture characteristics and intensities can be compared

between wells, and qualitative estimates can be made of the effects of fractures on reservoir plumbing.

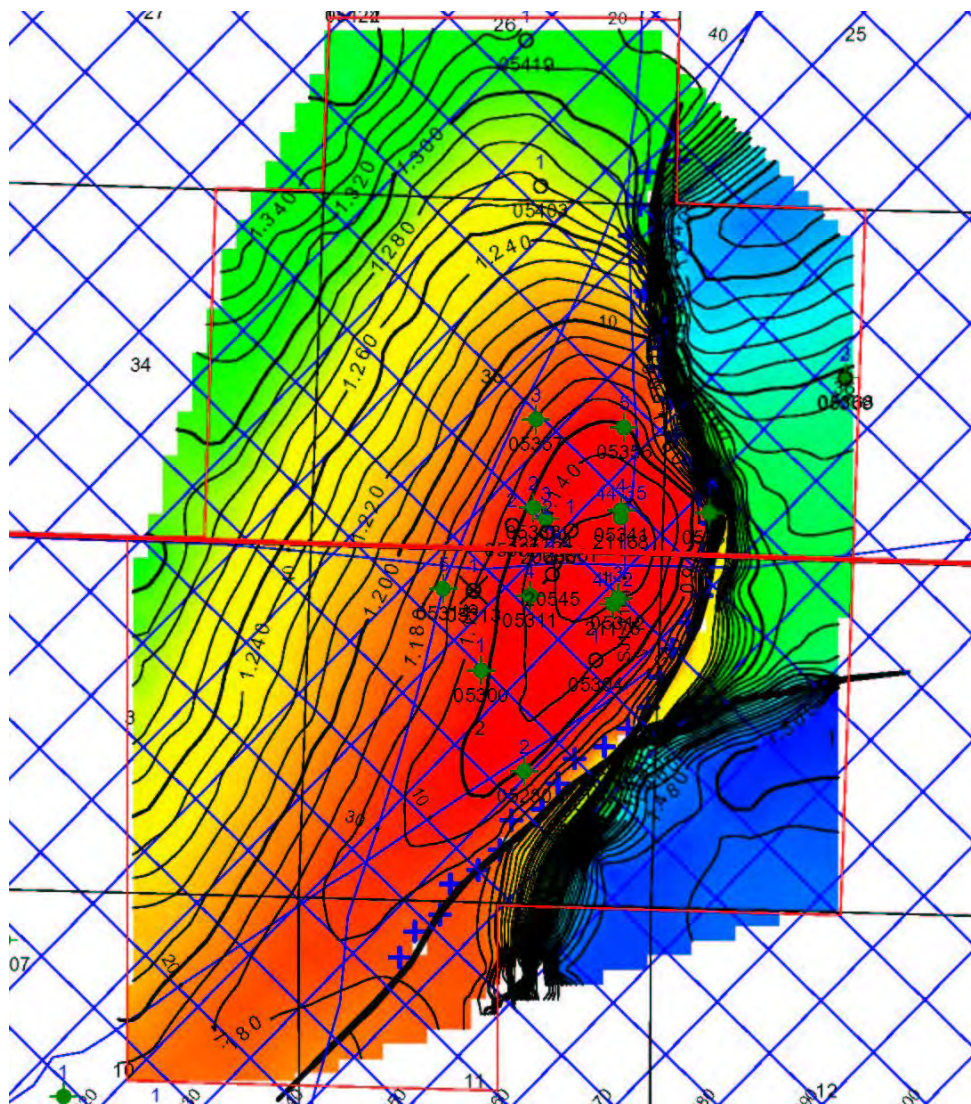
STRUCTURAL SETTING

Hatfield field is located on an east-vergent anticline that is about three-miles long but that culminates in a more localized crest. The anticline has a mapped structural closure of about 600 ft. The structure-contour maps suggest that the backlimb of the anticline has an 8°-10° dip to the west while the forelimb, where it is at its steepest due east of the crest, dips about 35° to the east.

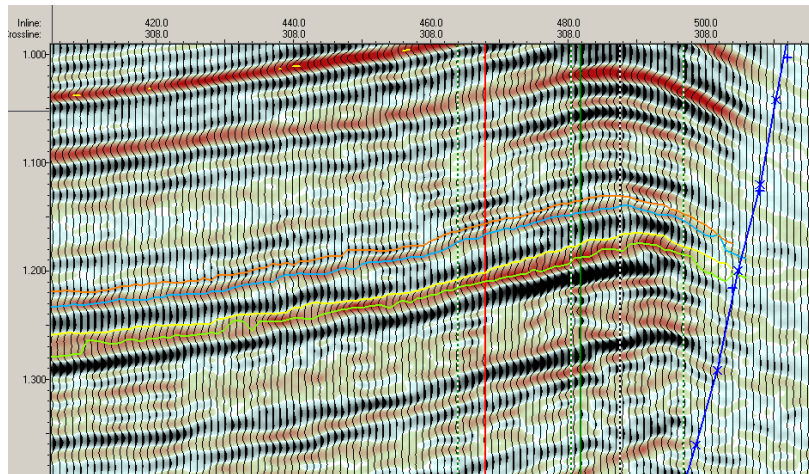


Conventional structure-contour and cumulative-production “bubble” map of the Hatfield oil field, provided courtesy of Lee Robinson, Nadel and Gussman.

The 3-D seismic structure map shows more detail, including a curved, concave-westward bounding thrust fault on the east side of the structure, a steeper eastern flank, and a slightly different, more easterly location for the crest. The upper plate of the thrust that forms the Hatfield structure seems to have been lifted and thrust eastward over an E-W trending arch, possibly accounting for the relatively small, localized crest of the Hatfield anticline compared to the elongate crests that are more common on these structures. An underlying arch such as this in most structural settings would have impeded eastward motion of the thrust, thus the concave-westward thrust front shown on the seismic map is unusual.



Seismic time-structure map of the Hatfield oil field, provided courtesy of Lee Robinson, Nadel and Gussman.



E-W seismic cross section across the Hatfield anticline, courtesy of Lee Robinson, Nadel and Gussman.

The position of the highest part of the Hatfield dome over the crest of the underlying anticline suggests that a lot of energy was expended in moving rock over this obstacle. The high degree of fracturing found in the Hatfield cores accommodated much of that energy. Large, repeatedly offset fractures accommodated significant amounts of strain during thrusting.

The Tensleep Formation at Hatfield is anomalous in several respects. It produces Cretaceous-age oil rather than the more common Paleozoic oil found Wyoming's Tensleep reservoirs. The eolian Tensleep dune deposits which typically have poor cementation and high porosity elsewhere in the state, have relatively low porosity (a reported average of only 3%; unpublished Nadel and Gussman report), and they are tightly cemented in the Hatfield reservoirs. Moreover, the cement is calcite, whereas most Tensleep sandstones are cemented with anhydrite. Induration of the rock with calcite cement has made the Tensleep strata at Hatfield brittle and more susceptible to fracturing. Hatfield represents an end member in the spectrum of Tensleep reservoirs in Wyoming.

FRACTURE CHARACTERISTICS

Fracture types and orientations

Cores of the Tensleep Formation at the Hatfield Dome are intensely fractured. The different fracture types, and pieces of core containing intersecting fractures show that multiple fracture orientations are present in the subsurface. However, the cores are not oriented, thus the strikes of those fractures cannot be determined and the number of different fracture orientations can only be estimated. Many of the fractures are shear fractures with high to low dip angles: relatively few of the vertical extension fractures that are common in other Tensleep reservoirs are present in the Hatfield cores, and where they are present they have commonly been secondarily sheared: many of the fractures show evidence for multiple opening and shear events. Moreover, some of the Tensleep bedding planes were oriented optimally relative to the deformation stresses and were sheared to form bed-parallel fractures.



Fractures with opposing dips. Ohio Government #1



Two intersecting fracture orientations. Union Pacific #5



Fractures with three orientations (outlined by dashed lines). Tesoro Skyline #1

Other structures are common in the Tensleep reservoirs at Hatfield. Stylolites, those irregular, pressure-solution surfaces within a rock oriented normal to the maximum compressive stress, are locally common. Numerous faults are represented by multiple inclined, sub-parallel to anastomosing shear planes with obvious offset and slickenlines. Shear fractures grade into faults as displacement increases and the zone of deformation widens, and the distinction between them is not always apparent.



Box-shaped stylolites. Union Pacific #3 well. Thumb for scale

Fracture Mineralization, Ornamentation, and Apertures

Calcite mineralization is common, though it rarely completely occludes a fracture. Shear offset, both before and after calcite precipitation, has produced irregular fracture apertures that have retained significant amounts of porosity along most of the fractures. Within the larger fractures, calcite has typically occluded the narrow zones but has merely lined the walls of the wider slots with euhedral calcite crystals. Significant porosity, and presumably permeability, remain within most of the fracture apertures.



Parallel fractures with large-scale open porosity lined by crystalline calcite. Ohio Government #3.



Calcite-occluded shear fractures showing vertical bedding offset. Union Pacific #5

Bitumen also lines many of the fractures. It typically underlies the calcite mineralization, indicating that bitumen emplacement predates the precipitation of calcite along the fractures.



Inclined fracture showing an early coating of bitumen, slickenline striations on the bitumen, and calcite-crystals lining a hollow in the shear plane. Union Pacific #5



Bitumen with a papillary texture coating an inclined fracture. Union Pacific #5

Many of the fractures show offset bedding across the fracture walls and slickenlines along the fracture faces. Slickenlines, indications of the direction of offset across fracture walls,

have been imprinted onto the host rock and/or onto the bitumen and calcite mineralization. Where slickenlines decorate the mineralization they indicate a sequence of fracturing followed by mineralization and secondary shear. Many of the slickenlines rake across fracture faces at angles to the dip azimuth of the fracture. Raking slickenlines also suggest reactivation of fractures: the fracture geometry typically records the stress field during initial fracturing, and rake shows reactivation in shear under re-oriented, oblique stresses.



Inclined shear fracture showing raking slickenlines on a bitumen-coated surface and patches of calcite cement precipitated in the hollows behind asperities.



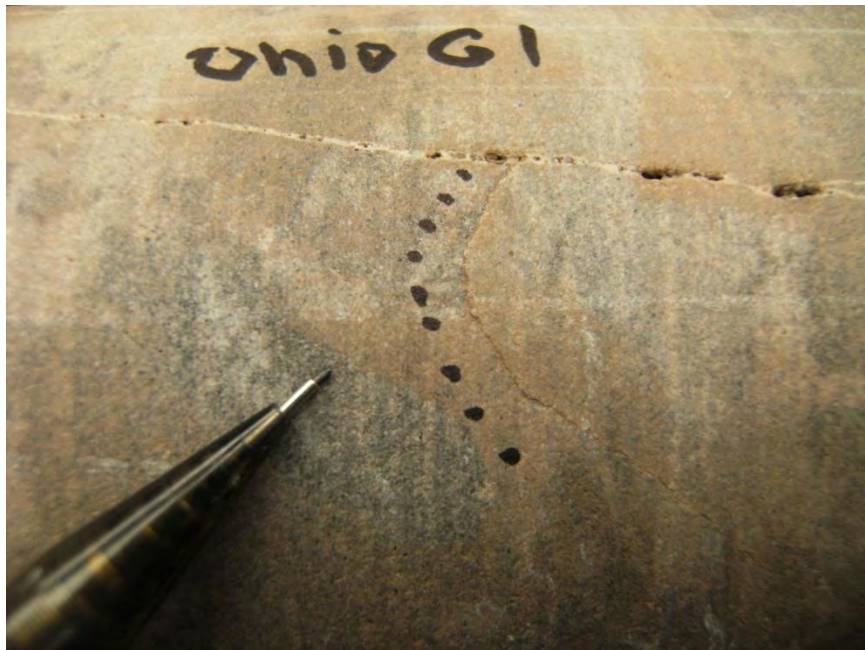
Inclined shear fracture coated with calcite displaying a raking –slicken-cryst” texture, probably indicating mineral precipitation during shear. Ohio Government #2



Inclined shear fracture. Left: edge-on, showing pinch and swell texture of the calcite mineralization. Right: face-on showing patchy calcite and slickenlined bitumen. The fracture strikes oblique to the maximum horizontal compressive stress as recorded by the associated petal fracture (outlined by the dotted line). Union Pacific #5.

Fractures and Stresses

The strikes of coring-induced petal fractures record the present-day orientation of the maximum in situ horizontal compressive stress. Petal fractures are not common in the Hatfield core, but enough of them are present, and can be associated with natural fractures, to document normal to oblique relationships between the in situ stresses and some of the natural fractures. Unfortunately the orientation of neither the maximum horizontal compressive stress nor the fractures can be determined in the absence of oriented core or an image log.



Petal fracture (outlined by the dotted line) strikes normal to the strike of a vertical, calcite-mineralized fracture. Ohio Government #1

The most recent Tensleep core, taken in 2007 from the Hatfield #16-35 well, contains no petal fractures, and only one drilling-induced fracture was picked on the image log in the Tensleep interval. However, induced fractures higher in the hole are consistently NE-SW, suggesting that that may also be the orientation of the maximum horizontal compressive stress in the Tensleep interval.

Faults

Numerous faults were cored in the 1948-49 wells. Faults consist of numerous sub-parallel shear planes and local fault breccias, the composite zones of disturbance being up to several tens of centimeters wide. Bitumen and calcite commonly fill and line the shear fractures that comprise faults. Significant open void space is common along the fault planes, the voids commonly being slot-shaped parallel to the fault and lined with crystalline calcite.

Faults are inclined, dipping from 30° to 70° relative to the presumably vertical core axes. Associated slickenlines indicate dip-slip and oblique slip motion, and sometimes both: many of the faults have been reactivated, possibly several times.



Fault breccia along a shear plane. Government Cunningham #1



Large-scale porosity along inclined shear planes of a fault: Government #1



Large-scale porosity along high-angle shear planes. Note the reverse sense of offset on bedding. Tesoro Skyline Federal #1



Occluded shear planes of a fault system. Union Pacific #5

Origin of the Fractures at Hatfield

Several phases of fracturing can be deciphered from the core data although the details are obscure. The compound structural history of the rock may have means that evidence for some of the fracturing events may have been altered or even destroyed. In essence, an early phase of fracturing is recorded by the bitumen that lines many fractures. Later fractures, locally reactivating the bitumen fractures, opened and calcite was precipitated on top of bitumen. Many of the fractures were then reactivated in shear and new shears were created in virgin rock at the same time. Some of the shear planes grew into faults.

Bitumen, essentially a devolatilized oil, is pervasive in the Tensleep pores in the upper parts of the Hatfield reservoir, staining the core gray to dark brown. Pegui Yin (personal communication) suggests that it is remnant from Permian oil that originally charged the reservoir. This oil must have been pressurized, either thermally during burial or by mechanical compression of the strata during thrusting, early in the structural history of the reservoir. Overpressurization created the observed fractures lined with bitumen, along which the Permian oil escaped from the reservoir trap. Subsequent healing of the reservoir seal allowed later filling of the trap with Cretaceous oil.

Thrust faulting, probably of Laramide age, was the primary source of strains that led to pervasive shear fracturing of Tensleep sandstones at the Hatfield anticline. If the fracture patterns in similar Wyoming basement-cored anticlines can be taken as a guide, the main fractures should trend parallel and normal to the axis of the hinge of the anticline. However, the

rock is more heavily fractured, and more shear fractures are present at Hatfield, than in most Tensleep reservoirs. The most likely reason is that sandstone induration by calcite cement at Hatfield 1) made the rock more susceptible to fracturing, and 2) prevented pervasive strain accommodation at the intergranular level.

A more specific model relating fracturing to the formation of the anticline cannot be constructed without information about the orientations of the Hatfield fractures. Nevertheless, thrusting and folding of the strata were obviously of sufficient magnitude to create a suite of closely spaced shear fractures in the fracture-prone Tensleep strata.

FRACTURE EFFECTS ON THE HATFIELD TENSLEEP RESERVOIR

The drilling mud that had to be washed off the 1948-49 cores during this study contained a fibrous Lost Circulation Material (commonly known as LCM), much of it lodged into the open void spaces in fractures. The drilling and well records for these wells are not in the USGS files and have presumably been lost, but the LCM indicates that drilling these wells was not easy, that the drilling engineers had to fight to reduce the loss of drilling mud into the voids of the highly fractured reservoir.



Fibrous Lost Circulation Material in the mud was used to slow the loss of mud into the fractured formation during drilling. Government #5



Lost Circulation Material was forced into fractures with the drilling mud, with the intent of reducing fracture permeability and thus the loss of mud. Government #5

The need to use LCM shows that fractures and faults make the formation highly permeable despite tight cementation and the 3% matrix porosity. Once the wells are drilled, presuming no drilling damage, the fracture-related system permeability is instrumental in conducting oil to the wellbores at economic rates. Fracture and fault conduits are also probably the preferred pathways for fingering water up from the oil-water contact when the reservoirs are pumped hard.

Fractures are numerous and occur in a spectrum of sizes from hairline fractures to faults tens of centimeters wide, thus fractures may contribute not only to the conductivity in the formation but also to the storage capacity.

MISCELLANEOUS TRIVIA

The longer sticks of the 1948-49 cores appear to have been broken into pieces that would fit into the core boxes by some sort of bending device no longer in use today. A distinctive, repetitive type of core break starts as a smooth planar surface normal to the axis of the core, without any percussion marks or scars from a hammer, and at $\frac{3}{4}$ of the way across the core

diameter the plane bends smoothly yet abruptly to become nearly parallel the core axis. The plane of the break then bends back to become normal to the core axis to complete the break across the core. This suggests that the break started in tension, as at the outside of a bend, changing direction as it propagated into a region of compression at the inside of the bend in the core.



Man-made break in the core caused by bending. Union Pacific #2

Another bit of interesting information is the excellent preservation of the impressions of 1948 Hughes tri-cone bits at the tops of two of the cores. The drillers used the Hughes tri-cone down to core depth then changed to diamond coring bits. The inefficacy of a tri-cone bit on the indurated Tensleep is shown by the deep tool marks preserved in the top of the core, suggesting that the bits rotated in place for some time without penetrating the formation.



Fossil imprint of a 1948 Hughes tri-cone bit at the top of the core in the Union Pacific #2 well.

FRACTURE DISTRIBUTIONS

An attempt has been made to compare the fracture types and intensities between the different wells, and to compare those with the cumulative production from the various wells. This semi-quantitative comparison must be interpreted subjectively since the incomplete cores as described above have skewed the statistics an unknown amount in unknown directions. Core diameter in the different wells ranges from 3 1/8 inches to 4 inches, and only the slabbed core was available for the Tesoro well: this does not severely alter the number of fractures intersected since most of the fractures are not vertical. The amount of core cut in each well ranged from 71 ft. to 306 ft., but the amount of that core that was boxed, preserved, and is now available for study ranges from 25-62% (except for the Tesoro well where all 71 ft. of slabs are available).

In addition, correlations between fracturing and production must be used carefully: fracture spacing, interconnectedness, and permeability are prime controls on production rates, whereas cumulative production will depend more on fracture spacing and porosity: fractures are important to volume only if they comprise a significant percentage of the reservoir storage volume.

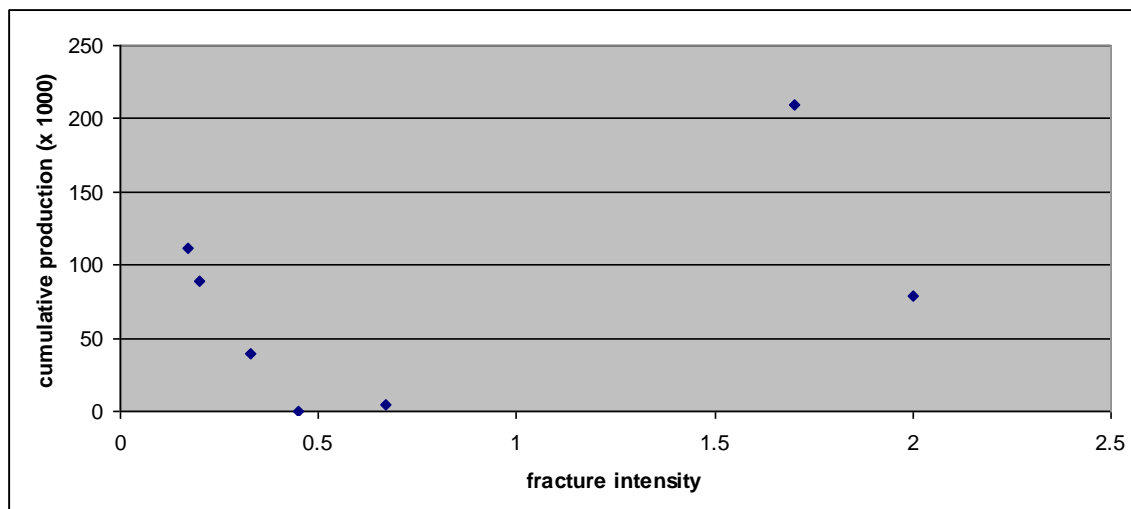
TABLE 1: Comparison of Fracture Measurements

	OG1	OG3	OG5	UPR2	UPR3	UPR5	CUN1	TES1
ft. F/ft. core	0.17	0.33	0.45	1.70	0.20	0.67	2.00	0.17
avg F height	0.4	0.5	1.0	0.8	.4	0.9	.4	0.5
shear faults	some	some	some	mod	some	heavy	HVY	some
F sets	-	3	1	2	-	1	5	1
avg F width mm	2	>3	1	3	>3	>3	>3	3
avg F porosity %	0.9	0.5	0.8	0.8	0.7	1.3	1.6	0.3
production	60	-	35	25	15	20	30	40
bubble size	med	sm*	dry	b ig	med	sm	med	-

*Bubble as plotted on the map is small, but the associated production number suggests it should be medium-sized.

The following parameters are used in the table above:

ft. F/ft. core: this is an estimate of fracture development or fracture intensity in the core, derived by dividing the cumulative feet of fracture height along the core axis by the length of core available. At Hatfield, this ratio varies by an order of magnitude, from slightly less than 0.2 to 2.0 ft. of fracture height per ft. of core length. The chart below suggests that fracture intensity may be one of the controls, though not the only one, on cumulative production. If all other parameters are equal, i.e., assuming that the wells have been producing for roughly equal lengths of time, that they have equal oil saturations and fluid pressures etc., then fracture intensity should be one or the more important controls on cumulative production. The relationship is ambiguous, and several factors may account for it. The data population may be too small, the measurements may be to crude, or, quite likely, the other parameters may not be equal.



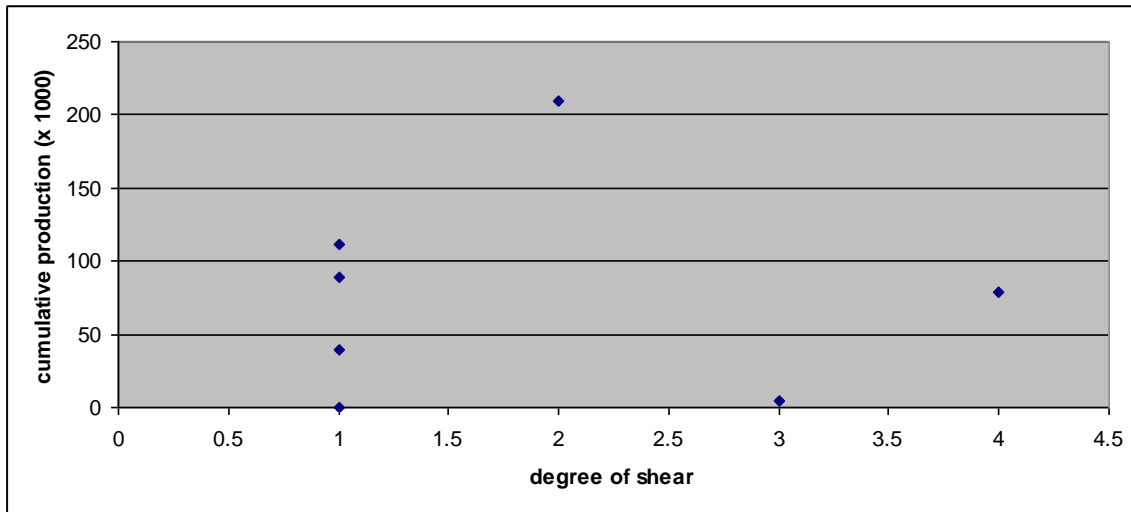
Fracture intensity, measured as ft. of fracture length per length of core, correlates roughly to cumulative production.

The correlation between degree of fracturing and structural position is also ambiguous. The two wells with the highest degrees of fracturing and faulting are found in different places. The Cunningham #1 well, with the highest measurement of 2.0 ft. of fracture per ft. of core is on the forelimb where high fracture intensity would be expected. The Union Pacific #2 well, with 1.7 ft. of fracture per ft. of core, is located on the backlimb. The other wells all have less than half of the fracture intensity of these two wells, none having more than 0.7 ft. of fracture height per ft. of core.

Fracture Spacing: Numbers for fracture spacing are important for reservoir modeling, but they are also difficult to acquire. There is no reliable way to determine an empirical dimension for fracture spacing in this reservoir from the incomplete and discontinuous core data, but the ratio of fracture length to core length can be used to qualitatively estimate fracture spacing. In many reservoirs considered to be fractured, one foot of fracture height per ten feet of core length in the reservoir lithology is an average ratio and corresponds to lateral fracture spacings of two to five feet. The fracture-to-core ratio is well above this average in the Hatfield core, thus fracture spacings of less than a foot would not be out of line for the more fractured parts of the reservoir.

avg F height: the average fracture height was calculated by dividing the cumulative fracture height measured in the cores by the number of fractures measured. This is a severely truncated data set since the measurable fracture height was all too frequently limited by missing pieces of core. In fact, in these cores, this parameter is probably more a measurement of the average length of the preserved core pieces than it is of fracture heights.

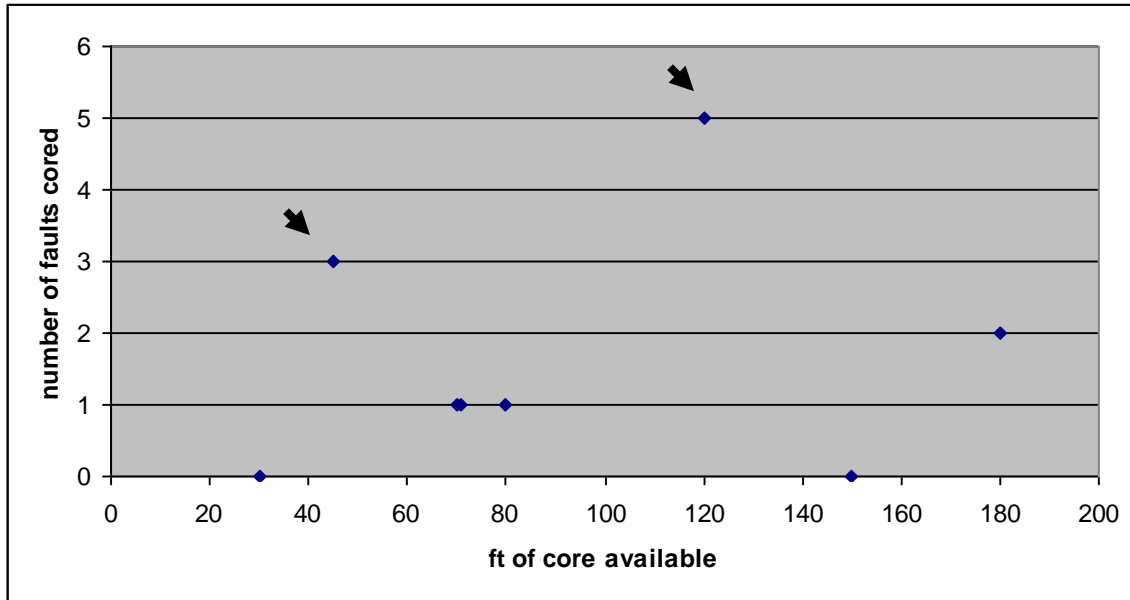
shear: the degree of shearing in a core was estimated subjectively based on the number of shear fractures and an estimate of shear offset for each. The degree varies from —somè to —moderate” to —~~heavy~~” to —HEAVY.” Although the well with the highest degree of shear fracturing has only a medium-sized production bubble and the well with the largest bubble has only moderate shearing, there is a very rough trend, if one is willing to believe, of more production with increasing degree of shear. As would be expected, the well with the highest degree of shear (The Cunningham #1) is also the well with the highest ratio of fracture height to core length.



Cumulative production is roughly related to degree of shear

faults: The number of faults encountered in the available core for each well is also given in the table above. The probability of finding a fault increases with the length of core examined, and indeed the plot below shows, roughly, that more faults are present in the longer cores. The

wells with the highest ratio of faults encountered per ft. of core are both on the forelimb where studies have shown deformation on similar structures is typically highest. Interestingly, a correlatively high degree of fracturing is present in only one of these two wells, the Cunningham #1. It is possible that a representative sample of fractures is not present in the other well where only 45 ft. of core were available for study.



Longer cores encountered more faults. However the two wells on the forelimb of the anticline (the Cunningham #1 and Government #3, arrows) are well above the average.

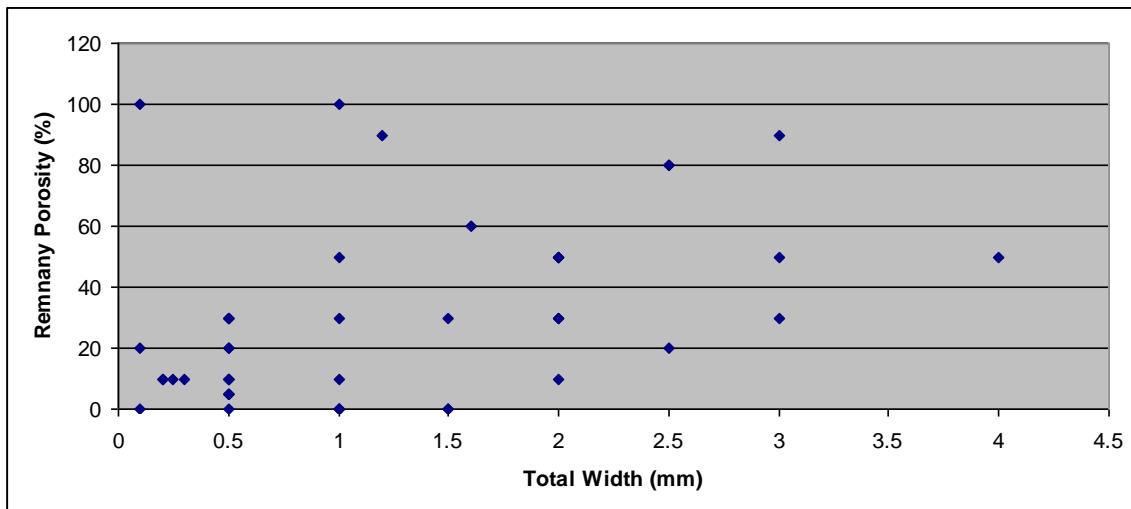
Faults are likely to provide vertically extensive conduits for flow within a reservoir. This can be good, in that faults can connect various fracture systems across different lithologies, but faults can also connect a reservoir to unwanted water below the oil leg. In fact, the two wells with high degrees of faulting on the forelimb have only moderate cumulative production records, thus enhanced faulting does not seem to be desirable in Hatfield-type reservoirs.

F sets: This is a record of the number of probable intersecting fracture sets with different orientations in the subsurface, based on observations of intersecting fractures in the cores. If three sets are listed on the table, at least three different intersection angles could be measured between fractures in that core.

The only core where a single fracture set could be documented is the only dry hole on the table. This suggests that fracture intersections are as important as fracture intensity. The dry hole, the Ohio Government #5 well, is located on the modestly deformed distal back limb of the anticline, where outcrop studies suggest that single fracture sets with parallel, non-intersecting fractures are common.

avg F width mm, and avg F porosity % are averages for the measured and estimated (respectively) values of these parameters in the cores. They do not correlate well with production, in part because the data set is relatively small (most of the fractures are broken open and reliable measurements of these parameters are difficult to obtain), and in part because other parameters such as fracture intensity and degree of intersection are much more important. Width and porosity would be more important parameters if the fractures in this reservoir were smaller and tighter.

A plot of the width and porosity data from several of the wells (below) shows that the larger fracture widths, as measured between the fracture walls including mineralization, tend to have a larger percentage of remnant porosity. Nevertheless, even the smaller fractures commonly have sufficient remnant porosity to contribute to the volumetrics and permeability of the reservoir.



Wider fractures tend to have more remnant porosity despite mineralization, but many the smaller fractures also retain significant porosity and will also contribute the reservoir plumbing system. n = 45.

CONCLUSIONS

These descriptions and discussions suggest that although fractures are intensely developed and must dominate production, no one fracture parameter controls fluid flow at the Hatfield oil field. Rather, a family of interrelated and supporting parameters is necessary to create good production from these heavily fractured reservoirs. Fractures and faults are best developed on the steep forelimb of the anticline, but wells located there are not the best producers. Fractures are locally well developed on the backlimb, possibly related to local structure such as a tear fault in the thrust plate, and good production on the back limb correlates, in at least the best producer, to good fracture development and multiple fracture sets. The only dry hole is also located on the backlimb, but core in that well suggests the presence of only one set of poorly developed fractures and no shearing. The presence of intersecting fracture sets is an important parameter, but the presence of numerous faults does not add to the quality of the reservoir.

APPENDIX: SYNOPSES OF CORE DATA FROM INDIVIDUAL WELLS

Summaries of the fracture data from the individual wells are presented below, along with pencil-sketch summaries of the more detailed logs that were made during this study. The pencil sketches are rough, but they are presented for visual impact since they show qualitatively the relative intensity of fracturing. The following symbols are used in the sketches:

-The relative incompleteness of most of the cores is indicated by the degree of dashing in the lines on the right side of the lithology column.

-Oil stain is indicated by shading to the left of the lithology column.

-Shear fractures are indicated by double-headed arrows to the right, raking shear by a circled dot.

-Near-vertical fractures are depicted by vertical lines within the lithology column.

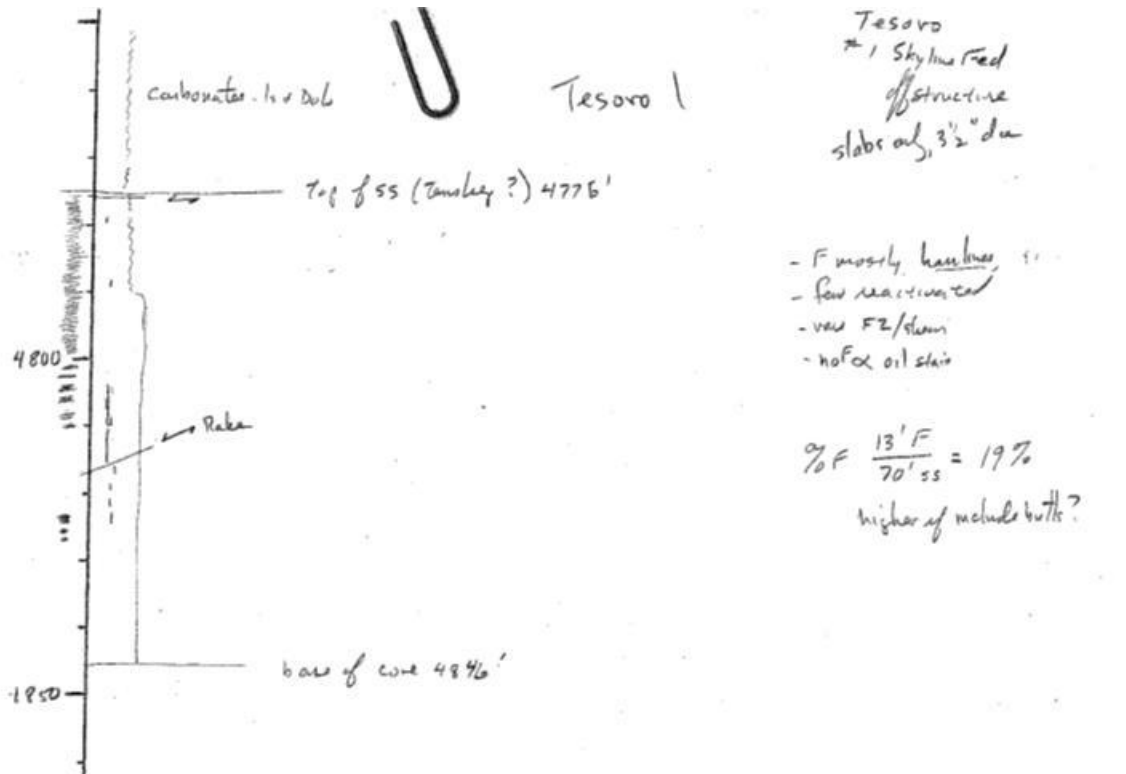
- The locations of bitumen fractures are indicated by "B" to the right of the column.

-Stylolites are indicated by jagged lines to the right of the column.

-Faults are indicated by "FZ" (Fault Zone).

The more important of the penciled comments have been translated into print in the accompanying text for each well.

[Note: the Tesoro well is off structure, 4 miles to the southwest of the anticline and is not on the maps presented above.]



Tesoro #1 Skyline Federal, section 28, T. 19 N., R. 88 W.

3½ inch core, 4775-4846' MD

71 ft. of Tensleep core cut, 71 ft. of the core preserved *but slabs only*

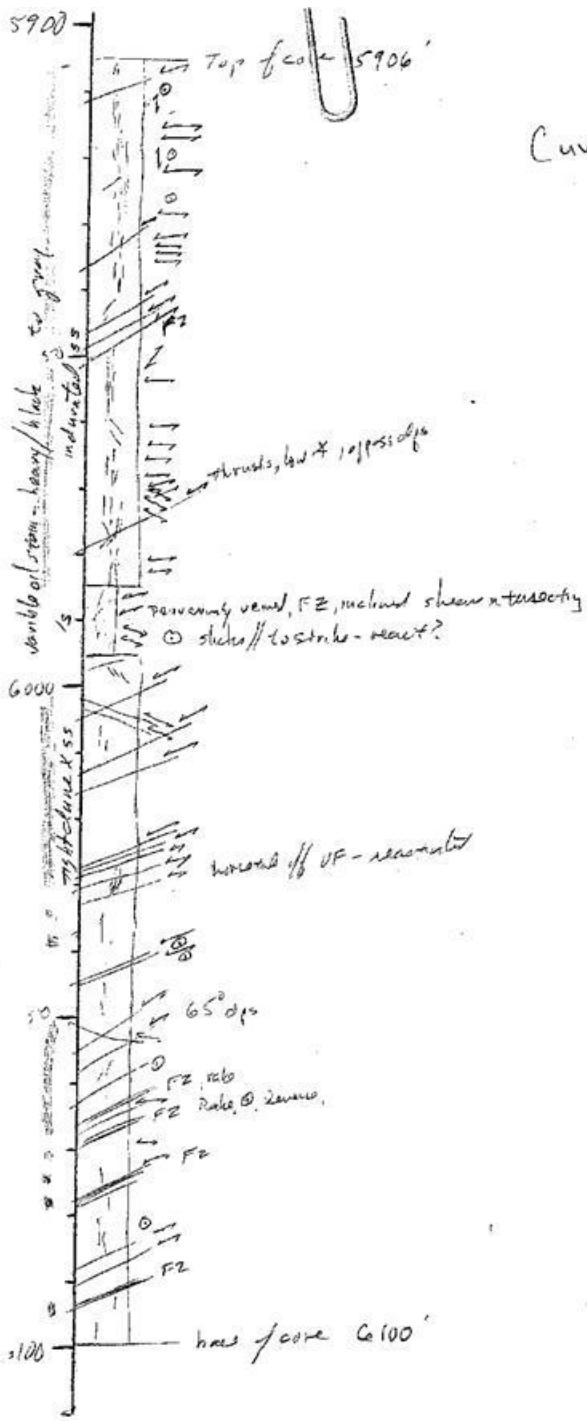
Well location: off structure, approximately four miles to the southwest

Production unknown

Fractures are mostly vertical hairlines, a few reactivated.

One shear fracture/fault with breccia and raking slickenlines in the Tensleep, another smaller shear at the top of the formation

Moderate oil stain over the top 25 ft. of core, irregular diminishing to unstained below 4800'. Two types of oil stain, gray and tan



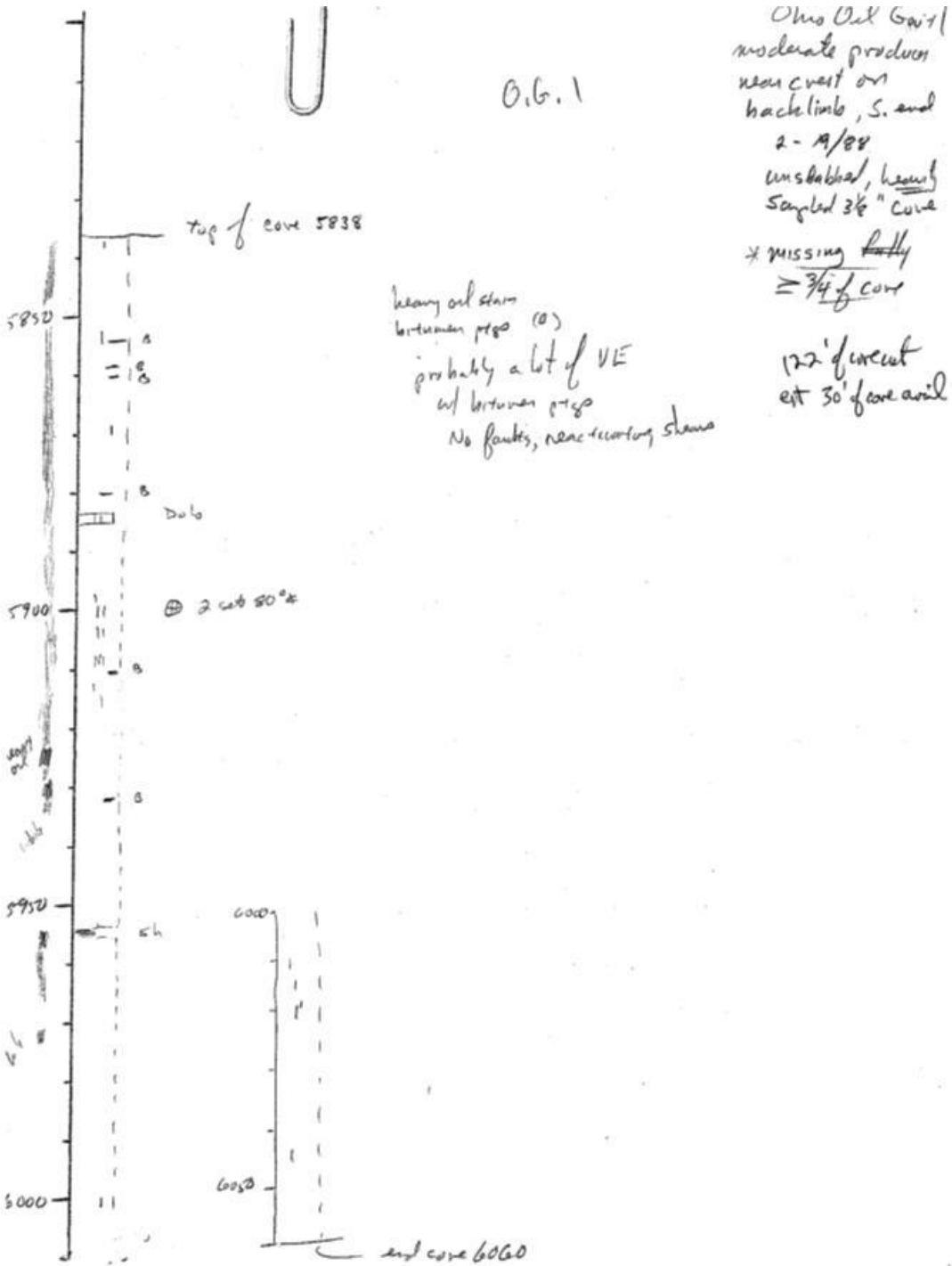
Cunningham #1

Ohio Oil
Gov't Cunningham
#1 2-19/88
Southern forelimb
modest production
unstable/heavily
sampled 3.5" core

heavily fractured
but few VF
(no more than in
the skyline?)

195' of core cut
est 120' of core avail

Ohio Oil Government Cunningham #1, section 2, T. 19 N., R. 88 W.
 3½ inch core, 5906-6100' MD; 194 ft. of core cut, est. 120 ft. of core preserved
 Well location: forelimb of the anticline in the southern part of the field
 Modest cumulative production
 Heavily shear fractured and faulted, with multiple slickenline orientations even on the
 same plane. Few vertical fractures
 Moderate oil stain over most of the core, irregular below 6030'



Ohio Government #1, section 2, T. 19 N., R. 88 W.

3 1/8 inch core, approx. 5388-6060' MD

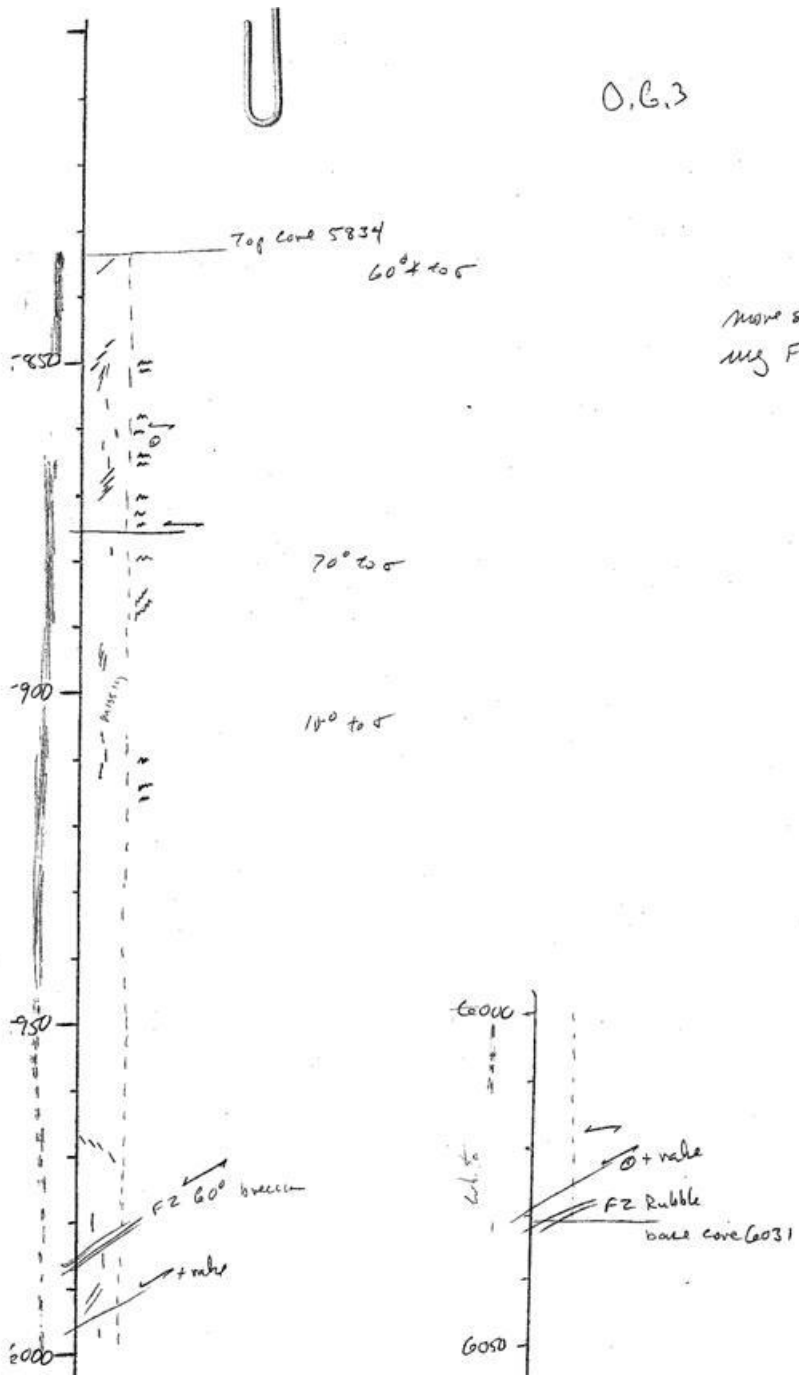
122 ft. of core cut, only 30 ft. of the core preserved

Well location: slightly behind hinge south of the crest, on the backlimb

Modest cumulative production

Relatively poorly fractured but some intersections; no shears or faults

Horizontal bitumen-filled partings; mod oil stain top 2/3rds, irreg. below 5940'



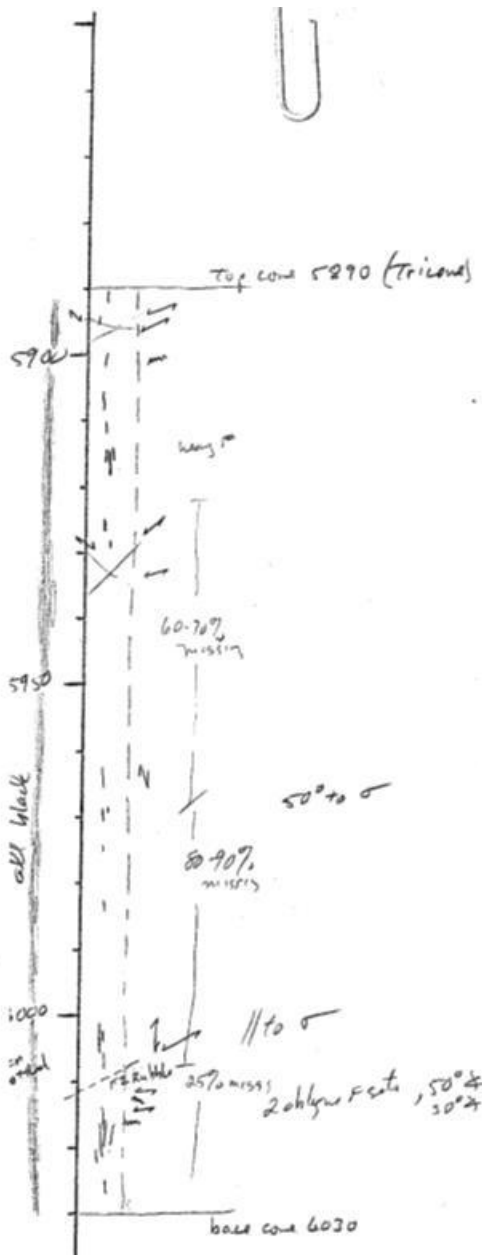
O.G.3

Ohio Gov't #3
 2-19 N/88 W
 Small producer,
 mid forelimb
 heavily sampled -
 large sections
 missing, 50%
 of core missing

more stylolites
 mg F strike to 5 = multi, 6
 stylolites/f

97' cut
 ~45' preserved

Ohio Government #3, section 2, T. 19 N., R. 88 W.
 3½ inch core, 5834-6031' MD
 97 ft. of core cut, estimated 45 ft. of core preserved
 Well location: forelimb of the anticline 1000 ft. SE of the crest
 Moderate cumulative production
 Moderately fractured, several faults; numerous stylolites
 Moderate oil stain over top half of the core, irregular below 5950'



O.G. 5

Ohio Govt #5
 2-19N/88W
 Far back limb
 ≠ P+A
 heavily sampled
 3 1/2" dia. Unalaska
 ~50% core missing
 locally to 80%
 full of oil
 lots of cm
 140 ft cut
 ~70' in logs
 3 1/2" core

} Fault F zones but not clear zone, doesn't help oil

Ohio Oil Government #5, section 2, T. 19 N., R. 88 W.

3 1/2 inch core, 5896-6030' MD

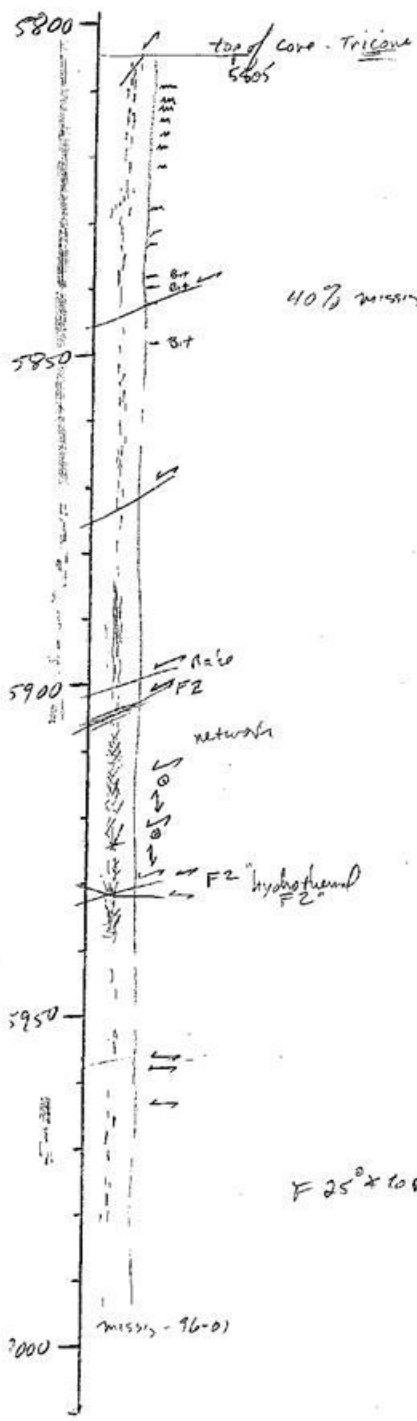
140 ft. of core cut, estimated 70 ft. of core preserved

Well location: far backlimb of the anticline

Dry hole

Moderate fracturing but no indications of intersecting sets. One fault

Heavy oil stain over most of the core, lighter below 6000'



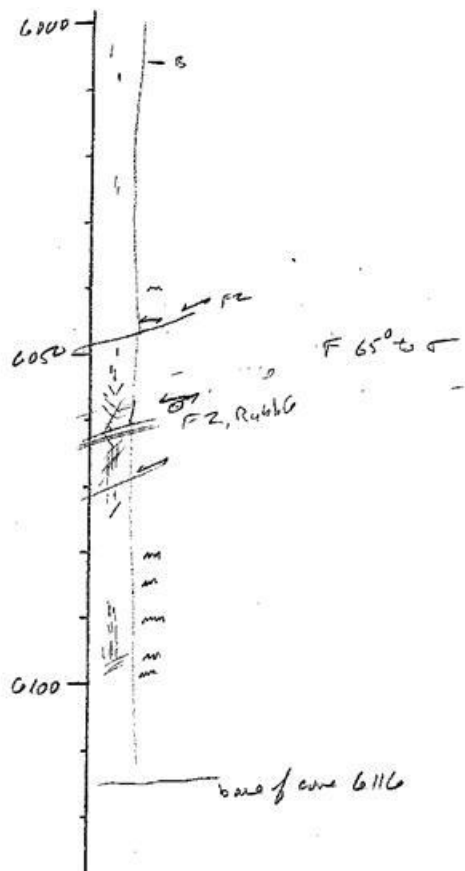
UPR 2

ldj ✓ UNO UPR-C
 35-20M/82W
 good producer
 on the middle
 back limb
 unstable 3 7/8\"/>

40% missing 306' cut, ~ 180' present, 3 1/8\"/>

Hit some good fault cores - (2x) -
 = hi Q?

F 25° x 10 r



Ohio UPR #2

Ohio UPR #2, section 35, T. 20 N., R. 88 W.

3 5/8 inch core, 5805-6116' MD

306 ft. of core cut, estimated 180 ft. of core preserved

Well location: middle of the backlimb, 1000 ft. west of the crest

Good cumulative production

Heavily fractured and faulted. Zones of numerous intersecting fractures.

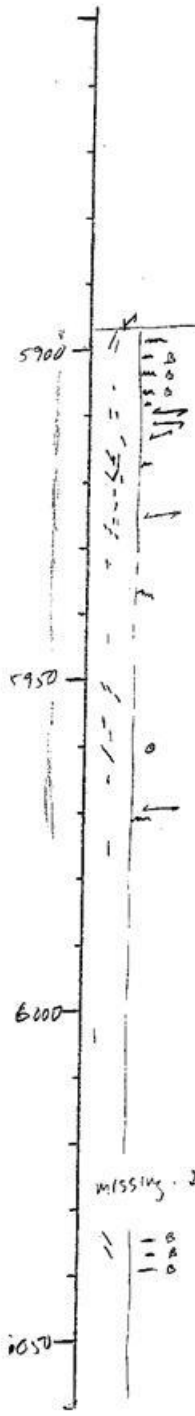
Moderate oil stain in the top 100 ft., irregular below 5870', none below 5970'

UPR 3

Ohio UPR #3
35-20, N 88W
moderate producer
on back hole, N/W pad
unlashed, heavily sample
4" core

* oil stained but not heavily stained
is that why not big producer??

top of core 5898' - (see notes top 43' of tubing above this was not cased)



20-60% missing

40% miss

missing - 25-35'

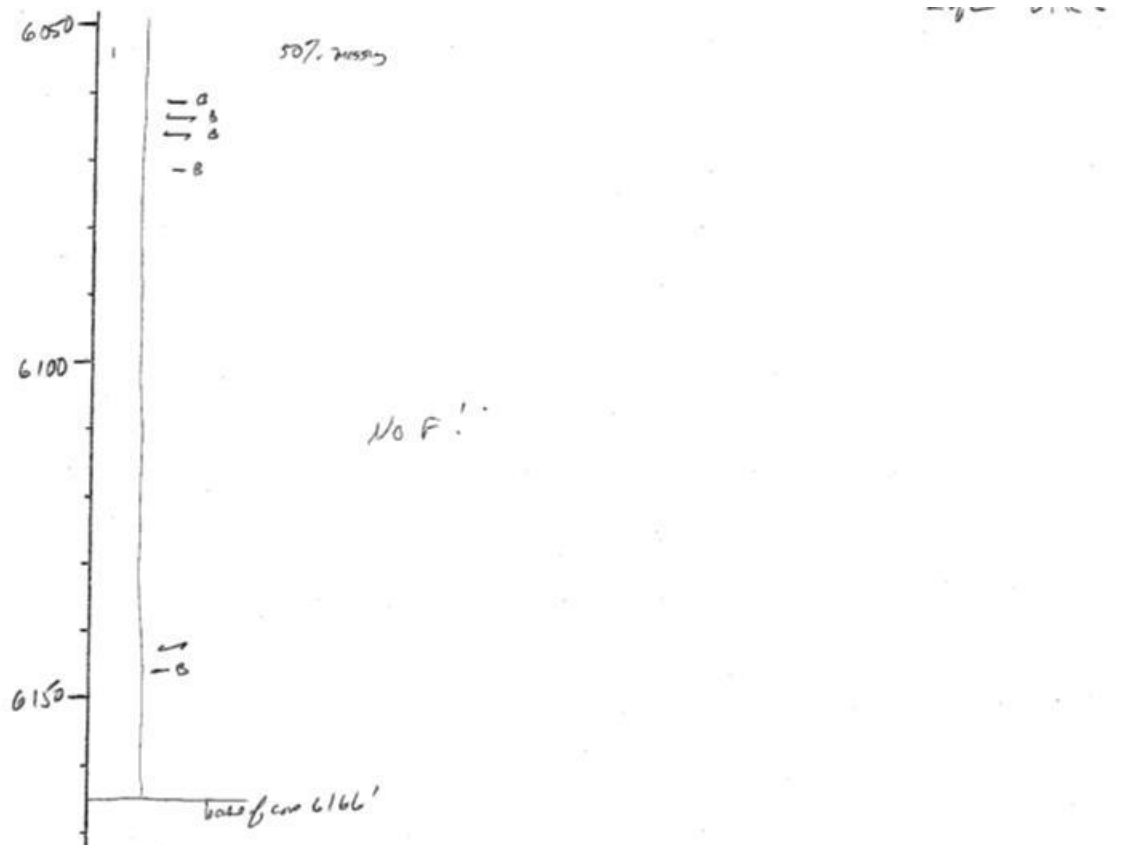
50% miss

— B
— A
— O

also no Faults. lack of F
& lack of Faults cause low
Q or due to low oil sat?
or low oil sat due to No F, F2

few D B's anywhere

Very low F in water log - why?
(few also in oil core but
still, some!)



Ohio UPR #3, section 35, T. 20 N., R. 88 W.

4 inch core, 5906-6100' MD

269 ft. of core cut, estimated 142 ft. of core preserved

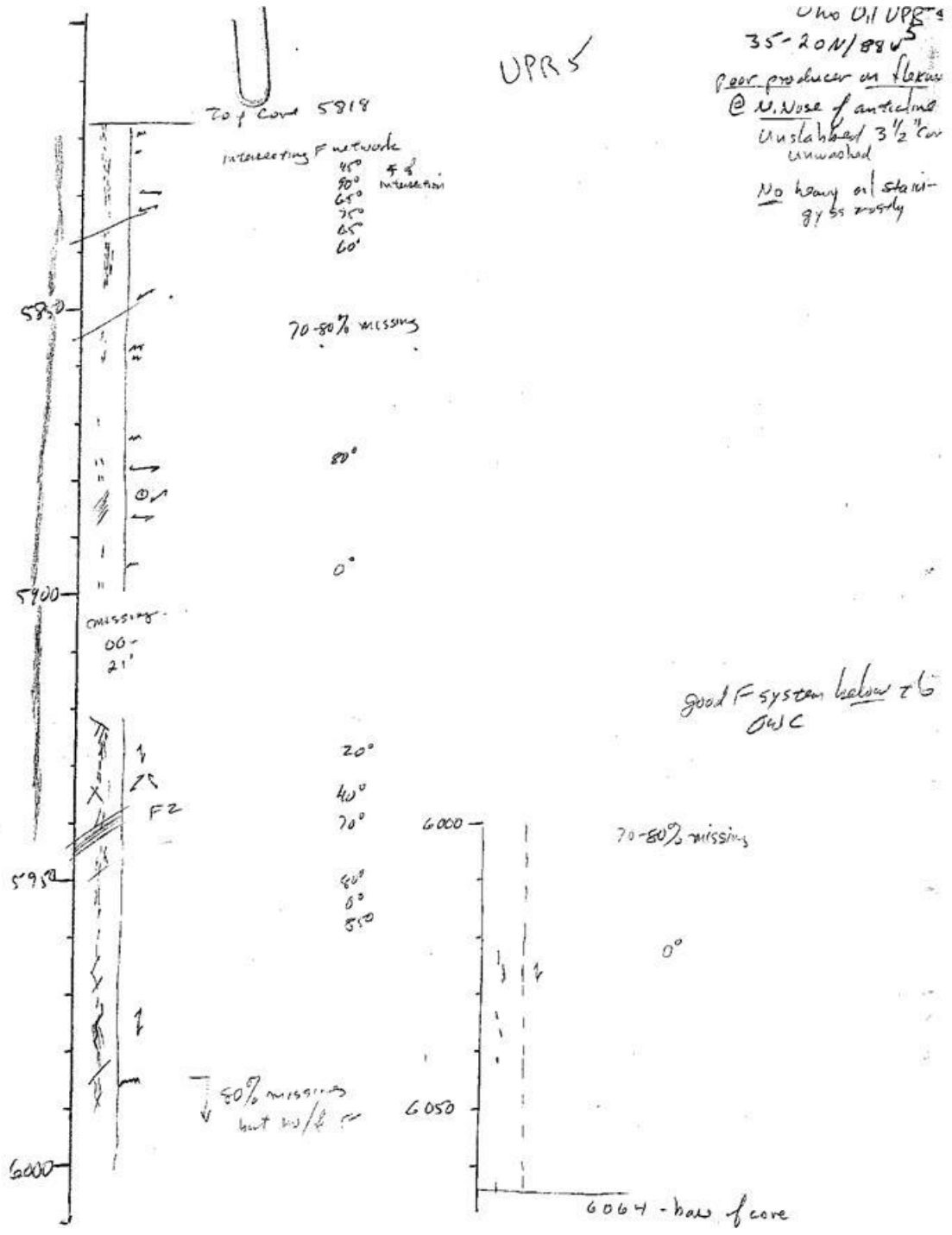
Well location: backlimb of the anticline, 2000 ft. NW of the crest

Modest cumulative production

Moderately fractured; no faults. Some stylolites and bitumen. Few fractures below the

OWC (compare to good fracturing below OWC in UPR #5)

Moderate oil stain over the top third of the core, unstained below 5970'



Ohio UPR #5, section 35, T. 20 N., R. 88 W.
 3 1/2 inch core, 5906-6064' MD
 146 ft. of core cut, estimated 80 ft. of core preserved
 Well location: along the broadened hinge, 1500 ft. north of the crest
 Poor production
 Numerous small intersecting fractures, some faulting. Good fracturing below the
 OWC. Moderate oil stain in the top half of core, unstained below 5950'

MAHONEY DOME

REPORT ON FRACTURES IN CORE FROM THE MAHONEY DOME #12 AND #20 WELLS

John Lorenz, July 3, 2008

SUMMARY

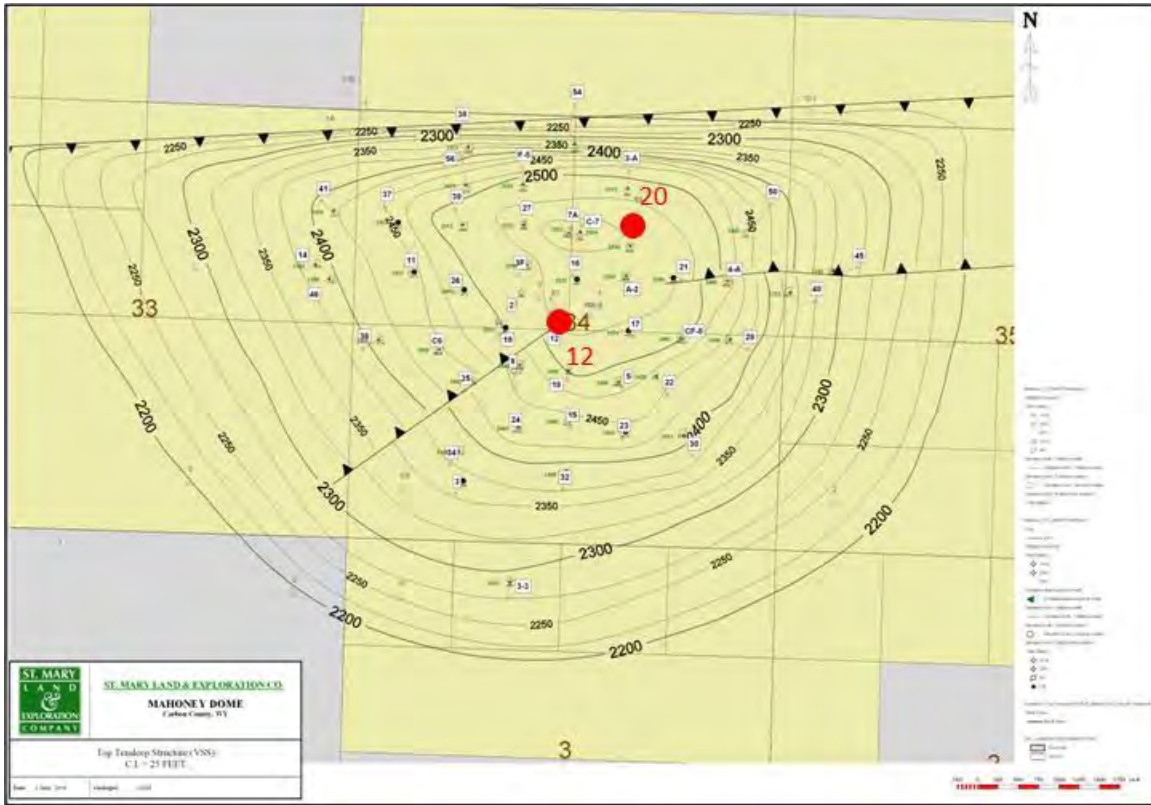
Vertical, anhydrite-mineralized extension fractures are common in sandstones of the Mahoney Dome #12 and #20 cores. Frequency of fractures is such that there is one foot of fracture height per every seven-eight feet of sandstone thickness in the core even though only the slabs are available for study: fracture development derived from whole core would have been more intense. Significant porosity remains in the fractures despite variable degrees of mineralization and along individual fractures. An effective fracture width of 0.02 mm and an effective fracture spacing on the order of five-ten feet, although not valid in terms of strain or the mechanics of fracturing, would be reasonable parameters for use in reservoir models. Fractures may form an interconnected permeability network in the reservoir, as several examples of intersecting fractures can be documented in the Mahoney Dome # 12 core from the backlimb of the anticline. However, fracture permeability may be dominated by one fracture set, the orientation of which is unknown. Vertical fracture permeability is probably unlimited in most of the reservoir strata.

INTRODUCTION

Two of the three Mahoney Dome cores were examined and logged at the BEG core library in Houston on June 24-25, 2008. Space was unavailable to lay out the third core, which will have to be examined at a later date and which will be the subject of a later report.

Only about half of the fracture data that was present in the cores originally was still available for this study, as sampling and slabbing have left the core pieces unblockable, thus the relative orientations of fractures in different parts of the core cannot be determined. Moreover, only the slabs are available so about three-quarters of the volume of the core is missing, with an

equivalent reduction in the probability of finding and studying fractures. Nevertheless, fracture characteristics and a qualitative estimate of fracture intensity and distribution can be determined.



Structure-contour map of Mahoney Dome, with locations of the two cores reported here.

Induced fractures such as petal and centerline fractures record the orientation of the maximum horizontal compressive stress in a reservoir, but few are present in these cores. The fragmented nature of the cores means that the few that were found cannot be related to the strikes of the natural fractures.

These two wells are located near the crest of the relatively small, structurally simple Mahoney Dome structure. The wells were drilled in the late 1970's with oil-based drilling fluid, and the core was not oriented. The core is now part of the University of Texas collection.

FRACTURE CHARACTERISTICS, MAHONEY DOME # 12

This well is located on the backlimb of the Mahoney Dome anticline, about a quarter of a mile south of the crest and near the termination of a secondary fault. A total of 445 ft. of core was cut, of which about 420 ft. is sandstone (primarily from the crossbedded dune facies), the rest consisting of reddish siltstones and shales from strata overlying the Tensleep Sandstone at the top of the core, and some dolomite interbeds. Much of the core is stained with oil, some of it from the reservoir, some introduced by the mud-based drilling fluid. The staining from the reservoir oil stain is darker, commonly brown-black, whereas oil stain from the drilling mud a lighter brown. This is the longest of the three available Mahoney Dome cores.

Most of the fractures in the core are small, hairline fractures and are less than spectacular, but numerous fractures are present even though only the slabs were studied.

Fracture Types

Some 73 fractures were recorded from this core, most being vertical to sub-vertical extension fractures. The actual number of fractures is uncertain since some of the fractures counted separately here may have originally been connected as a single plane between core pieces. The resulting fracture data set is skewed, both in terms of fracture numbers and in terms of fracture heights, discussed below.

Five of the 73 fractures are inclined, dipping between 65° and 80°, but they are otherwise similar to the vertical fractures and are inferred to be local variations on the vertical fractures rather than to comprise a separate fracture set.

A few of the fractures have poorly developed plume structures, but most of the fracture faces are un-ornamented except for anhydrite mineralization. Some of the fractures show a few millimeters of offset of bedding planes and asperities that indicate both normal dip-slip and strike-slip offset. However, none of the fracture faces show slickenlines or slickensides, so most of these fractures are probably trans-tensionally reactivated extension fractures, an interpretation supported locally by fish-scale patterns in the anhydrite mineralization that indicate offset during mineral precipitation. Only one fracture plane shows small-scale steps suggestive of an origin in incipient shear.

Distributions

All of the 73 logged fractures occur in the sandstone facies. Most occur in the cross-bedded dune facies but that merely reflects the predominance of that lithology in the core. Most fractures terminate top and bottom blindly in the core for no apparent reason, although where lithology contrasts occur they commonly create mechanical discontinuities that arrested fracture propagation.

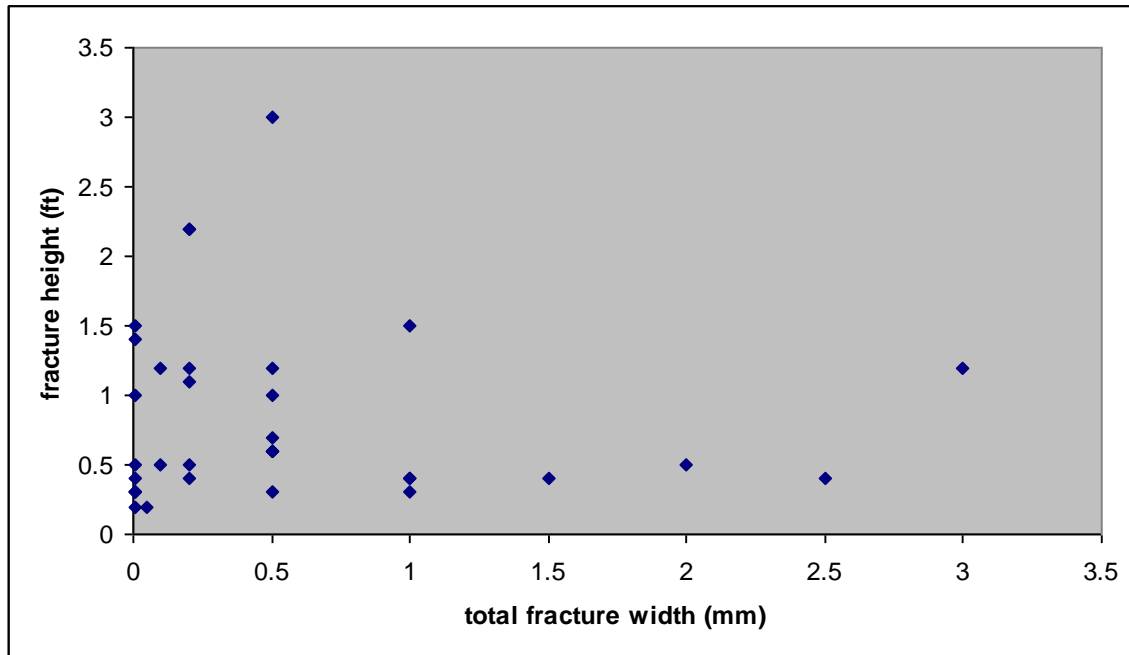
The 73 logged fractures have a range of apparent heights from 0.2 ft. to 2.9 ft., and an average height of 0.72 ft. This is a minimum average height given the truncated nature of the data set as discussed above. The cumulative height of all logged fractures is 52.7 ft.: given the 420 ft. of sandstone core, this is about 8 ft. of core per foot of fracture. Experience suggests that a ratio of about 10:1 is common in fractured reservoirs, so this core has a slightly higher, more fractured ratio than many other reservoirs considered to be fractured. If whole core had been available for study, the degree of fracturing would have been significantly higher, perhaps as much as 50%. The data qualitatively suggest that fractures are common in this reservoir.

Vertical, fracture-related permeability is probably impeded at gross lithology changes (sandstone-siltstone, clay partings), and is certainly arrested at the interbedded dolomites, but few lithology changes mean that the fractures and fracture-controlled permeability are well connected vertically within the sandy reservoir facies.

Mineralization and Apertures

Fracture permeability depends in large part on the size and character of the aperture of the fracture: how wide is it, how much is occluded by mineralization, and how tortuous a pathway is left for fluid flow. Although even very narrow slot fractures will afford significant permeability, few natural fractures are bounded by parallel-plate, slot-type walls. Rather, mineralization, typically anhydrite in the Mahoney Dome cores, is present in all of the Tensleep natural fractures, partially to completely occluding fractures. Fracture width and degree of occlusion varies along the length and height of most fractures, and commonly all that's left for flow enhancement is an irregular, tortuous pathway around and over the anhydrite patches and crystals. The total measured width of a fracture, wall to wall including mineralization and remnant aperture, does not translate well into permeability estimates, and irregular remnant apertures make estimates of aperture widths meaningless: the fractures rarely have parallel walls.

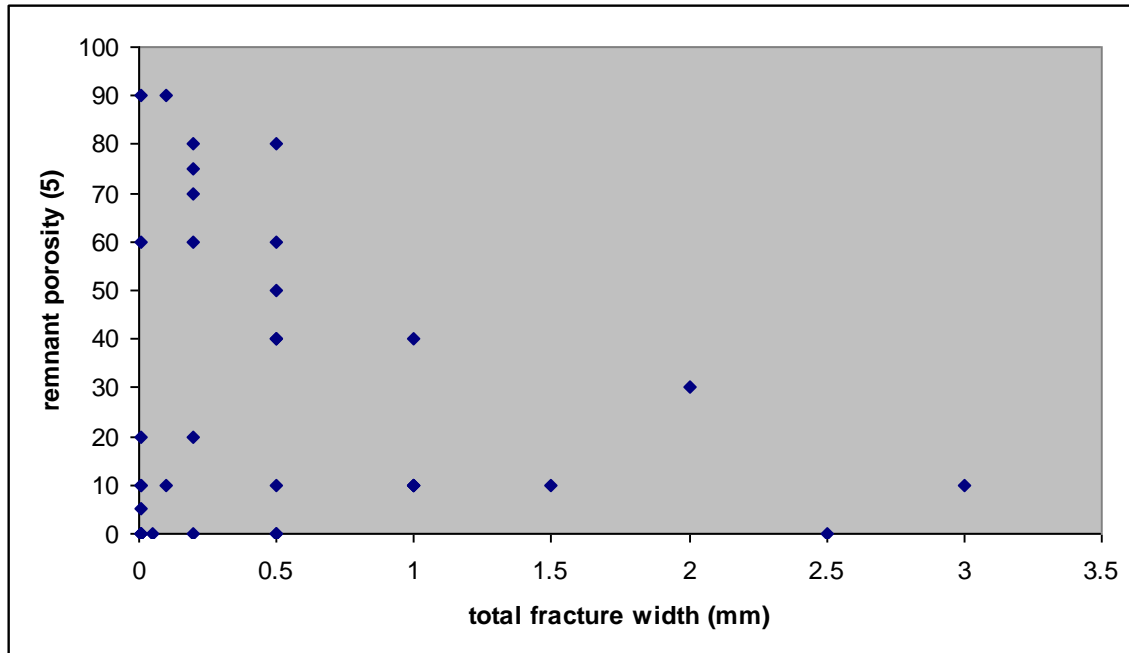
Rather, a visual estimate of the remnant void space, expressed in percent of the total aperture, was made instead of an estimate of remnant fracture aperture.



Fracture height does not control fracture width. n = 34

Most fracture-aperture populations are not related to fracture length or height since mechanically, large extension fractures do not need to have to have larger apertures. Rather, the aperture of an extension fracture commonly varies along its length and height, and in fact the taller fractures in the Mahoney Dome #12 core do not have consistently larger total widths (see chart above).

Fracture widths in the Mahoney Dome core contain anhydrite, the degree of filling ranging from a light coating of hard-to-see crystals to complete occlusion. Smaller fractures tend to be more completely occluded by mineralization because capillary forces keep mineralizing pore waters in the fracture longer, but the Tensleep fractures with larger total widths do not have consistently higher percentage of remnant aperture. In fact the data seem to suggest the reverse relationship, but it is more likely that the data points that suggest this apparent fall-off on the graph shown below are too few to define a reliable trend.



Total fracture width is not related to the remnant porosity (estimated % of open void space within the mineralization). n = 34

Average total fracture aperture is 0.55 mm, and the average estimated remnant porosity in those fractures is 30%. 30% of 0.55 mm is 0.17 mm, but that 30% represents tortuous permeability pathways rather than parallel-plate slots. A plausible estimate of the effective fracture permeability pathways would be to use a tenth of that, or about 0.02 mm, as an average of the open fracture aperture in modeling a reservoir, regardless of fracture height.

About a quarter of the fractures contain a black, solid bitumen. The bitumen typically underlies later anhydrite layer or crystals and is thus the first phase of fracture mineralization. It is unclear whether the bitumen was injected into the rock to form fractures or whether it migrated into existing fractures. The distribution of bitumen in the sandstone adjacent to such fractures suggests that imbibed into the porosity, supporting the latter interpretation.

Fracture Orientations and Spacing

This core is not oriented, so no absolute fracture orientations could be obtained from it. However, relative fracture orientations where they can be determined provide interesting insights into the probable fracture-related reservoir plumbing at Mahoney Dome. At least 12 examples of closely spaced, parallel fractures are present in the core, indicating that at least one strong set of

systematic, parallel fractures is present in the reservoir. However, five examples of intersecting natural fracture planes in one piece of core are also present. The intersection angles are 40°, 42°, 55°, 70°, and 80°, indicating that more than one and probably three fracture sets are present. The relative importance of the different sets, their actual orientations, and effects on the reservoir cannot be determined, but the data do suggest that the reservoir's fracture plumbing may be reasonably well connected.

The 12 examples of closely spaced parallel fractures, in combination with the relatively high degree of fracturing calculated above from feet of core per fracture, all suggest that fracturing is well developed in the Mahoney Dome Tensleep reservoirs. Lateral fracture spacing cannot be calculated from the available, one-dimensional, vertical core data, but a qualitative estimate of spacing can be inferred. Spacings of fractures in this kind of regional fracture population are commonly distributed in log-normal fashion, i.e., numerous closely spaced fractures and fewer more widely spaced fractures.

The closely spaced, parallel fractures captured by several pieces of four-inch diameter core represent the low end of the spacing spectrum. More widely spaced fractures with unfractured rock between them are the other end of the spectrum. Experience with other reservoirs where horizontal and vertical core data have been taken from the same unit suggests that effective fractures in the Mahoney Dome Tensleep reservoirs are spaced on the order of 5-10 ft.

FRACTURE CHARACTERISTICS, MAHONEY DOME #20

This well is located a few hundred feet east of the crest of the anticline, along the strike of the anticlinal hinge. Only 187 feet of core were taken from the well, all of it in the sandy Tensleep dune and interdune facies. Original reservoir oil staining is scattered, and is complicated by the use of oil-based drilling mud. Fractures are similar to those in the Mahoney Dome #12 core. A somewhat simpler fracture system is suggested by the data, but may in part be merely the effect of a significantly smaller data set.

Two features that resemble the sand-filled hydraulic fractures that have been found in the Tensleep Sandstone in outcrops at Flat Top Mountain are present in this well. They are not

common so they are not discussed further here, but several photos are included in the Appendix, and at least one of the two has an effect on the distribution of oil.

Fracture Types

All of the 55 fractures recorded from this core are anhydrite-mineralized, vertical to near-vertical extension fractures. As with the Mahoney Dome #12 core, the number of fractures and their heights are artificially skewed by slabbing and sampling of the core, i.e., the data suggests there are more fractures and that they are shorter fractures than the actual subsurface population. The artificially enhanced population numbers may partially offset the fact that a smaller population of fractures is to be found in the slabs alone than would have been found in the whole core, but this is not quantifiable. Some of the fractures in this core occur as small families or swarms of short, parallel associated fractures.

Distributions

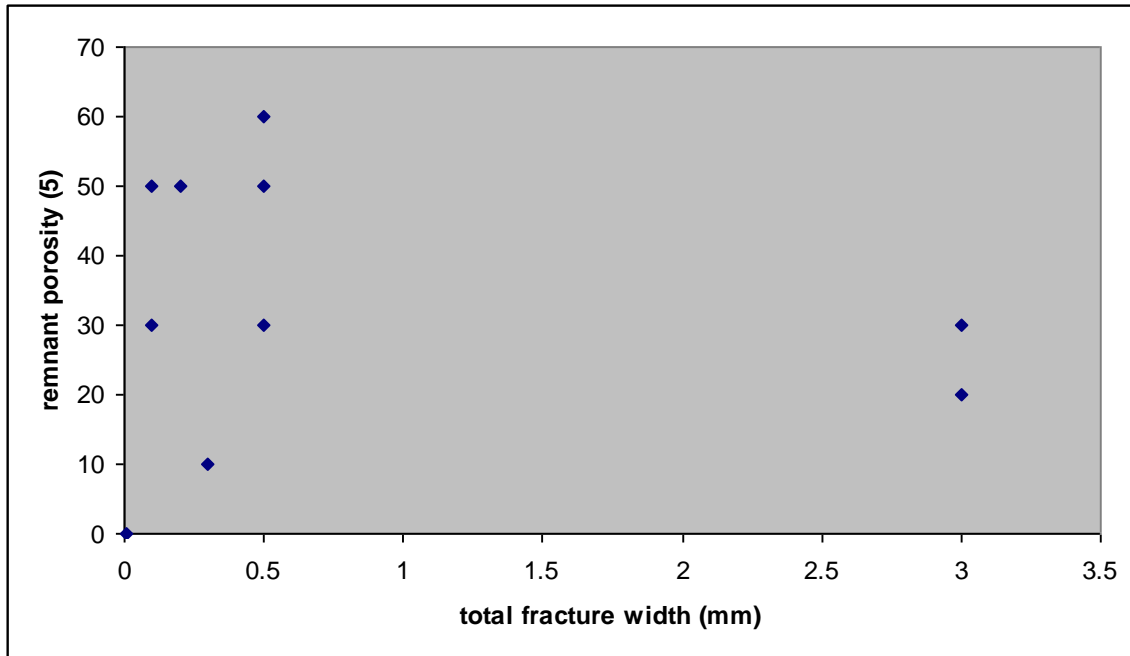
As with the Mahoney Dome #12 core, all fractures occur in the sandstone facies, primarily within the cross-bedded dune facies. Most fractures terminate top and bottom blindly in the core within thick beds of crossbedded sandstone, but local lithology contrasts also arrest fractures.

The 55 logged fractures have a range of apparent/minimum height from 0.1 ft. to 4.5 ft., and an average of 0.46 ft., less probably not significantly so, than the 0.72 ft. average fracture height found in the Mahoney Dome #12 core. The total core footage divided by the cumulative 25.5 ft. of height of all logged fractures gives slightly more than 7 ft. of core per foot of fracture, comparable to the 8 ft. per fracture in the Mahoney Dome #12 core. This degree of fracturing would be higher if whole core had been available for study, but even this partial data set suggests that fractures are common and therefore that fractures and fracture-controlled permeability are well connected vertically.

Mineralization and Apertures

Aperture and mineralization data for the smaller population of fractures in the Mahoney Dome #20 is similar to that of the Mahoney Dome #12 core. Anhydrite is the mineralization agent, and it partially to completely occludes the fractures. The average total width of the ten

measurable fractures in this core is 0.82 mm, somewhat wider than the other core (0.55 mm), but the average percent remnant porosity is nearly identical: 33% (vs. 30%). An average 0.02 mm of open/effective fracture aperture would still be a valid estimate for use in reservoir modeling.



Remnant porosity (%) plotted against total fracture width (includes both mineralization and void space in the fracture) shows an essentially random distribution. n = 10

Fracture Orientations and Spacing

At least eight examples of parallel natural fractures in one piece of core exist in this well, and no examples were noted of intersecting fractures. The fracture system in this well may be dominated by a single set of parallel fractures, although the data set is fragmented and small and does not exclude the possibility of intersecting fracture sets.

The fracture data from this well resembles that from the Mahoney Dome #12 core, thus a similar estimate of the spacing of the larger, effective fractures (5-10 ft.) can be made.

CONCLUSIONS

Vertical, anhydrite-mineralized extension fractures are common in the Mahoney Dome #12 and #20 cores. The broken and slabbed core is less than optimum for fracture study, yet a high ratio of one foot of fracture height is present per every seven to eight feet of sandstone thickness in the core is present in the available core. Significant porosity remains in the fractures despite variable degrees of mineralization, and vertical fracture permeability is probably unlimited. Several examples of intersecting fractures are present in the Mahoney Dome # 12 core on the backlimb of the anticline, and they may form an interconnected permeability network although one of the fracture sets may be dominant.

Most of the fractures are extension fractures, although a few shear structures are present and some of the extension features may have been reactivated in shear.

An effective fracture width of 0.02 mm and spacing on the order of five-ten feet are suggested as reasonable parameters for reservoir modeling.

APPENDIX: Representative fracture photos



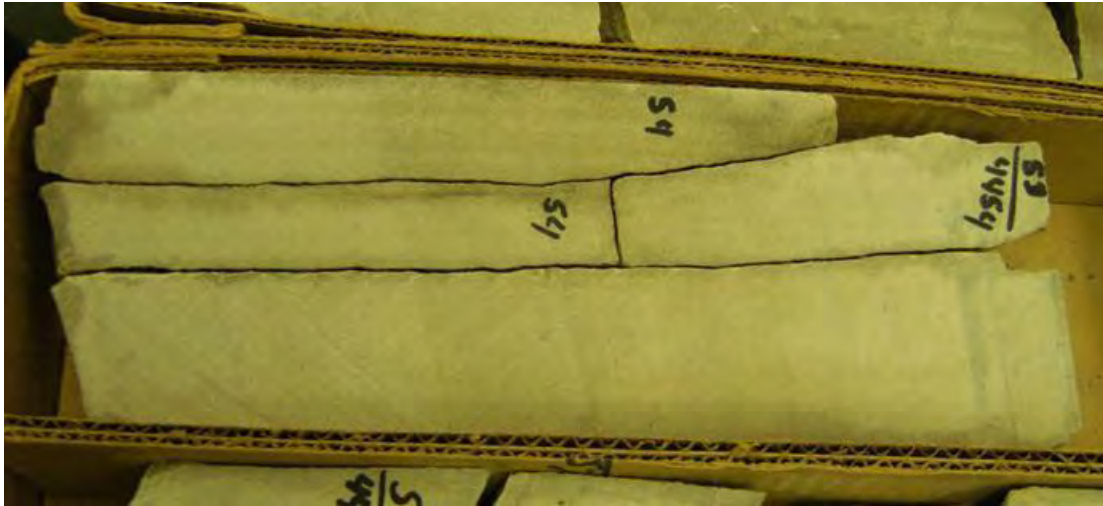
Anhydrite mineralization coating the opposing faces of a fracture. The apparent patchy mineralization distribution is due to the thin anhydrite layer adhering irregularly to alternate faces.



Fish-scale texture in anhydrite suggests small offset during mineral precipitation.



Patchy mineralization (white) and vuggy porosity along an inclined fracture with several millimeters of dip-slip offset (up-hole is to the left).



Parallel, closely spaced fractures.



Black bitumen lines a fracture face.



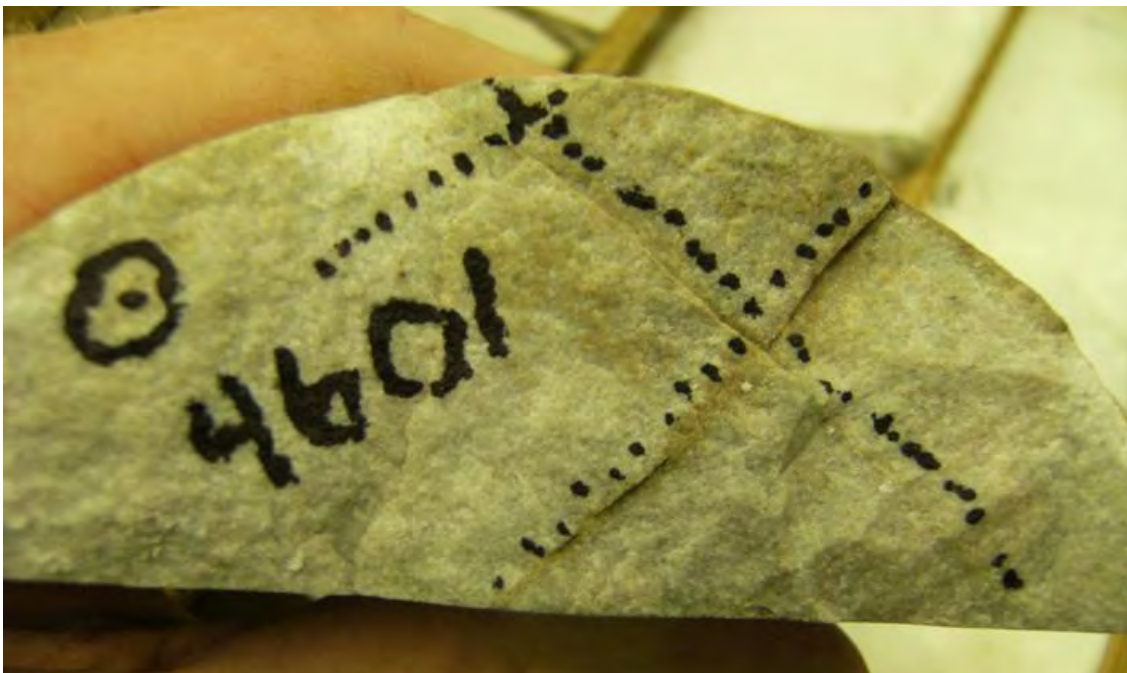
Imbibition pattern of bitumen along a hairline fracture.



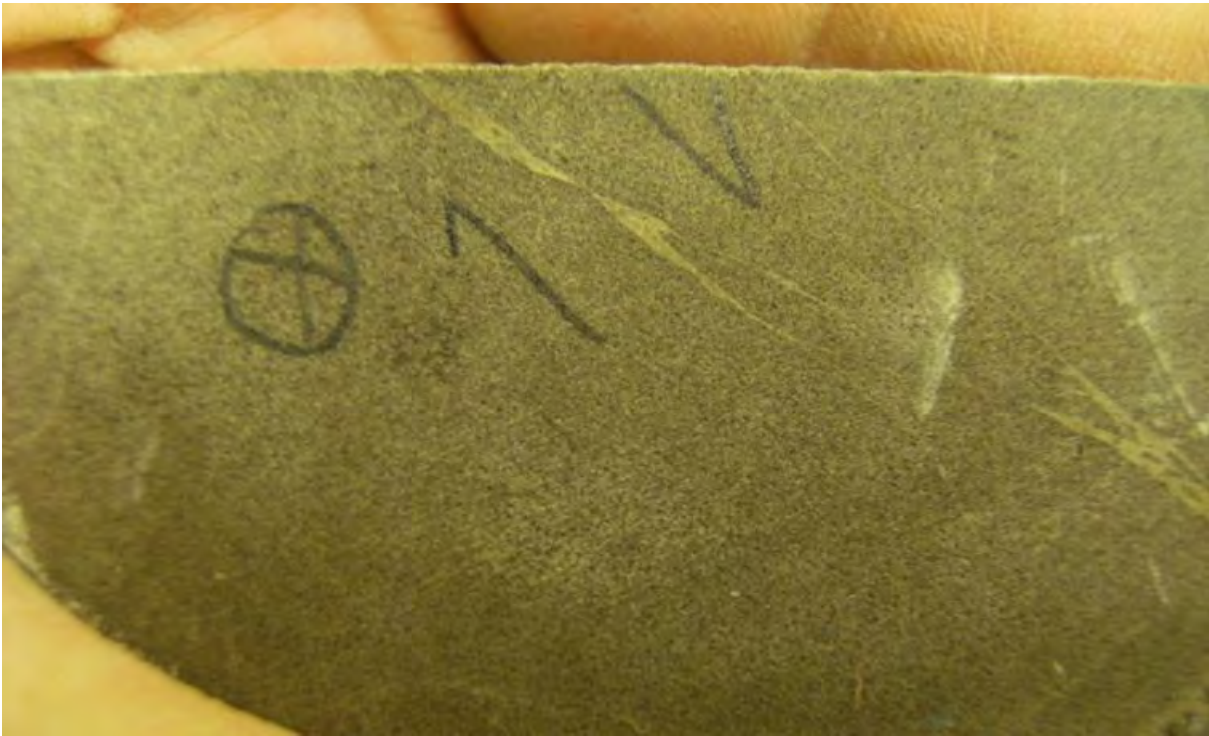
Inconsistent slabbing planes (the planar surfaces marked with footages) from one piece of core to the next mean that the fracture present in the upper core piece is not present in the next piece below even though the two core pieces lock together as shown. Even though the fracture obviously extended further vertically, it cannot be determined how far with the available core.



Semi-crystalline anhydrite indicates significant remnant porosity despite mineralization in this fracture.



Two sets of fractures (highlighted by dotted lines parallel to the fracture planes) intersecting at an 80-degree angle. Circled dot indicates view is down-hole.



A few millimeters of left-lateral offset (circled X indicates view is up-hole) on an anhydrite-filled fracture.



Vertical, anhydrite-mineralized, hairline fractures in sandstone: 0.5 mm pencil lead for scale.



Irregular tan oil stain, from the mud-based drilling fluid, along a fracture indicates permeability along the fracture is enhanced over matrix perm.



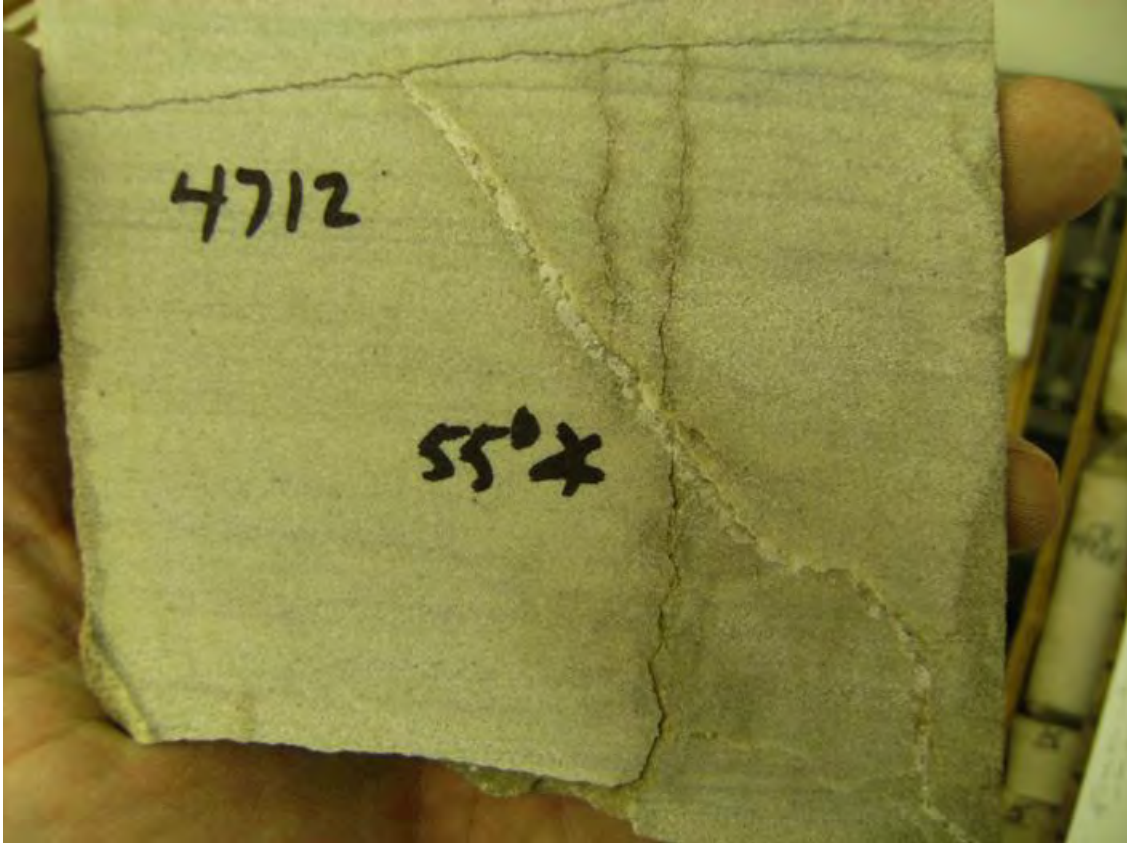
End view of the same piece of core showing staining at the core surface and into the core along the two parallel natural fractures.



Hydraulic fracture in sandstone, terminates at an erosional surface marked by color change and small rip up clasts.



Oil staining is different on one side of a sand-filled hydraulic fracture than on the other, suggesting that the structure is relatively impermeable.



Intersecting fractures, both terminating at a small stylolite. The white, anhydrite-mineralized fracture is both narrower and closer to vertical than apparent in this photo, being foreshortened by the shallow angle between slab surface and fracture plane. The two oil-stained, higher-permeability fractures are younger, as indicated by termination of one and by offsetting where the other crosses the white fracture.

**NATURAL FRACTURE CHARACTERISTICS IN CORE FROM THE MAHONEY
DOME #24 WELL, WYOMING, AND COMPARISONS WITH FRACTURES FROM
THE MD #12 AND #20 CORES**

John Lorenz, August 26, 2008

SUMMARY

The average natural fracture in the Mahoney Dome #24 core is a vertical extension fracture, 1.4 ft. high, 0.37 mm wide, and with 54% remnant porosity despite common mineralization. Mineralization phases include, in order of abundance, calcite, anhydrite, dolomite, and bitumen, but a third of the natural fractures are unmineralized. Data from 360 ft. of sandstone core show that fractures strike predominantly parallel to the maximum horizontal in situ compressive stress (the trend of which cannot be determined in this un-oriented core), but at least one secondary set of fractures is present. Fractures range up to 10 ft. in height along the length of the core, the bedding contacts that create mechanical discontinuities and terminate fracture propagation being relatively rare. Fractures are numerous, some 23% of the sandy, fracture-prone lithologies being fractured, but few shear fractures are present and no faults were encountered. Fractures are probably relatively closely spaced, less than 5 ft. by analogy to the similar frequency of fractures in analog cores.

INTRODUCTION

Core from the Mahoney Dome #24 well (located in section 34, T 26 N., R. 88 W., Carbon County, Wyoming), was examined on August 21, 2008, at the Bureau of Economic Geology core library in Houston, Texas. The core was taken from the Tensleep Sandstone, between the depths of 4360 and 4733 ft., an interval of 373 ft., although only approximately 360 ft. of core was available for study. About 19 ft. of the core consist of dolomite or limestone, leaving about 340 ft. of fracture-prone, sandy reservoir facies.

The 4-inch diameter core had been slabbed and only the slabs were examined (the butts are apparently in Norman, Oklahoma). The core is in good shape, with only minor missing sampled intervals, although it was slabbed along random planes and therefore could not be locked back together in order to assess fracture continuity and relative orientations. The core was not scribed or oriented. This is the last of the three Mahoney Dome cores to be logged.

Nearly all of the fractures in this core are vertical extension fractures, though one shear fracture and two probable hydraulic fractures were noted. Few shear fractures and no major fault zones were cut by the core, although many of the fractures appear to have a millimeter or less of vertical and/or lateral offset.

The Mahoney Dome #24 well is located on the backlimb of the anticline, away from mapped faults and in a relatively simple structural setting.

FRACTURE DATA

Fracture Types

A total of 58 natural fractures is present in the MD #24 core. The fractures contain several types of mineralization, and many display significant remnant porosity despite mineralization. Most of the fractures are vertical extension fractures, though one low-angle, inclined shear fracture is present near the top of the core and two poorly-defined, syn-sedimentary hydraulic fractures were logged.

Most fractures occur in sandstones. Hairline fractures less than 0.1 mm wide are locally abundant in the dolomite facies but they are completely occluded by mineralization and are not described here. No fractures were observed in the three feet of limestone core.

Extension Fracture Distributions

All of the 55 vertical extension fractures recorded occur in the sandy facies of the Tensleep formation, primarily the cross-bedded dune facies, if only because this facies comprises most of the reservoir lithology in the core. Sandstones with several degrees of cementation are present, and no fractures occur in the 20 ft of poorly cemented, even friable, sandstone at the top of the second core (4526-4546 ft). The dense, well-cemented white sandstones at the opposite end of the cementation scale, however, are well fractured. As with the MD #12 and #20 cores, this core contains few coring-induced petal and petal-centerline fractures.

Twenty-three percent of the sandstone contains fractures, or about 4.3 ft. of core per every foot of fracture height. Fractures vary from 0.1-10.0 ft. tall and have an apparent average height of 1.4 ft., forming a cumulative 79.1 ft. of fracture height in the core. The true average fracture height is taller since sampling and slabbing have destroyed the ability to trace many of the fractures from one core piece into the next, thus some fractures have been counted as two short fractures even though they probably originally extended across the pieces as one longer

fracture. Nevertheless, six composite fractures could plausibly be traced over significant lengths of core despite missing pieces. These families consist of overlapping, closely spaced fracture segments and have aggregate heights of 1.7, 3.0, 3.3, 3.8, 4.5, and 10.0 ft.

Similar to the Mahoney Dome #12 and #20 cores, few of the extension fractures in the Mahoney Dome #24 core are strata-bound. Only a quarter (9 of 34) of the fracture terminations that are not core exits or that are unknown in a missing core piece occur at an obvious lithology contrast. The rest terminate blindly in a homogeneous lithology for no apparent reason, possibly due to en echelon offsets that stepped beyond the core volume.



The fracture on left terminates at a bedding boundary, whereas the fracture on the right extends across bedding. Pencil point for scale.

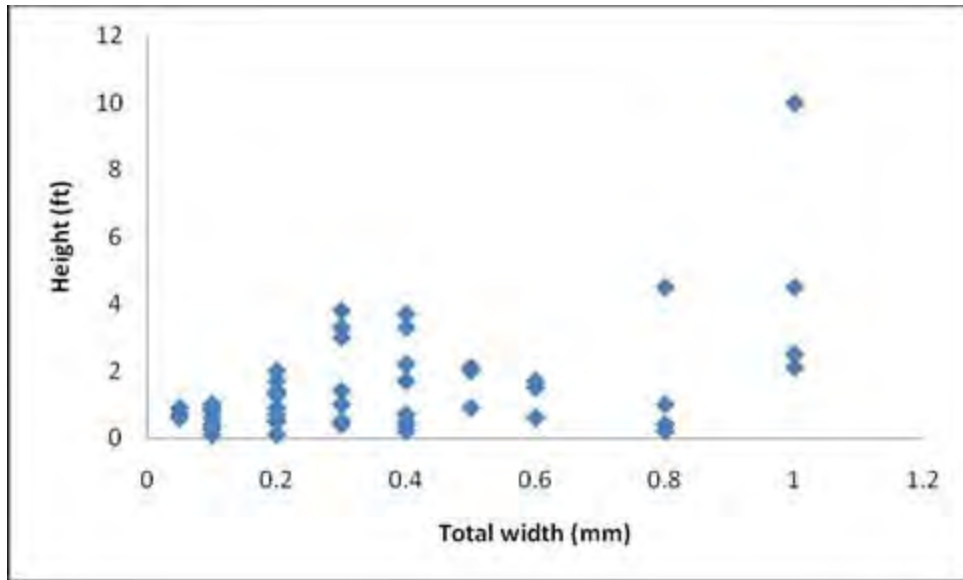
A quarter of the vertical fractures have a distinct pinch and swell character in both vertical and horizontal cross section. Minor bedding offsets, and small calcite-filled voids located consistently on one side of asperities, show that this pinch and swell character is related to offsets of half a millimeter to a millimeter along the fractures. However, bedding-plane

shears that might be expected to accompany such minor adjustments were not documented from this core.



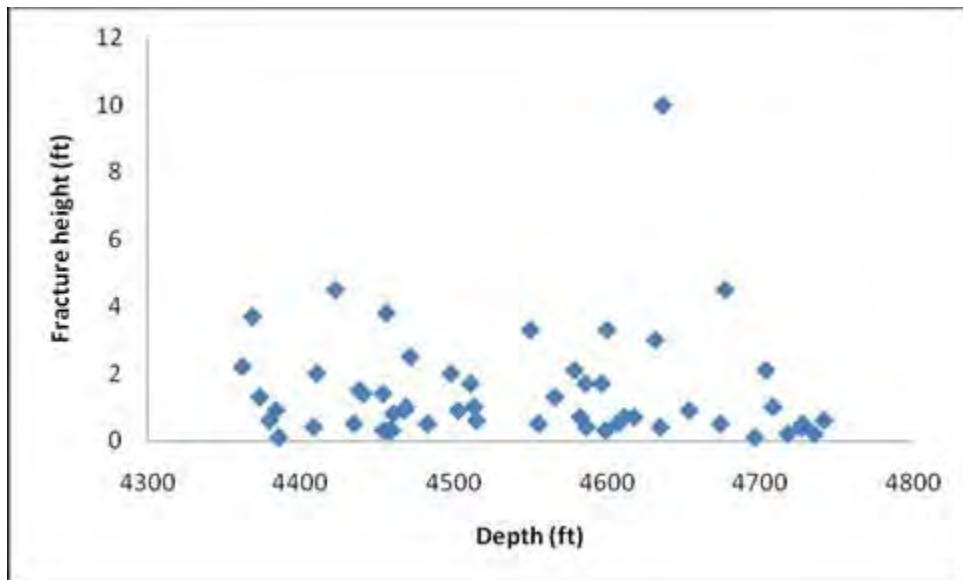
Pinch and swell along a fracture, suggesting a minor component of shear. Much of the offset is probably into and out of the plane of the photograph (i.e., horizontal).

In contrast to the ME #12 and MD #20 cores, where the relationship is vague at best, fractures in this core show an irregular trend of taller fractures being wider, although even some of the tall fractures have very narrow widths.



Many of the tall fractures are wider, but other tall fractures are as narrow as short fractures.

Fracture height is consistent, albeit within a broad range, over the length of the core. No change in fracture size is apparent with depth.



Fracture height, ranging from 0.1 to 10.0 ft and averaging 1.4 ft, does not vary with depth. Fracture spacing

Lateral fracture spacing cannot be calculated from vertical fracture distributions, but it can be derived by analogy. An average of at least one foot of fracture height per ten feet of core length is typical of a fractured reservoir in other provinces such as the Permian basin, and this

ratio commonly translates into a lateral fracture spacing of 5-10 ft. where corroborated by horizontal data from core or image logs.

This ratio is 7-8 ft. in the Mahoney dome #12 and #20 cores, but it is much lower in the Mahoney Dome #24 core, only 4.3 ft. of core per foot of fracture height. This suggests a much closer average fracture spacing, possibly on the order of 3-5 ft., in the MD #24 reservoir.

An average implies a spacing distribution, and in fact several pieces of the MD #24 core contain two or more parallel fractures, capturing the lower end of the spectrum. Eight measured spacings of parallel fractures range from 0.5 cm to 5.0 cm, averaging 3.2 cm, indicating the closest fracture spacings in the range.

Fracture mineralization and apertures

Fractures are mineralized with a wider variety of minerals in the Mahoney Dome #24 core than in the two cores reported previously. Most fractures (22, or 40%) contain good calcite, documented by effervescence with hydrochloric acid. The calcite was unexpected, since the fractures in the other cores are mineralized almost exclusively with anhydrite, and since the host sandstones are not cemented with calcite. The percentage of calcite-mineralized fractures increases downhole.



Partially mineralized fracture: pencil point for scale.

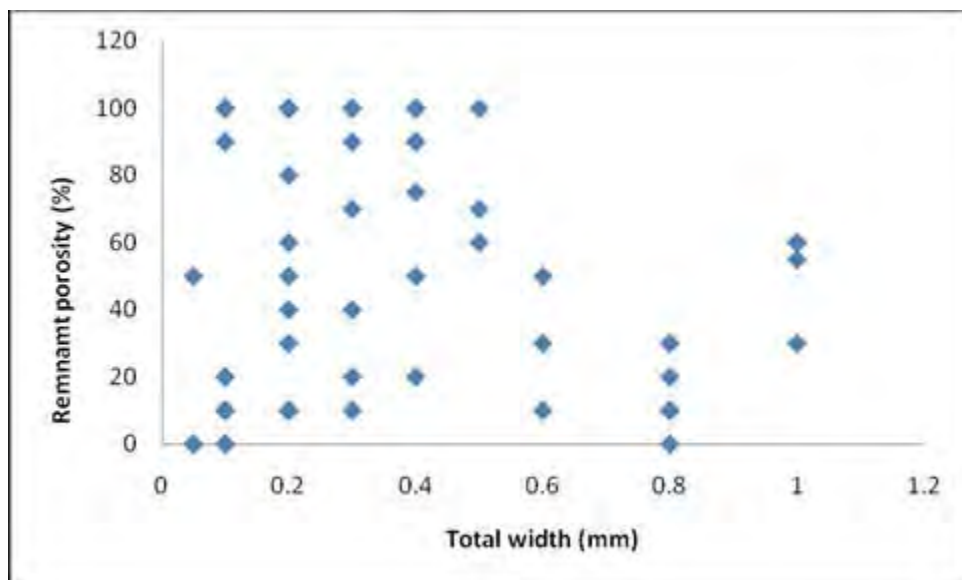
A smaller but still significant percentage of the fractures (33%) are unmineralized, at least within the confines of the core, and the distinctions between them and coring-induced fractures is not always definitive. Relatively few fractures (13, or 22%) contain anhydrite mineralization, and at least one fracture contains a calcareous, sandy gouge that is probably related to minor offset along the fracture plane, although obvious slickenlines are absent.

TABLE 1: Mineralization Phases in Fractures in Core from the Mahoney Dome #24 well

<u>Mineralization</u>	<u>Number</u>	<u>Percent</u>
Calcite	22	40
None	19	33
Anhydrite	13	22
Dolomite	2	3
Gouge	1	1
Bitumen	1	1
TOTAL	58	100

Many of the fractures retain a percentage of the fracture aperture despite mineralization. The original fracture apertures range from 0.05-1.0 mm (average 0.37 mm), and the remnant open void space ranges from 0-100% of that aperture, averaging 54%. The relationship between original aperture and remnant porosity is random below half a millimeter of aperture (total width), but above that the percentage of fracture fill diminishes irregularly with fracture total width.

This threshold of half a millimeter was also apparent in the fracture-width/remnant aperture data from the MD #12 and MD #20 cores.



The original aperture (total width) of a fracture is unrelated to the degree of mineral occlusion below half a millimeter, but some of the larger fractures are less mineralized.

Fracture orientations

The MD #24 core is not oriented and therefore absolute fracture strikes cannot be obtained from it. However, in addition to the core pieces where parallel fractures are present as described above, five pieces of core display intersecting fractures. The intersection angles range from 20-55 degrees, but the data population is not large enough to allow a distinction of fracture sets. It does allow the inference that more than one fracture set exists at depth.

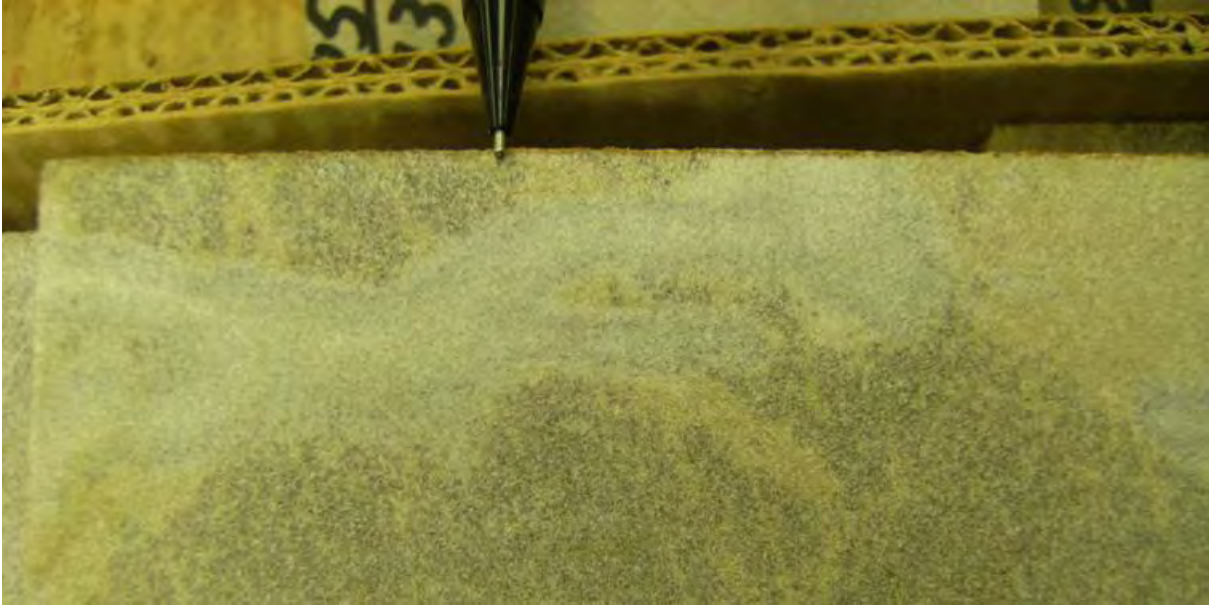
The strikes of six petal fractures can be related to strikes of associated natural fractures, with five parallel relationships and one 70-degree relationship. Making the plausible assumption that the petal fractures have a constant orientation along the core length, these angular relationships suggest a dominant fracture trend striking parallel to the maximum horizontal compressive stress and a subordinate trend striking nearly normal (70 degrees) to it, again indicating more than one fracture strike in the subsurface.



Intersecting fractures on the end of a piece of core. Note also the pinch and swell character.

Other

Two poorly defined hydraulic fractures are present in the core. These fractures are filled with sand, making them hard to distinguish from the sandy host rock. They occur as irregular and divergent bands cutting across bedding and having slight differences in grain size, sorting, and coloration from the host sandstone. They do not extend more than a foot along the length of the core, primarily because they are irregular and exit the core: the core captured neither the upper or lower terminations.



Probable hydraulic fracture, pencil point for scale. Distinction between the sand-filled fracture and the sandy host rock is difficult.

One inclined shear zone is present, cutting obliquely across and offsetting dune foresets at a low, 22-degree angle, with minor oil staining along the fracture planes. The lack of mineralization suggests that this may be an early feature. Similar features are present in outcrop at both Flat Top Mountain and at Sand Creek.

COMPARISONS WITH FRACTURES IN THE MAHONEY DOME #12 AND #20 CORES

The Mahoney Dome #24 fractures are somewhat narrower than those in the other two cores, but on average they are two to three times taller and have a higher percentage of remnant porosity. They are more intensely developed, with nearly twice as much fracture height per core length compared to the other two cores, and therefore their lateral spacing is inferred to be closer. The presence of calcite and dolomite in the fractures in addition to the more commonly found anhydrite, as well as the development of fractures without mineralization, is unique to the MD #24 core. These attributes were not expected in this relatively undeformed part of the reservoir.

TABLE 2: Comparison of Fracture Characteristics

	<u>MD #12</u>	MD #20	<u>MD #24</u>
no. fractures	73	55	58
ft. of ss core	420 ^c	187 ^c	340 ^c
cum frac height	52.7 ^c	25.6 ^c	79.1 ^c
frac height range	0.2-2.9 ^c	0.1-4.5 ^c	0.1-10.0 ^c
avg frac height	0.72 ^c	0.46 ^c	1.4 ^c
est. eff. frac spacing	5-10 ^c	5-10 ^c	3-5 ^c
ft. core/ft. frac	8	7	4
frac widths range	0.1-3.0 mm	0.1-3.0 mm	0.05-1.0 mm
frac widths average	0.55 mm	0.82 mm	0.37 mm
remnant porosity avg	0-90%	0-60%	0-100%
remnant porosity avg	30%	33%	54%
no. frac sets	3	1	2
mineralization*	A	A	C, A, D, B, none

*A anhydrite; C calcite; D dolomite; B bitumen

CONCLUSIONS

Core from the Mahoney Dome #24 well is highly fractured even though only the slabs of 4-inch diameter core were examined. The high degree of fracturing is surprising given the location of the well on the backlimb of the anticline, away from known faults, and in a relatively undeformed province. Most fractures are vertical-extension fractures, and average 1.4 ft. high. they have an average width of 0.37 mm and average remnant porosity of 54% despite partial occlusion by various minerals including calcite, anhydrite, dolomite, and bitumen. A third of the natural fractures are unmineralized. The fractures strike predominantly parallel to the maximum horizontal in situ compressive stress, but at least one secondary set of fractures is present. Twenty-three percent of the 340 ft. of sandy, fracture-prone lithologies are fractured, fractures ranging up to 10 ft. in height, and effective fractures are probably spaced at less than 5 ft. Few shear fractures and no faults are present. Although many of the vertical fractures have sub-millimeter offsets, they did not originate in shear.

TEAPOT DOME

Fracture Interpretations of the Teapot Dome Tensleep Formation Core taken from Well # 45-4-X-21

John Lorenz, August 16, 2007

SUMMARY

Tensleep core from the 45-4-X-21 well contains numerous vertical extension fractures in the dolomite intervals, and deformation bands in the best reservoir sandstones. It also contains enough petal fractures to reconstruct probable fracture orientations relative to the trend of the maximum horizontal in situ compressive stress. Intersecting sets of extension fractures in the dolomite facies, probably striking NE-SW and NW-SE, although numerous, may not provide conductivity between reservoirs because they are vertically limited by numerous well developed horizontal stylolites. Deformation bands, probably striking NE-SW, may have a deleterious effect on system permeability, creating baffles and compartmentalizing some zones of the reservoirs.

INTRODUCTION

Approximately 90 feet of unoriented core, taken from the RMOTC 45-4-X-21 well between the depths of 5429-5524 feet, were examined at the Omni Labs workshop in Casper, Wyoming, on August 13-14, 2007. The 3½-inch diameter core contains no spinoffs, rubble zones, or missing intervals. At the time of examination the core was unslabbed and unsampled, and in excellent condition. There is only one break in the core where the pieces of core could not be locked back together, at 5495.5 ft. where core-catcher scars indicate that a connection was made in the drill pipe while coring, and where coincidentally the presence of a system of closely spaced natural fractures in a dolomite bed facilitated breakage of the core during the temporary raising of the drill-string off bottom. The core is erratically oil-stained along bedding planes in some of the sandy intervals, but the core surface was clean enough to allow reliable fracture detection and identification.

Fifty-seven feet of the core consist of sandstone and dolomites of the upper part of the Tensleep Formation. Thirty-three feet of core taken from the overlying Opeche Shale consist

dominantly of red mudstone, siltstone, and shale, and contains numerous local, irregular, slickenlined compaction features and several irregular filled fractures. The Opeche interval is not significant to the Tensleep permeability system: it was not examined in detail and is not included in the following discussion.

FRACTURE TYPES AND CHARACTERISTICS

Three types of fractures are present in the Tensleep interval of this core: vertical extension fractures (numerous in the dolomites but several also present in the finer grained sandstones), deformation bands (present only in the sandstones), and coring induced petal fractures.

Extension Fractures in Sandstone

Only two, parallel, near-vertical extension fractures, totaling one foot of cumulative fracture height, are present in the Tensleep sandstones, in a finer-grained sandy interval near the top. These fractures are not obviously mineralized: although sparkling reflections off of what may be crystal faces are apparent in some light conditions, the small fracture apertures (less than 0.1 mm) are not occluded. These fractures terminate at the top at a change to a coarser sandstone, but they exit the core at the base so the bottom terminations are unknown and only a minimum fracture height is present. Nevertheless, two fractures totaling only one foot of height within 42 feet of sandstone is not a high percentage of fracturing, thus extension fractures do not seem to be well developed in the local Tensleep sands. Even though the permeability along these individual, open fractures may be high, there may not be enough of them to contribute significantly to the sandstone reservoir system conductivity.



Parallel, steeply dipping extension fractures in a very fine-grained sandstone at 5468 ft.

Extension Fractures in Dolomite

On the other hand, numerous vertical extension fractures are present in the dolomitic facies. Counting individual fractures in the dolomites is problematic given the numerous short en echelon fractures that commonly combine to form compound fractures, but at least ten fractures form 11.5 ft. of cumulative vertical feet of fracture height within the two cored dolomite beds (total of 15 feet of dolomite core). This is a high ratio given the improbability of intersecting vertical fractures with vertical core and indicates that extension fractures are very well developed in the dolomitic facies.



Partially mineralized extension fracture with an irregular fracture plane, in dolomite

Fractures in the dolomites have apertures up to half a millimeter, although patches of anhydrite or dolomite cement (locally with crystalline faces indicating growth into open void space) occlude 20-80% of the aperture. These fractures provide local planes of high permeability but their effectiveness in creating connectivity between the sandstone reservoirs is restricted by the common fracture terminations at numerous horizontal stylolites. Nevertheless, one five-foot tall fracture is present in the ten-foot thick dolomite bed: although this fracture is best developed in an interval with few stylolites, it does cut cross several stylolites near its top and base.



Patches of mineralization on a fracture plane (exposed at the right side of photo), in a dolomite.

Deformation Bands

Three well developed deformation bands are present in the sandstone at the lowest six feet of core. Each band dips 65-70 degrees, with the top and bottom bands being nearly parallel and the intermediate band having a parallel strike but an opposing dip. These form a conjugate shear system that creates an upright “X” fabric of baffles within the reservoir. Each deformation band traverses the core diagonally, exiting the core top and base, and each band spans slightly more than a foot of the core length. The actual band intersections were not cored but their positions can be inferred to be in the nearby rock by projecting the steeply dipping planes beyond the core to the point where they would intersect.



Deformation band cutting obliquely across the core. Offset along the band is obscured by circumferential drilling scars that circle the core like threads on a screw, recording downhole progress during bit rotation, but the inclined coloration bands are differentially oil stained sand-dune cross-bed foresets that show about half a centimeter of normal dip slip.

Each deformation band consists of a non-calcareous white zone about half a millimeter to a millimeter thick, locally splitting into several smaller sub-parallel bands that indicate several events of micro-shear along the plane. Half a centimeter bedding offset can be demonstrated locally, and should be more easily visible after slabbing. Small planar voids are present locally along some of the deformation bands, but the white bands that mark the planes consist of a micro-fault gouge of reduced grain size and diminished porosity, created during shear slip along the band. Reduced porosity is usually associated with reduced permeability, and these bands would retard transverse fluid flow. Flow should be channeled into elongated matrix block, bounded by the intersecting bands and several feet on a side, but unlimited in length in the direction parallel to the bands.

Given the high probability of intersecting such systematically inclined fractures with a vertical well, the absence of deformation bands from the 12 feet of reservoir-quality sandstone overlying the banded interval suggests that they are truly absent from that upper zone and not just missed by the core. The compartmentalized zone of deformation bands may continue downward below the base of the core.



Pockets of remnant aperture along a deformation band. White material is non-calcareous microgouge created during minor shear offset prior to significant lithification. Splaying of the band to the right of the photo indicates multiple shear events along this plane.

Petal Fractures

Six definitive coring-induced petal fractures are present in this core. They have consistent strikes, parallel to one another even where they occur on opposite sides of the core as in the arrangement of a family of four fractures between 5486 and 5487 ft. The consistency of petal fracture orientation along the core suggests a consistent horizontal in situ stress anisotropy. If the local trend of the horizontal stress anisotropy is known or can be reliably inferred, these features can be used to orient the core, and, ultimately, to orient the associated natural fractures, as attempted below.



One of a family of four parallel-striking petal fractures, two on each side of the core within a one-foot interval. The curved pencil line parallels the fainter actual fracture trace immediately to the right.

FRACTURE ORIENTATIONS

The petal fractures in the 45-4-X-21 core should strike ESE-WNW if the Tensleep maximum horizontal in situ compressive stress at this location has the same trend as that documented by the wellbore breakouts and induced fractures in the nearby 48-X-28 well. The orientations of the natural fractures in this core can be measured relative to the petal fractures, and, if the assumption that the petal fractures strike ENE-WNW is correct, then:

1. The three deformation bands strike NE-SW.
2. The two extension fractures in the sandstone also strike NE-SW.
3. The 10-12 extension fractures in the dolomites have two trends, striking NE-SW and NW-SE, but with 20-30 degrees of variability in each trend.



Fracture face (plane of the photograph), looking downhole, showing whiter patchy mineralization. A second set of intersecting, shorter, oblique fractures shows as gray traces parallel to the core axis, top to bottom in this photo. This is the same fracture shown on page 3, upper photo.

COMPARISON WITH 48-X-24 DATA

Fracture intensity

Only two short extension fractures occur in the 45-4-X-21 core, significantly fewer than found in the 48-X-24 core. However, if the three deformation bands described below are included in the 45-4-X-21 fracture count as a measure of overall strain in the sandstones, and if the highly fractured red dolomitic sandstone facies, which is not present in the 45-4-X-21 core, is excluded from the calculation of the 48-X-24 core statistics, then the degree of fracturing in the two wells is comparable at about one foot of fracture height per ten feet of sandstone core.

Likewise, fracture intensity of the dolomites is also comparable in that fracturing is significantly better developed there than in the sandstones of both wells. Dolomite fracture intensities range from three to seven feet of cumulative fracture height per ten feet of dolomite

core, some of the range of variability probably being attributable to the short sampled dolomite intervals and the difficulty in getting representative averages.

Fracture Orientations

These inferred fracture orientations are consistent with the hinge-normal and hinge-parallel fracture orientations measured by Scott Cooper in outcrops of Cretaceous strata around the anticline. However, they are not consistent with the fracture orientations measured in the FMI log run across the Tensleep Formation in the 48-X-24 well, where a consistent and dominant ESE-WNW orientation prevails according to my copy of the FMI log. Nevertheless, one figure in a recent paper published by Friedman and Stamp suggests that the Tensleep fractures have a more NE to ENE-WSW trend, more in line with the fracture orientations inferred here.

In addition to better fracture development in the dolomite intervals, the cores from both wells contain multiple, intersecting fracture orientations in this lithology. However, none of the bitumen-lined fractures noted in dolomite core from the 48-X-24 well were noted in the 45-4-X-21 core.

Conjugate Fractures

The definitive conjugate deformation bands present in the 45-4-X-21 have no direct equivalent in the 48-X-24 core. Several inclined fractures are present in the sandstone in a thin zone in the latter core, and these may be precursors to deformation bands which have not sheared enough to form the distinctive micro-gouge zones, or that may have formed after lithification when such gouge zones do not form. Regardless, the effect on reservoir conductivity will be entirely different: whereas deformation bands are deleterious and compartmentalize a reservoir, the apertures common along conjugate fractures should enhance system permeability and connectivity.

IMPLICATIONS

The Tensleep Formation at Teapot Dome does not contain a widely-developed and uniform suite of fractures. The two cores compared here demonstrate that although fracturing is ubiquitous in the subsurface, fracture intensity, style, and orientation can be variable from location to location in a single field.

Different fracture styles affect reservoirs differently: strong development of a systematic suite of conjugate deformation bands will compartmentalize a reservoir, with maximum permeability being the matrix permeability within blocks, and the blocks being bounded by permeability baffles created by the deformation bands. Conjugate fractures will have the opposite effect, enhancing system permeability and creating good connectivity across a reservoir. Single sets of extension fractures have intermediate effects, creating permeability systems that have higher values than matrix permeabilities but enhanced only in the horizontal direction parallel to fracture strike. Multiple sets of intersecting extension fractures have the potential to improve a reservoir nearly as much as conjugate fractures unless restricted vertically by stylolites.

All of these types of fracture systems are present in different areas and at different levels within the two cores compared here. The number and characteristics of the fractures noted in the cores suggest that they should be controlling features, as important as diagenesis, structure, and sedimentary patterns, on fluid flow within the subsurface Tensleep sandstones at Teapot Dome.

Fracture interpretations of the Tensleep core taken from well # 48-X-28

John C. Lorenz and Scott P. Cooper, June 24, 2004

BACKGROUND

Twelve cores from the RMOTC 48-X-28 well, Teapot Dome, Wyoming, were examined between May 15th and June 4th, 2004. These are unoriented, two and five-eighths inch diameter cores that were relatively broken up by the coring process, especially so in the intervals containing numerous natural fractures. The core is broken along spin-offs, commonly initiated at bedding planes and fracture surfaces, and where rubble zones were created while coring natural fractures; long pieces of continuous/intact core are rare except where the core missed fractures in the sandstones.

Twelve back-to-back cores were taken between 5300 and 5653 ft depth. This interval includes un-recovered core and one short drill-ahead zone. About 197 ft of core was recovered from the Tensleep Formation. Top of the Tensleep Formation is at 5437 ft: core above this was logged and photographed, but was not examined in detail, and the numerous fractures it contains were not included in the analysis below.

The Tensleep core is highly fractured, containing both natural and coring-induced fractures. Omni Labs recovered the core from the well site, removed it from the inner aluminum barrels, and pieced it back together on a layout table in Casper. We examined the core immediately after it was laid out, before it was plugged and sampled. This allowed for acquisition of the maximum amount of fracture information.

FRACTURE DESCRIPTIONS

Over forty natural fractures are present in the cored Tensleep sandstones and dolomites (216 ft cored, 197 ft recovered). Numerically counting the fractures, this is about one fracture per five feet of core, a relatively high fracture count. The percentage of cumulative fracture height (fracture length along the core) is also high, but varies significantly by lithology, with fracture intensity ranging from 11 to 70 feet of fracture length per 100 feet of core length (Table 1). The average fracture intensity for all cored facies is 20 ft of fracture height per 100 ft of core

length over the entire Tensleep core (compatible with the numerical fracture count of one fracture per five feet of core).

The natural fractures are mostly vertical to near-vertical, although dips up to 75° are present locally, and individual fracture heights range from seven ft to a couple tenths of a foot in length along the core axis. Fractures most commonly terminate vertically at bedding planes and stylolites, although many terminate within a homogenous lithology for no apparent reason. Many fractures exit the core and terminations cannot be observed. Most of the fractures are less than a millimeter in total width, and much of that width is occluded in the smaller fractures by partial mineralization of quartz and/or dolomite. Nevertheless, significant porosity, 10-80%, remains in most fractures, especially within the larger ones. The larger fractures also typically split the rock and the core is no longer intact across the fracture, indicating that mineralization provides only an incomplete and weak seal between fracture faces.

Fractures in the oil-stained sandstone interval are essentially the same as those in the non-stained intervals, suggesting that fracturing occurred prior to oil migration or at least that the presence of oil did not change the fracture susceptibility of the rock. A zone of inclined fractures is present between 5591 ft and 5595 ft, and these fractures are suggestive of a conjugate shear system similar to that seen in Tensleep outcrops immediately south of the Alcova reservoir.

The natural fractures commonly strike parallel to the coring-induced fractures where this relationship can be observed, but a few data points suggest locally intersecting fracture trends. The FMI log indicates that the maximum horizontal in situ compressive stress and most of the natural fractures strike E-W to WNW-ESE.

A short interval of white, micritic dolomite with numerous bitumen-stained natural fractures is present between 5495 and 5498 ft, overlying the oil-stained reservoir facies. These fractures may be related to escape of oil from the reservoir.

TABLE 1

Lithology	Cumulative Thickness (ft)	Cumulative Frac Height (Ft)	Fracture Intensity (-%")
white sandstone	116.5	13.2	11.3
oil-stained sandstone	15	2	13
micritic dolomite	39.1	8.9	22.7
dolomitic sandstone/ sandy dolomite	5	1.6	32
red well-cemented sandstone	16.1	11.4	70.8
micritic dolomite w/ bitumen-filled fractures	5	2.5	150
Total	196.7	39.6	
Average			20.1



Quartz-crystal mineralization (note the crystal faces reflecting a points of light) on a natural fracture within the clean sandstone reservoir facies. Fractures in this part of the wellbore measured by the FMI log were interpreted as induced and strikes E-W.



Intersecting fractures (top and bottom arrows) in fine-grained dolomite. The bottom fracture is 70-80% filled with dolomite. The top fracture shows an alteration halo of lighter rock (middle arrow) suggesting the flow of leaching fluids along the fracture, and is only about 20% mineralized, leaving large open voids along the fracture.



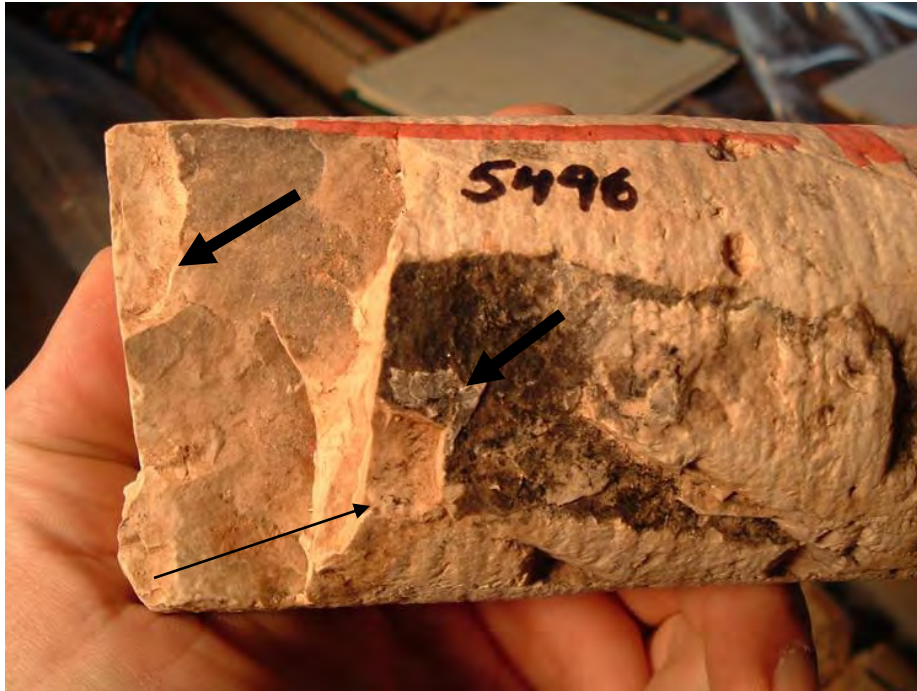
Two parallel, dolomite-mineralized fractures (two "N" arrows) in a well-cemented sandstone, part of a seven-ft high fracture system that weaves along the core axis. Fractures in this part of the wellbore strike E-W on the FMI log.



A natural fracture face that is partially covered with crystalline dolomite. The estimated in situ total fracture total width is one millimeter, with 40% estimated remnant void space irregularly distributed along the fracture plane.



A near-horizontal shear plane within a massive dolomite facies. Such shear planes are relatively rare in the Tensleep but are not uncommon within core from the overlying strata.



Parallel, bitumen-lined fractures (large arrows) and patchy calcite overlay (thin arrow), in the fine-grained, white dolomitic facies that overlies oil-stained reservoir sandstone. Only four feet of core was recovered from the coring run that penetrated this zone, the numerous fractures having broken up during the coring process and jammed the core barrel before a significant amount of core could be cut.



Side view of the same piece of core.



A natural fracture that terminates top and bottom for no obvious reason within a crossbedded but otherwise homogeneous sandstone reservoir lithology.

OUTCROP STUDIES

Fractures and Strain Accommodation in the Tensleep Formation at Flat Top Anticline, Carbon County Wyoming: Implications for Analog Reservoir Systems

John Lorenz, November 13, 2007

SUMMARY

Fractures accommodated strain in Tensleep sandstones during the formation of Flat Top Anticline, a compound structure of three sub-anticlines developed in the hanging wall of a thrust sheet. The fractures include two sets of tectonic fractures: early-formed hinge-oblique and later-formed hinge-parallel extension fractures. In addition, newly described hydraulic injection fractures, both micrite-filled and sand-filled, strike sub-parallel to both of the tectonic-fracture trends and probably formed at about the same time. Other structures include deformation bands with a variety of strikes, local faults, and both bedding-parallel and bedding-oblique shear planes. These structures formed as the strata were extended parallel to the anticlinal hinge due to folding, and oblique to the hinge due to extension related to thrust translation.

Similar, parallel structures probably formed at several different times during development of the anticline, and existing structures were reactivated from time to time. The result is a suite of meter-scale features, locally compound, that were not simply and sequentially formed, but that do record the structural history of the anticline.

The intensity of the tectonic fractures varies by structural position: only hinge-normal fractures are present on the anticline backlimbs where folding is minimal, but two sets of fractures are developed on the forelimbs and crests. Hydraulic injection fractures are thicker and more common at Pine Butte on the western end of the anticline where it is most acutely folded. Tectonic fractures are poorly developed in the same area, where most of the strain was taken up by hydraulic fracturing and the reactivation of hydraulic fractures, and by bedding-related shear planes. Hydraulic fractures are locally better developed in the thickly, horizontally-bedded sandstones than they are in dune foreset facies with large-scale cross-beds, but development of

the tectonic fractures was not affected by differences in lithology. Most of these structures will degrade permeability in the otherwise high-porosity, good quality Tensleep reservoirs, and most of the observed structural patterns should create a significant permeability anisotropy.

ACKNOWLEDGMENTS

This report has benefited from discussions with Scott Cooper, Shaochang Wo, and Peigui Yin. Scott Cooper reviewed drafts of the report and offered many useful suggestions and ideas. Peigui Yin made the thin sections and photomicrographs presented here and helped formulate their interpretations. This study was funded by and conducted for the Enhanced Oil Recovery Institute at the University of Wyoming, Jim Steidtmann director.

INTRODUCTION

Purpose of the study

This study has been undertaken in order to understand the characteristics and distributions of fractures and other reservoir-scale structural features that might affect fluid flow in Tensleep anticline reservoirs in Wyoming. Detailed characterization and knowledge of the heterogeneities should lead to more efficient strategies for oil extraction from these reservoirs. Fractures of various types have been noted by most of the published reports that have described cores or wellbore-image logs in the Tensleep reservoirs of Wyoming (see earlier Lorenz report of April 20, 2007). However, these subsurface data are quite limited in extent relative to the size of typical reservoirs: i.e., it is difficult to reconstruct a three-dimensional permeability network that may extend over several square miles using only the one-dimensional data acquired from a few 8-inch diameter wellbores. Nevertheless, the published sketchy descriptions indicate that Tensleep reservoirs are highly fractured and that the effects of fractures on permeability systems should be accounted for during flow modeling.

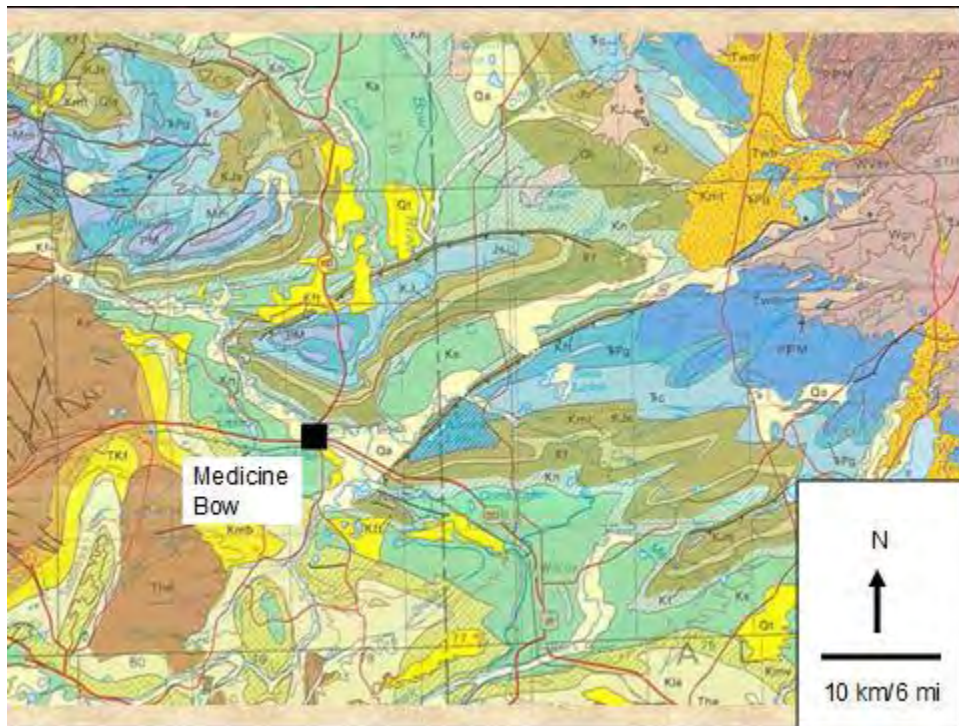
Outcrop data can be used to develop a model for permeability networks, conceptually filling in the large unknown areas between wellbores. Outcrops afford extensive, three-dimensional views of fracture systems, and outcrop data can often be used to create quantitative models of fracture permeability in a reservoir. Outcrop data are never perfectly analogous to the

subsurface, but if used and filtered properly these data can indicate the probability of fracturing as well as the most likely fracture intensities and orientations.

The outcrop study reported here is one of a series of project reports on fractures in the Tensleep Formation and the effects of fractures on fluid flow in Tensleep reservoirs across Wyoming.

Location and Structural Setting

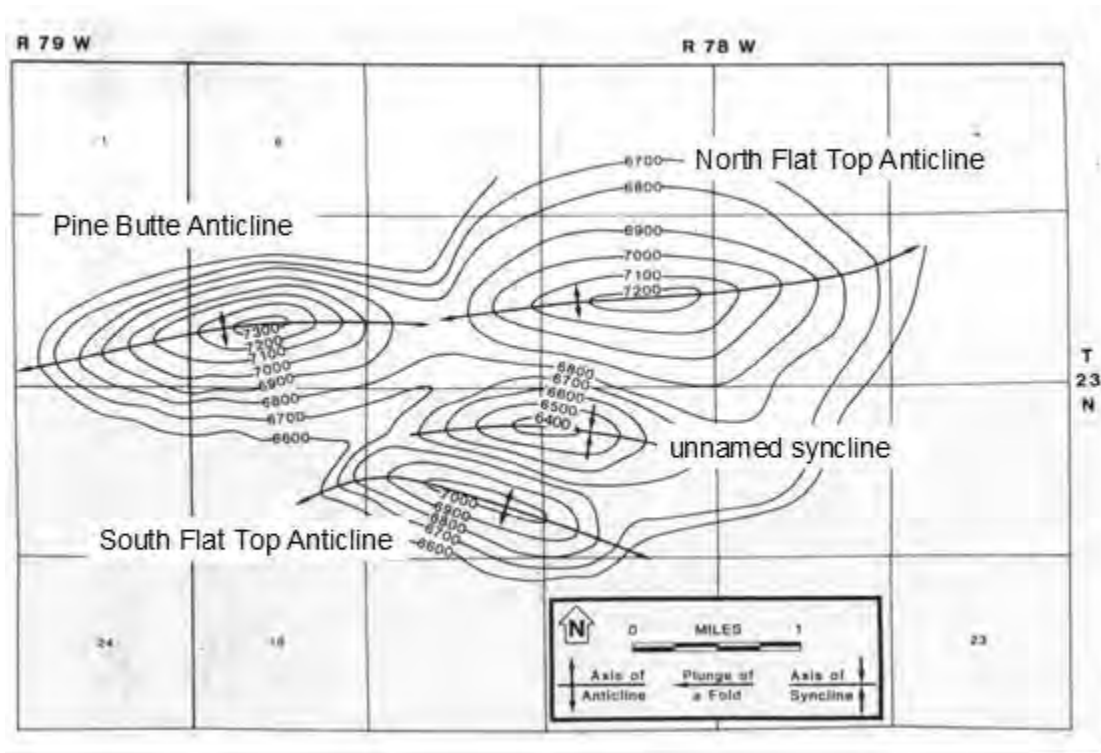
Flat Top Anticline is located in southeastern Wyoming, about six miles north of the small town of Medicine Bow, at the northern margin of the Hanna basin and just south of the Shirley Mountains. At the time of this writing, access to the structure had become restricted due to a change in land ownership. Flat Top Anticline is the northernmost of several ENE-WSW trending, asymmetric anticlines in the area (Blackstone, 1994; Lillegraven and Snoke, 1996), each overlying a north-vergent, deep-seated thrust fault a few tens of miles long.



Section of the geologic map of Wyoming showing the northeast-trending Flat Top Anticline (middle of the figure, just north of Medicine Bow) in southeastern Wyoming. The structure widens and becomes more complex at the western end of the anticline.



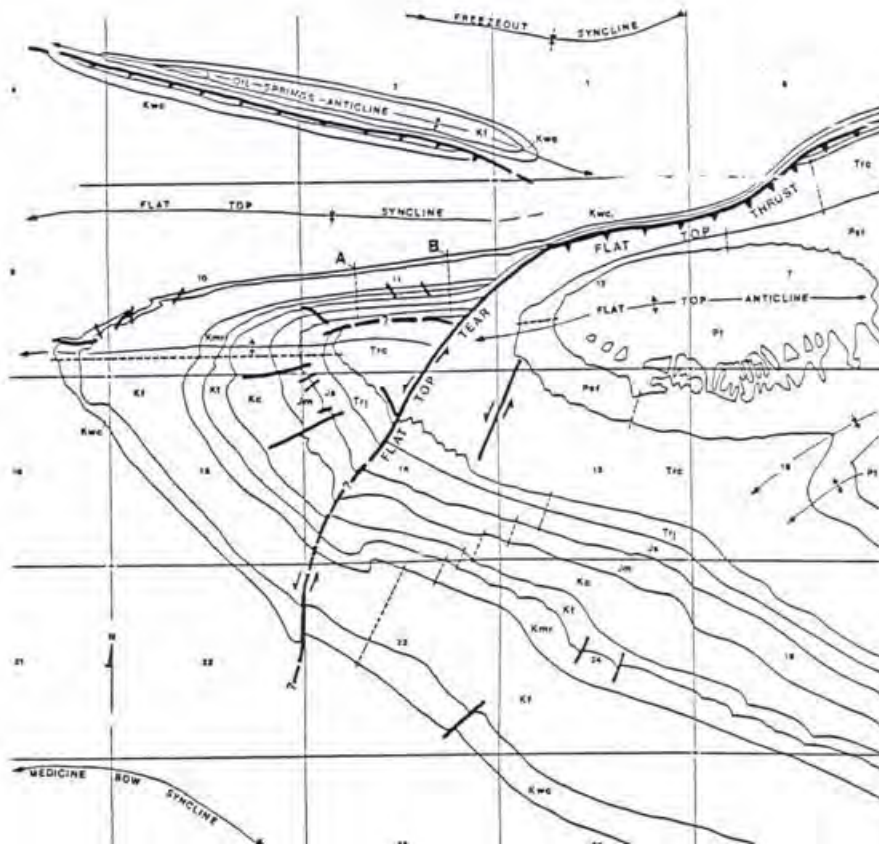
Flat Top Mountain viewed from the eastern slope of Pine Butte. View is to the east, along the axis of the Flat Top Anticline.



Structure-contour map of the sub-structures forming the composite west end of Flat Top Anticline (from Kelly, 1984). The mapped surface is the top of the Tensleep Formation and the datum is sea level. Only a few wells penetrate the structure, and the top of the Tensleep Formation is exposed, eroded, and missing in many areas, thus Kelly must have inferred much of this structure. Pine Butte Anticline is labeled as “Flat Top Anticline” on the following map from Blevins (1984).

Since several similar names are used in the following discussions, the terminology should be clarified. Flat Top Anticline refers to the 26-mile (42 km) long, composite structure that includes three sub-anticlines (Kelly, 1984): North Flat Top Anticline, South Flat Top Anticline, and Pine Butte (also referred to as Pine Mountain) Anticline. Flat Top Mountain is the prominent mesa at the crest of the North Flat Top Anticline, and it gives its name to the broad-scale structure. Pine Butte is the slightly higher and more vegetated knob at the western end of the compound structure, and for which the Pine Butte Anticline is named.

Several M.Sc. theses (Knight, 1944; Carey, 1950; Blevens, 1984) are the only published references that have described the structure of Flat Top Anticline in detail. These theses describe Flat Top Anticline as being approximately 26 miles long with an overall strike of N70° E. A south-dipping thrust fault underlies the anticline, breaking to the surface immediately to the north. Based on small-scale structures, both Blevens (1984) and Carey (1950) concluded that motion on the thrust fault was left-lateral oblique-slip, and that the transport direction of the strata above the fault was not normal to the strike of the thrust fault, but rather towards N35° E and N50° E for the western and eastern parts of the anticline respectively.



Blevins' (1984) geologic map of the Pine Butte Anticline (labeled "Flat Top Anticline") at the westernmost end of the Flat Top Anticline. The Tensleep Formation (Pt) is the oldest unit exposed at the center of the anticline. The grid shows the one-square-mile section lines.

Blevins also concluded that maximum displacement is at the western end of the thrust fault, accommodated by an inferred tear fault. Blackstone (1994) disputed this interpretation, suggesting instead that offset along the fault is highest in the middle and zero at the ends, and that the proposed western tear fault is, rather, a bend in the thrust fault. Blackstone's interpretation seems to have been based primarily on theoretical arguments as he presented no field data to support it, and Blevins' interpretation, based on observations of numerous small-scale structures in outcrop, is accepted here.

Regardless of the interpretation, folding of the Tensleep strata becomes more acute westward along the fault. From a narrow, relatively simple anticline at its eastern end, the anticline widens westward into a compound structure comprised of three sub-anticlines. The northern two sub-anticlines, at Flat Top Mountain and Pine Butte, are aligned along the main axis of the overall anticline and separated only by a poorly defined structural saddle. Meter-scale

strain-accommodation structures including natural fractures become larger and more frequent westward along the anticline, also recording increased strain in that direction. Tensleep strata are relatively tightly folded at Pine Butte, where northward structural dips of as much as 40° are present in the forelimb of the anticline. Younger strata may even be overturned on the northeastern flank (Blackstone, 1994). Northward-dipping strata of the forelimb at North Flat Top Anticline are poorly exposed, and this structure is less tightly folded (Carey, 1950). Strata are horizontal at the crest of both sub-anticlines, and dip southward at about 10° and 20° on the backlimbs of North Flat Top Anticline and Pine Butte Anticline, respectively.

The southernmost of the three anticlines that comprise the Flat Top Anticline, South Flat Top Anticline, was examined only briefly during this study. It contains fractures and other structures similar to those found elsewhere in the area, but data were not collected systematically from this structure and it will not be discussed further.

None of the published studies have reported fracture characteristics from the Tensleep Formation.

Stratigraphic Setting

Tensleep strata exposed at Flat Top Mountain are about 110 ft. (34 m) thick (Kelly, 1984). A thicker section, about 300 ft. (90 m), is exposed at Pine Butte, and although the base of the Tensleep Formation is not exposed anywhere on the Flat Top Anticline, this may represent nearly the full thickness of the formation since Kelly reported that the Tensleep section in a well drilled near the crest of Pine Butte is also about 300 ft. thick, with an estimated additional 50 ft. (15 m) of the formation having been eroded from the top of the section at that location. This is about 30% thicker than equivalent strata in nearby wells off the structure, and Kelly suggested that this anomaly could be related to thrust-repeated section. However there is no evidence for thrusting or repeated section in the Tensleep sandstones that are well exposed in the short, deep canyons around the margins of the butte. Blevens (1984) and Kelly (1984) report that the well drilled near the top of Pine Butte reached basement at either 855 or 870 ft. (260 or 265 m), and that the Tensleep Formation overlies Paleozoic marine limestones, shales and sandstones.

A five- to six-meter thick shale with a capping meter-thick carbonate, part of the Opeche Shale interval, overlies the Tensleep eolian sandstones. The shale-carbonate couple is best exposed where it dips under the overlying strata along the northern edge of Pine Butte. The last

erosional remnants of a similar section are present at the very top of Flat Top Mountain, thus the local 34-meter section exposed at this location probably represents the top of the Tensleep strata even though the sedimentary sequence in the underlying Tensleep sandy layers does not correlate well with the uppermost 30 m of the sedimentary sequence at Pine Butte.

Several sedimentary facies are present in the Tensleep strata along Flat Top Anticline. In addition to the heroic, large-scale crossbedded eolian dune facies with planar-tabular cross-bed sets 4-5 (12-15 ft.) meters thick, several layers contain smaller-scale trough cross beds only 1-2 meters (3-6 ft.) thick. Parallel-horizontal bedding, assigned by Kelly to interdune environments, dominates several units. Some of these units are thickly bedded, but the thinner, better-cemented, horizontally bedded sandstone near the top of the section is finely laminated.

Remnant dead oil stains many of the sandstones at both Flat Top Mountain and Pine Butte. Oil stain is most prominent in the lower third of the exposed section at Flat Top Mountain but is irregularly distributed at Pine Butte. Prominent beds of marine dolomite, common in other outcrops and in most subsurface reservoirs, are notably rare in the Tensleep section at Flat Top Anticline.

Strain Accommodation: General

Extension fractures are common in the Tensleep sandstones. Shear fractures are present but less common. Hydraulic injection fractures, described below, are locally the most prevalent strain-accommodation features, especially where they have been reactivated multiple times. The 300 to 350-ft (90- 120 m) thick package of poorly cemented Tensleep sandstone behaved as a relatively homogeneous, easily deformed unit during anticline development. Most of the strain-accommodation structures occur indiscriminately throughout the section, without regard to bedding or sedimentary facies. Although differential weathering in the different sedimentary facies commonly makes it appear so, bedding contacts between different sedimentary facies did not arrest the propagation of most bed-normal fractures.

Millimeter-scale slip can be discerned locally along large-scale dune crossbed foresets, and several good examples of bed-parallel shear along major bedding contacts between sedimentary units were found, but for the most part bedding contacts did not accommodate much shear. Either bedding planes and changes in lithology did not present major mechanical

discontinuities, or the structural conditions were such that such flexural slip was not required to accommodate strain during deformation.

Only a few large faults are present, those noted having a few meters of strike-slip and oblique-slip offset. Most strain during deformation was taken up along numerous, pervasive, small, non-sedimentary structures, described below, and by the repeated reactivation of those structures to form larger compound structures.

The Tensleep Formation on Flat Top Anticline presents a variety of irregularly distributed and superimposed strain-accommodation structures. Many of these structures are fractures in the classical sense, being planar to sub-planar breaks in the rock, and formed in extension or shear. Others, although occurring as similar planar discontinuities, have significantly different mechanical origins, having formed primarily as injected, natural hydraulic fractures. In addition, many of these primary structures have been reactivated several times and thus have a compound history that obscures the mode of origin and complicates the interpretation.

Many of the structures were puzzling when first encountered in the field because they are not the classic fracture breaks in the rock with easily interpretable fractographic characteristics that were expected. Some of the structures have not been previously described in detail in the literature, and it was necessary first to determine how they formed in order to make valid measurements. Moreover, many features are composite, where the original structure has been activated and/or mineralized more than once. Because not all of the compound features are built from the same primary structures or formed in the same order, it took a while to separate the components and to discern patterns and the order in which they formed. Finally, the hydraulic injection fractures were first encountered at Flat Top Mountain where they are relatively small and obscure. Only as the study expanded westward to Pine Butte, where the features are larger and more definitive, did much of their nature become apparent. The following report contains a seemingly inordinate number of photographs but they have been useful in conveying the wide variety and complexity of these features that are relatively new to the Tensleep literature.

The structures observed in the Tensleep Formation at Flat Top Anticline include deformation bands with micro-fault gouge, extension fractures, hydraulic injections filled with sand and/or micrite, faults, slots filled with centimeter-scale calcite crystals and/or clasts derived from the host rock, and both bedding-parallel and bedding-oblique shear planes.

Permeability along these structures must have changed during their development as they were alternately opened, sheared, injected, and mineralized. Estimates of their current permeability may not be directly applicable to subsurface reservoirs due to the mineralogical changes, primarily conversion of anhydrite to calcite, which may have accompanied exposure and weathering at the surface (Yin, personal communication).

DEFORMATION BANDS

Deformation bands are millimeter-scale shear zones and are common strain-accommodation structures in poorly consolidated, high-porosity sandstones. Deformation bands are present at Flat Top Anticline, but they are not pervasive as might be expected, given that the high-porosity Tensleep sandstones have mechanical properties that are susceptible to banding.



Northeast-southwest striking set of deformation bands on a bedding plane (boot toe, lower right, for scale). The en echelon offsets suggest a small degree of right-lateral shear.



Multiple, sub-parallel to coincident deformation bands that locally diverge to show that at least five small-scale shear events contributed to forming this composite feature. Thumb tip (lower left) for scale.

Deformation bands in outcrop are commonly marked by raised, erosion-resistant ridges that consist of collapsed porosity and comminuted sand grains formed during small-scale shear. Because the ridges resemble the resistant mineralization of garden-variety fractures, each ridge in the Tensleep outcrops needs to be examined carefully in order to distinguish between deformation bands and mineralized fractures.

Deformation bands in the Tensleep Formation occur as irregular sub-parallel planes, and in anastomosed, sub-parallel lacework and reticulate boxwork patterns. Where they formed in cross-bedded sandstones, they commonly follow the inclined fine-coarse laminations of the cross-bed foresets. In such cases the bands are relatively inconspicuous except where they locally break across several foreset planes to join an adjacent plane.



Lacework deformation bands (left) and an east-west striking, inclined deformation band (top to bottom, center of the photo) that follows the foreset of a large cross-bed set.



Box-work of deformation bands in oil-stained, cross-bedded sandstone.



Composite photomicrograph (taken by Peigui Yin) of a thin section made from the sample shown in the previous figure, showing contorted bedding, shear zones of finer-grained/comminuted sand, and irregularly distributed porosity (blue epoxy zones). The black bar and series of small 2-mm yellow bars at the top of the figure gives the scale.

Deformation bands were some of the first structures to form in the Tensleep sandstones at Flat Top Anticline, as shown by cross-cutting relationships where they are offset by most other structures. The exclusion of oil stain from the low-porosity zones adjacent to deformation bands at Flat Top Anticline suggests that oil migrated into the sandstones after the deformation bands formed.

Deformation bands create low-porosity permeability baffles in reservoirs where they are present, but at Flat Top Anticline they are not common enough to provide a significant control on permeability. They never comprise more than three percent of the total fracture population at any location, and are entirely absent in many areas. Although the deformation bands in meter-

scale outcrops are commonly roughly aligned, they show no preferred orientation or trend at the kilometer-scale of the anticline. They probably formed early in the burial history of the rock in response to local compaction stresses.

TECTONIC FRACTURES

Tectonic fractures in the Tensleep Formation at Flat Top Anticline are defined here as relatively planar features that may have plumes on the fracture faces, millimeter-scale calcite mineralization of the fracture aperture, and/or that merely consist of planar breaks in the rock. Plume structures, indicative of extension fracturing, are in fact rare in these strata, in part because poor cementation did not leave the rock prone to plume formation during fracturing, and in part because the same poor cementation allowed plumes to be quickly destroyed during weathering. Moreover, some plumes seem to have been obscured or destroyed by shear reactivation of the extension fractures. Regardless, hints of plume structures are present on some fracture faces, and, along with the absence of offset, suggest that most of the planar breaks in the Tensleep sandstones formed initially in extension. Tectonic fractures comprise between a third and 100% of the fractures in various beds around the Flat Top Anticline.



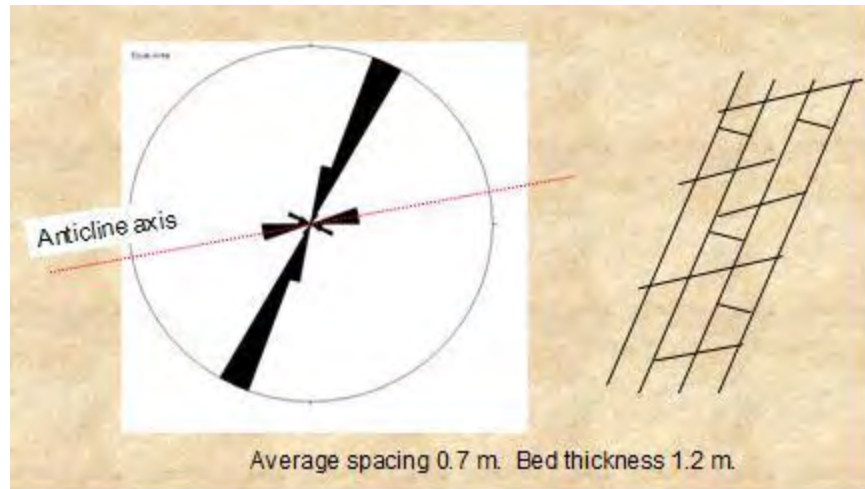
Tectonic fracture plane with suggestions of a broad plume structure. Orange iron stain on the fracture face indicates that it was a conduit to ground water. Remnants of white materials on the face include calcite mineralization and a layer of gouge (see the following photograph).



Close-up from the previous photograph, showing that the materials on the fracture face consist of an early layer of white gouge and a later layer of off-white calcite crystals. This fracture is inferred to have formed in extension (indicated by the fracture-face plume), to have been reactivated in shear (to form the gouge), and, finally, to have been mineralized.

Basic Tectonic Fracture Pattern

Two tectonic fracture strikes are present in most of the Tensleep sandstones at Flat Top Mountain, although those two basic strikes vary around the structure and with stratigraphy at any given locale. In general, fracture patterns are both more regular and relatively simple in thin, well-cemented sandstone beds, and the Tensleep fractures are no exception: the basic Tensleep tectonic fracture pattern is well developed and well preserved in the calcareous, thinly and horizontally bedded, 1.2 meter thick sandstone layer at the top of Flat Top Mountain.



Rose diagram and schematic showing the relatively simple strikes and geometric relationships of 42 fractures in the thinly bedded, well cemented calcareous sandstone at the top of Flat Top Mountain

Three fracture sets are present in this bed:

1. an early, through-going set of tectonic fractures that strike NNE-SSW
2. an intermediate-age set of tectonic fractures that strike ENE-WSW, parallel to the general axis of the anticline. These fractures locally cut across, locally abut fractures of the NNE-SSW set
3. a youngest, irregularly developed set of short, non-tectonic fractures that are generally normal to the earliest set and that terminate against fractures of either of the older sets

Interpretation

This most regular of the observed fracture patterns is plausibly interpreted as follows. The oldest, NNE-SSW fractures formed as load-parallel extension fractures (Lorenz et al., 1991) just prior to or contemporaneously with early stages of anticline development, prior to extensive thrust translation or folding. These fractures do not strike normal to the trend of the anticline or to the map trace of the thrust fault, as might be expected if the direction of thrust translation is assumed to be normal to the thrust front. However, as noted above, the probable direction of transport for the Flat Top Mountain thrust, as interpreted by Blevins (1984) and Carey (1950) from small-scale structures, is oblique to the trace of the thrust fault, towards the NNE. Thus the early set of Tensleep fractures strikes parallel to that interpreted direction of motion and the

strikes are consistent with an interpretation of their formation as load-parallel extension fractures under same the stress conditions that initiated thrusting.

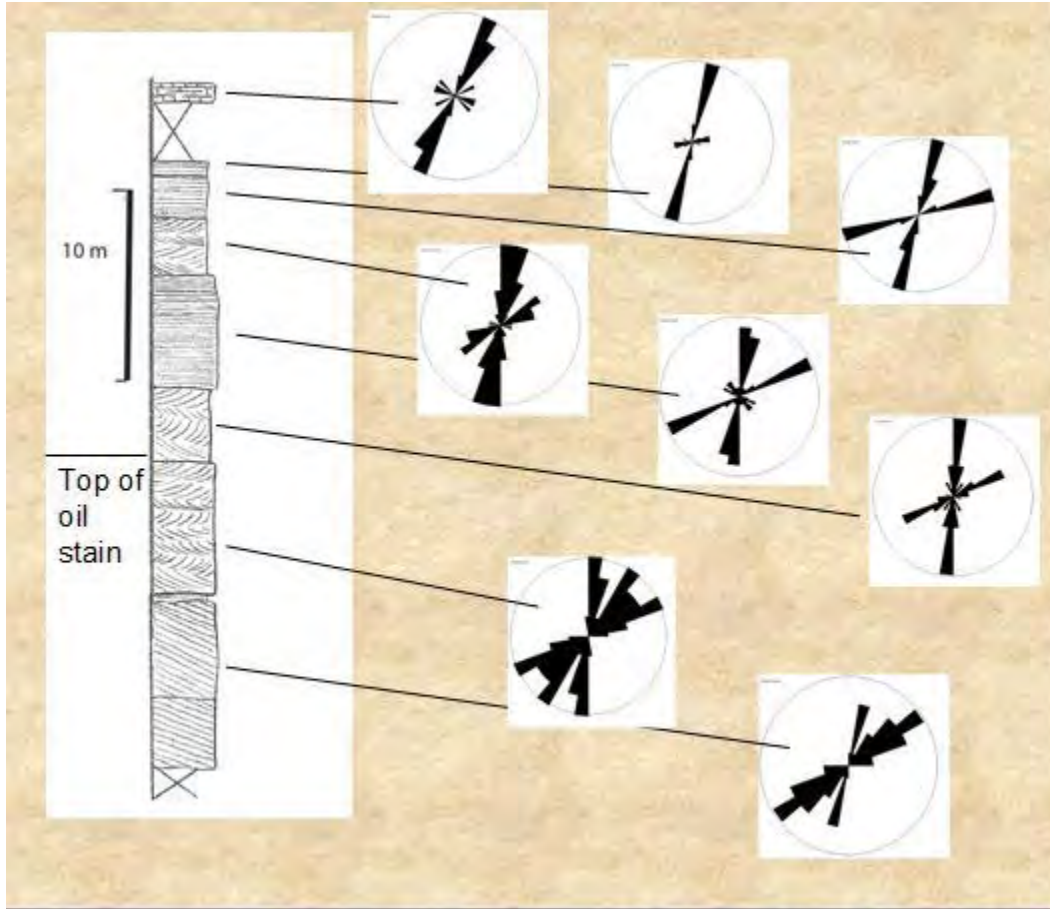
The intermediate-age, ENE-WSW striking fractures, striking parallel to the anticlinal hinge, can easily be interpreted as having formed slightly later, during fold-related extension across the developing anticline. Finally, the short youngest fractures formed by stress release during uplift and exposure. These fractures would not be present in subsurface reservoirs, but the older two sets would be.

Variations on a Theme

Fracture patterns in the other sandstone beds that crop out at and around Flat Top Mountain are less regular and less systematic than those in the well-cemented bed, yet the basic pattern of an oldest, approximately NNE-SSW set and a younger, approximately ENE-WSW can be recognized in most areas. Such patterns and age relationships are complicated in the thicker, less well cemented sandstones where fractures tend to be less regular and systematic as a rule anyway, by reactivations of many of the fractures, and by the presence of other structures, as described below.



Plan-view surface showing the interactions between a through-going pair of N-S fractures and ENE-WSW trending fractures in a thick, cross-bedded sandstone at Flat Top Mountain. Disruption of the ENE-WSW set shows that the N-S set was present in the rock when the ENE-WSW set propagated across the area.

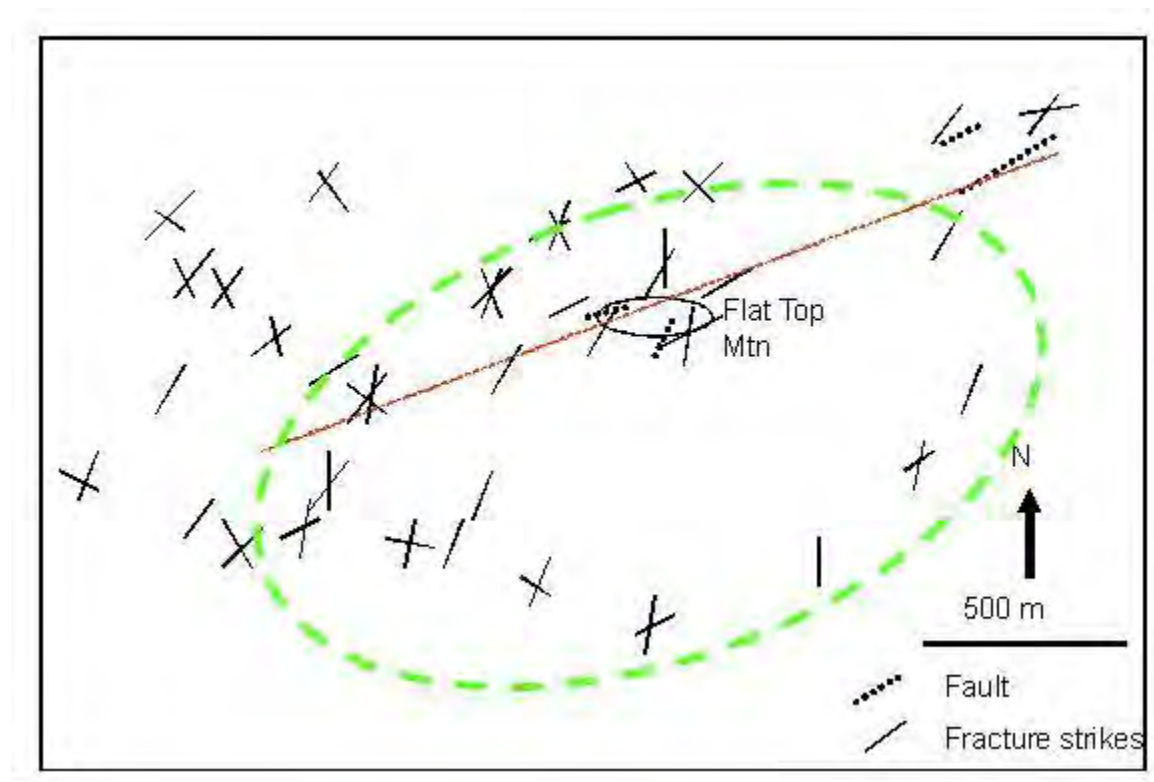


Summary of fracture orientations in the different sedimentary facies that crop out on the south side of Flat Top Mountain. Most beds contain a set of older NNE-SSW, through-going fractures and a younger set of approximately ENE-WSW fractures. Variations in the population ratio of the two fracture sets depend in part on the angle of outcrop exposure relative to fracture strike. Between 12 and 40 fracture measurements were taken from each bed. The thin-bedded, 1.2 meter thick calcareous sandstone described above as displaying the basic fracture pattern is the unit immediately below the covered interval near the top of this measured section.

Variation by Structural Position

Fracture orientations were measured at numerous stations in the outward-dipping Tensleep beds that define the perimeter of the North Flat Top Anticline. These measurements show that, with some variation, the early-formed, NNE-SSW-striking, thrust-transport-parallel fractures are ubiquitous. Some variation in strike is present, especially on the forelimb, but the earliest, through-going fracture set in all outcrops strikes approximately parallel to the earliest fracture set measured at Flat Top Mountain.

Flat Top Mountain is located along the hinge of the North Flat Top Anticline, where folding, flexural strain, and the related fracturing would be expected to be greatest. However, the folding is not acute: bedding dip changes only from 10° to the south on the backlimb to an estimated 20° to the north on the forelimb, therefore fold-related fractures are not intensely developed along the crest. The data do suggest that hinge-parallel fractures are absent from much of the unfolded backlimb (although stress-release cross-fractures are present there), whereas an additional, possibly fault-related fracture set is present locally in the forelimb.



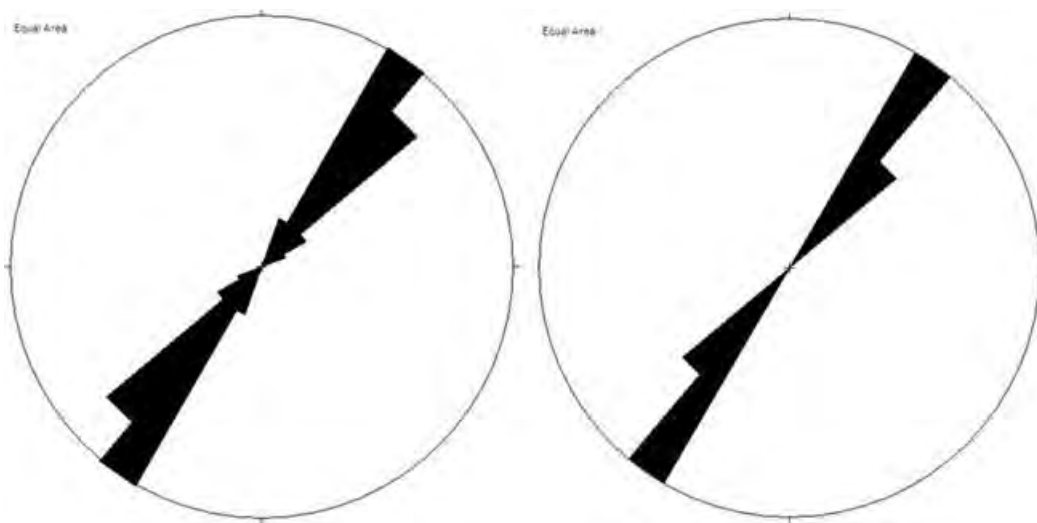
Strikes of faults and the dominant fracture trends around the perimeter of North Flat Top Anticline. The red dashed line indicates the approximate hinge of the anticline; the green dashed line indicated the approximate outline of the anticline. Lines rather than roses are shown on this figure, the lines being tracings of the well-defined dominant fracture strikes from air photos in each location, all of which were verified by examination on the ground.

Similar tectonic fracture patterns are not present immediately to the west at Pine Butte Anticline, where hydraulic fractures, discussed next, are so well developed and were so commonly reactivated they accommodated almost all strain in the rock. Despite the significantly tighter folding at Pine Butte (20° dips on the back limb, up to 40° dips on the forelimb), tectonic fractures are rare.

Fracture patterns as a function of sedimentary facies

One of the goals of this study was to determine whether fracture patterns vary appreciably as a function of variations in sedimentary facies (which control composition, cementation, and porosity, and thus the mechanical properties, of a rock). To that end several specific comparisons were made between the fracture populations in different facies of adjacent beds of similar thickness, thereby eliminating structural variability as a controlling factor. Two beds on the southwestern slope of Flat Top Mountain, each about 2 meters thick, and each with a good exposure of the bedding surface that eliminated outcrop-orientation bias in data collection were selected. One was a cross-bedded unit and the other a horizontally bedded one. Only the older, NNE-SSW striking fractures were considered at this site.

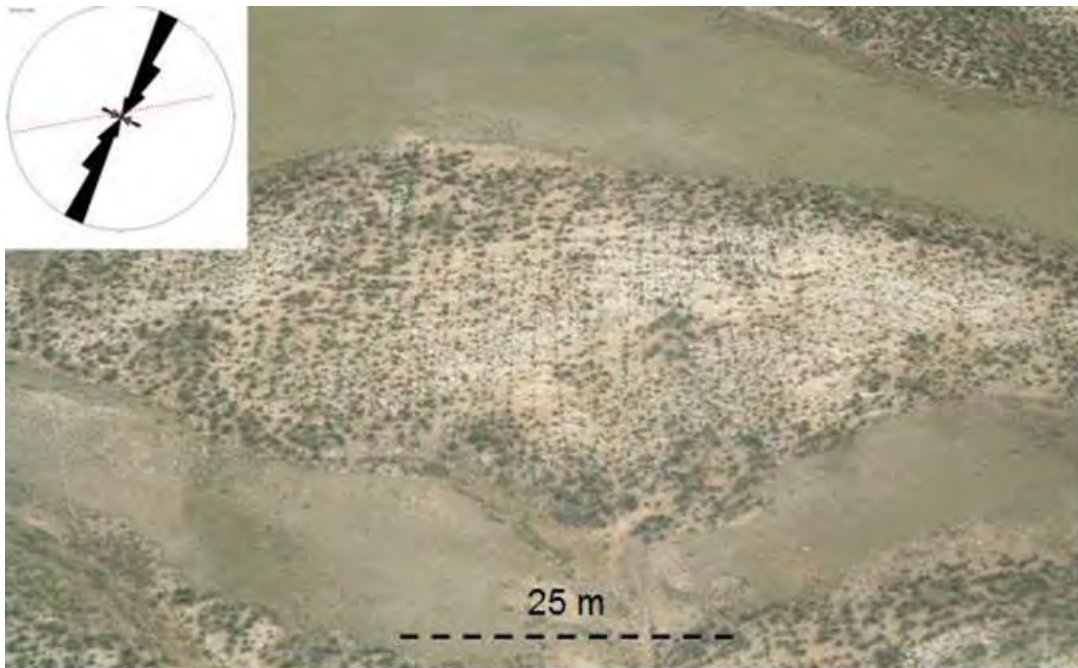
The data suggest that no statistically important difference exists between the fracture populations of the two beds, and that the mechanical properties, the fracture susceptibility, and therefore the resulting fracture populations, are similar.



Left: Scan line including 22 fractures on a pavement at the top of a parallel-bedded sandstone on the southeastern slope of Flat Top Mountain: mean strike is 38.4° , average spacing is 1.47 m.
Right: Scan line including 19 fractures on a pavement at the top of the immediately underlying cross-bedded dune facie: mean strike is 37.6° , average spacing is 1.65 m.

Another but broader scale comparison was made on the gently south-dipping ($<10^\circ$) flank of North Flat Top Anticline, approximately one kilometer southwest of Flat Top Mountain. Bedding-plane pavement exposures again allowed data collection without outcrop orientation bias.

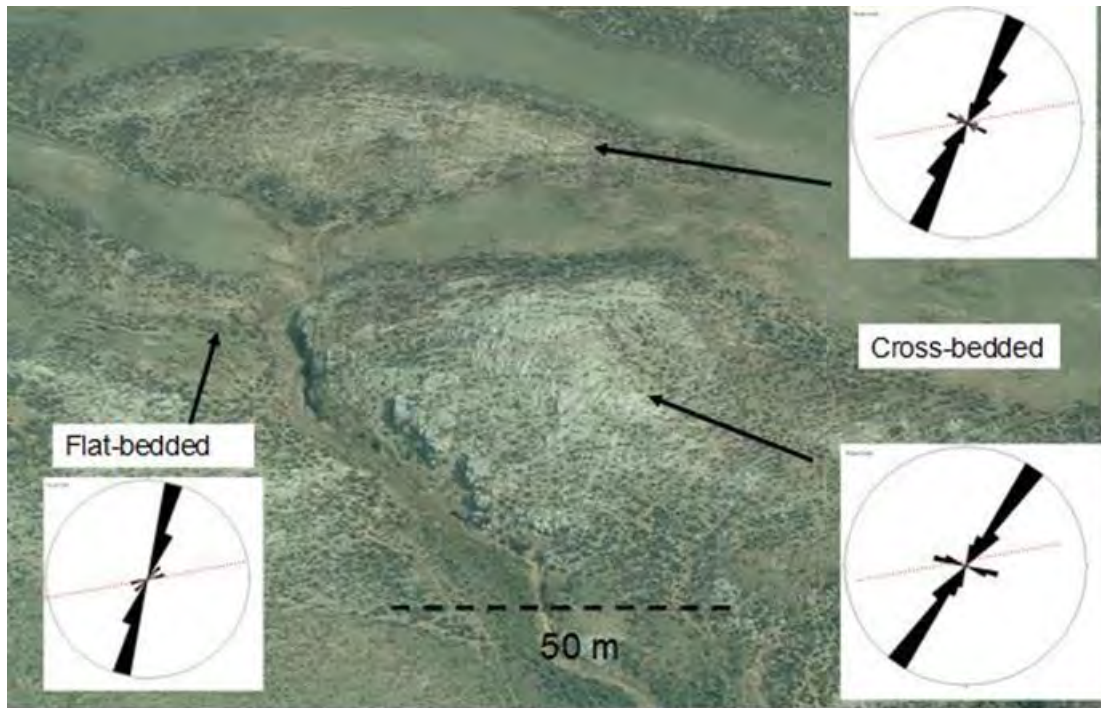
All fracture orientations were recorded at these outcrops, making it obvious that the ENE-WSW, hinge-parallel fracture set is notably absent. This is probably due to the structural position on the relatively planar, unfolded backlimb of the anticline. Rather, the cross fractures at these locations are normal to the NNE-SSW fractures and are related to stress release during uplift and exposure, as indicated by the paucity of cross fractures in the parallel bedded facies which is exposed primarily in a gully floor and which has had little exposure or chance to develop such cross fractures.



Aerial photograph of a bedding-plane exposure of systematic NNE-SSW striking fractures in cross-bedded sandstones on the shallow, unfolded back-limb of the North Flat Top Anticline. A youngest set of abutting cross fractures is also present, but the hinge-parallel, ENE-WSW fracture set is absent because these strata have not been folded. The red dotted line across the rose diagram indicates the strike of the anticline hinge. Scale is approximate.

The differences in fracture strikes ($10-15^\circ$) between the three outcrops are not significant. However, average fracture spacings do vary, from between 1.2 and 1.5 m in the cross-bedded facies, to 3.2 m in the parallel-bedded facies. The thicknesses of these beds could not be

determined due to cover and thus could not be factored out of consideration, but the difference in measured spacings, a factor of over two, is probably related to differences in mechanical properties of the different sedimentary units, which could be determined by laboratory testing.



Aerial photograph of three adjacent bedding-plane pavements, two in cross-bedded facies (including the same one shown in the previous photograph), and one in a parallel-bedded facies. Twenty-six to 30 measurements were taken at each location. The oblique trends in the whiter outcrop in the center of the photo are traces of cross-beds, not fractures. Fracture strikes are not significantly different in the three outcrops, but fracture spacings are. The red dotted lines indicate the trend of the anticline hinge, the indicated scale is approximate.

Summary, Tectonic Fractures

Two types of tectonic fractures exist on North Flat Top Anticline: early-formed fractures that strike approximately NNE-SSW, parallel to the direction of transport during thrusting, and later fractures that formed parallel to the ENE-WSW trending hinge of the anticline in response to extension across the anticline during folding. The former are ubiquitous, the latter are absent from the unfolded backlimb of the anticline. A third set of non-tectonic, stress-release fractures is also common, striking normal to the NNE-SSW fractures and abutting them.

Fracture strikes and spacings do not vary significantly with changes in depositional facies in the thick, high-porosity sandstones, i.e., there is no significant difference between the strikes or spacings of fractures found in the thick, parallel-bedded sandstones and those found in the cross-bedded eolian dune facies. However, fractures tend to be more regular and systematic in thinner, better-cemented sandstones when compared to the fractures thicker, more poorly cemented sandstones.

Tectonic fractures can usually be distinguished from other fracture types discussed below by their better planarity, plume structures, and calcite mineralization, although repeated reactivation of fractures in different conditions blurs the distinctions as early fractures have acquired some of the characteristics of later fractures during reactivation. Tectonic fractures, which comprise the dominant fracture type found at North Flat Top Anticline, are virtually absent from the Tensleep strata at Pine Butte Anticline.

HYDRAULIC FRACTURES/CLASTIC DIKES

Introduction

Natural hydraulic injection fractures or clastic dikes are not uncommon in the sedimentary record (e.g., Peterson, 1968; Duranti and Hurst, 2004), and they have even been previously reported from equivalents of the Tensleep Formation (Ahlbrandt and Harris, 1975). Some of the features described as “sand-filled fractures” in Tensleep cores elsewhere in Wyoming (e.g., Emmett et al., 1971; Shebl, 1996) probably originated in this way, although others may be deformation bands.

Meter-scale clastic injections have been reported from modern eolian environments (e.g., Glennie, 1970), and larger, reservoir-scale sandy “injectites” are well known (e.g., Hurst and Cartwright, 2007). However, descriptions of locally pervasive, small-scale hydraulic fractures such as those presented here are not common in the Tensleep literature. They represent an unanticipated structural complication in modeling fluid flow through Tensleep reservoirs and therefore will be described in detail.

Millimeter- and Centimeter-Scale Characteristics of Hydraulic fractures

Variations in the style of hydraulic fracturing exist along the Flat Top Anticline, and it is often difficult to categorize any single fracture since many of the planes have been exploited on two or more occasions to accommodate repeated strain or to accept different types of injected material. Features that are taken here to be diagnostic of hydraulic fractures include allochthonous, irregularly planar filling material ranging from less than a millimeter to 20 centimeters wide. The injected material is commonly banded or layered parallel to the fracture walls, and may consist of sand, silt, and/or micritic microcrystalline limestone. Where sandy, the cementation, grain-size populations, and roundness characteristics are typically distinct from those of the host sandstones.



Simple hydraulic fracture in a hand sample of sandstone ("8/11-3" indicates the third sample taken on August 11th). The fracture fill is about 1 cm wide and composed of microcrystalline limestone: see following photo for detail.



Montage of photomicrographs, taken by Peigui Yin, of sample 8/11-3 showing that the fracture is filled with microcrystalline limestone and has layering near the edges suggestive of either flow or multiple injections. The sharp-edged, broad lighter band in the middle is due to different lighting in one of the component photos. The white bar and smaller series of yellow bars at the top of the figure are 2-mm scale bars.



A 17-cm thick, NW-SE trending micrite injection in sandstone, near the crest of Pine Butte. This is among the thickest of the injections found. Thin sections of the micrite show a subtle chaotic to swirled texture suggestive of flow. Bands of calcite crystals near the edges of this injection suggest opening of void space during shear reactivation along the walls of this vein. Notebook (12 cm x 19 cm) for scale.



Small, simple injection fracture in an oil-stained, calcite-bearing sandstone. The fracture displays a central micrite fill and a halo of calcite cement: see the following figure for details.



Photomicrograph collage (taken by Peigui Yin) of sample 8/12-7 shown in the previous photo. Fracture has a narrow silty micrite filling with a central calcite-crystal zone, and is surrounded by a halo of pink-stained, highly cemented, low-porosity sandstone that contrasts with the blue-epoxy filled, high-porosity zones of the normal host rock at the edges of the figure. The black bar and series of smaller yellow bars at the top of the figure are 2-mm scale bars.

Injected micrites may or may not include dispersed, floating sand grains. Layers of entirely different injected materials (sand, micrite) are commonly found as adjacent layers in the same vein. Some veins are filled with different materials at different locations along their length, transitioning from sand to micrite to large, white calcite crystals (suggesting precipitation in open void space) along strike over distances of a few tens of meters.



Sample 8/12-2: simple hydraulic fracture of sandstone injected into sandstone. See the following photo for details. Alhbrant and Harris (1975) described similar features in the Casper Formation.



Photomontage, taken by Peigui Yin, of a thin section across sample 8/12-2, showing the difference in cementation between the better-cemented, low-porosity, pink-stained injection material and the blue, epoxy-filled porosity in the host sandstone. This figure also shows a distinct difference between the two sand grain-size populations which indicates that the source of the injected material was not the host rock. Black bar is 2 mm



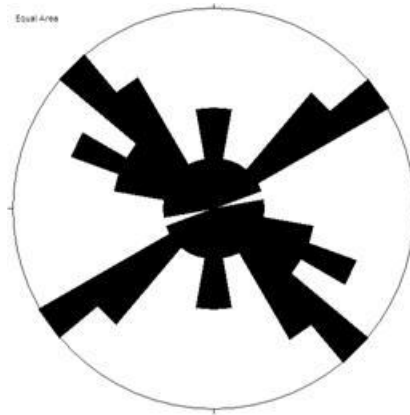
A two-cm thick vein filled with large calcite crystals. Hydraulic fractures locally transition abruptly from sand and/or micrite filling to such crystalline calcite along the length of an injection. Similar calcite-crystal layers are also found in layers parallel to clastic injection materials along some of the planes.

Meter-Scale Characteristics of Hydraulic Fractures

Strikes and Dips

Hydraulic fractures, whether or artificial such as those created during oil reservoir stimulations or natural such as those described here, form in the plane defined by the maximum and intermediate principle stresses, opening their walls against the minimum principle stress since that requires the least amount of energy. In poorly consolidated sands where little stress anisotropy can be supported, any pre-existing fabric in the rock such as sedimentary structures will play an important role in controlling the directions of fracture propagation. If no structures are present and the stresses are nearly isotropic, hydraulic fractures are poorly constrained and will have irregular orientations.

At Flat Top Mountain, and more so at Pine Butte, the orientations of the smaller hydraulic fractures tend to wander along their length, and rose plots of their strikes are correspondingly diverse. In some places adjacent fractures cut across one another several times in confusing, mutually cross-cutting relationships. The strikes of these smaller fractures as a whole are highly variable, especially when large numbers of them are measured in adjacent outcrops. Larger hydraulic fractures however, tend to strike sub-parallel the tectonic fractures.



Irregular strikes of small hydraulic fractures on a bedding-plane pavement at Pine Butte, as measured by an 8-m diameter circular scan line. $n = 33$



Poorly constrained strikes in a mesh of small hydraulic fractures at Pine Butte. Fractures splay, branch, and cut across each other, suggesting that little stress anisotropy and no strong sedimentary fabric was present at the time of fracturing. The sandstone immediately adjacent to the hydraulic fractures is better cemented, supporting weathering-resistant ridges.

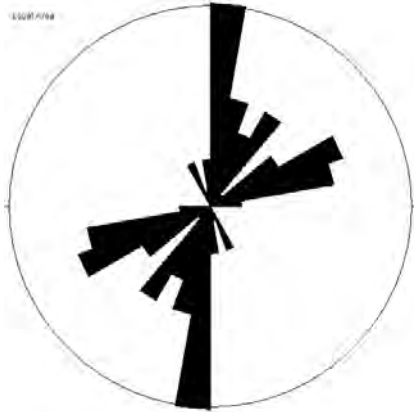


A system of hydraulic fractures that turns and splays as it approaches the viewer. One branch diverged abruptly from the system and would be expected to be younger than the other, more similarly-oriented fractures. However, the prominent intersection in the middle of the photo (arrow) suggests that the divergent branch is in fact older (see next photo for detail). Field notebook for scale.



Intersection between two hydraulic fractures of the same system. The diagonal, upper left to lower right fracture is the divergent fracture noted in the previous photo; refraction of the left to right fracture as it crosses suggests that the divergent fracture was present when the left to right fracture propagated across the area. (boot for scale).

At Flat Top Mountain on the Flat Top Anticline, the larger hydraulic fractures and the tectonic fractures are both dominantly vertical and strike NNE-SSW, and, less commonly, ENE-WSW. At Pine Butte, however, the larger hydraulic fractures strike irregularly north-south, whereas the rarer tectonic fractures have widely dispersed strikes.



Flat Top Mountain. Left hydraulic fractures (n = 64). Right: tectonic fractures (n = 79).



Pine Butte: Left, hydraulic fracture (excluding the circular scan line data) (n = 93). Right: tectonic fractures (n = 33)



Planar, 10-degree striking tectonic fracture, sub-parallel to a group of more irregular hydraulic fractures (marked by raised weathering ribs).

Hydraulic fractures have systematic strikes at Pine Butte. They are more numerous and more systematic than the few local tectonic fractures, with N-S strikes dominating in the backlimb, crest, and forelimb of the structure (see Appendix). Small, obliquely striking fracture populations are present on the Pine Butte in the eastern part of the crest nearest to the NNE-SSW striking fractures of North Flat Top Anticline, and in the backlimb.

Vertical Extents of Hydraulic Fractures

Exposures of several tens of meters of Tensleep section in single outcrops, and deep erosion in different parts of the section at Pine Butte, enable tracing many of the hydraulic fractures vertically for ten meters or more and allows investigation of their distribution throughout the section. In spite of the good exposures, the vertical terminations for these structures, top or bottom, are rarely obvious, most of them extending the entire height of an outcrop. Many of the apparent terminations at bedding boundaries turn out on close inspection to be related only to changes in fracture expression between the two lithologies, i.e., in the less well cemented host lithologies, the cementation halos adjacent to a hydraulic fracture create a conspicuous weathering rib as the host rock weathers, whereas little weathering relief exists across a hydraulic fracture in better-cemented lithologies: many of the apparent hydraulic fracture terminations at bedding contacts are illusory.

In many cases, however, there is a change in fracture character as it transitions between two lithologies. Some of the noted differences include fractures that are multistranded in one lithology and single-stranded and singular in another, and fracture surfaces that are planar in one lithology but irregularly curved in another, suggesting differences in cementation and/or stress conditions in the two lithologies. However, no rule of thumb could be extracted from the observations: i.e., a given fracture characteristic could not be associated consistently with a given lithology. Although at Flat Top Mountain the thick-bedded, horizontally bedded sandstones contain the highest percentage of hydraulic fractures and while those hydraulic fractures are the least planar and most commonly branching fractures at that outcrop, that relationship does not extend to the horizontally bedded sandstones at Pine Butte.



Closely spaced hydraulic fractures in an eight-meter high canyon wall on the southwest flank of Pine Butte. Individual fractures can be traced for many meters vertically, but obvious tops and bases have not been found.



Hydraulic fractures, most of which seem to terminate at the contact between a cross-bedded sandstone and the overlying horizontally bedded sandstone. Close inspection shows that most of the fractures do in fact continue between the two beds rather than terminating at the contact.



Hydraulic fractures that do terminate at a bedding contact, suggesting that they formed prior to deposition of the overlying, horizontally bedded sandstone.



A hydraulic fracture that is multi-stranded in the lower, cross-bedded sandstone but that has a singular plane in the overlying horizontally bedded sandstone.



Hydraulic fracture that is a single, regular plane in the crossbedded sandstone below the yellow field notebook, but that becomes irregular and curved in the overlying horizontally bedded sandstone.

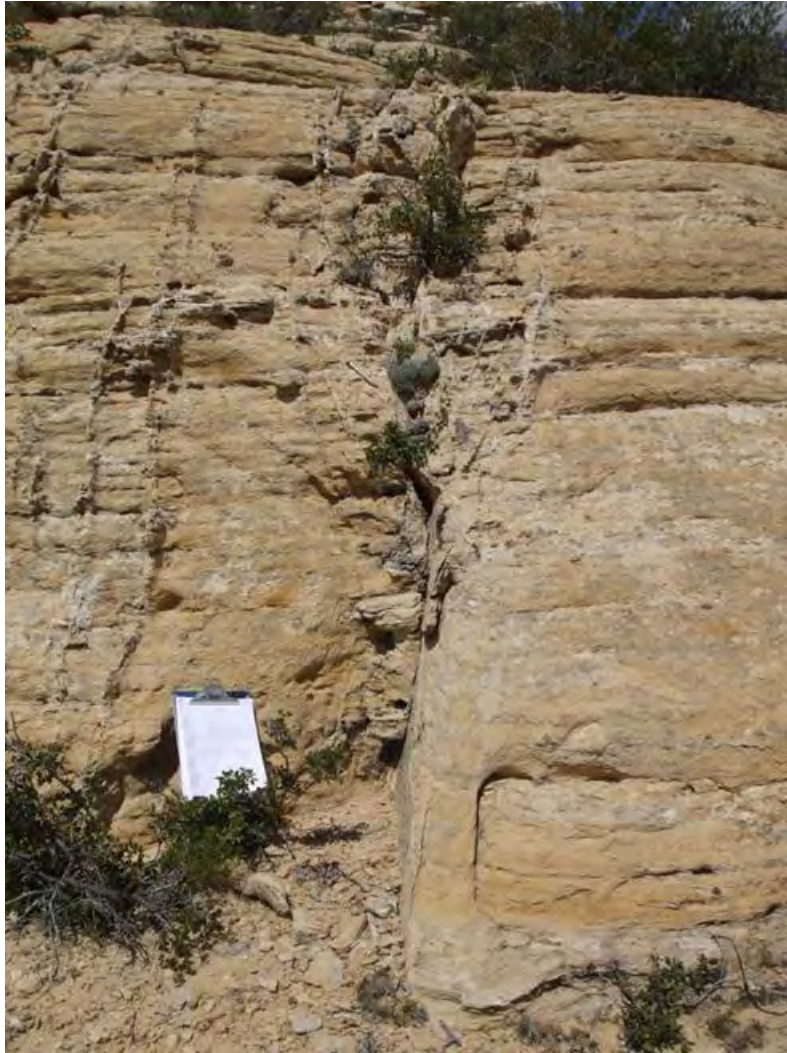
The lower terminations of the hydraulic fractures were never obvious, and they could never be traced to an obvious underlying source. The inability to correlate hydraulic fractures with sources is frustrating, yet, according to Holly and Lonergan (2002), it is also apparently common.

Branching

Some of the Tensleep hydraulic fractures branch, either upward or downward. In these cases multiple injections used a common pathway in the trunk of the fracture. Assuming an upward migration of fluid (most common according to Holly and Lonergan, 2002), the trunk system either gathered fluid and injectite from the rock below towards a common pathway, or dispersed materials from the trunk into the rock above. In the latter case, the trunk of the branching hydraulic fracture originated at a more planar fracture with a parallel strike in the underlying bed of cross-bedded sandstone.



Left: a branching-downward hydraulic fracture in horizontally bedded sandstones at the southwest edge of Flat Top Mountain, backpack for scale. The orange arrow shows the location of the close-up at right, which shows the trunk of the system, displaying at least seven distinct layers of micritic limestone (finger for scale). This unit of horizontally-bedded sandstone contains numerous hydraulic fractures, including the upward-branching one shown in the following photo.



NNE-SSW-trending hydraulic fracture, from the same horizontally bedded sandstone as the previous photos but several hundred meters to the east, on the south slope of Flat Top Mountain. This fracture branches upward from a more planar fracture in the underlying cross-bedded sandstone. Clip-board for scale.



A thin, bedding-parallel splay (above the knife), branching off of an inclined, sandstone-filled hydraulic fracture in cross-bedded, oil-stained sandstone. The sill orientation implies a low level of injection energy required to lift the overburden during dike emplacement, and thus shallow burial.

Distribution

The abundance of hydraulic fractures in the Tensleep Formation on Flat Top Anticline varies with both location and stratigraphy. At Flat Top Mountain, hydraulic fractures are most common in the thick, horizontally bedded sandstone bed near the middle of exposed stratigraphic column, where locally they comprise as much as 60% of the observed structural features. Westward, at Pine Butte, hydraulic fractures become larger and pervasive, locally dominating the system almost to the exclusion of all other types of strain-accommodation features, but with no preferred host lithology.

Hydraulic injection fractures are apparently more common along Flat Top Anticline than they are in other Tensleep deposits. None were noted in several Tensleep cores taken from the Teapot Dome, but the “sand-filled fractures” that have been reported other Tensleep cores (e.g., Emmett et al., 1971) are probably hydraulic injections. Outcrop examples were reported from the stratigraphically similar Casper Formation in southeastern Wyoming (Ahlbrandt and Harris,

1975), but only a few small examples were noted in the Tensleep Sandstones that crop out at Alcova Dam and at the upper end of Alcova Lake, despite an intentional search for them. The abundance of hydraulic fractures at Pine Butte indicates that conditions were more favorable for their formation at that location, although whether it was due to optimum stress conditions or to the presence of more easily fluidized injectite sources is not obvious.

Time of injection

Much of the evidence suggests that the clastic dikes were injected when the rock was incompletely lithified. The sand grains along the walls of the injections are never broken, and isolated sand grains are commonly included in micritic vein fillings, suggesting that they were easily stripped from the wall rock during injection. Evidence for poor lithification also includes pinch and swell along many injections and small inclusions of the host rock within them. Unfortunately, this does not really constrain the time of injection because the Tensleep sandstones have never been strongly indurated.

Many examples show calcite crystals lining both walls of the host rock with the injectite material occurring between the calcite layers, suggesting that some of the injections may have intruded pre-existing, mineralized tectonic fractures. Alternatively there may have been a chemical reaction between injected fluids and formation waters that caused precipitation of calcite along the fracture walls as well as out into the porosity of the host rock to form the present-day weathering-resistant ridges.

An analysis of the evidence and theories for the timing of injection is presented below.



Photomicrograph, by Peigui Yin, showing unbroken sand grains and mis-matched walls along a micrite-filled injection fracture, suggesting poor lithification of the host sandstone at the time of injection. 0.5 mm yellow scale bar.



Irregularly shaped injection of micritic material with inclusions of the host-rock sandstone, suggesting that the rock was incompletely lithified at the time of injection. Pencil point (top center) for scale.



Hand sample showing a layered fracture in oil-stained (dark brown) sandstone. The fracture consists of a layer of micrite (tan zone at the arrow head) between two layers of white calcite, and includes an irregular halo of better cemented sandstone (light brown) that is not stained with oil.

Ahlbrant and Harris (1975) reported bedding in the Casper Formation that is upturned at the edges of injections as if poorly lithified sand had been drag-folded by the flow of the injection. This has not been observed at Flat Top Anticline, but a few instances were found where bedding in the sandstone has been thickened immediately adjacent to a hydraulic fracture, having been shouldered aside by the lateral force of the added material in the injection, and there are many examples of un-sheared yet mis-matched fracture walls, indicating differential expansion and poor lithification.

In the oil-stained parts of the formation, the bands of cemented rock next to the fractures are not stained with oil. This suggests that fracturing and the associated halo of oil-excluding cementation occurred before oil migrated into the formation, or before Early Jurassic time, if the scenario suggested by Stone (1967) is correct and assuming that the cementation halo is associated with the injection processes. Alternatively, precipitation of cement may have driven out pore-filling oil during cementation.



Inclined, heavily calcite-cemented white sandstone injection in a poorly-cemented, cross-bedded, oil-stained sandstone. Poor lithification of the host rock at the time of injection is indicated by bending and thickening of the bedding within a few centimeters of the injection.

Several exposures of the contact surface between an injection fracture and its host rock show an irregular pattern of curved and wavy, generally concave-down ridges. I have found no other reported examples of this type of pattern in the literature on clastic dikes, and although they are not listed in Peterson's (1968) catalog of "Flow structures in sandstone dikes", one possibility is that they record flow patterns during injection.



Possible flow structures on the host rock-wall, exposed where a clastic dike has been weathered away; southern slope of Flat Top Mountain.

Multiple Injection Events

Multiple injection events along the same planes are suggested by layering and locally by the presence of significantly different components (micrite, sand) in adjacent layers in the injections. Although layering in single-component bands may be related to flow during injection, repeated injections are also indicated by local disruptions of previously-deposited layers by later injections and the resulting centimeter-scale intraclast breccias composed of fracture-filling material.



Multiple micrite layers in a hydraulic fracture, some of which have been broken up by subsequent injection along the same plane to form an intraclast breccia.

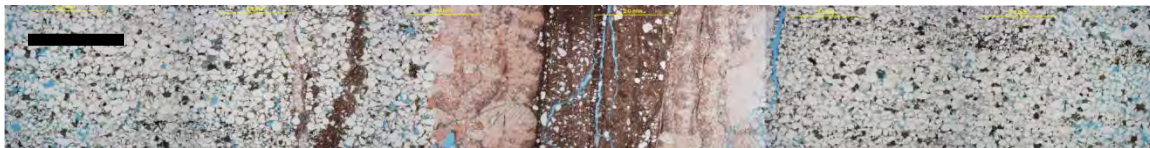


Thin-section montage by Peigui Yin, of a different fracture, showing pink-stained micrite (left-center, layered and with included sand grains), sand with an intraclast breccia and calcite-crystal void fillings (center, formed from another micrite layer and apparently disrupted by the injection of sand), and other layers of micrite, calcite crystals, and calcite-cemented sand, all indicating multiple injection events.



Hydraulic fracture filled with micrite layers and breccia in a sandstone host rock. The breccia suggests disruption of deposits left by earlier injections, the bulbous form of the fracture plane suggests that the host rock was not well indurated at the time of injection.

Bands of twinned calcite crystals are also common along the hydraulic fractures, most commonly as the layer(s) immediately adjacent to the host rock. Calcite crystals suggest that open void spaces were present at times, and the common injection of other materials between two bands of crystals suggests that the injections may have taken advantage of pre-existing weakness planes along mineralized fractures.



Photomicrograph montage, taken by Peigui Yin, showing micrite injected between two layers of calcite mineralization. Black 2 mm scale bar.



Photomicrograph montage, taken by Peigui Yin, showing sand injected between two layers of calcite mineralization. Black 2 mm scale bar.

Twinning of the crystals indicates that they were subjected to pressures in excess of 200 bars (2900 psi) at least once during the geologic history of the strata, and argues against an origin of the calcite as a replacement for anhydrite during weathering at the surface.



Photomicrograph montage, taken by Peigui Yin, showing twinned calcite crystals as one of the bands lining this hydraulic fracture. The photo also shows well cemented sandstone immediately adjacent to the fracture, grading on the right to higher-porosity sandstone. Black 2 mm scale bar.

Hydraulic Fracture Interpretations

The characteristics of the sand- and micrite-filled clastic dikes, and their comparisons with published examples, confirm that these structures are natural hydraulic injection fractures, but the timing of injection and the sources of pressure and materials are obscure. It must be possible because it happened, yet constructing plausible conceptual models for the origins of these structures is difficult because there are many unknowns and because the data are contradictory.

In order to inject foreign material into a formation, there must be an unconsolidated or easily fluidized source of that material, fluid to help transport it, and a pressure gradient to drive

it from one area to the other. A pressure seal is usually considered to be necessary to create a temporary but steep pressure gradient, along with some triggering event that breaches the seal and allows localized, abrupt injection (see Holly and Lonergan, 2002).

As noted above, the points of origin of these hydraulic fractures have not been found even though nearly the entire thickness of the Tensleep Formation is exposed at Pine Butte. A source of sandstone injection material is not problematic in this sandy formation, but there are few obvious sources for the microcrystalline micritic limestone since only a few of the carbonate interbeds that are common elsewhere in the Tensleep Formation are present in this area: those that are present are thin and laterally restricted, and are composed of dolomite rather than limestone.

Interpretations of the origin of these injections should be compatible with most of the data, the exceptions being accounted for, and should be compatible with theory. Two possibilities are considered here, each with strengths and weaknesses:

1. The injections may be syn-depositional, the strength of this theory being that injection would have taken place when the sediments were unconsolidated and easily mobilized.
2. The injections may have occurred much later, during Laramide folding, the only well-known tectonic event to have affected the strata, which would explain the parallelism between injections and the tectonic fractures.

Syn-depositional injection

Some clastic dikes form during deposition and early burial. Most examples of syn-sedimentary hydraulic fractures world-wide come from non-analogous marine environments, but Oomkens (1966) suggested that the weight of migrating sand dunes over crusted-over, soupy, muddy/evaporitic interdune sabkha deposits is one possible source of both localized pressures and foreign injection material in eolian sandstones. The upper terminations of some of the Tensleep hydraulic fractures at bedding planes suggests that some of them formed soon after or even during deposition of the rock.

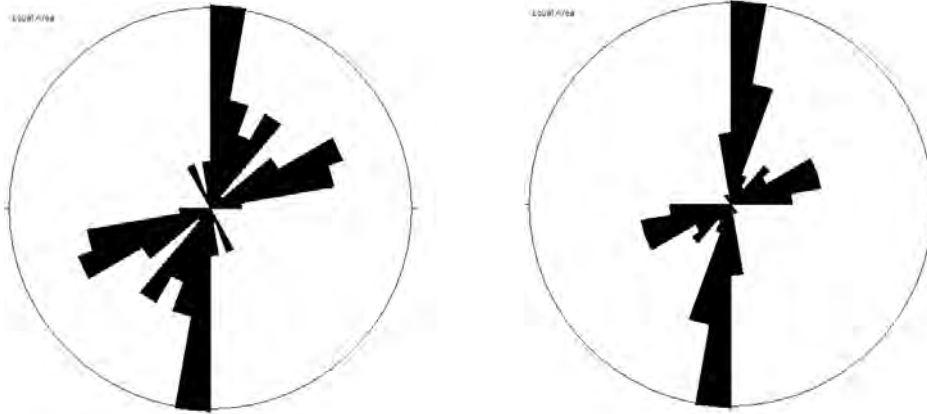
One possible mechanism for producing injection fluids and transporting foreign sand into another bed of Tensleep sandstone during early burial is the conversion of the pervasive gypsum that originally cemented the sandstones to anhydrite plus water during burial. This transition

occurs at about 50° C (Jowett et al., 1993), or at about a kilometer of burial under normal geothermal gradients. The volume of anhydrite after the phase transition is 30% less than the original volume of gypsum, but it releases water and the combined volume of anhydrite plus water exceeds the original volume of gypsum by 10%. If the water was trapped by bedding and loaded to high pressure by the overburden, it would be prone to being squirted out of the system, upward towards lower pressures, carrying with it foreign material to be injected into the newly formed cracks.

Such a system could account for the absence of obvious injectite sources since the entire stratigraphic section of sandstone was cemented predominantly with gypsum, but it does not offer a source for the micrite injections. It could explain, though not uniquely, the dominantly vertical, dike orientation of the injections, since the overburden stress usually exceeds the horizontal stresses at depths deeper than about 500 m, making it difficult to form horizontal sill injections.

This scenario does not explain why, other than by unlikely coincidence, the strikes of the hydraulic and tectonic fractures should be so similar. One possible source of early folding stress that might account for this similarity is the orogeny that formed the Ancestral Rocky Mountains, the duration of which included the span of Tensleep deposition. Although the major structures of this orogeny are found south of Wyoming (e.g., Ye et al., 1996), the Front Range/Laramie Mountains that are part of it extend into southeastern Wyoming. It is possible that a pre-Laramide structure was formed at Flat Top Anticline, a Pennsylvanian, syn-depositional fold with related injection fracturing. Syn-depositional deformation might also account for the reported 30% thicker Tensleep section at this location, but this reconstruction remains speculative.

Some of the hydraulic fractures appear to have been injected into existing tectonic-fracture weakness planes, whereas some of the tectonic fractures apparently followed planes of weakness provided by existing hydraulic fractures. Once again the age relationships of structures and events are ambiguous, suggesting multiple events of formation for many structures, and a single theory of origin may not accommodate all the data.



Parallelism between hydraulic and tectonic fractures at Flat Top Mountain.
 LEFT: hydraulic fractures (n = 64). RIGHT: tectonic fractures (n = 79).

Post-depositional injection

Another possibility, not necessarily mutually exclusive with the syn-depositional theory, is that injection took place well after deposition, at or nearly at the same time as the known tectonic fracturing, i.e., during Laramide folding in Late Cretaceous-early Tertiary time. This could more easily explain the parallelism between tectonic and hydraulic fractures and the ambiguous age relationships, and fits well with the best-known tectonic events and stresses. Such compression could easily have created strong local pressure gradients necessary for hydraulic fracturing, and the better development of hydraulic fractures on Pine Butte could be explained by the more acute folding of this structure.

In this scenario, the larger hydraulic fractures would have tended to form parallel and sub-parallel to tectonic fractures because they were forming under the same stress conditions, but also because locally they were exploiting existing tectonic-fracture planes of weakness. As noted, many of the hydraulic injections seem to have been intruded between calcite layers that could be the remnants of mineralized tectonic fractures, although it's unclear why so many tectonic fractures should have been mineralized with double layers of calcite.

This scenario of post-depositional hydraulic fracturing related to Laramide folding does not solve the enigma of the micrite source, a problem common to both theories. More importantly, it requires the fluidization of sands that had ostensibly been buried and cemented, albeit only by gypsum, for millions of years, and it does not mesh with the observation that the

fracture cementation halos do not contain oil and therefore seem to predate the hypothesized Early Jurassic migration of oil (Stone, 1967).

The first question is addressed by observations of widespread fluidization of lithified strata, including the fluidization of conglomeratic and volcanoclastic sandstones of the Andean thrust belt and their injection into advancing thrust sheets (Winslow, 1983). A modern example of fluidization despite cementation is the problematic “produced sand” that disaggregate and enter many industry wellbores during the stress changes associated with production. Thus the need to mobilize cemented sand, especially poorly indurated sand such as that of the Tensleep Formation, does not vitiate the theory of late injection.

The evidence that suggests fracturing prior to oil migration (i.e., the cementation halos that exclude oil from the matrix rock immediately adjacent to many hydraulic fractures) may be conclusive. The presence of oil in a formation slows but may not entirely arrest the precipitation of cement on sand grains (e.g., Bjorkum et al., 1993). Growth of cement could either prevent invasion by oil, or it could have driven oil out of sandstone pores during cementation. Fracturing could be later than oil emplacement.

Having Your Cake and Eating It Too

Many of the hydraulic fractures are inferred here to be post-depositional in age, probably related to thrusting and anticline formation during Laramide tectonics. However, it is likely, given the numerous conflicting and even mutually-exclusive age relationships between different structures observed along the Flat Top Anticline, that there were several episodes of both hydraulic and tectonic fracturing. Early hydraulic fracturing related to the gypsum-anhydrite conversion during burial may account for the smaller, hydraulic fractures with wandering and irregular strikes, while most of the larger hydraulic fractures may have developed later, during Laramide folding.

Fracture Mineralization

Almost all Tensleep fracture mineralization and matrix cement in the subsurface across Wyoming consists of anhydrite, therefore the calcite cement and fracture filling at Flat Top Anticline is plausibly interpreted as a replacement of anhydrite and gypsum during recent exposure to surface conditions (Yin, personal communication). However, the larger calcite

crystals in the fractures are obviously twinned, indicating that they must have been subjected to significant differential stresses at some time in their history (e.g., Jamison and Spang, 1976). Twinning is unlikely in surface-related anhydrite-replacement calcite since they would never have been subjected to high differential stresses, therefore the calcite crystals in the fractures are inferred to be primary.

Fracture reactivation

Evidence for several stress and fracturing events, in addition to the multiple injections along individual fractures, includes indications of post-injection shear offset on many of the hydraulic and tectonic fractures. This is especially common at Pine Butte, where the paucity and irregular strikes of tectonic fractures can be plausibly explained by preferential strain accommodation along reactivated hydraulic fractures during folding rather than by the formation of new tectonic fractures. Evidence for reactivation includes lozenge-shaped, diagonal pull-aparts between parallel fractures, local breccias along the fractures, and bands of calcite crystals within the fractures that display a poorly interlocking, disrupted/granulated texture.



Shear re-activation of two NNW-SSE-trending hydraulic fractures on Pine Butte is indicated by calcite-filled lozenges, showing centimeter-scale left-lateral shear along the fracture planes that opened sigmoidal void spaces along diagonals between them.

Implications of Hydraulic Fractures for Reservoirs

The presence of pervasive injections of well-cemented sandstone and/or dense micrites will severely compartmentalize a reservoir and degrade the efficiency of hydrocarbon recovery, since the injected materials have significantly less porosity and permeability than the high-porosity host rock. Even the smaller injection fractures have a cementation halo of much-reduced porosity a few centimeters wide that will significantly degrade permeability transverse to the fractures.



Heavily cemented zones around a network of hydraulic fractures, developed in poorly cemented sandstone which has weathered away to leave the network standing out in relief. Such zones will significantly degrade permeability and compartmentalize reservoirs.

Where the injection fractures are parallel, with spacings on the order of meters to a few tens of meters and vertically continuous across bedding as they are at Pine Butte, reservoirs would be segmented into vertical, high-permeability slabs that trend parallel to the injections. The slabs would have to be either drilled through horizontally or broken across with artificial hydraulic fractures in order to access trapped hydrocarbons. Vertical wells would only access the few slab compartments adjacent to the well.



The lavender-colored ribs in this photo are 15-cm thick, parallel, micritic injection fractures that would be capable of compartmentalizing a reservoir in one axis. Hammer (center of the photo) for scale.

However, the micritic injections, if not the sandy ones, are internally cracked and may merely create permeability baffles rather than complete permeability barriers. Meter-square expanses of the sides of injections are exposed in several outcrops, and in all cases the sheet of injected micrite is cracked and broken into decimeter-scale blocks. The cracks often have an irregularly horizontal fabric. The reason for this cracking is unclear but could be related to shrinkage during lithification after injection. It does not appear to be caused by weathering, since it is not a dissolution texture and since the crack patterns on northeast-facing outcrops are similar to those on the southwest faces that get more sunlight and weathering. Peterson (1968) included an un-interpreted figure of a few similar cracks, which he called “irregular cleavage” (his Figure 9) in a sandstone dike. The numerous igneous dikes that transect the Raton Basin in

New Mexico-Colorado display similar cracking at a larger, meter scale, that are probably related to cooling and related shrinkage after magma injection.



Side view of a micrite-filled, centimeter thick injection fracture, showing numerous cracks that would allow fluid flow across the low-porosity baffle. Pencil point for scale. See also the similar cracks on the sides of the thicker injections in the previous photo.

FAULTS

Several small faults cut the Tensleep section on the Flat Top Anticline. One cuts across the eastern end of Flat Top Mountain, trending N20°E and consisting of a zone up to 1.5 m wide of shear planes, minor fault breccia, and local voids filled with large calcite crystals. Offset must have been primarily strike-slip since little vertical offset of the bedding is apparent. Local en echelon shear planes suggest associated left-lateral motion although the numerous fault planes indicate multiple reactivation events, possibly with several senses of offset. Centimeter-scale calcite crystals of several colors indicate that this fault was permeable to fluids at several times in its history: it would form an irregular permeability conduit in a reservoir, enhancing both vertical and lateral conductivity along the fault plane.



Strike-slip fault on the south side of Flat Top Mountain, striking 20° - 200° . The fault consists of numerous shear planes and local voids filled with cm-scale calcite crystals. Heavy mineralization makes this zone into a weathering-resistant rib protruding from the outcrop. Field notebook for scale.

Other widely-spaced and obscure faults at Flat Top Mountain strike ENE-WSW, and are apparent only from a few meters of vertical bedding offset in covered zones. Strike-slip motion in addition to the dip-slip offset is probable but cannot be documented. These faults are present along the crest and in the forelimb of the North Flat Top Anticline, where the parallelism between fault strikes and the anticline hinge suggests that they are related to folding.

Faults at Pine Butte are smaller but more somewhat more numerous, six having been noted. The faults occur in the relatively steeply dipping (30° - 35°) forelimb and consist of discrete planes marked by slickensides. Their strikes are dominantly ENE-WSW, sub-parallel to the generally E-W bedding strike. Slickenlines indicate dominantly dip-slip motion, and bedding is offset in both normal and reverse fashion by a few meters or less. These faults are probably related to folding and bed-normal strain accommodation on the forelimb during bending on this more acutely deformed part of the anticline.



Slickensided vertical fault on the forelimb of Pine Butte. Fault strikes ENE (-60°), and the slickenlines rake to record oblique-slip motion. A micrite-filled hydraulic fracture (arrow) intersects the fault plane but is not offset by it, suggesting that the injection post-dates faulting.

BEDDING-PARALLEL SHEAR

Strata on the more severely deformed Pine Butte Anticline also display local bedding-parallel shear, primarily on the forelimb, at sandstone-on-sandstone bedding contacts and along thin carbonate interbeds. The most dramatic of these shear planes occurs between a thick parallel-bedded sandstone and a thick cross-bedded sandstone in the upper third of the Tensleep section on the forelimb of the Pine Butte Anticline. The bedding contact is marked by 1-15-cm thick zone containing up to seven bedding-parallel, polished and lightly slickenlined planes. This sheared bedding contact can be traced for a few tens of meters along the bottoms of several adjacent canyons. The muted slickenlines consistently indicate shear motion along a NNW-SSE trend, normal to the hinge of the anticline. Thin sections show millimeter-thick, bedding-parallel zones of sheared sand grains interlayered with normal sandstone. This shear is interpreted to be layer-parallel flexural slip created during Laramide folding.



Shear zone (the tan-orange plane on which the hammer is lying) of comminuted sand grains between underlying crossbedded sandstone and overlying parallel-bedded sandstone, at the bottom of a canyon on the north slope of Pine Butte. Lichen grows preferentially on many of these shear planes, probably because of the greater surface area and the related easier extraction of nutrients from the crushed sand grains in these zones.



Close-up photo of the bedding contact, showing several tan-orange shear planes developed in the rock.



Polished shear surface showing low-relief slickenlines (left to right) and a cracking fabric, of unknown origin, that commonly marks the shear surfaces.



Photomicrograph montage taken by Peigui Yin, showing bedding-parallel shear planes at a bedding contact. Rock with the high percentage of blue-epoxy filled porosity is the normal rock, while the gray, low-porosity, horizontal zones of smaller (comminuted) sand are the shear zones. Top of the photo is up in the rock, black and yellow 2 mm scale bars.

One example was also noted of bedding-parallel shear localized along and within a 30-cm thick carbonate unit between two thick sandstones on the forelimb of Pine Butte Anticline. The shear zone is marked locally by a fault breccia with centimeter-scale clasts, and calcite-filled voids created by combined dilation and shear. Offset moved the bed overlying the shear zone uphill/up-dip (to the south) in a reverse sense of motion.



Sheared carbonate unit (from top to base of the hammer) consisting of disrupted bedding and shear breccia (see the next photo for details) between two sandstones. Asymmetric void spaces at the base of the unit suggest reverse, bedding-parallel offset (i.e., the top bed moved uphill, to the right). Forelimb of Pine Butte. North is to the left.



Disrupted bedding within the carbonate bed of the previous photo, created during bed-parallel shear.

Another though subtle example of bed-plane shear was noted on the backlimb of Pine Butte Anticline, on the southwestern corner of the Butte. A series of sub-horizontal, en echelon/ladder-form deformation bands below a bedding contact are oriented oblique to bedding, and suggest bedding-parallel shear with the top block offset down-dip, to the south, in normal shear.



Ladder structures in deformation bands below a bedding contact, indicating bed-parallel shear offset, top block to the south. Surface on which the azimuth (-295°) is written is nearly bedding-parallel, thus the ladders are shorter in the vertical plane.

BEDDING-OBLIQUE SHEAR

In addition to faults, fractures, and bedding-parallel shear, a more subtle and locally pervasive form of deformation is present in many of the thicker sandstones, particularly at Pine Butte. This deformation consists of sub-parallel, decimeter-spaced planes that cut across bedding at oblique angles. Individual planes can be traced for a few meters and are most common, or perhaps most commonly apparent, in the cross-bedded dune sandstone facies where they superficially resemble irregular cross-bed foresets and suggest at first look an impossible pattern of superimposed, bi-directional crossbedding in a single bed. The shear planes are less regular and more widely spaced than cross-bed foresets, and are commonly characterized by millimeter-scale ridges with adjacent grooves. These structures are difficult to sample and thin sections have not been made of them, but hand-lens examination suggests that the ridges are resistant ledges of comminuted grains formed by small-scale shear similar to deformation bands

even though offset cannot be documented. The few exposures of the surfaces that were found are not ornamented.



Closely-spaced horizontal shear planes cutting obliquely across inclined sedimentary cross-bed foresets. The shear planes are less regular and less continuous than sedimentary bedding, and are commonly marked by thin ridges.

The shear planes are most noticeable where they cut obliquely across foreset bedding, resulting in a cross-hatched pattern of intersecting, closely spaced planes. An estimated 20% of the sandstone beds in some outcrops on Pine Butte display this type of bedding-oblique shear. The shear planes typically cut across the cross-bed foreset bedding, often at nearly right angles to the foresets, but locally they curve at the centimeter scale to abut bedding, and locally they curve to join it. In the latter case it is likely that strain accommodation by shear has been transferred to the foreset bedding planes.

These shear planes seem to have developed locally where potential shear zones along bedding planes were oriented at angles that did not easily accommodate strain during folding. Shear planes are also present on the forelimb of Pine Butte where they have generally E-W strikes and where their northerly dips are steeper than bedding dips, suggesting reverse offset related to folding.



Oblique relationship between sedimentary foreset bedding (upper left to lower right) and closely spaced, more irregular, incipient shear planes (upper right to lower left) in a cross-bedded sandstone.



Intersection of three sets of planar features: hydraulic fractures (top to bottom), cross-bed foresets (nearly horizontal in this photo but dipping towards the viewer) and shear planes (upper right to lower left). Hammer for scale.

STRUCTURAL INTERPRETATION

The earliest structures in the Tensleep Formation on the compound Flat Top Anticline are deformation bands and small, highly irregular hydraulic fractures. These are inferred to have formed during diagenesis and compaction of the sediments in the early stages of burial.

Flat Top Anticline may have had a precursor structure related to the Ancestral Rocky Mountains, but the major structure formed as a bend over a developing Laramide thrust fault. Northeastward, oblique translation of the thrust sheet, rather than north-northwest translation normal to the surface expression of the thrust fault, created an early-formed set of N-S to NNE-SSW trending extension fractures during the initial stages of thrusting and before folding, parallel to the maximum horizontal compressive stress. Before, during, and after the formation of tectonic extension fractures, formation pore pressures were elevated due to the thrust-related compression. Sandstone and carbonate beds were fluidized and entrained in formation fluids by local pressure releases, to create intra-formational injected clastic dikes as natural hydraulic injection fractures.

Continued thrusting led to folding in the hanging wall. Hinge-normal extension during folding created hinge-parallel younger tectonic and hydraulic fractures; such fractures did not form on the anticline backlimbs where the strata are not folded. This mode of semi-synchronous, bi-directional extension is compatible with the mechanism of fracture formation on basement-cored anticlines developed by Cooper et al (2006).

More acute folding at Pine Butte at the western end of the Flat Top Anticline thrust fault suggests a higher level of compression, accommodated by the thrust-terminating tear fault mapped by Blevins (1984). Higher compression and tighter folding are consistent with the more highly developed hydraulic fractures in this area. Tectonic extension fractures are poorly developed at Pine Butte because strain was accommodated by the development and reactivation of a pervasive system of large, N-S-striking hydraulic fractures.

Tectonic and hydraulic fractures, as well as local deformation bands, were all formed during the course of thrusting and folding at Flat Top Anticline. Contradictory cross-cutting relationships indicate that these structures developed during multiple sequential and synchronous deformation events.

Faulting is not common except on the forelimb of the acute fold at Pine Butte, where the fold-related strain was too large to be accommodated entirely by tectonic and hydraulic fractures

or their reactivation. Bed-parallel and bed-oblique shear is also developed here as part of the suite of structures that developed to accommodate the higher levels of strain.

COMPARISONS WITH OTHER ANTICLINES

A basic pattern consisting of hinge-parallel and hinge-normal fractures is present in Tensleep strata on most anticlines in Wyoming. Fractures at Flat Top Anticline fit this general pattern, with a few significant dissimilarities. In most of the published studies from other areas of Wyoming (Alcova Anticline: Gilbertson, 2002; Zeisman Dome: McGinty, 2002, 2003; Aviantara, 1996, 1999; Sheep Mountain: Bellahsen et al., 2006a, b; Hennier and Spang, 1983), numerous fracture orientations but few fracture characteristics have been reported. Since the published fracture orientations on these anticlines suggest that most of the measured fractures are extension fractures, this will be assumed for the purposes of comparisons with Flat Top Anticline.

A pre-folding background pattern of anticline-oblique regional fractures is present at both the Alcova and Sheep Mountain anticlines, but absent from Flat Top Anticline and has not reported from Zeisman Dome. This set predates folding and its presence or absence would depend on the local pre-fold structural history.

The earliest-formed tectonic fractures are hinge-oblique at Flat Top Anticline but are analogous to the hinge-normal fracture sets that are present at all other sites. Similar fracture relative-age relationships that support this have been reported by Bellahsen et al. (2006a,b), but most authors have not noted the relative ages of their fracture sets. This set formed in extension during the early stages of layer-parallel strain that eventually led to thrusting, uplift, and folding. Since most anticlines formed during hinge-normal translation of the thrust plate, hinge-normal extension fractures were the result. At Flat Top Mountain however, the inferred hinge-oblique translation of the thrust plate explains the difference in fracture orientation from the normal pattern. This fracture set probably continued to develop by local hinge-parallel extension during subsequent uplift and folding, leading to some of the observed ambiguous relative-age relationships.

The second set of fractures common to the Tensleep strata on anticlines strikes parallel to the fold hinges and developed due to hinge-parallel extension during folding. Gilbertson (2002) indicates that fractures of this set are more closely spaced along the actual hinge of the tightly

folded Alcova Anticline, and he reports that they commonly occur as two parallel-striking sets with opposing dips, suggestive of conjugate fractures. Conjugate fracturing is not unexpected, but it did not develop at the Flat Top Anticline and has not been reported elsewhere. The change in fracture spacing noted at the crest of the Alcova Anticline is compatible with enhanced strain at the more acutely folded crest, but a similar change is not apparent on the less acutely folded Flat Top structure.

Hinge-parallel fractures are not developed on the planar back limb of Flat Top Anticline, and McGinty (2002) briefly suggests that this fracture set is also locally absent from Zeisman Dome. This fracture set is developed on the backlimbs the Alcova and Sheep Mountain anticlines, suggesting that these parts of the anticline are folded to some degree. Bellahsen et al. (2006a, b) also report differential development of fractures in five domains around Sheep Mountain Anticline.

Minor oblique fracture sets are present in most of the anticlines and probably formed at local, minor structural complexities and due to different degrees and orientations of folding during anticline development. The reactivation of fractures, as observed at Flat Top, has been reported by Bellahsen et al. (2006a, b) at Sheep Mountain but not elsewhere, probably not because it has not happened but because it was not looked for. Likewise, the bed-parallel shear that is present at Pine Butte has been noted in other Tensleep outcrops only by Hennier and Spang (1983) at Sheep Mountain. Bellahsen et al. (2006a,b), studying the same outcrops, did not report bed-parallel shear.

McGinty (2002, 2003) reports qualitatively that fractures are better developed in the parallel-bedded than in the cross-bedded sandstone facies, a relationship that was not observed at Flat Top Anticline despite data that were deliberately collected to test this relationship. Deformation bands and a few small hydraulic fractures were noted during the brief inspection of the Alcova outcrops done for this study, but Gilbertson (2002) did not break the former out of his data as a distinct fracture population and did not recognize the latter. In fact, hydraulic fractures are apparently not common in the Tensleep outcrops around Wyoming, at least not on the grandiose scale seen at Pine Butte. The extensive development of hydraulic fracturing at Pine Butte on the west end of Flat Top Anticline is the major difference between fracturing at this structure and elsewhere, at least as the other structures have been described. Hydraulic injection fractures have been noted in some Tensleep-equivalent outcrops (Ahlbrandt and Harris, 1975)

and have been described if not named from some Tensleep cores (Emmett et al., 1971; Shebl, 1996). They are likely to be significant structures in some reservoirs.

IMPLICATIONS FOR TENSLEEP RESERVOIRS ON ANTICLINES

Any fracture-permeability model for Tensleep reservoirs on anticlines based on observations from Flat Top Mountain would include a suite of permeability baffles, barriers, and conduits. Deformation bands, tectonic fractures, and hydraulic fractures would create reservoirs that would be highly compartmentalized, requiring numerous wellbores, deviated wellbores, and/or stimulation fractures to efficiently access and recover hydrocarbons. Simple systems composed primarily of hinge-normal tectonic fractures are present only on the backlimb of North Flat Top Anticline. Relatively simple two-set systems of hinge-normal and hinge-parallel fractures are present only in the thin-bedded, horizontally bedded sandstones near the top of Flat Top Mountain. All other fracture systems consist of mixes of tectonic and hydraulic fractures, the dominant trends being parallel and nearly normal to the anticlinal hinge.

Hydraulic fractures, consisting of heavily cemented sand and/or dense micrite, would create permeability barriers except that they are commonly cracked and are more likely to be baffles. Compartments created by the smaller hydraulic fractures can be as small as decimeters in scale, whereas the larger, more effective baffles created by the larger hydraulic fractures would create baffles on the tens-of-meters scale. On acutely folded anticlines such as Pine Butte Anticline, hydraulic-fracture compartments would be slab-shaped and aligned primarily across the anticline. In less deformed folds such as North Flat Top Anticline, where hydraulic and tectonic fractures are more equal in development and are also developed equally in two directions, compartments would be larger and more equilateral. Fracture patterns on anticlinal crests should consist of two intersecting sets, whereas fractures on backlimbs that were not significantly folded would consist only of the hinge-normal or hinge-oblique fracture set.

Permeability conduits would be found along the hinge-parallel faults of the forelimb and along the less frequent transverse faults. No difference in fracture development by major sandstone depositional facies is apparent at Flat Top Mountain: thick-bedded/horizontally-bedded sandstones have fracture orientations and spacings that are indistinguishable to the spacings and orientations of fractures found in the large-scale cross-bedded sandstones. Only

fractures in the meter-thick, thin-bedded to laminated sandstones are distinguishable, being more closely spaced and more regular.

CONCLUSIONS

The suite of strain-accommodation structures at Flat Top Anticline consists of early-formed hinge-oblique and later-formed hinge-parallel tectonic extension fractures, hydraulic fractures that strike sub-parallel to both of these trends and that probably formed at about the same times, deformation bands with a variety of strikes, local faults, and both bedding-parallel and bedding-oblique shear planes. These structures formed during anticline development, as the strata were extended parallel to and oblique to the anticlinal hinge. The strains leading to fracturing formed by folding, and by extension related to thrust translation, respectively. Similar structures with the same orientations probably formed at several different times during structural development of the anticlines, and were also reactivated from time to time with differing senses of offset, leaving a suite of compound features that do not record a simple, linear, progressive sequence of structures.

Development of the tectonic fractures varies by structural position but not by sedimentary facies. Only hinge-normal fractures are present on the anticline backlimbs, where hinge-parallel fractures did not develop because folding is minimal. Fractures are better developed where the degree of folding was higher on the forelimbs and anticlinal crests of the sub-structures that comprise the Flat Top Anticline. Hydraulic fractures are thicker and more common, and most of the bedding-related shear planes occur, at Pine Butte on the western end of the anticline where it is most acutely folded and where thrust translation has been inferred to be greatest. Tectonic fractures are poorly developed in this area, most of the strain having been taken up by hydraulic fracturing and reactivation of the hydraulic fractures. Hydraulic fractures are locally better developed in the thickly, horizontally-bedded sandstones than they are in large-scale dune foreset facies.

Most of these structures have been observed in and reported from the Tensleep Formation at other anticlines, although sandstone-filled hydraulic fractures have only been noted in one locality where they are not nearly as well developed as at Pine Butte. Micrite-filled hydraulic fractures have not been reported, and sand-filled fractures have been reported from a few cores. Bedding-related shear planes have also been noted by only one other author, the apparent rarity

probably being a function of non-recognition rather than absence. Most of these structures will degrade permeability in the generally high-porosity Tensleep reservoirs.

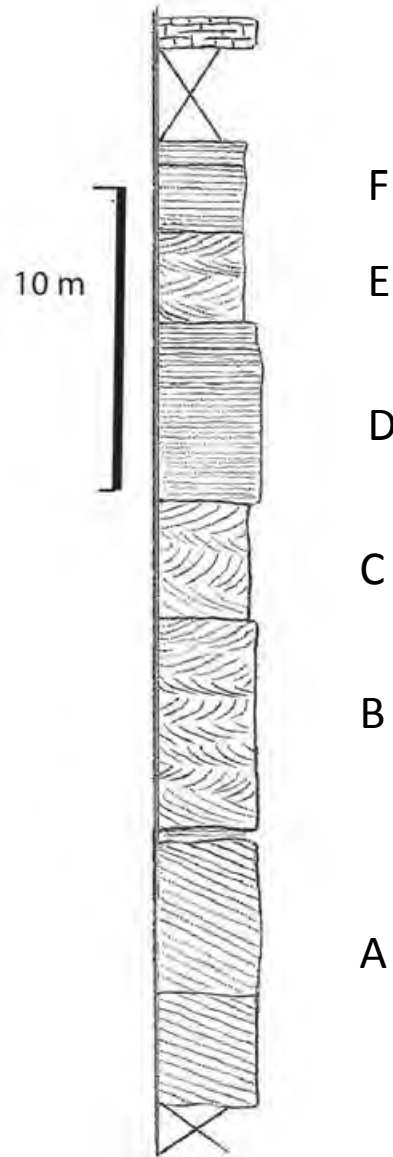
REFERENCES

- Ahlbrandt, T.S., and R.E. Harris, 1975, Clastic dikes in the Fountain and Casper formations (Permo-Pennsylvanian), southeastern Wyoming: *Rocky Mountain Geology*, v. 14, p. 51-54
- Aviantara, Arya, 1996, Facies and fracture architecture of the Tensleep sandstone, Bighorn Basin, Wyoming: preliminary result of outcrop and subsurface study (abstract): *American Association of Petroleum Geologists Bulletin*
- Aviantara, A.A., 1999, Facies architecture of the Tensleep Sandstone, Bighorn Basin, Bighorn County, Wyoming: PhD thesis, University of Tulsa.
- Bellahassen, Nicholas, Patricia Fiore, and David D. Pollard, 2006a, From spatial variation of fracture patterns to fold kinematics: a geomechanical approach: *Geophysical Research Letters*, v. 33, p. L02301, 4 p.
- Bellahassen, Nicholas, Patricia Fiore, and David D. Pollard, 2006b, The role of fractures in the structural interpretation of Sheep Mountain Anticline, Wyoming: *Journal of Structural Geology*, v. 28, p. 850-867.
- Bjorkum, P.A., Walderhaut, O., and Aase, N.E., 1993, A model for the effect of illitization on porosity and quartz cementation of sandstones: *Journal of Sedimentary Research*, v. A63, p. 1089-1091.
- Blackstone, D.L. 1994, Oil Springs and Flat Top anticlines, Carbon County Wyoming: An unusual fold pair: *The Mountain Geologist*, v. 31, p. 53-60.
- Blevens, D.M., 1984, Computer assisted structural analysis of the western termination of the Flat Top anticline, Carbon County, Wyoming: Master's thesis, University of Wyoming, 119 p.
- Carey, B.D., 1950, Geology of the eastern part of the Flat Top anticline, Albany and Carbon Counties, Wyoming: Master's thesis, University of Wyoming, 62 p.
- Cooper, S. P., Goodwin, L. B., and Lorenz, J. C., 2006, Fracture and fault patterns associated with basement-cored anticlines: The example of Teapot Dome, Wyoming: *American Association of Petroleum Geologists Bulletin*, December 2006. v. 90, p. 1903-1920.
- Duranti, D., and A. Hurst, 2004, Fluidization and injection in the deep-water sandstones of the Eocene Alba Formation (UK North Sea): *Sedimentology*, v. 51, p. 503-529.
- Emmett, W.R., K.W. Beaver, and J.A. McCaleb, 1971, Little Buffalo Basin Tensleep heterogeneity—its influence on drilling and secondary recovery: *Journal of Petroleum Technology*, February, 1971, p. 161-168.
- Gilbertson, N.J., 2002, 3D Geologic modeling and fracture interpretation of the Tensleep Sandstone, Alcova Anticline, Wyoming: PhD thesis, Colorado School of Mines.
- Glennie, K.W., 1970, Desert sedimentary environments, *in* *Developments in Sedimentology*, no. 15, New York, Elsevier Publishing Company, 222 p.
- Hennier, Jeff, and John H. Spang, 1983, Mechanisms for deformation of sedimentary strata at Sheep Mountain Anticline, Bighorn Basin, Wyoming: 34th Annual Field Conference, Wyoming Geological Association guidebook, p 97-111.

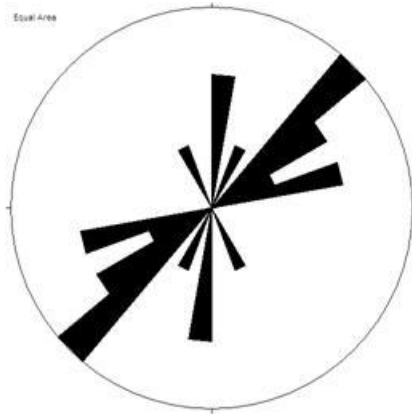
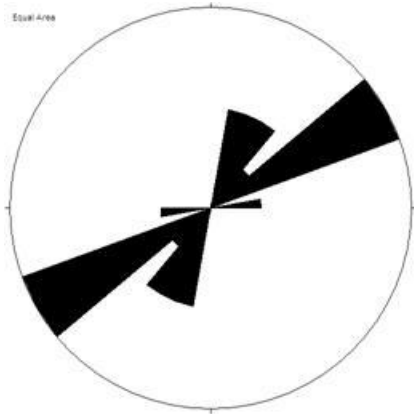
- Holly, R.J.H., and L Lonergan., 2002, Mechanisms and controls on the formation of sand intrusions: *Journal of the Geological Society*, v. 159, p. 605-617.
- Hurst, A., and J Cartwright, 2007, Sand injectites: implications for hydrocarbon exploration and production: *American Association of Petroleum Geologists, Memoir 87*, 274 pages.
- Jamison, W.R., and Spang, J.H., 1976, Use of calcite twin lamellae to infer differential stress.
- Jowett, E.C., L.M. Cathles, and B.W. Davies, 1993, Predicting depths of gypsum dehydration in evaporite sedimentary basins: *American Association of Petroleum Geologists Bulletin*, v. 77, p. 402-413.
- Kelly, A.O., 1984, Significance of interdune deposits in the upper Casper Formation: 34th annual field conference, Wyoming Geological Association, p. 97-110.
- Knight, W.H., 1944, Geology of the western part of the Flat Top anticline, Albany and Carbon Counties, Wyoming: Master's thesis, University of Wyoming, 30 p.
- Lorenz, J.C., Summary of the published information on Tensleep fractures: memo to distribution, April 20, 2007, 36 p.
- Lorenz, J.C., Teufel, L.W., and Warpinski, N.R., 1991, Regional fractures I: A mechanism for the formation of regional fractures at depth in flat-lying reservoirs: *American Association of Petroleum Geologists Bulletin*, v. 75, p. 1714-1737.
- McGinty, Sheila R., 2002, Fracture architecture of the Tensleep Sandstone at Zeisman Dome and Brokenback Anticline, Wyoming: PhD dissertation for the University of Tulsa, 170 pages plus appendices.
- McGinty, Sheila R., 2003, Fracture architecture of the Tensleep Sandstone at Zeisman Dome and Brokenback Anticline, Wyoming (abstract): *American Association of Petroleum Geologists, Annual Meeting*, June 3-6, Denver, Colorado
- Oomkens, E., 1966, The environmental significance of Sand dikes: *Sedimentology*, v. 7, p. 145-148.
- Peterson, G.L., 1968, Flow structures in sandstone dikes: *Sedimentary Geology*, v. 2, p. 177-190.
- Winslow, M.A., 1983, Clastic dike swarms and the structural evolution of the foreland fold and thrust belt of the southern Andes: *Geologic Society of America Bulletin*, v. 94, p. 1073-1080.
- Shebl, M.A., 1996, Geochemical and diagenetic investigations of the Tensleep Sandstone, Bighorn Basin, Wyoming: PhD dissertation, University of Wyoming, Laramie, Wyoming
- Stone, D.S., 1967, Theory of Paleozoic oil and gas accumulation in Big Horn Basin, Wyoming: *American Association of Petroleum Geologists Bulletin*, v. 51, p. 2056-2114.
- Ye, H., Royden, L., Burchfiel, C., and Schuepbach, M., 1996, Late Paleozoic deformation of interior North America: the greater ancestral Rocky Mountains: *American Association of Petroleum Geologists Bulletin*, v. 80, p. 1397-1432.

APPENDIX

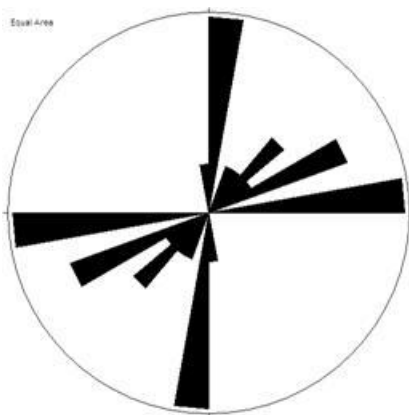
Fracture orientation data from the Flat Top and Pine Butte Anticlines



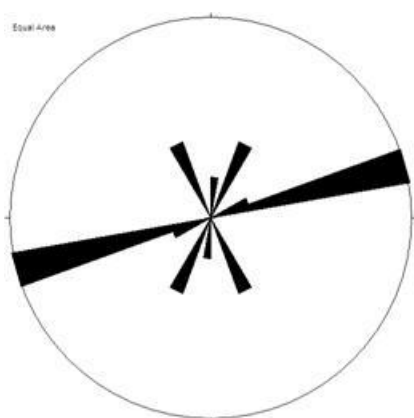
Measured section at Flat Top Mountain: lettered units correspond to the following rose diagrams.



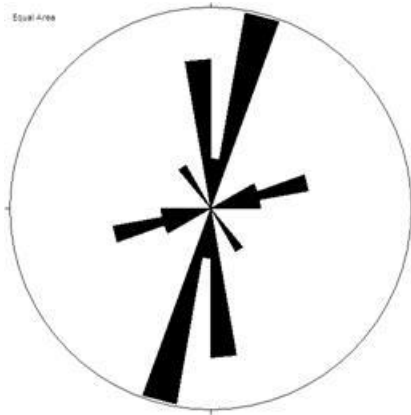
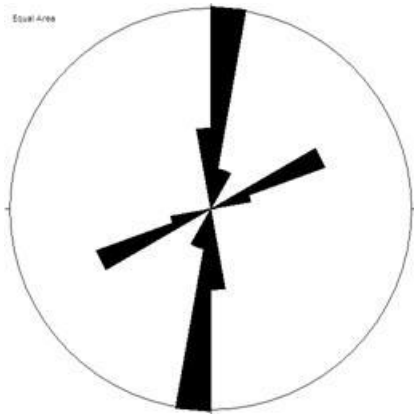
UNIT A. Left: Hydraulic fractures, $n = 16$; RIGHT, Tectonic fractures, $n = 12$.



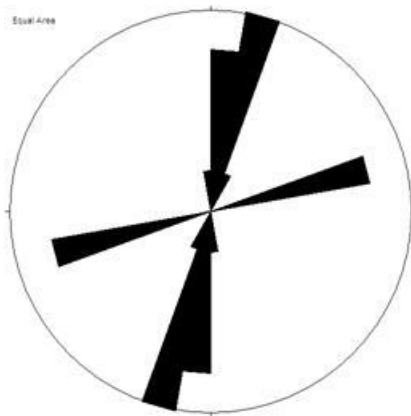
UNIT B. Left, Hydraulic fractures, $n = 8$; RIGHT, Tectonic fractures, $n = 17$.



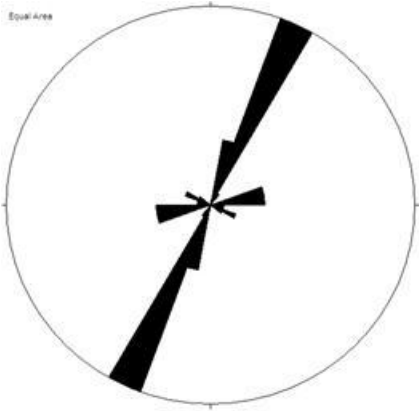
UNIT C. Left, Hydraulic fractures, $n = 11$; RIGHT, Tectonic fractures, $n = 22$.



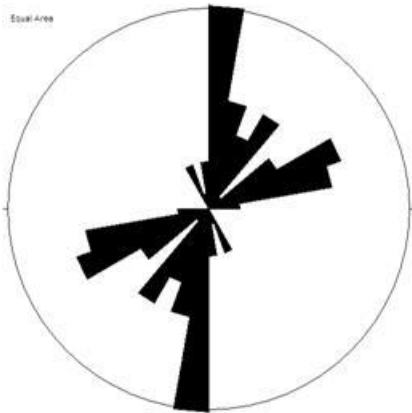
UNIT D. Left, Hydraulic fractures, $n = 13$; RIGHT, Tectonic fractures, $n = 13$.



UNIT E. Left, Hydraulic fractures, $n = 15$; RIGHT, Tectonic fractures, $n = 15$.

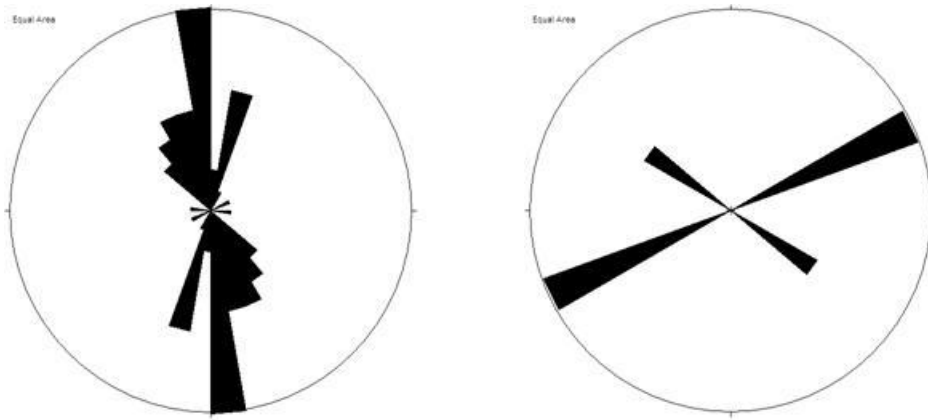


UNIT F, Tectonic fractures, n = 33. (No hydraulic fractures)

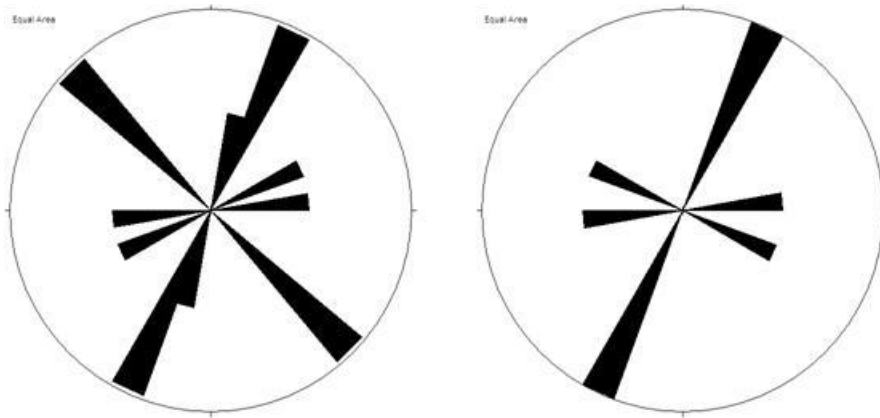


Units A-E combined: Left: hydraulic fractures, n = 64. Right: tectonic fractures, n = 79.

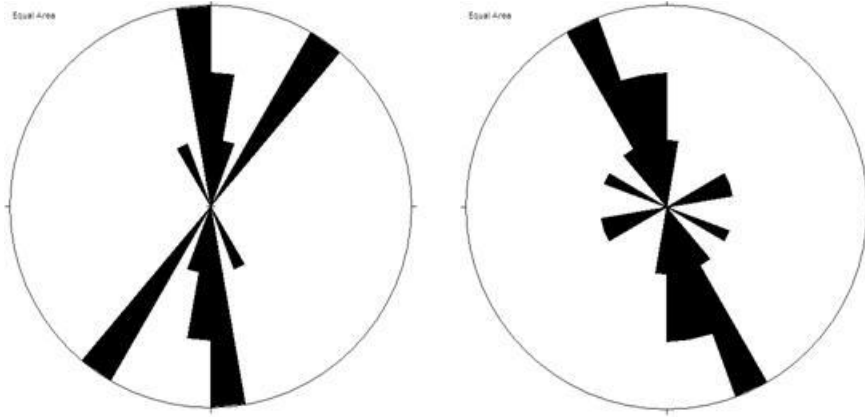
PINE BUTTE FRACTURE DATA



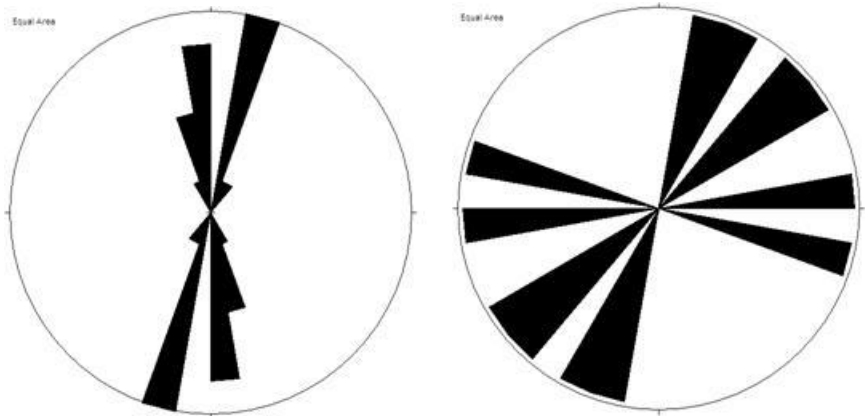
Crest of Pine Butte: Left, hydraulic fractures, $n = 38$. Right, tectonic fractures, $n = 3$. Spacings of the larger hydraulic fracture range from 1.5 to 20 m, estimated average is 10 m.



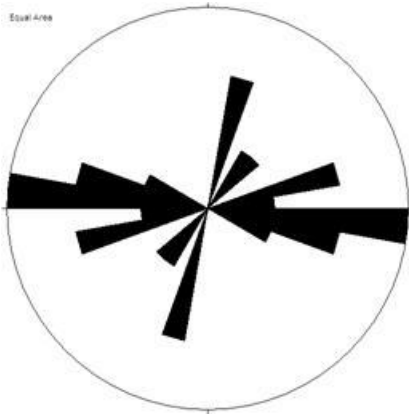
Eastern slope of the Pine Butte crest: Left, hydraulic fractures, $n = 7$. Right, tectonic fractures, $n = 4$.



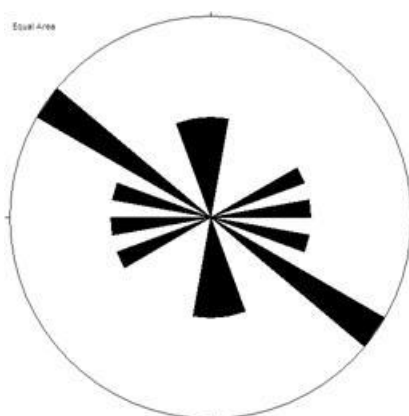
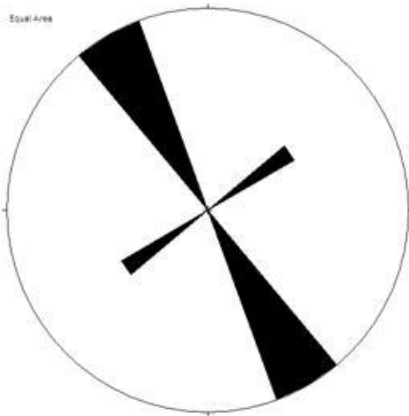
Backlimb of Pine Butte Left, hydraulic fractures, $n = 10$. Right, tectonic fractures, $n = 12$. Rare cross fractures. Many of the north-south hydraulic fractures have been reactivated in left-lateral shear.



Western and southwestern sides of Pine Butte: Left, hydraulic fractures, $n = 17$. Right, tectonic fractures, $n = 6$. Hydraulic fractures are more widely spaced in this area; some have been reactivated in left-lateral shear. Tectonic fractures are rare.



Northwestern side of Pine Butte: Hydraulic fractures, $n = 13$ (no tectonic fractures)



Forelimb of Pine Butte: Left, hydraulic fractures, $n = 5$. Right, tectonic fractures, $n = 8$.

OUTCROP STUDIES

BEER MUG ANTICLINE

Natural Fracture Patterns and Strain Accommodation in the Tensleep Formation within a Tightly-Folded Laramide Anticline, Beer Mug Anticline, Carbon County Wyoming: Implications and Data Sets for Analog Reservoirs

Scott Cooper and John Lorenz, December 2010

SUMMARY

Beer Mug Anticline, with a near-vertical forelimb and backlimb dip up to 50 degrees provides an ideal analogue for fracture systems that will have a significant effect on fluid flow in tightly folded Laramide reservoirs. Outcrop data collected over the 2009 summer field season indicate that the entire exposed sedimentary package, Tensleep Formation through the Alcova Limestone, is cut by numerous intersecting fractures.

The Pennsylvanian Tensleep Formation in south-central Wyoming is a complex package of repeated limestones and/or dolomites, and sandstones. Strata of these varied lithologic units are folded over Beer Mug Anticline and are cut by numerous intersecting fractures. Fracture type and degree of development vary systematically with lithology, structural position, and degree of folding. Fracturing is most intense towards the core of the anticline, which consists of brecciated, oil-stained rock with large-scale vuggy porosity. Most of these strata exhibit inherited F_0 fracture patterns that pre-date folding, as well as fold-related extension fractures that trend approximately normal (F_1) and parallel (F_2) to the axis of folding. The age relationships of the fracture sets are commonly ambiguous since offset is minimal and most intersections are mutually crosscutting, but pre-fold and fold-related fracture sets can be recognized. Many of the early-formed fractures were reactivated in shear and/or extension, and additional fracture sets developed as the degree of folding increased.

Within the Tensleep Formation, bedding-parallel slip, commonly along the large dune cross-bed foresets, accommodated much of the pervasive strain. Bed-parallel shear also occurred along bedding contacts between limestone and sandstone. Small offsets were also documented

on irregular calcite-mineralized planes oblique to bedding. The meter-scale limestone beds interbedded within the thicker Tensleep sandstone units accommodated much of the larger-scale bed-parallel shear through brecciation, but brecciation is not always obvious due to cementation and weathering. In fact, at a gross scale, many of the limestone beds give the appearance of being massive and completely unfractured. Granulation, brecciation, pressure solution, and cementation likely occurred nearly simultaneously with deformation. Natural hydraulic or injection fractures with random strikes occur within both sandstone and limestone strata. Some injection fractures are parallel to the ESE-WNW striking early-strain extension fractures, suggesting an age and/or mechanical relationship. Many injection fractures contain not only micritic mudstone fill but also euhedral calcite crystals suggesting extension and open aperture at depth.

Shales overlying the Tensleep Formation accommodated strain by localized bedding-parallel shear faulting. Large-scale bed parallel shears were documented at bedding contacts between limestone and sandstone in the Tensleep Formation. Small thrust faults and shear fractures in the overlying Alcova Limestone provide additional evidence that the maximum stress was in the horizontal plane and approximately ESE-WNW prior to tilting of the beds. These data suggest that the Beer Mug anticline was not passively draped over an underlying basement thrust.

ACKNOWLEDGEMENTS

The authors would like to thank the landowners; without their help, support and interest none of this work could have been accomplished. The authors would also like to acknowledge Dr. Jim Steidtmann, who initiated this project while director of the University of Wyoming's Enhanced Oil Recovery Institute (EORI). We greatly benefited from interactions with the entire staff and contractors at EORI, including Lon Whitman, Juliann Hamilton, Carolyn Coolidge, Glen Murrell, Laura Rehmeier, Brian Reyes, Geoff Thyne, Mark Tomasso, and Shaochang Wo. Dr. Peigui Yin at EORI made the thin sections and photomicrographs presented here and helped formulate their interpretations. This study was funded by and conducted for the Enhanced Oil Recovery Institute, with thanks to David Mohrbacher director.

INTRODUCTION

This field study was undertaken in effort to understand the characteristics and distributions of fractures and their influence on fluid flow within analogous Tensleep Formation reservoirs. Outcrop data from the Pennsylvanian-age Tensleep Formation can be utilized for developing models of the fracture network that can then be used to reconstruct the permeability network, thus knowledge of the fracture network and subsequent modeling can lead to more efficient strategies for enhanced oil recovery.

Fractures of various types within the Tensleep Formation have been reported in published reports (see Lorenz report of April 20, 2007) and nearby outcrops of the Tensleep Formation at Flat Top Anticline (see Lorenz report of November 13, 2007) were found to vary as a function of lithology, structural position and degree of folding. These natural fractures dominate fluid flow in Tensleep reservoirs and are therefore a dominant control on the recovery of oil from the subsurface.

The supporting data are available as Excel files available through EORI and can be utilized in a variety of modeling software. The outcrop study reported here is one of a series of projects on fractures in the Tensleep Formation from anticlines, outcrops and cores from across Wyoming for the Enhanced Oil Recovery Institute (EORI) at the University of Wyoming. When completed, copies of the longer compilation report can be requested directly from the EORI at The University of Wyoming or from their website at www.eori.uwyo.edu.

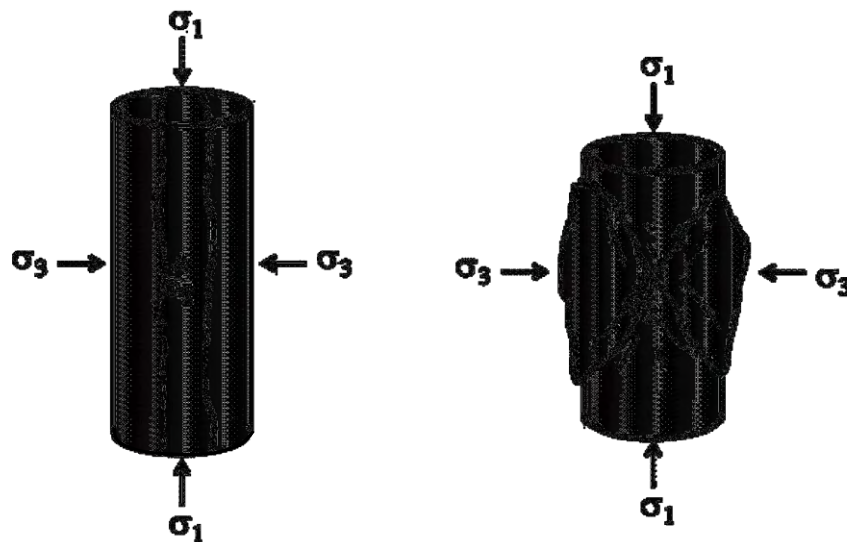
BACKGROUND

Fracture Terminology

Consistent with the terminology utilized in the fossil-energy industry, discontinuities in rock are described as either extension or shear fractures. Extension fractures, also termed joints, tensile fractures, dilation fractures, or Mode 1 fractures (Pollard and Aydin, 1988), are characterized by displacement perpendicular to the fracture wall. Extension fractures form perpendicular to the least compressive stress and would bisect the acute angle between conjugate shear fracture pairs formed in the same stress regime (Peng and Johnson, 1972; Long et al.,

1997). Tectonic fractures are extension fractures that are interpreted to have formed during a tectonic event such as the formation of Beer Mug Anticline.

Shear fractures are characterized by displacements parallel to the fracture wall, also termed Mode II or III fractures depending upon relative displacement to the fracture front (Pollard and Aydin, 1988). Deformation bands were also documented at Beer Mug Anticline. These structures are roughly planar features that record small amounts of displacement and typically form in high-porosity, poorly cemented sandstone. Deformation bands have been also referred to as coherent shear fractures or small-displacement faults (millimeters to centimeters of displacement; Aydin, 1978; Antonellini et al., 1994; Mair et al., 2000). Larger amounts of displacement can be accommodated by zones of multiple, composite deformation bands (Aydin, 1978; Aydin and Johnson, 1983; Antonellini et al., 1994).



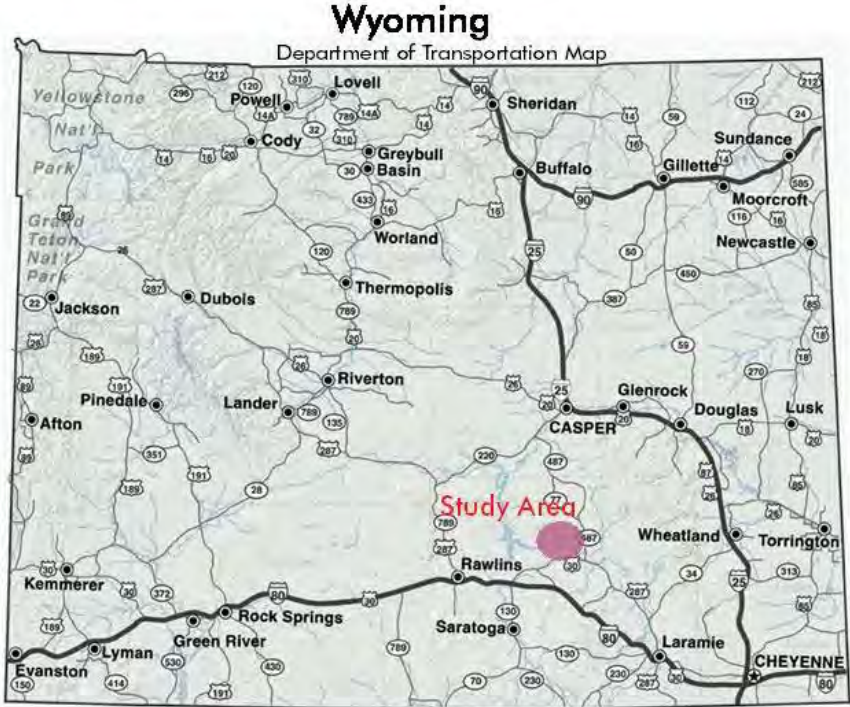
Both extension and shear fractures can be formed in laboratory compression tests with specific orientations with respect to the applied stress. Extension fractures form perpendicular to the least compressive stress (s_3), parallel to maximum compressive stress (s_1) and bisect the acute angle between conjugate shear fractures (modified from Weijermars, 1997).

Location and Structural Setting

Beer Mug Anticline is located in southeastern Wyoming, approximately 15 miles northwest of the small town of Medicine Bow. Both are at the northern margin of the Hanna basin and just south of the Shirley Mountains. Beer Mug Anticline has a near vertical forelimb and a steeply dipping backlimb (up to 50°) and has been previously interpreted as a basement involved Laramide structure by Maravich (1941), Stone (1993) and Taylor (1996).



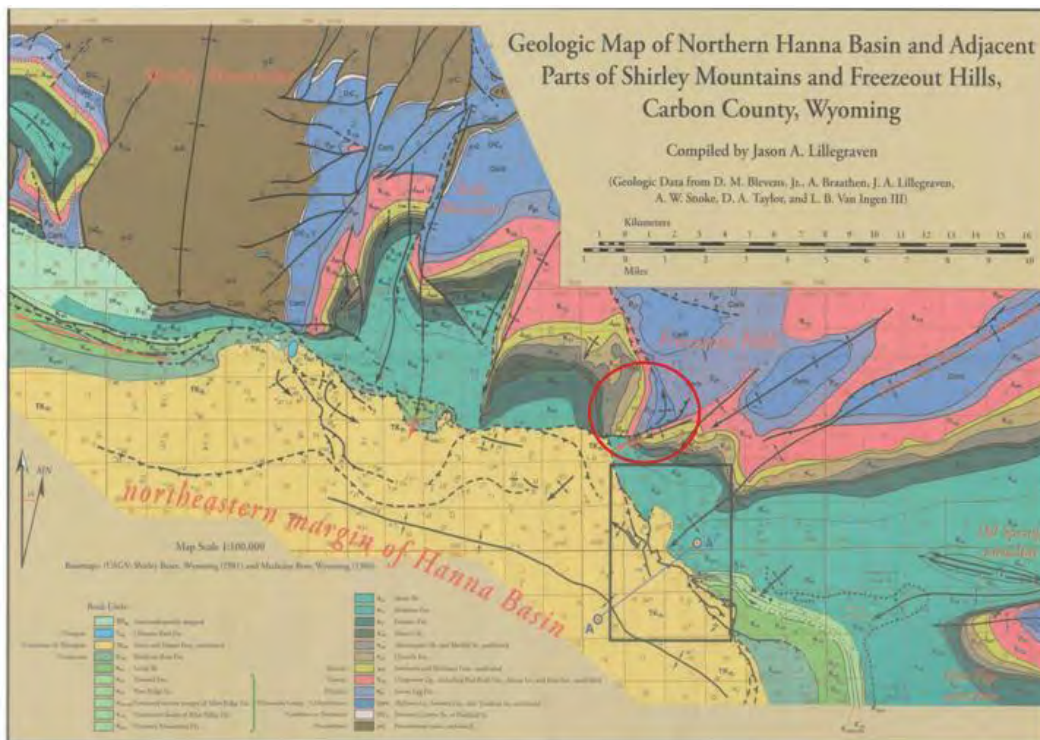
Aerial photograph (view to the northwest) showing the tightly folded and steeply dipping Tensleep Formation on Beer Mug Anticline (twenty foot wide gravel road in the foreground for scale).



The general location of the Beer Mug Anticline study site is shown in red; the base map is a Wyoming Department of Transportation state highway map.

Some of the earliest work done in the area was a survey of the stratigraphy and invertebrate fossil assemblages in the Freezeout Hills area by W.T. Logan in 1900, while S.H. Knight (1900) published a stratigraphic column of the Jurassic section from this general area. W.T Lee (1927) detailed the stratigraphy within the Difficulty Creek area. Maravich (1941) described the general stratigraphy and structure of the Freezeout Mountains just northeast of the study area. Maravich's cross-sections show the Freezeout Mountain anticlines as basement-involved thrust structures.

Lillegraven and Snoke (1996) and Lillegraven et al. (2004) provide a general geologic map of the northeastern margin of the Hanna basin and sections of the Shirley Mountains and Freezeout Hills within which is Beer Mug and the associated Ellis Ranch anticlines. These researchers document thrust faults directed out of the basin and infer they are related to volume constraints within the basin and basin margins. As shown on their geologic maps these faults do not intersect with either the Beer Mug or Ellis Ranch anticlines.

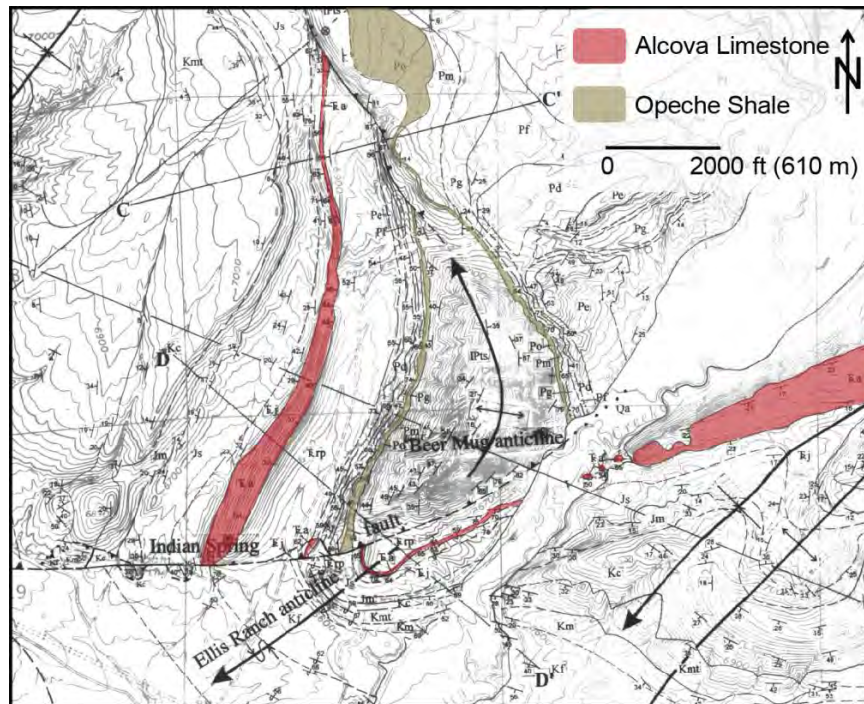


Geologic map of the northern Hanna Basin from Lillegraven et al. (2004); Beer Mug Anticline study area is highlighted in the red circle near the center of the map just north of the Hanna Basin (Lillegraven et al., 2004).

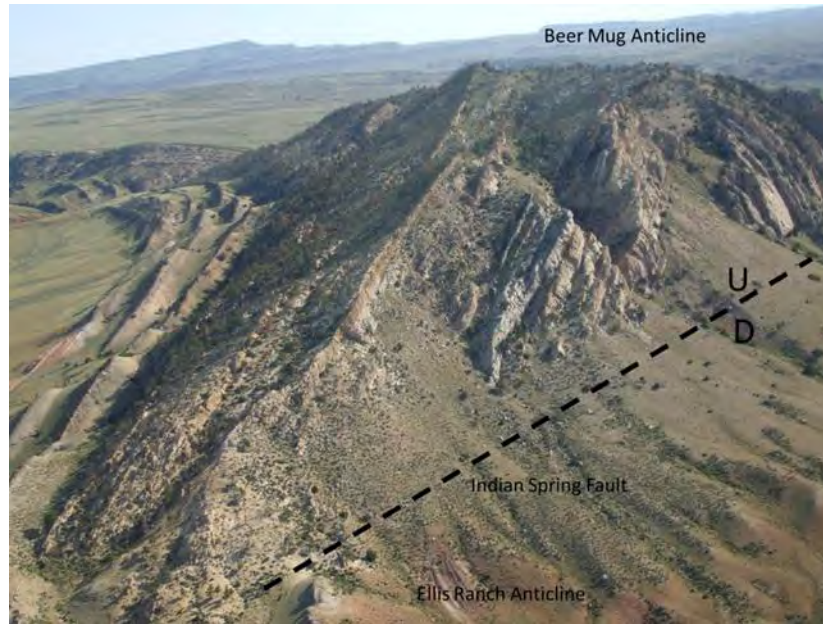
A Google Earth image coupled with a geologic map by Taylor (1996) and low-angle aerial imagery of the Beer Mug Anticline help to visualize the general structure of this tightly-folded anticline and the associated Ellis Ranch Anticline. These structures are also detailed and described in the sequence of aerial photographs that follows the geologic maps. The smaller anticline (Ellis Ranch Anticline) is in the footwall and was overridden by the larger Beer Mug Anticline. David Taylor documented these structures and more in his 1996 Master's Thesis at the University of Wyoming titled "Structural geology of the Difficulty Creek area, Carbon County, Wyoming". Brown also documented these structures in his thesis "The geology of the Difficulty-Little Shirley Basin area, Carbon County, Wyoming" at The University of Wyoming in 1939, though some of his terminology is different both interpret Beer Mug as a basement-involved structure.



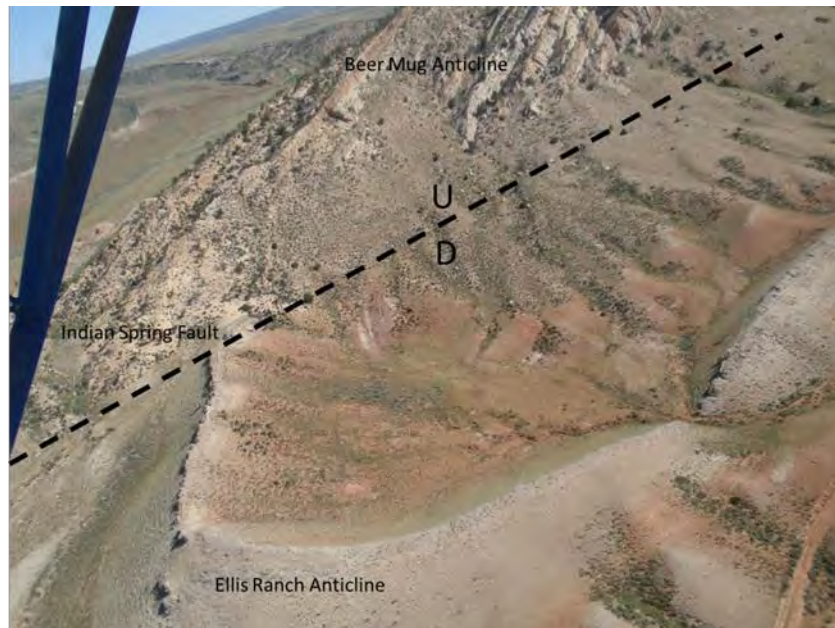
Aerial view (Google Earth) of Beer Mug Anticline and surrounding area with fault and fold interpretations on image. Image is at the same scale as the geologic map below.



Geologic map of Beer Mug Anticline and the surrounding area (modified from Taylor, 1996). The Alcova Limestone is highlighted in red to help highlight the Ellis Ranch Anticline and the Alcova Limestone exposures along the backlimb of Beer Mug Anticline. These outcrops are described in detail in later sections of this report.



Aerial view to northeast from southern end of Beer Mug Anticline; backlimb (left side of photograph) dips up to 50 degrees, forelimb (top right) dips are near vertical. Forelimb in lower right is cut by the Indian Spring Fault.

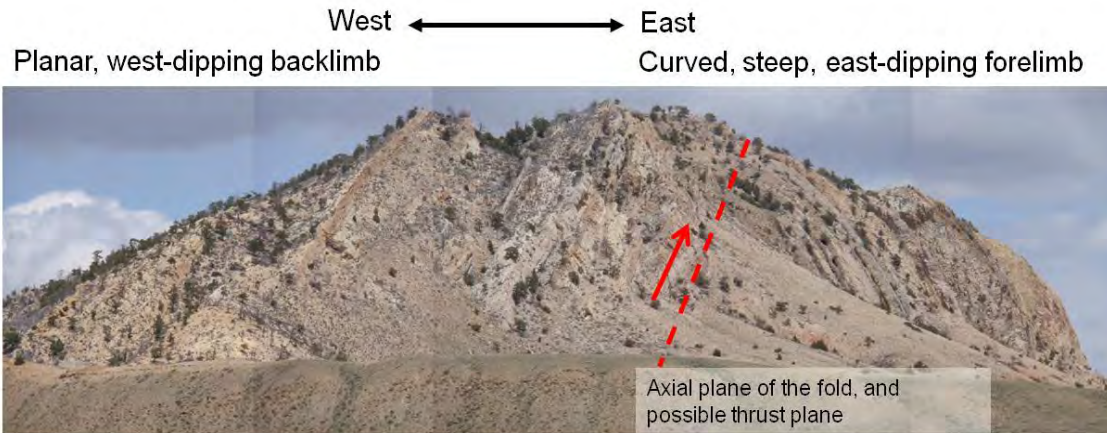


Aerial view to north-northeast from southern end of Beer Mug Anticline; this view is just below (south) of the photograph above. The forelimb of Beer Mug Anticline is cut by the Indian Spring Fault and overrides the Ellis Ranch Anticline in the footwall. The formation outlining the Ellis Ranch Anticline in gray is near to slightly overturned exposures of the Alcova Limestone.



Aerial view to the southeast from the northwestern section of Beer Mug Anticline; note dotted line highlights the valley at the north end (left) is an area of increased faulting and fracturing related to a dip reversal within the Tensleep Formation from east-vergent south of the fault valley to west-vergent north of the fault.

The next figure is a photograph of the southern end of Beer Mug Anticline as viewed along strike of the fold axis. The photograph shows the anticline in a near cross-sectional view because the anticline has been cut oblique to the axis by the Indian Spring fault. The rim of the Ellis Ranch Anticline is in the foreground. The abrupt change in dip of the Tensleep Formation strata of 45° on the backlimb to nearly 90° on the forelimb and the breccia at the center of the axis indicate there is likely a fault parallel to the anticlinal axis (highlighted as the dashed red line).

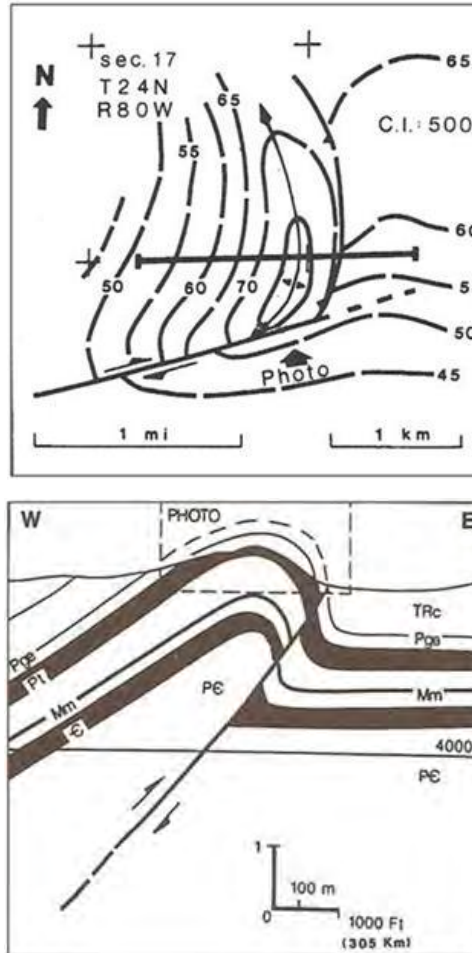


Beer Mug Anticline view is to the northeast along strike of the fold hinge. Southeastern section of the anticline cut by a fault exposing a cross sectional view of the anticline and the Tensleep Formation. Beds on the forelimb have near vertical dips at the far right (east) base.

There are different working hypotheses as to the underlying fault fold structure at Beer Mug Anticline. Stone (1993) and Taylor (1996) support a basement-involved fault propagation fold. There are some differences between their models and these are detailed in the next figures. We have also included a cross section by Hennings et al. (2000) from Oil Mountain west of Casper, Wyoming to initiate another working hypothesis (favored by the authors of this report) that Beer Mug Anticline may have a thrust in the sedimentary units that repeats the sedimentary section at the Tensleep level.

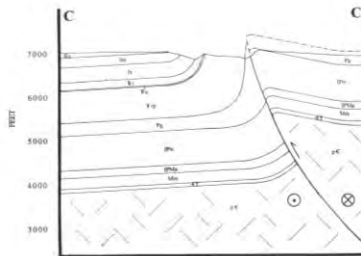
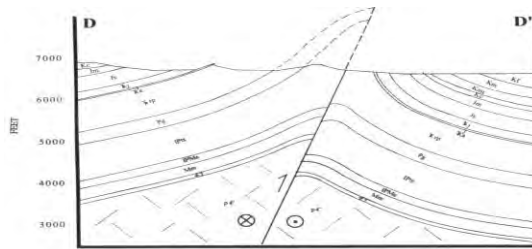
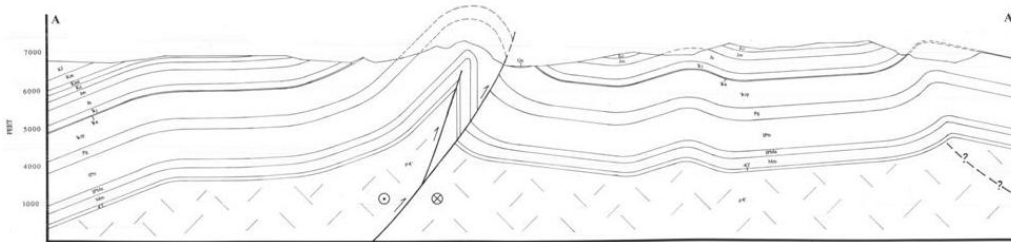
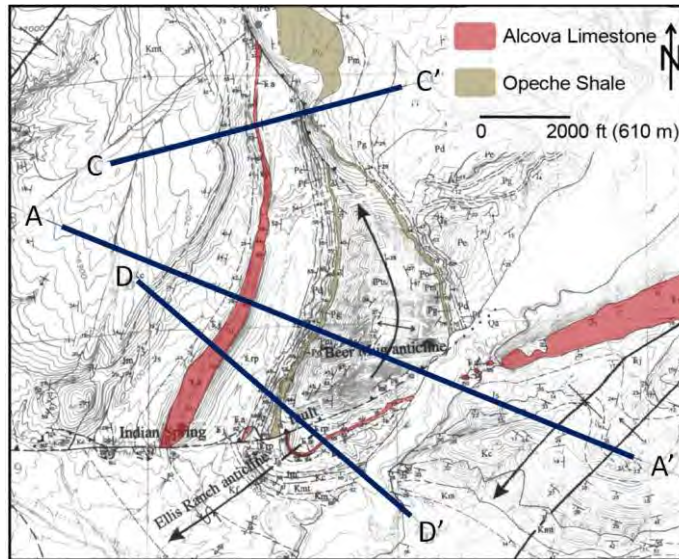
Stone coined the phrase “trapdoor structure” for Beer Mug Anticline. In this interpretation a thrust fault along the eastern edge terminates against a tear fault (Indian Spring fault; figures below) and uplift along the tear produces a trapdoor, pop-up style structure. This interpretation is similar to the Master’s thesis work by Brown (1939), though Brown has a slight change in terminology with the Indian Spring fault labeled the Beer Mug Fault and no fault along the north eastern limb of the anticline, though he does infer the Indian Spring fault as continuing further to the east like the map by Stone (1996) below.

As noted by Lillegraven et al. (2004), Lillegraven and Snoke (1996) and based on mapping by Taylor (1996) there is recognizable thrust fault along the eastern and northeastern limb as shown in the figure below.

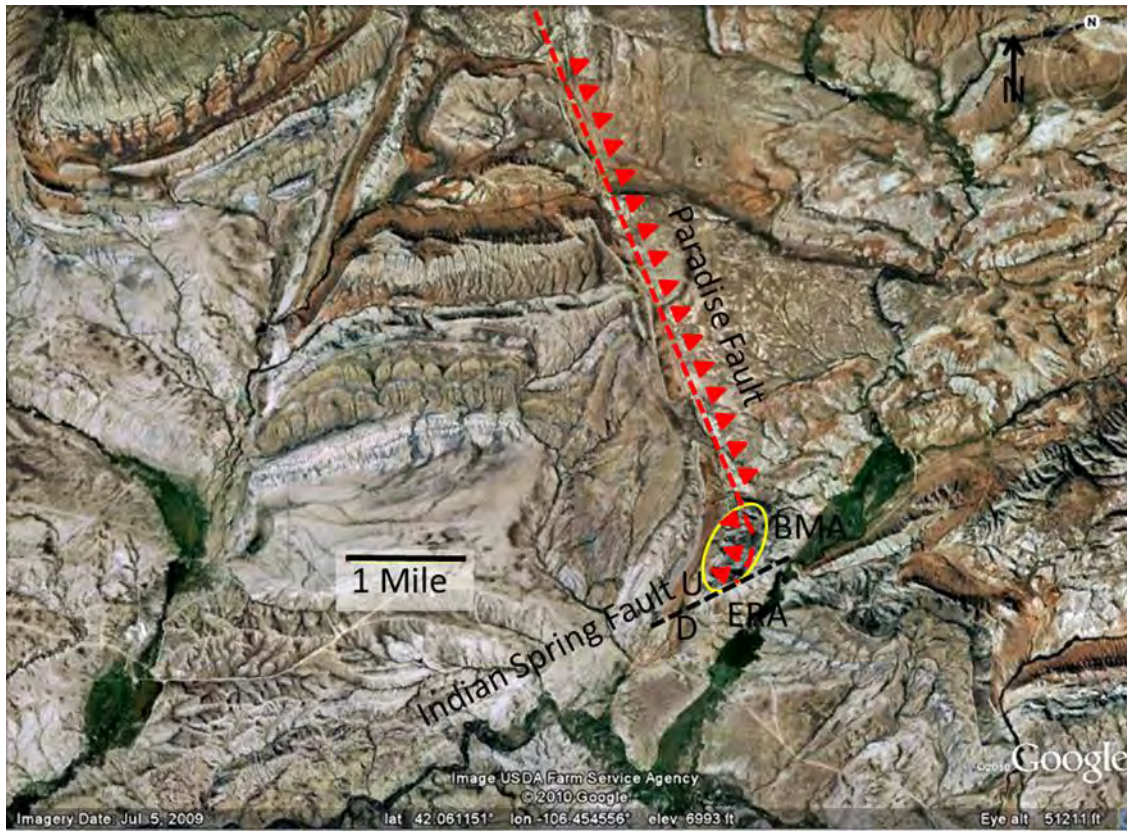


Top figure is a structural contour map from Stone (1993) based on thesis work by O. Brown (1939); structural contours are in feet x 10^2 . Bottom figure is a cross section from west to east along the line in the upper figure. These figures highlight the hypothesis that Beer Mug Anticline is basement cored with no shortening in the stratigraphic section.

Extensive field work by Taylor (1996) shows that the strike and dip of the stratigraphy, the surface location of faults and their associated strikes and dips, and other associated structures such as the Ellis Ranch Anticline are rather complex and somewhat counterintuitive. The following figures detail Taylor's hypothesis of a more complex basement fault system as detailed in his cross sections and we utilize Taylor's naming convention for the fault system at Beer Mug Anticline.



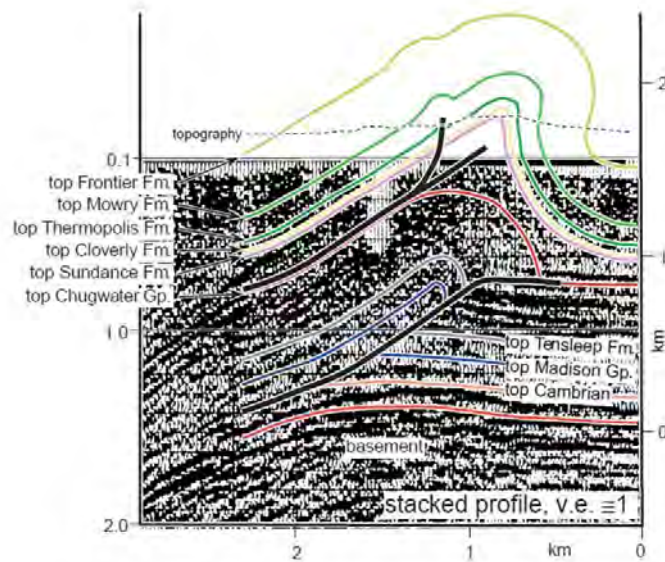
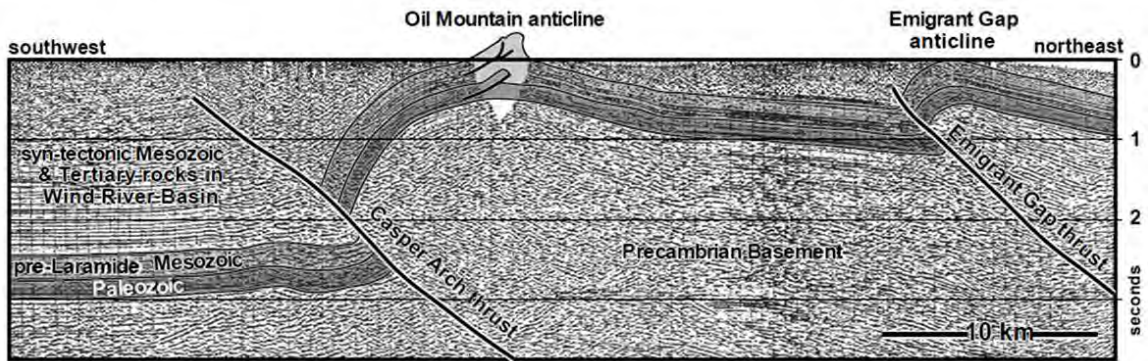
Cross-sections of Beer Mug Anticline by Taylor (1996) are shown above. Section A-A' is through the central portion of Beer Mug Anticline; and illustrates the basement-involved fault propagation fold with a secondary fault through the axis of the anticline and the main fault is the Indian spring fault. The middle cross-section D-D' is through the southern section (Taylor, 1996) and shows that Beer Mug Anticline is actually overriding the smaller-scale Ellis Ranch Anticline. C-C' is north of the main Beer Mug anticlinal structure and shows that this basement fault is dipping in the opposite direction is the thrust faults to the south (compare to cross sections A-A' and D-D').



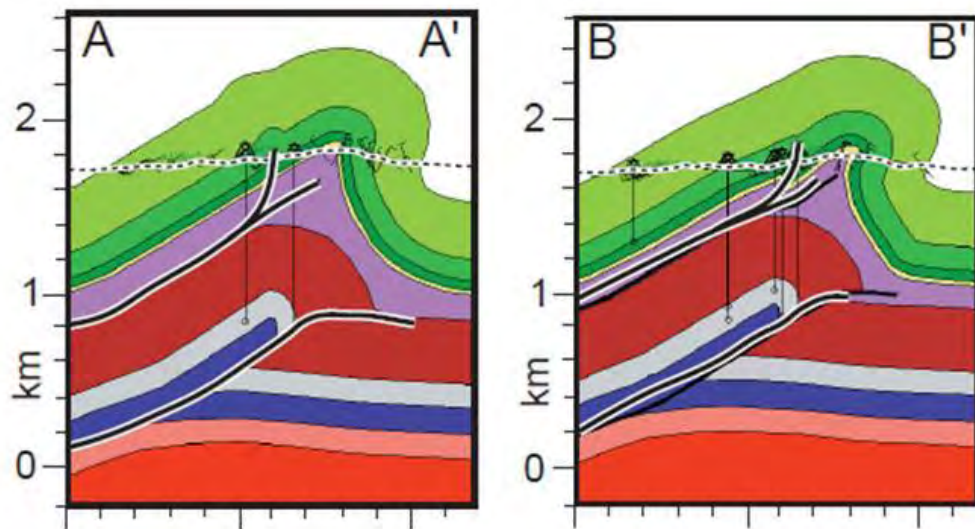
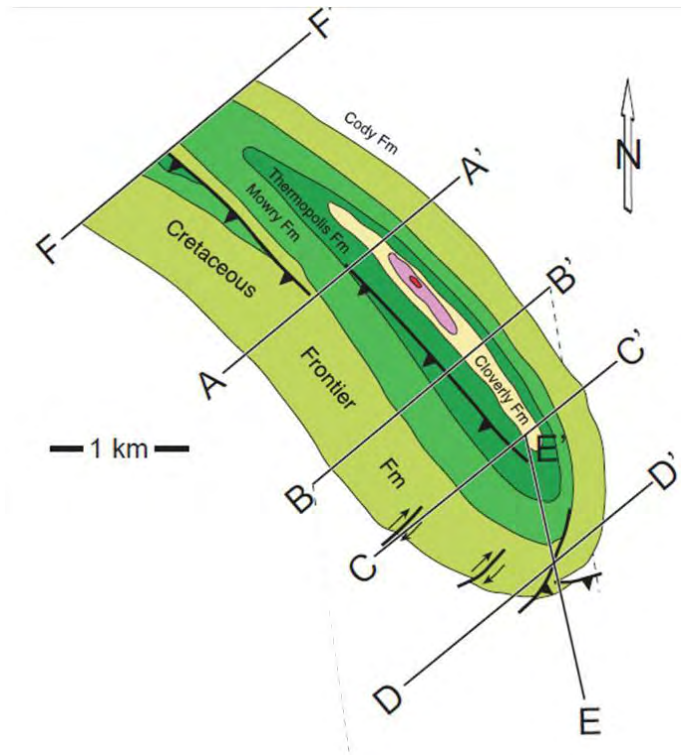
Aerial view (Google Earth) of Beer Mug Anticline and the surrounding area; Beer Mug (BMA: highlighted by the small yellow circle) is the southern extension of the Paradise Fault at the intersection with the Indian Spring Fault. Note that the vergence of the Paradise thrust changes along strike, from southwest-vergent along the northern extension of the Paradise Fault to east-vergent at BMA. This suggests that Beer Mug Anticline may be a back thrust on the larger Paradise Fault and related to possible volume constraints near the intersection of the Paradise Fault and the Indian Spring Fault (black dashed line). The Ellis Ranch Anticline (ERA) is south of the Indian Spring Fault.

In the structural interpretation section of this report we propose an additional hypothesis of the Beer Mug Anticline structure (as a thin-skinned style fault propagation fold perhaps as a back thrust over a deeper seated basement-involved fault) that fits the larger-scale data from the figure above and work by Hennings et al. (2000) at a similar structure. To facilitate that discussion provided below is a description of Oil Mountain west of Casper Wyoming in work by Hennings et al. (2000) as a potential analog for subsurface structures at Beer Mug Anticline. Hennings et al. (2000) have not only extensive surface data but also subsurface seismic data and well data to help constrain the fault/structural interpretation which includes thrusting in the sedimentary section and some doubling of the Tensleep Formation stratigraphic section. Thus

thin-skinned style thrust faulting can occur in an overall Laramide basement-involved structural setting.

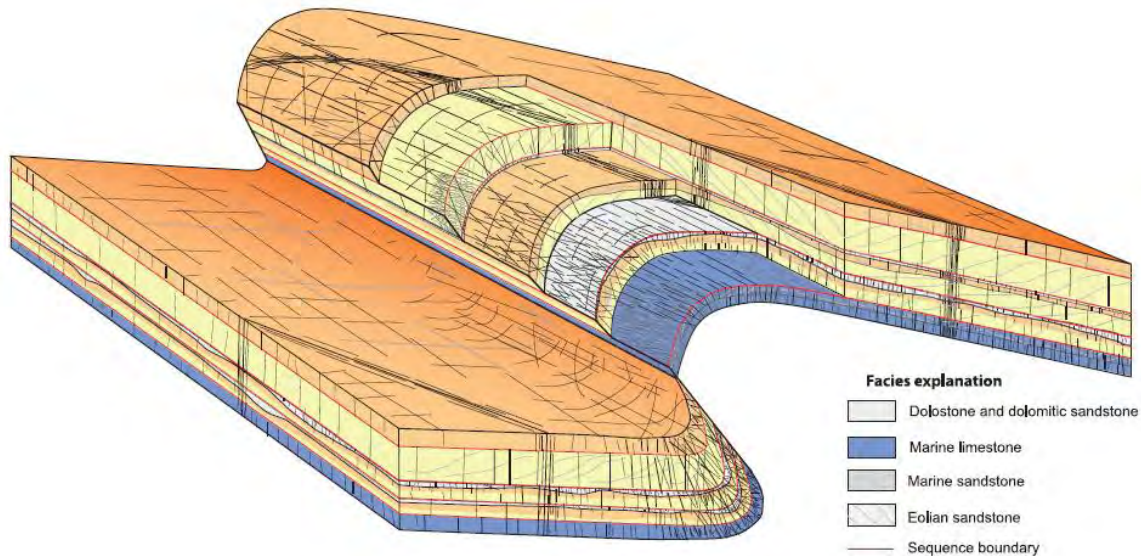


Upper figure is a time-migrated seismic section showing the location of Oil Mountain relative the larger basement-involved Casper Arch and Immigrant Gap thrusts (Hennings et al., 2000). Bottom figure is one of four seismic profiles combined with well data that was utilized by Hennings et al. (2000) to constrain the following cross sections.



Upper figure shows the locations of the cross section examples (A-A' and B-B') from Hennings et al. (2000). These data and interpretations indicate it is hypothetically possible for thin-skinned thrust faulting in the sedimentary section with duplication of sectional thickness in a Laramide tectonic setting and structure. This structure has a similar shape as the relatively unconstrained (no seismic or well data) structure at Beer Mug anticline.

Outcrop and LIDAR data analysis by Zahm and Hennings (2009) at the Alcova anticline, indicate that fractures within the Tensleep Formation are controlled in part by facies, depositional sequences and structural position. These relationships are similar to but not identical to those observed at Beer Mug anticline. In particular, Beer Mug anticline has more limestone vs dolomite beds and bed-parallel slip on the forelimb than the Alcova anticline.



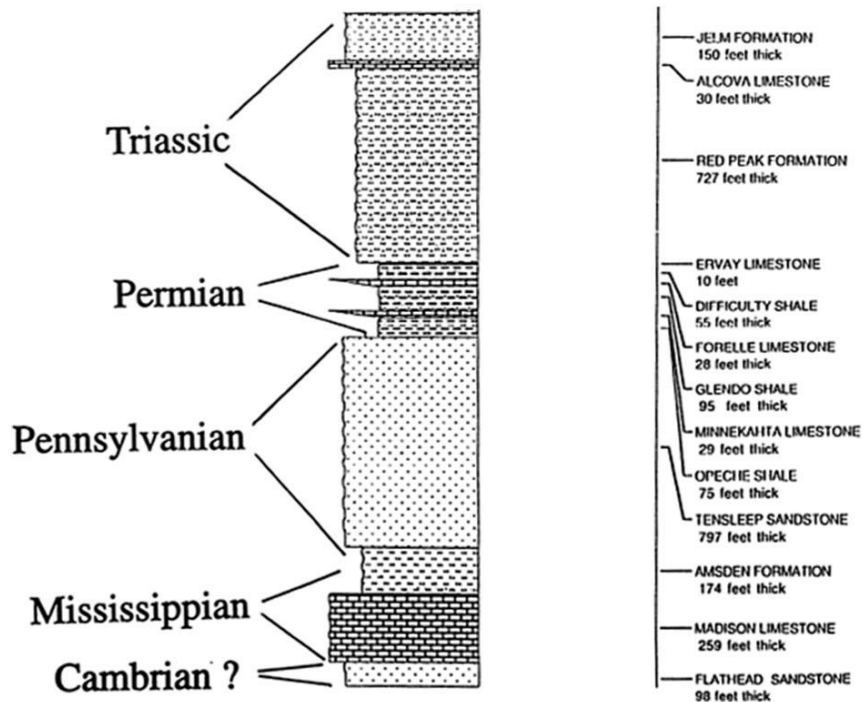
Zahm and Hennings (2009) conceptualized fractures hierarchy for the Tensleep Formation at the Alcova anticline, at the Alcova Reservoir. Fractures can be facies-bound, sequence-bound and/or throughgoing. The model also highlights their conceptualization of fracture intensity with increased fracturing on the forelimb relative the backlimb. Many of these relationships were also found within the Tensleep formation at Beer Mug anticline.

Lithologic Units

The lithologic units of interest within the study area range from Cambrian to Triassic in age. The stratigraphic section below is from Taylor (1996). The Ervay Limestone, Difficulty Shale, Forelle Limestone, Minnekahta Limestone, and Opeche Shale are the interbedded limestone and shale members of the Goose Egg Formation. Fracture data were also obtained from the Alcova Limestone and presented in a separate section within this report. The Alcova limestone is approximately 30 feet thick and is thinly bedded limestone with some stromatolites at the base. The majority of the data were collected from the Tensleep Formation because it is large producer of hydrocarbons within Wyoming and thus the primary unit of interest in this study.

Tensleep Formation Sedimentology

The Tensleep Formation in south-central Wyoming is Middle to Upper Pennsylvanian in age, and consists of a complex package of repeated marine limestones and/or dolomites, and eolian sandstones formed in near-shore dune and interdune environments with both horizontal and large scale cross-bedding (Boyd, 1993; Love et al., 1993). While both upper and lower units of the Tensleep are composed of eolian-marine sequences the upper is dominated by eolian sandstones and lower by marine facies (Carr-Crabaugh and Dunn, 1996; Dunn, 1997). Outcrop data enhanced with LIDAR survey data by Zahm and Hennings (2009) at Alcova Reservoir (west of Casper, Wyoming) indicate that these eolian-marine sequences range from meters to decimeters in thickness and that the different facies therein are a significant control on fracturing, with many fractures being facies-bound. The eolian sandstones are fine- to very fine-grained, feldspathic quartz arenites with varying amounts of quartz, carbonate and anhydrite cements (Carr-Crabaugh and Dunn, 1996). The Tensleep Formation is laterally equivalent in part to the Minnelusa Formation to the north and east, to the Casper Sandstone to the east and south, and to the Weber Sandstone to the west (Love et al., 1993).



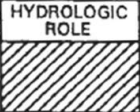
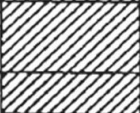
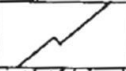
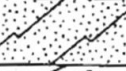
This figure illustrates the Cambrian to Triassic stratigraphic division and thicknesses of the lithologic units at the Beer Mug Anticline study area from Taylor (1996).

Of note to later discussions of inferred faulting is the stratigraphic thickness from top of the Tensleep Formation to the Cambrian basement. Taylor (1996) estimates the thickness as approximately 1300 ft. and Johnson and Huntoon (1994) give a range from 830-1010 ft. These thickness estimates are on the same order as the amount of Beer Mug Anticline above the surrounding plain and the Indian Spring fault.

Groundwater and Fluid Flow

Work by Johnson and Huntoon (1994) shows that the area just north of the Hanna Basin study area is separated into flow compartments by the basement faults. The Paradise Fault which is the northern extension of the fault underlying Beer Mug Anticline is the edge of one of these compartments as evidenced by a 400 ft. hydraulic head change across the fault and different water chemistry within Tensleep Formation aquifers.

The figure below details the flow characteristics of the major rock units in the study area. Difficulty Creek starts as a spring within the Tensleep Formation north of Beer Mug Anticline and flow along it's the eastern margin.

UNIT	HYDROLOGIC ROLE	PERMEABILITY	DESCRIPTION
ALCOVA LIMESTONE			
CHUGWATER FORMATION			Shale, siltstone, and sandstone with thin beds of anhydrite and gypsum obstructing groundwater flow.
GOOSE EGG FORMATION			
TENSLEEP FORMATION			Thick sandstone containing alternating limestone and sandstones in lower interval. Excellent water supply where saturated and penetrable.
MADISON LIMESTONE		 	Limestone with interbedded dolomite and an upper cherty unit. Aquifer with good quality water.

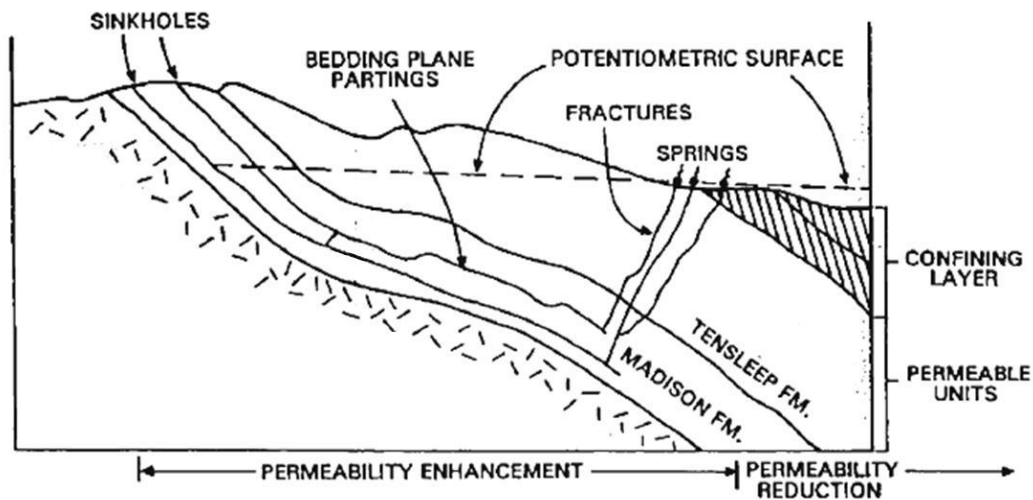
				
Confining Layer	Aquifer Where Saturated	Fracture Permeability	Inter-Granular Permeability	Solution Features

Hydraulic characteristics as defined by Johnson and Huntoon (1994) by formation within the Difficulty Creek area. Note Chugwater Formation of Johnson and Huntoon (1994) is equivalent to the Red Peak Formation of Taylor (1996).

Johnson and Huntoon (1994) study of the Difficulty Creek area shows that this groundwater compartment is actively recharged in the Shirley Mountains to the west and the Freezeout Mountains to the east. The water flows down gradient to numerous springs and seeps in the Tensleep Formation.

Below is a diagram illustrating groundwater movement from sinks in the Tensleep Formation and Madison Limestone down gradient to a spring, for example the Difficulty Creek Spring. Groundwater at the spring flows through vertical fractures that connect the Madison and Tensleep aquifers.

Johnson and Huntoon (1994) also note an increase in the Difficulty Creek stream flow of $3.4 \text{ ft}^3/\text{sec}$ from seeps and springs along the eastern margin of Beer Mug Anticline. These seeps and springs are inferred by Johnson and Huntoon (1994) to be associated with fractures parallel to the strike of the anticline.



A diagrammatic cross-section by Johnson and Huntoon (1994) illustrating groundwater flow from highland sinks through permeability pathways to vertical fractures where the potentiometric surface meets the topographic surface/ground level and is not confined by overlying confining layers.

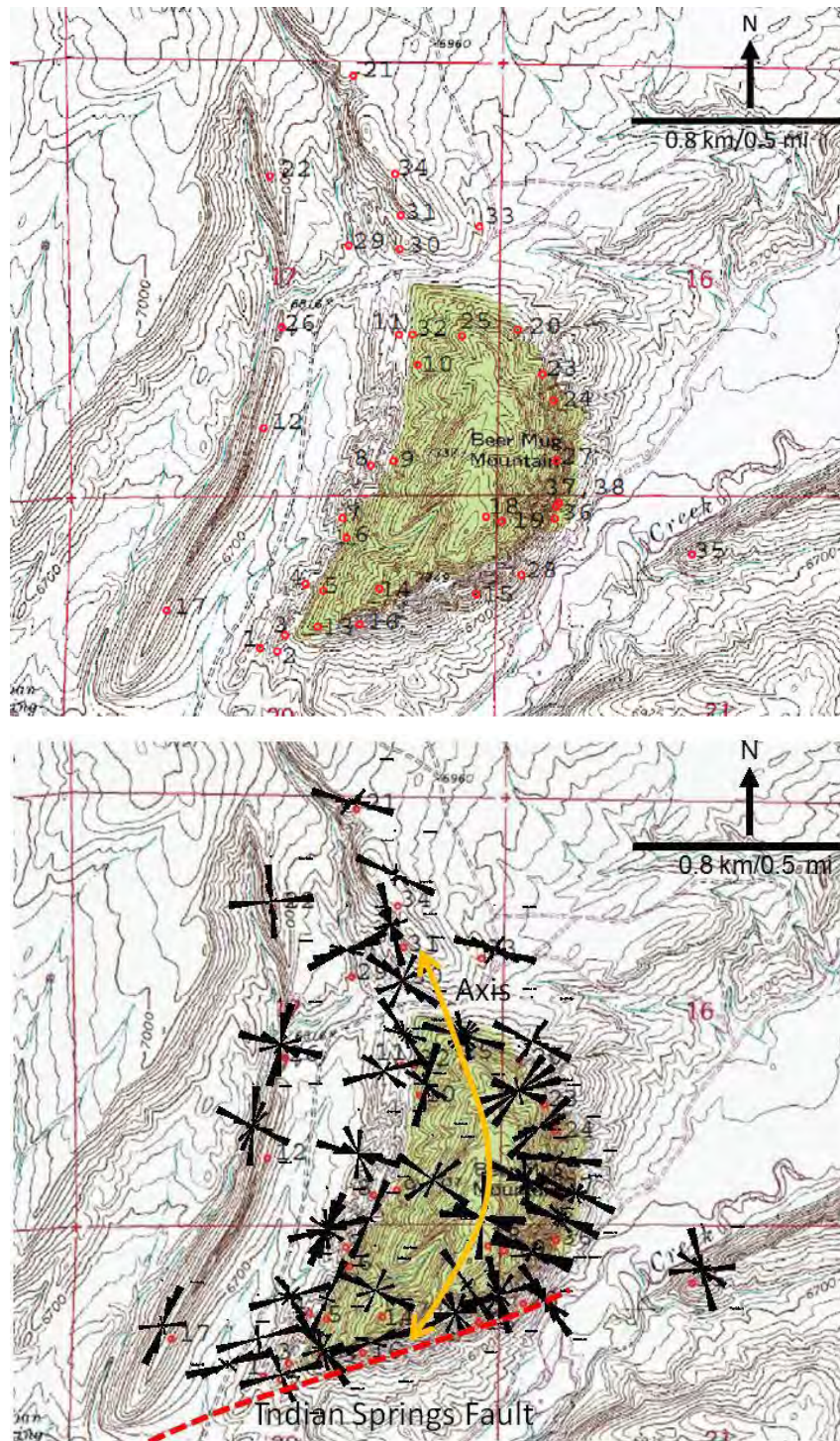
STRAIN ACCOMMODATION: GENERAL

Laramide-age thrusts have folded the Tensleep Formation into a spectrum of anticlines; from broad anticlines with low angle bedding dips to steeply-folded anticlines with vertical to overturned beds. Many of these anticlines exhibit inherited F_0 fracture patterns that pre-date folding, as well as fold-related extension fractures that are approximately dip-parallel (F_1) and strike-parallel (F_2); normal and parallel to the axis of folding respectively. The F_1 set can strike oblique to the hinge in anticlines where the stress orientation that caused both folding and fracturing was oblique to the inherited basement structure that dictated the hinge trend as at Flat Top Anticline (Lorenz, 2007). Areas on anticlines that were not significantly folded, i.e., relatively planar backlimbs, contain only the early, F_1 fractures caused by dilation perpendicular to thrusting during initial uplift, although locally it is superimposed on prethrust F_0 fractures. Intensified folding 1) reactivated earlier-formed fractures in shear and/or extension, 2) formed additional strike-parallel F_2 fractures caused by folding and the related hinge parallel extension, and 3) wrench-fault related F_3 fractures present at Beer Mug Anticline.

Fracture data were collected at numerous stations and transects across Beer Mug Anticline. The thirty-eight data collection sites are shown in the next figure. The figure following that and at the same scale illustrates all the fracture data in present day orientation and outlines the fold axis and location of the Indian Spring Fault.

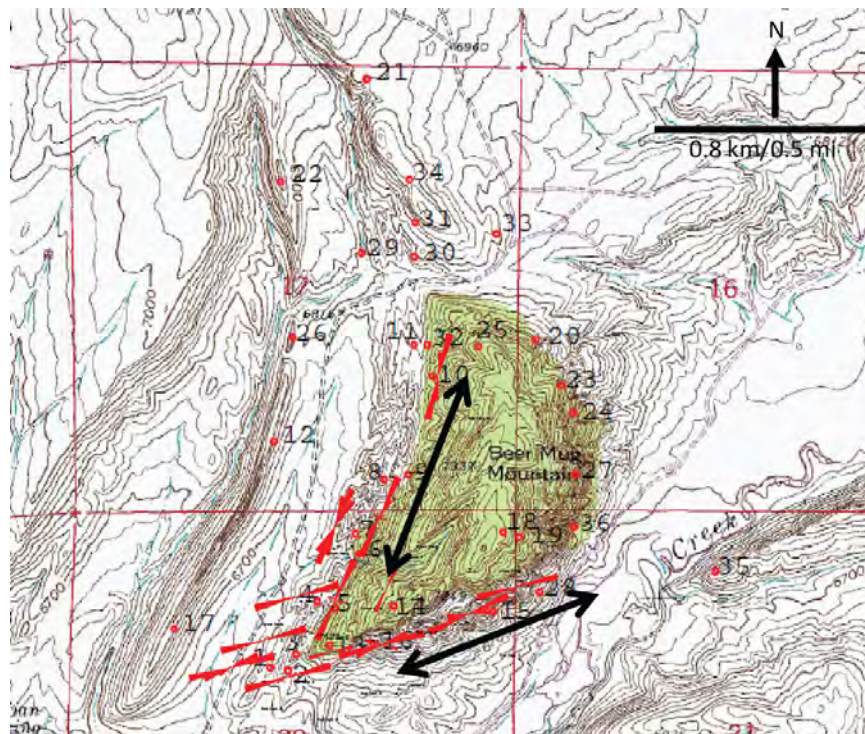
Early regional	Dip parallel	Strike parallel	Wrench parallel	Stress release	Micrite filled	Bed parallel shear	Bed oblique shear	Deformation band shear
F_0	F_1	F_2	F_3	F_x	F_m	S_1	S_2	S_3

The table above summarizes the nomenclature used and the fracture sets and types documented at Beer Mug Anticline. The following sections will describe each of these different fracture types and detail how these features vary and production implications.

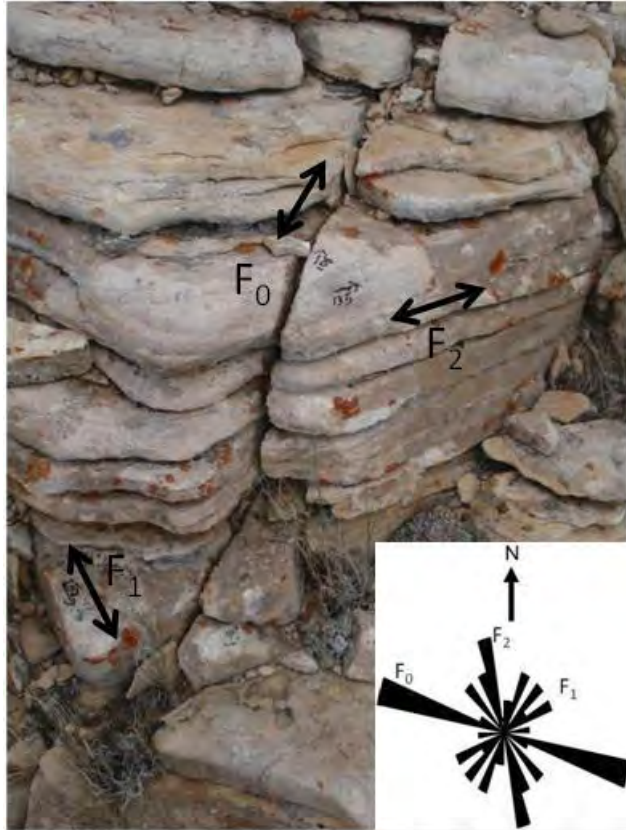


Top figure shows all the thirty-eight singular data collection sites, these sites are keyed to all the following figures and the associated data tables. Bottom figure shows rose diagrams of present-day fracture orientations at the thirty-eight stations. The axis of anticline is curved; it strikes NE in the south and rotates to a NW strike in the northern sections. The Indian Springs fault cuts the southeastern section of the anticline. Base map is the Difficulty Quadrangle from United States Geological Survey 7 ½ Minute Topographic Map Series.

Natural fractures include a NW to WNW striking (F_0) set of fractures. The next extension fracture sets have orientations that are dip-parallel (F_1) and strike-parallel (F_2). Shear fractures and faults parallel (S_1) are common at major lithologic discontinuities and shear fractures oblique (S_2) to bedding are documented within all units but thrust oriented shears are particularly common within the Alcova Limestone. Additional shear structures, such as deformation bands (S_3), are parallel, normal and oblique to bedding, including cross bedding. Another set of fractures (F_3), along the southeastern section of the anticline, strikes parallel to the Indian Springs wrench fault. This fracture set is localized within approximately 300 meters (1000 ft.) of the wrench fault. Early micrite-filled and probably injection related fractures (F_m) are observed within the Tensleep Formation. Only a few stress release (F_x) fractures are recorded at Beer Mug Anticline, probably because the numerous pre-existing fractures accommodated enough of the stress release to preclude the need for an entirely new fracture set.



Rose diagrams of typically bed normal extension fractures. This is a subset of the data that illustrates these two primary fracture orientations. One parallel to the fold hinge (F_2), the second parallel to the Indian Springs fault at the southeastern edge of Beer Mug Anticline (F_3).



A



B

A) Photograph of cross bedded sandstone unit within the Tensleep Formation at site 25 on the northwestern section back limb of Beer Mug Anticline. It contains a combination of F_0 , F_1 and F_2 extension fractures; F_1 and F_2 tend to terminate against F_0 at this location. Rose diagram of present-day fracture orientations ($n = 24$). B) Photograph of cross bed-parallel shears (S_1), and deformation bands (S_2) in the same outcrop.

TECTONIC FRACTURES (F_0 , F_1 , F_2)

Introduction

The tectonic fractures in the Tensleep Formation at Beer Mug Anticline are relatively planar structures with little surface features other than occasional millimeter –scale calcite mineralization. Plumose structure on the fracture faces which is an indicator of extension-style fracturing is quite rare in the Tensleep Formation at Beer Mug Anticline. This may be due to surface weathering or reactivation of the fracture surface which destroyed this typically fine texture. Tectonic extension fractures comprise a 30% to 100% of the fractures in select beds and sites around Beer Mug Anticline.



One of the best examples of preserved plumose structure is within sandstone of the Red Peak Formation on the eastern flank of the anticline. The plumes radiate from the center and right edge of the rock toward the left edge of the rock indicating that the fracture formed in extension and propagated from right to left.

Basic Tectonic Fracture Pattern

The early regional shortening, tightly-folded strata and curved fold hinge have produced numerous orientations of tectonic fractures but there are three general trends; the oldest is the northwesterly F_0 regional fracture set, and two fracture sets that are oriented relative to the

anticlinal structure. One set is dip parallel (F_1) the second is strike parallel (F_2); these fracture sets formed penecontemporaneously with the fold structure.

The fold is tight: bedding dip changes from 40° to 55° on the western backlimb to 90° on the eastern forelimb. Fold-related fractures are intensely developed along the crest. The core of Beer Mug Anticline is extensively fractured and brecciated with numerous void spaces and dead oil stain. At Beer Mug Anticline a NW to WNW striking (F_0) set of fractures is recorded. Where abutting relationships can be recorded it is the oldest fracture set. The next extension fracture sets have orientations that are dip-parallel (F_1) and strike-parallel (F_2).

As the fold tightened there was some shear reactivation along these fractures and some secondary reorientation related to changing fold curvature. The next two photographs and associated rose diagrams highlight these fracture sets.



Close-up of tectonic fracture face on the steeply-dipping (80°) forelimb (site 28) that has both gouge material and calcite mineralization. Unfortunately little plumose structure remains after both weathering and shearing of the fracture surface but it is likely this fracture formed in extension and was subsequently sheared as the fold tightened.

To reiterate at Beer Mug Anticline a NW to WNW striking (F_0) set of fractures is recorded. Where abutting relationships can be recorded it is the oldest fracture set. The next extension fracture sets have orientations that are dip-parallel (F_1) and strike-parallel (F_2). The next two photographs and associated rose diagram highlight these fracture sets.



Outcrop on the southwestern back limb of Beer Mug Anticline (site 5). Cross-bedded sandstone unit within the Tensleep Formation, bedding strike $N25^\circ E$, dip $40^\circ SW$. F_1 dip-parallel fractures are the exposed cliff face, F_2 strike-parallel fractures cut perpendicular to the cliff face. The rose diagram illustrates this combination of strike-parallel extension fractures (F_2), and dip-parallel extension fractures (F_1) ($n = 28$).



North is to the right in this photograph and the rose diagram. This outcrop is north of the main Beer Mug Anticline and highlights the three tectonic fracture trends very well with a documentable intersecting relationship showing the F_0 set is the older extension fracture set because the other extension fracture sets (F_1 and F_2) tend to terminate against it.

Interpretation

These three sets of fractures (F_0 , F_1 and F_2) are interpreted as follows: the oldest NW-SE set formed in extension and parallel in strike to regional shortening (Lorenz et al., 1991) prior to uplift of the anticline and are recorded both on and off the main anticlinal structure. Given the curved nature of the anticline the F_1 dip parallel set does strike parallel with the F_0 set along some sections of Beer Mug Anticline. Nevertheless the general shortening prior to uplift is in a Northwest-southeast orientation.

The dip-parallel (F_1) and strike-parallel (F_2) fracture sets are interpreted to have formed a little later and penecontemporaneous with the formation of the anticline. All three of the aforementioned fracture sets would be in the subsurface at this location. As an analog for other locations the dip-parallel and strike-parallel sets would be expected in the subsurface. However, the existence and orientation of any preexisting regional set at depth would need to be inferred qualitatively from the regional tectonic history and related quantitatively to the local site through outcrop studies, core analysis or borehole imagery.

Variations as a Function of Lithology

Where lithology is similar, fractures are also similar at Beer Mug Anticline. The extension fractures are relatively planar features and may have plumes on the fracture faces. Locally, there is millimeter-scale calcite mineralization. However, some fractures consist of simple planar breaks in the rock. Plumose structures and arrest lines, indicative of extension fracturing, are in fact rare in some strata; because poor cementation, 1) did not leave the rock prone to plume formation, and 2) allowed plumes to be quickly destroyed by weathering. In better cemented units some plumes have been obscured or destroyed by shear reactivation of the original extension fracture sets. Regardless, hints of plume structures are present on some fracture faces, and, along with the absence of offset, suggest that most of the planar breaks in the Tensleep sandstones formed initially in extension.

From a distance, many exposures of the limestone beds at Beer Bug Anticline appear to be unfractured relative to the interbedded sandy limestones and eolian sandstones. The limestones within the Tensleep Formation accommodated much of the larger-scale bed-parallel shear through granulation, brecciation and pressure solution although it is not always obvious due to weathering and secondary re-cementation. Re-cementation likely occurred nearly simultaneously with deformation. The dolomites in contrast were either not recemented or were re-cemented to a much lesser degree. Extensive fracture patterns are recorded from the capping dolomite at Flat Top Anticline (see Lorenz EORI report on Flat Top Anticline, 2007), as are unhealed fractures in Tensleep Formation dolomite cores from other locations.

Limestones and Sandstones

The limestones within the Tensleep Formation at Beer Mug Anticline accommodated strain by granulation through fracturing, and by repeated granulation with pressure solution and re-cementation. These beds also sheared, most notably on the crest and in the forelimb, (few Tensleep Formation limestones are exposed on the backlimb).

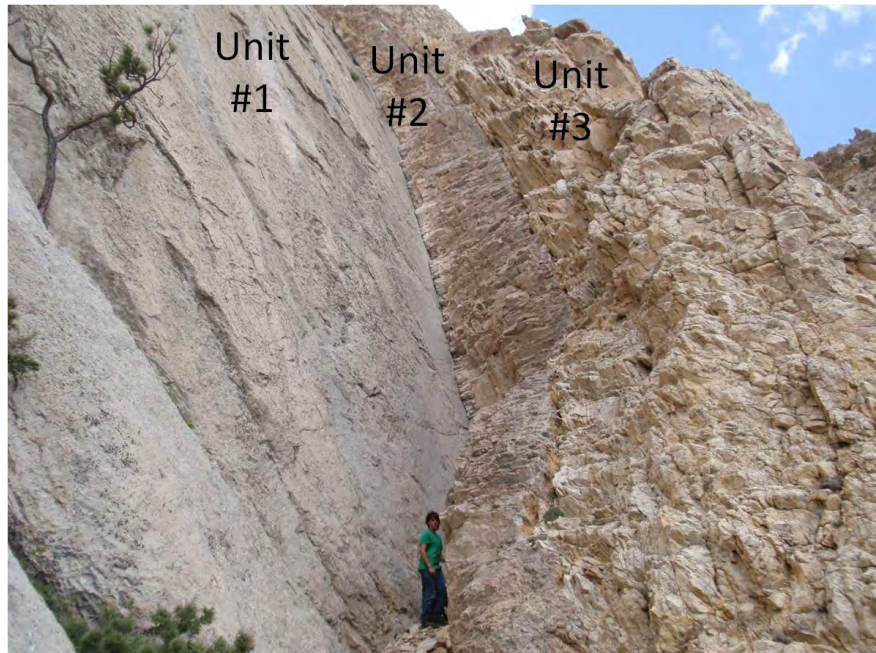
The limestones probably accommodate much of the larger-scale bed-parallel shear by brecciation. Brecciation is not obvious due to cementation and weathering and is most obvious on the cross sectional edge of bedding. In fact, at a gross scale, many of the dolomite beds appear unfractured but when observed at the small scale are brecciated or granulated.

Granulation, brecciation, dissolution, cementation and re-cementation were likely occurring simultaneously with deformation.

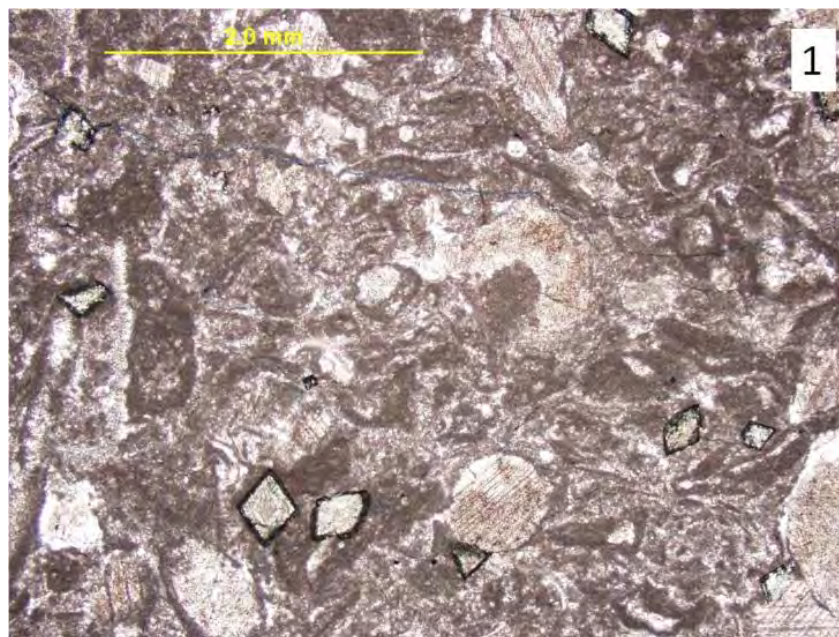
The following series of figures illustrate the nature of fracturing within a transitional sequence of limestone (unit 1), sandy limestones (unit 2), and sandstone (unit 3) lithologic units. Fracture intensity is different in these differing lithologies. At the macro scale there appear to be few fractures in the limestone (unit #1) a relatively uniform fracture pattern in the transitional sandy limestone (unit #2) and an almost brecciated appearance to the sandstones (unit #3).



Photograph above is an oblique aerial view of Beer Mug Anticline. The next series of figures highlight some of the fracture variability associated with lithology. These data were taken from the area within the red box on this photograph.



Upper figure shows the location (site 15) of the sequence described below on the eastern limb of Beer Mug Anticline. Lower figure shows a closer view of the transitional from limestone (unit #1), to sandy limestone (unit #2), to sandstone (unit #3); photomicrographs of each unit are provided below. Note that at this scale the limestone appears mostly unfractured (unit #1), a relatively uniform fracture pattern in the sandy limestone (unit #2), and an almost brecciated appearance to the sandstones (unit #3).



Photomicrograph of the limestone (unit #1), it is primarily composed of calcite with a few secondary dolomite rhombohedrons (scale bar 2 mm).



Photomicrograph of the sandy limestone (unit #2), it is fossiliferous and composed of silica sand grains floating in a calcite matrix (scale bar 2 mm).



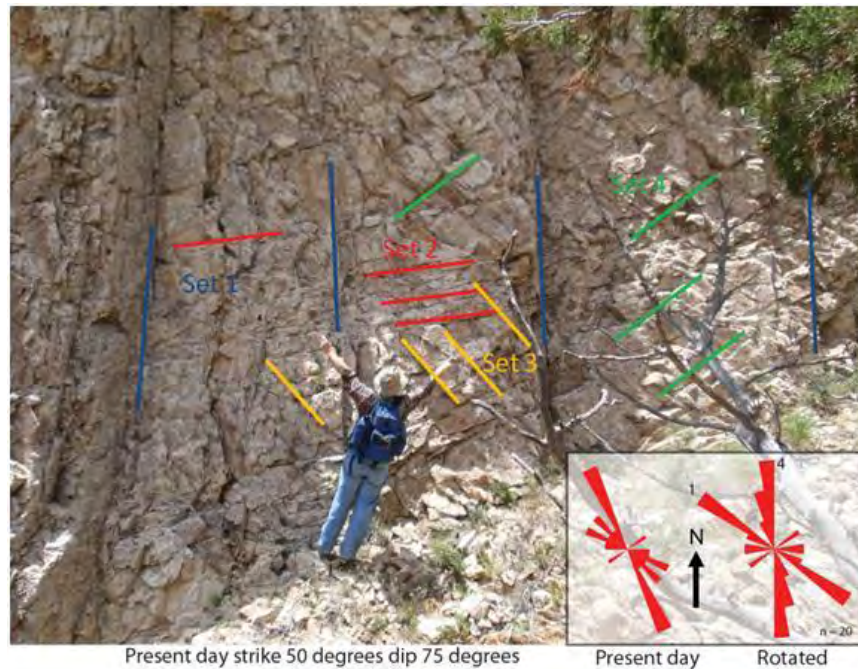
Photomicrograph of the sandstone (unit #3), it is well-rounded, fine-grained and cemented with calcite (scale bar 2 mm).

Close-up photo of the limestone (unit #1) shows that it is brecciated into centimeter scale pieces but that the limestone was self-healing by cementing the pieces with calcite

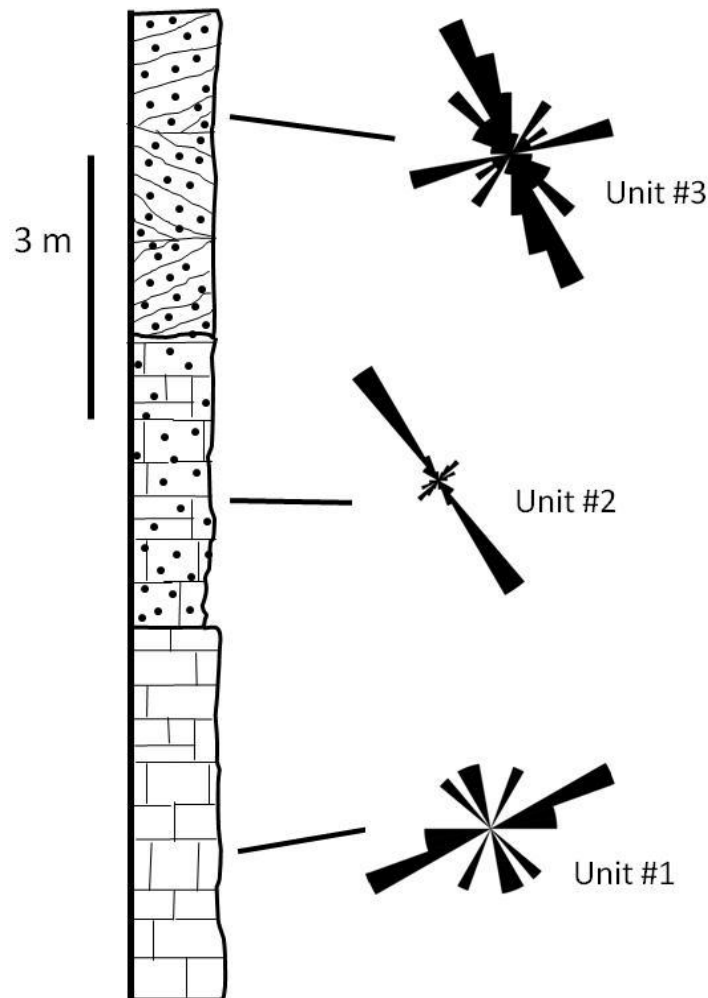
penesimultaneously with brecciation. When viewed on pavement surface rather than side view the sandstone (unit 3) exhibits an ordered fracture pattern.



Close-up image of the limestone (unit 1) surface, at this scale one can begin to see the granulation and clasts under the weathered and lichen covered surface.



When viewed on pavement surface rather than side view the sandstone (unit 3) exhibits an ordered fracture pattern. Rose diagrams are of fracture data taken from this pavement surface.



Summary of present-day orientations of all large-scale fractures within these three different sedimentary facies (unit #1 $n = 9$, unit #2 $n = 34$, unit #3 $n = 41$); at Beer Mug Anticline most beds contain the older NW-SE fracture (F_0) set.

Tectonic Fractures Summary

Three sets of tectonic fractures exist on and near to the main Beer Mug Anticline: early-formed (F_0) fractures that strike approximately NW-SE, parallel to the inferred direction of regional shortening. The latter sets formed in response to extension across the anticline during folding (Cooper et al., 2006). Fracture strikes vary with the curvature of the anticline and younger sets of slightly differing orientations overlay older sets as the fold tightened. As the fold tightened all of these sets were reactivated in shear at certain sites around the anticline. When

comparing fracture spacing in Tensleep Formation sandstones on the backlimb to the forelimb or the fracture sets on the northern extension to the forelimb spacing of fractures decreased in tighter portions of the anticline.

Tectonic fractures are typically planar and can have plumose structure but these are obscured due to reactivation during folding. Due to the curved nature of the anticline the oldest F₀ set does align with the F₁ dip-parallel set and was likely reactivated as F₁ during folding in these areas.

Tensleep Formation sandstones and sandy limestones tend to have a more ordered fracture pattern whereas the limestones brecciated. The brecciated limestones were likely healing by calcite cementation at the same time they were forming, thus the formation of breccia versus an ordered fracture pattern. These fracture characteristics relative to lithology was most evident on the forelimb. It is probable the limestones are partial baffles to fluid flow.

INDIAN SPRING FAULT-PARALLEL FRACTURES (F₃)

Introduction

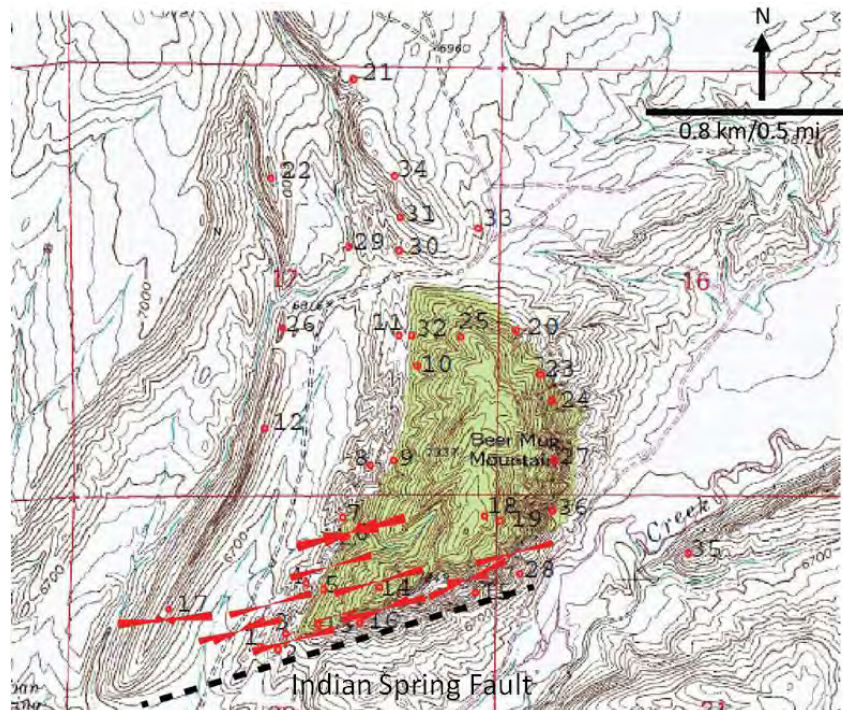
The southern section of Beer Mug Anticline is cut by the Indian Spring Fault. This fault exposes the anticline in cross-sectional view when viewed from the south to the north. Spatially related and parallel in strike to this fault is a set of natural fractures within the sedimentary units (Tensleep Formation through Forelle Limestone) along this fault. The Indian Spring fault is interpreted to be a right-lateral oblique slip thrust fault (Lillegraven et al., 2004; Lillegraven and Snoke, 1996; Taylor, 1996; Stone, 1993).



Aerial photograph view toward the northeast along the axis of Beer Mug Anticline, the Ellis Ranch Anticline is in the footwall at the bottom of the photograph). The Indian Spring Fault terminates to the northeast along the eastern edge of Beer Mug Anticline. It is not inferred to continue through the Difficulty Creek valley (Taylor, 1996). The fault terminates approximately one mile to the southwest, against an out of basin thrust (Lillegraven and Snoke, 1996; Lillegraven et al., 2004). Fractures (F₃) related to this fault were recorded in the hanging wall within a 1500 ft. distance perpendicular to the fault trace (primarily recorded within the red ellipse).

Basic Indian Spring Fault-Parallel Fracture Pattern

The set of fractures that strike parallel to the Indian Spring fault are typically well developed with uniform orientations, typically normal to bedding with relatively long trace lengths 10's of feet though some extend for a couple hundred feet. They are labeled as F_3 fractures in our naming sequence. The figure below highlights the parallel nature of this set and its special relationship to the Indian Spring fault. Spatially this fracture set was recorded in the hanging wall of the Indian Spring fault and within 1500 ft. or closer to the fault trace.



Map view of the location and orientations of the fracture set (F_3) parallel to the Indian Spring Fault. These are all within approximately 1500 ft. of the fault trace. Base map is the Difficulty Quadrangle from United States Geological Survey 7 ½ Minute Topographic Map Series.

The photograph below shows one of the best exposed fracture faces of this F_3 fracture set. The fracture is nearly perpendicular to bedding and very planar. There are other fracture sets in this upper Tensleep Sandstone as highlighted by the associated rose diagram. Most have been reactivated as the fold tightened bedding dip is nearly 50° to the west at this outcrop.



The above photograph and rose diagram ($n = 31$) of the site 13 outcrop. There are several sets of fractures in this outcrop but the most prominent is the cliff face itself with the young green shirted geologist for scale. This large-scale extension fracture (trace length over 200 ft.) is nearly perpendicular to bedding, very planar and along strike with the Indian Spring fault.

Interpretation

The fractures of set F_3 are within 1500 ft. and parallel in strike to the Indian Spring fault, therefore this set is interpreted to be directly related to displacement and associated applied stresses from the Indian Spring fault. Surface characteristics of this fracture set are planar with some evidence of remnant plumes, few shear indicators such as steps or slickenlines suggest these fractures formed in extension. Given the Alcova Limestone is resting against middle to upper Tensleep Formation sandstones along the Indian Spring fault trace, there is at least 1100 ft. of vertical displacement. This would suggest there should be shear fractures associated with shortening along the fault but these potential fractures were not observed. Therefore it is inferred that displacement along the fault occurred late in the folding process and shear was accommodated by the preexisting fractures sets (F_0 , F_1 , and F_2). Another working hypothesis that is consistent with the observed fracture patterns but not with previous mapped interpretations is that the fault has a component of normal displacement rather than thrust displacement.

Production Implications

This fracture set is essentially a fracture swarm associated with a fault. Fracture swarms have been observed in many areas (Hart, 2006). These fault parallel fractures can increase permeability and induce a high order of directionality to flow and can be “sweet spots” for hydrocarbon (Hart, 2006) and ground water production. The springs, bogs and increased creek flow documented by Johnson and Huntoon (1994) along the eastern margin of Beer Mug Anticline are likely related to this fracture set and are good evidence for increased fluid flow along this fracture set.

Summary of Indian Spring Fault-Parallel Fracture Set (F₃)

The F₃ extension fracture set is parallel in strike and spatially near the Indian Spring Fault. These fractures likely formed late relative to the folding of Beer Mug Anticline. These fractures are essentially a fault parallel swarm that likely allow for increased flow parallel to the fault. If this fracture type was intersected by a well in an analogous subsurface reservoir, that well would likely be a production sweet spot.

MICRITE-FILLED AND SAND-FILLED FRACTURES/INJECTION FRACTURES (F_m)

Introduction

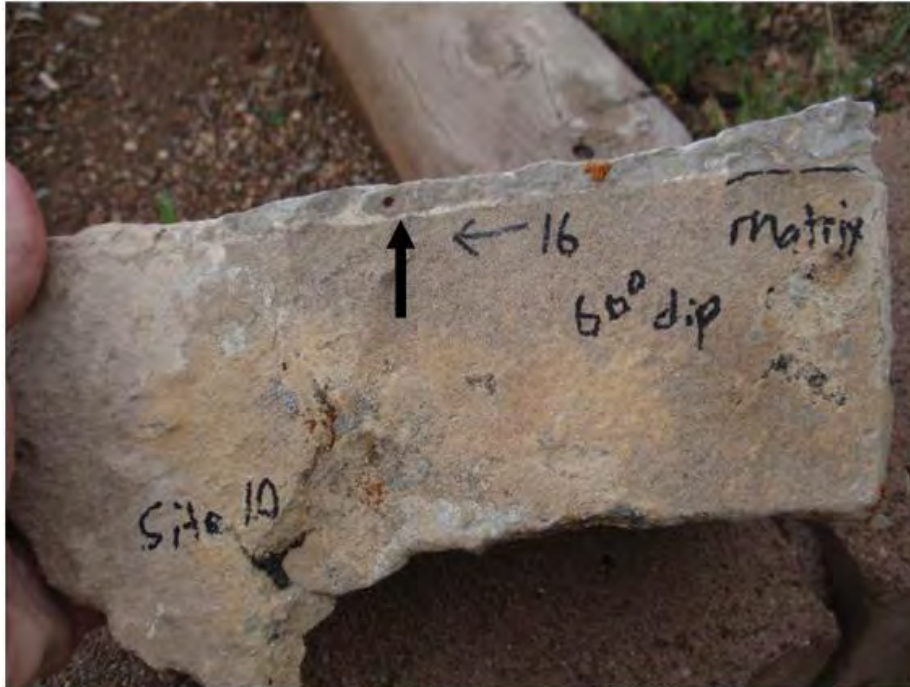
Micrite-filled fractures (F_m) were documented in several of the Tensleep Formation Sandstones. These fractures are similar to those documented by Lorenz (2007b) within Tensleep Formation sandstones at Flat Top Anticline approximately 10.5 miles to the southeast. Sand-filled fractures in some Tensleep Formation cores from Wyoming were recognized by Emmett et al. (1971) and Shebl (1996). Clastic style injections or dikes are documented at various locations around the world (Peterson, 1968, Duranti and Hurst, 2004, Hurst and Cartwright, 2007). As noted by Lorenz (2007a, 2007b) detailed analysis or even simple description of locally pervasive micrite and or sand-filled fractures are not common in the Tensleep Formation geologic or reservoir literature.

Lorenz (1997b) provides a in depth review of sand injectites and their similarity to these fractures within the Tensleep Formation. His review is not repeated within the report but will be included in the full compilation report on fractures within the Tensleep formation to EORI in the Fall of 2010. In the interim his report is available separately from EORI. This report will focus on the general characteristics of this fracture set in the Beer Mug Anticline study area.

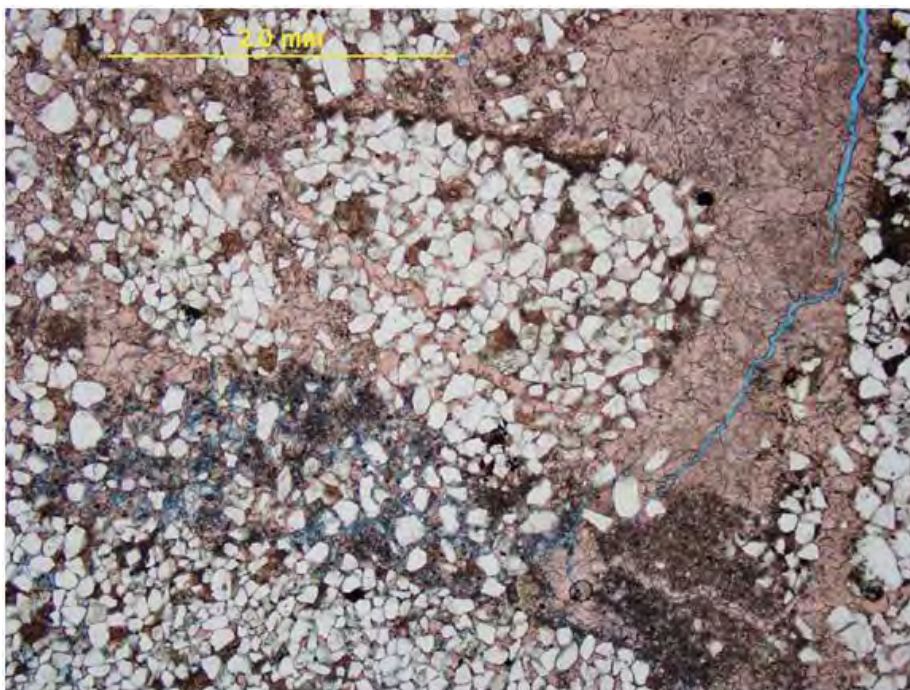
Characteristics of the F_m Fracture Set

Millimeter to Centimeter-Scale

This fracture set is observed in the Tensleep Formation sandstones over the main Beer Mug Anticline. The fractures are typically 1-15 centimeters wide and filled with a combination of fine-grained micrite, sand, silt and occasionally euhedral calcite. Photomicrographs (see following figures) show that some of the sands are likely brecciated clasts of the surrounding matrix rock that have been incorporated into the micrite fill. However, not every fracture is filled with sand grains or matrix clasts and this characteristic (i.e. amount of included sand) can change along strike.



Micrite, calcite and sand-filled fracture, strike 16 degrees. Photomicrograph of this fracture is provided below (site 10).



Thin section shows the fracture is filled with fine grained material, calcite and sandstone breccia clasts (site 10). Yellow scale bar at top left of the image is 2mm long.

At the millimeter-scale some of these fractures can be seen to have been filled with alternating layers of fine-grained micritic material. This suggests there were multiple episodes of emplacement of the fracture fill.



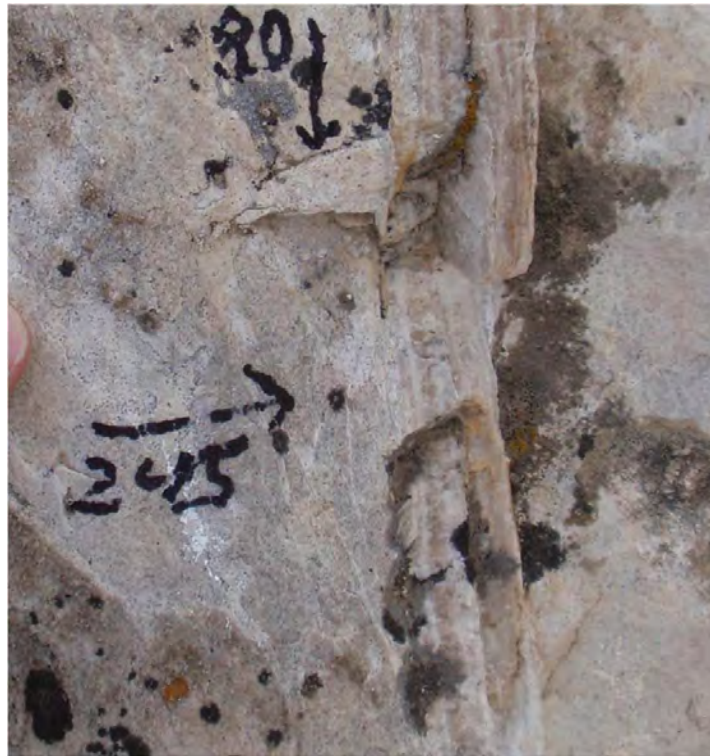
Multiple episodes of micrite emplacement evident by these multiple layers of fine-grained micrite (site 10; scale bar is in millimeters). Note there is less sand material in this fracture which is at the same site as the photographs above.

Mineralization

Some of these fractures contain euhedral calcite. This suggests the calcite was filling an open void space. The void spaces could be formed in a few ways; 1) the fill material was removed either immediately or penecontemporaneously with filling, 2) dissolved away post fill, and/or 3) that there was reactivation of these fractures that created open space along the fracture walls. Some cross-cutting relationships also suggest some of these may have been reactivated in and/or cut by later shear fractures.



Photograph of an F_m fracture with both fine-grained micritic material and crystalline calcite suggesting this fracture may have been reactivated in extension and subsequently filled with euhedral crystalline calcite (site 24).



Close-up image of the previous photograph (site 24); the calcite mineralization can be seen more clearly. The calcite crystals are growing from the opposing fracture walls to the center.



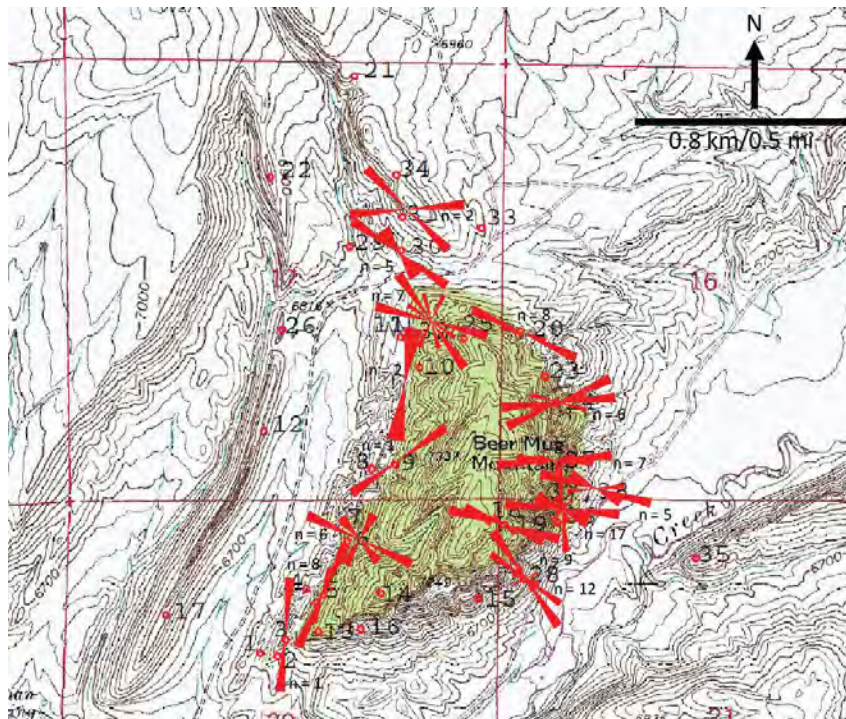
Multibanded F_m fracture cut by shear fracture with approximately 5 cm of displacement. There are smaller F_m fractures (1 cm wide or less) that parallel the shear fracture (Site 37). This intersecting relationship indicates the multibanded micrite-filled fracture is older than the shear fracture.

Meter-Scale

At the meter-scale the F_m fractures are not completely linear but the strikes and dips do suggest that they were aligned relative to an in situ stress. The fracture orientations are highly variable but some are not very dissimilar from the documented tectonic fractures (F_0 , F_1 and F_2) at Beer Mug Anticline. Interestingly few micrite-filled fractures were found to be parallel to the Indian Spring fault related set of fractures.



Micrite and calcite filled fractures (F_0), widths 1 to 15 cm. and spaced in this area a meter apart. These fractures are typically irregular along their trace length at lengths (scales) of more than one meter.



Present day orientation of micrite-filled fractures (F_m) at sites around Beer Mug Anticline. Base map is the Difficulty Quadrangle from United States Geological Survey 7 1/2 Minute Topographic Map Series. Compare to the previous Indian Spring fault-related fracture set (F_3) and note that few if any of F_m fractures actually parallel the Indian Springs fault.

These F_m fractures are best viewed in the sandstone units. These fractures are difficult to follow and in many cases absent in the interbedded limestones. This indicates the vertical extents are typically on the scale of the sandstone bed thicknesses of 1-5 meters. Top and bottom vertical terminations were not observed directly in the outcrop. Lorenz (2007b) observed some vertical terminations that indicated these fracture may have formed prior to deposition of the overlying sediments. No fractures of this type are found in the immediately overlying Opeche Shale or Minnekahta Limestone at Beer Mug Anticline.

Timing of Micrite-Filled Fracture Formation

Much of the evidence presented above suggests that these fractures formed by actual injection of poorly lithified material. This is similar to descriptions of sand injectites by Hurst and Cartwright (2007). The inference here is that the injections formed early in the loading process during Tensleep deposition. However, the Tensleep has not been heavily lithified nor hardened for significant period of its burial history. Therefore, the timing is not well constrained.

Given that many of these fractures are parallel to the tectonic fractures, would indicate that at least some of these fractures are related to Laramide tectonic activity. It is also recognized that many F_m fractures contain not only the lavender, banded dolomitic mudstone fill but also calcite crystals suggestive of opening in extension. Cross-cutting relationships also indicate that the micrite-filled fractures are younger than some of the shear fractures.

Interpretation

The age, origin, and significance of fractures filled with micrite and sand (F_m) are still ambiguous. The strikes are highly variable, and many curve irregularly within both sandstone and limestone strata. Poor planarity suggests low stress anisotropy, indicative of early formation. The current working hypothesis is these structures are similar in genesis and morphology to sand injectites.

However, others seem to follow or at least be parallel to the NW to WNW striking early-strain extension fractures (F_0), suggesting an age and/or mechanical relationship. Many contain not only the lavender, banded fill but also calcite crystals suggestive of opening or reactivation in extension and open voids at depth, especially on the eastern forelimb.

Production Implications

These fine-grained micrite and sand filled fractures are filled with low porosity and low permeability materials relative to the surrounding sandstone matrix, these fractures will be permeability baffles and barriers to flow. Where the fractures are wide 10 cm plus they will be significant barriers. Where these fractures have multiple orientations and spaced only meters apart the reservoir rock will be significantly compartmentalized.

In many instance the filling in these fractures is also fractured. It is likely then that instead of completely closed compartments these fractures are more of a baffle that will allow some flow across the fracture. However, where parallel to each other flow will still be best through the matrix. There will be an associated direction of permeability anisotropy parallel to fracture strike but again the flow will be primarily through the sandstone matrix.

BED-PARALLEL AND BED-OBLIQUE SHEAR FRACTURES/FAULTS (S_1 & S_2)

Introduction

Pervasive small-scale strain was accommodated in the sandstone dune facies both by subtle slip parallel to the large-scale cross bed foresets and by more prominent offsets oblique to bedding. Steps, slickenlines, slickencrysts (elongate calcite crystals) and gouge indicative of shear fractures are present in many outcrops, as well as local deformation bands.

Basic Bed-Parallel Shear Fracture/Fault Pattern

None of the thrust shear offsets in any of the lithologies are large but they are numerous and the cumulative effect is large. Bedding, especially the large dune cross-bed foresets, accommodated much of the pervasive strain and is difficult to document. Small offsets are also present on irregular calcite-mineralized planes oblique to bedding. The entire sedimentary package, especially on the forelimb, is intensely fractured with numerous crosscutting fractures. The age relationships of the fracture sets are commonly ambiguous since offset is minimal and most intersections are mutually crosscutting.

Bedding-parallel shear is present in the thinner-interbedded strata above the Tensleep on the western backlimb. The shales should have been able to accommodate much strain, both pervasive ductile and localized faulting, much of which is now hidden by weathering and vegetation.



The above photographs highlight in plan-view a shear on a cross-bed foreset surface (site 25). These (S_1) were observed on both the forelimb and backlimb.



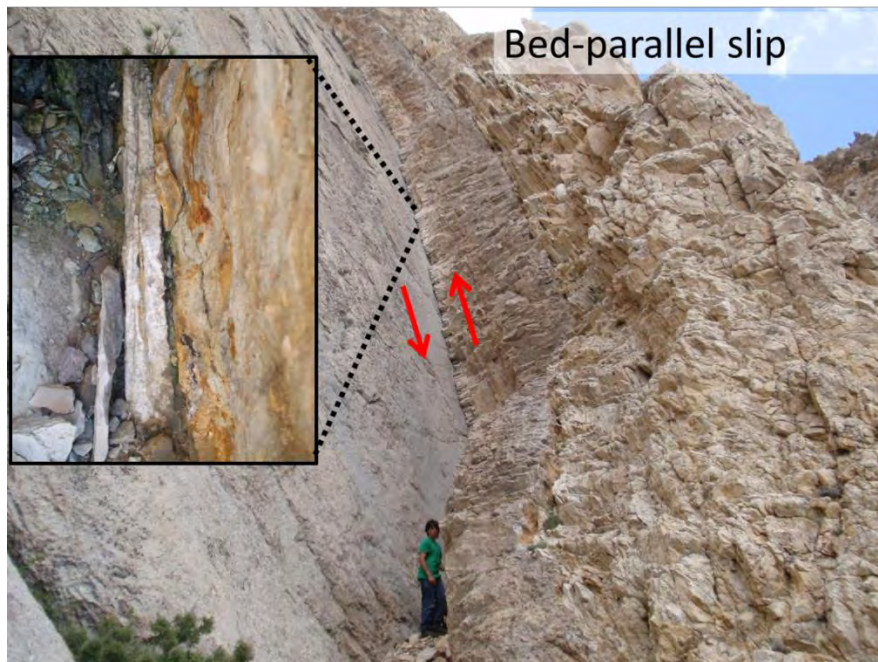
Gouge and calcite filled shear plane (S_1) at young geologist's feet is at a bedding contact between limestone (left) and sandstone (right) on the forelimb; beds are dipping approximately 75 degrees to the NE.



Close-up of the calcite and gouge zone shown in the previous photograph; the shear is parallel to bedding.



View of bed-parallel shear (S_1) and ramp within a limestone of the Tensleep Formation (pink limestone at center, tan sandstone on right).



Gouge and calcite filled bed-parallel slip plane at bedding contact between limestone (left) and sandy limestone (right) on the forelimb (site 15). Beds are dipping approximately 80 degrees to the NE.

Bed-parallel Shear in Soft Sediments on the Western Backlimb and Northeastern Forelimb

Bedding-parallel shear (S_1) is present in the Permian-age, thinner-interbedded strata above the Tensleep on the western backlimb and northeastern forelimb limb. These shear zones/faults were documented in the interbedded shales and limestones of the Goose Egg Formation. The members of this formation from youngest to oldest are Ervay Limestone, Difficulty Shale, Forelle Limestone, Glendo Shale, Minnekahta Limestone and Opeche Shale). The Opeche Shale rests unconformably on the Tensleep Formation. The interbedded shales, in particular the Opeche Shale, accommodated much strain, both pervasive ductile and localized faulting, much of which is now hidden by weathering and vegetation.

The following sequence of figures is of one of these shear zones along the western backlimb and illustrate the general character of these shear zones and faults.



Minnekahta Limestone outcrop, southwestern limb BMA (view to the north). In the area of the box within this photograph is a bed-parallel shear (S_1) at base of the unit and is highlighted in the next figures (near site2).



Photograph of a brecciated shear zone at the base of the Minnekahta Limestone along the southwestern limb of the anticline. The photograph is a close-up of the location highlighted in the box on the previous figure.

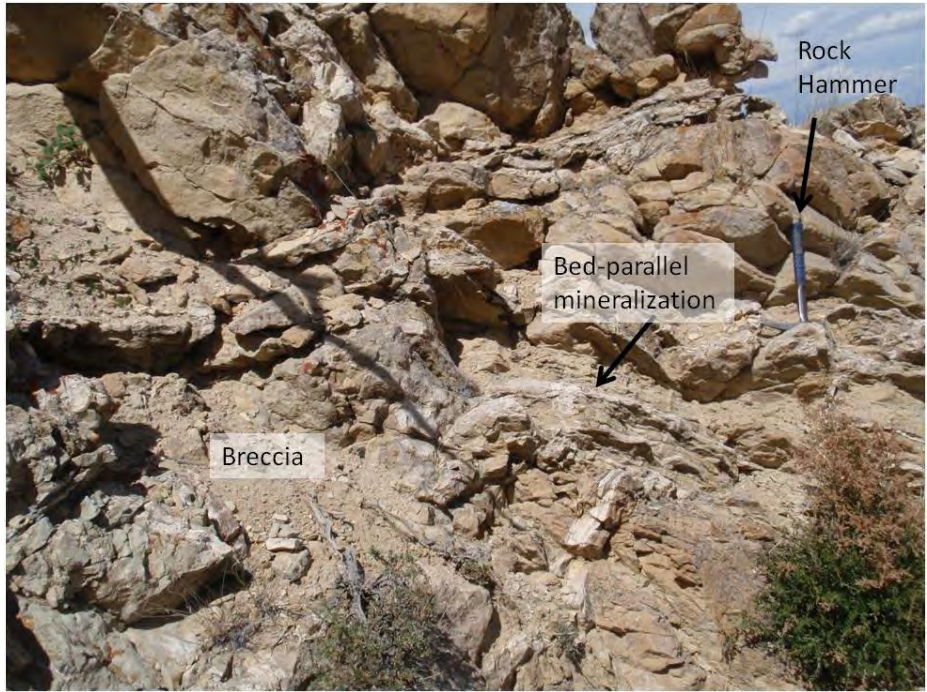


Photograph of a brecciated shear zone at the base of the Minnekahta Limestone and associated open void space filled with fine and large scale calcite mineralization (near site 2).

The following figures highlight one of the larger-scale bed parallel shear zones at the Opeche shale and Minnekahta Limestone contact on the northeastern forelimb. This is a similar structure to the bed parallel faults recorded on the southwestern backlimb of the anticline at the Opeche Shale and Minnekahta Limestone contact.



Photograph of bed-parallel fault zone at the base of the Minnekahta Limestone on the northeastern limb of Beer Mug Anticline (near site23).



Close-up of the bed-parallel fault/shear zone at the Minnekahta Limestone and Opeche Shale contact (near site 23). The zone contains breccia as well as bed-parallel mineralization similar to that observed on the southwestern limb.

Interpretation

These shear zones indicate the shales were zones of significant horizontal shortening and likely thickening/duplication of the stratigraphic section. These units may have been an area of actual detachment that may have duplicated the underlying Tensleep to basement section under the tightly-folded Beer Mug Anticline. It also likely these structures were reactivated by gravitational backsliding after the anticline was formed.

Production Implications

These structures were zones of increased bed-parallel permeability as evidenced by the thick mineralization and increased fracturing. Many of these zones still have some open vugs and thus increased permeability at the present day.

DEFORMATION BANDS (S₃)

Introduction

As previously described; deformation bands form in high-porosity, poorly-cemented sandstones. These structures record small amounts of shear displacement and can be utilized to determine the orientation of the principal stresses when they occur as conjugate shears (Olsson et al., 2004). Displacements are in the range of a few millimeters to a few centimeters. Larger amounts of displacement can be accommodated by zones of multiple, composite deformation bands (Aydin, 1978; Aydin and Johnson, 1983; Antonellini et al., 1994). This observation, that a single deformation band can accommodate only a limited amount of displacement, suggests the possibility of strain hardening (Rudnicki and Rice, 1975; Aydin and Johnson, 1983; Antonellini et al., 1994; Wong et al., 1997). Strain hardening leads to the sequential formation of more deformation bands adjacent to the original band (Rudnicki and Rice, 1975; Antonellini et al., 1994).

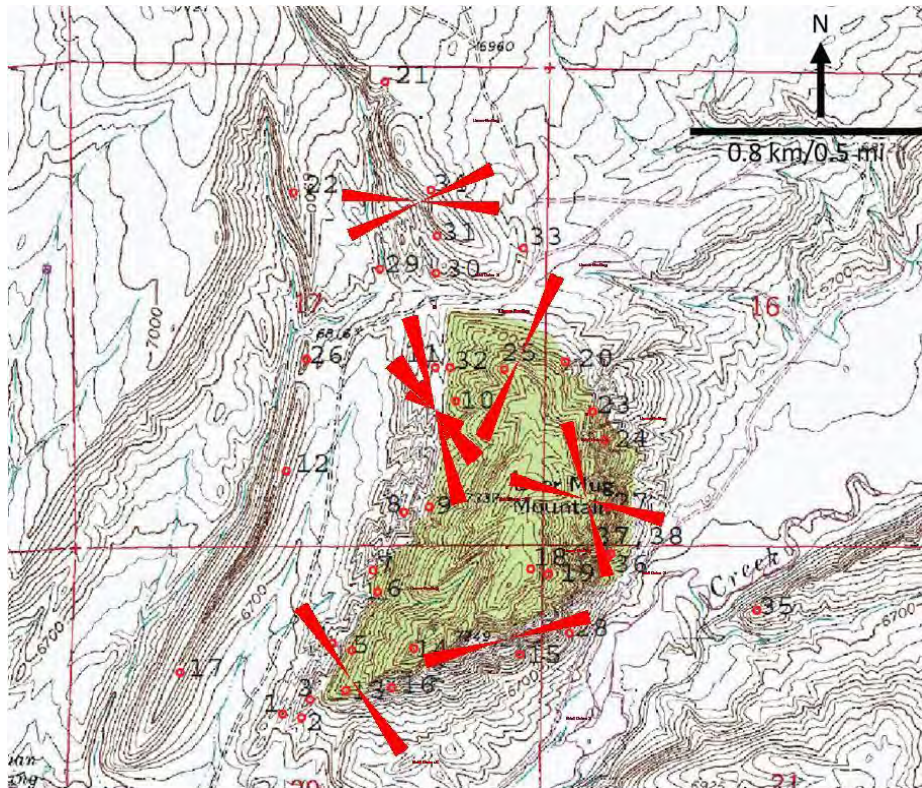
Mair et al. (2000) suggest a different mechanism for the sequential formation of deformation bands. The authors suggest that friction along the first deformation band makes slip more and more difficult, conversely nearby grains are preferentially loaded until a new sequential band is formed. This mechanism results in slip along a new band rather than the older band without strain hardening.

Cooper (2000) documented deformation bands in higher porosity sandstones within the Mesaverde Formation at Teapot Dome, Wyoming. These deformation bands were more resistant to weathering and due to permeability reduction in the bands were barriers to fluid flow across the bands.

Basic Deformation Band Pattern

Only six sites (10, 13, 15, 25, 27 and 31) were documented as having deformation bands. These sites and resultant rose diagrams are shown in the following figures. All the deformation bands are within relatively higher porosity Tensleep Formation sandstones. However, there are only 21 total deformation bands recorded from all six sites. This indicates deformation band formation was very limited. Though there is some alignment of strike at individual locations a comparison of one site to another shows an overall random orientation for

the deformation bands across the structure. It should be noted that only two deformation bands were recorded at each of 4 sites (sites 15, 25, 27 and 31), 3 from another site (site 13) and 10 from one site (site 10). Therefore the sample size at individual sites is very small.



Rose diagrams of deformation bands at six sites around Beer Mug Anticline. The overall pattern is relatively random (total $n=21$).



Example of deformation at site 10; the band is parallel to the arrow (strike 322° , dip is near vertical). The band is 0.8 cm wide.



This photograph illustrates a style of deformation bands formation parallel to strike and dip of cross-bedding. This indicates cross-bed parallel slip. This type of deformation band is difficult to differentiate from regular cross-bedding and likely under sampled.

Interpretation

Shearing of Tensleep Formation sandstones through the formation of deformation bands was not common at Beer Mug Anticline. Overall they are random in orientation though typically subparallel to each other at each individual documented site. Some are actually parallel to cross-bedding. It is difficult at times to differentiate between non-deformed cross-beds and cross-beds enhanced by deformation band shear. This style of deformation band was observed primarily along the northwestern margin of the anticline.

Production Implications of Deformation Bands

Given relatively few deformation bands were recorded in the outcrop these structures will not have a large influence on fluid flow in equivalent rocks and structures. However, deformation bands are a primary style of deformation in high porosity rocks (Olsson, 2004) and if the reservoir of interest has a less indurated matrix there is likely to be more deformation bands.

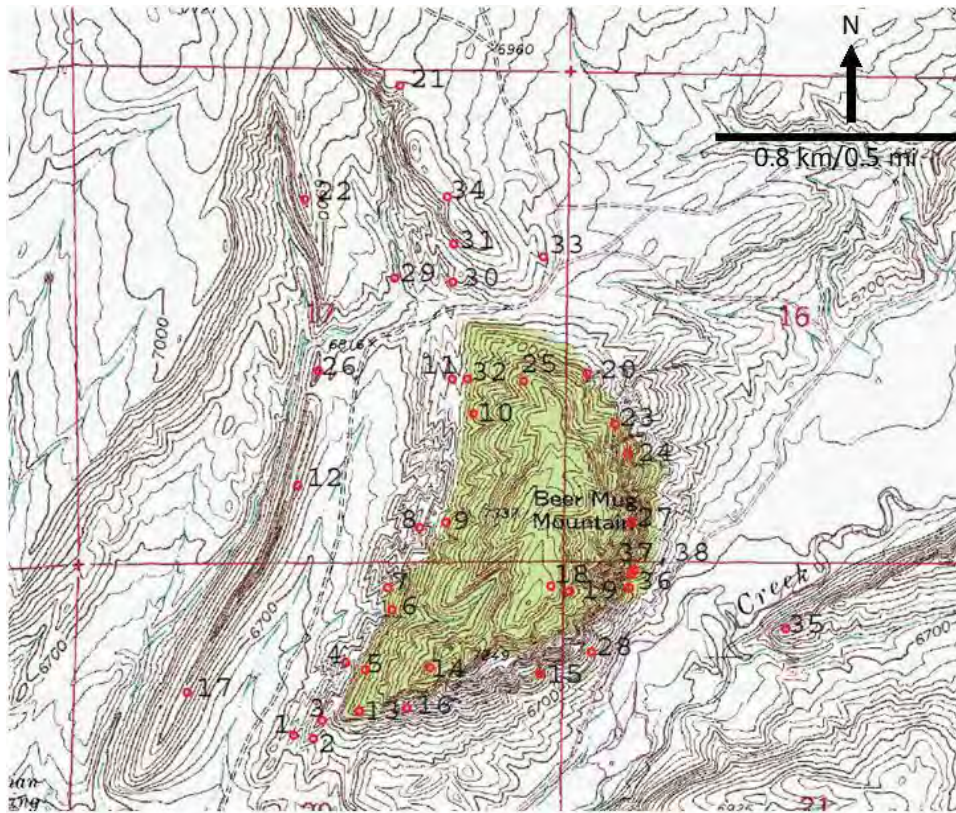
In general deformation bands will have decreased permeability across the band. This creates a permeability anisotropy that is parallel to deformation band strike. But all the fluids are carried through the matrix. At Beer Mug Anticline the previously described extension and shear fractures will break up these deformation bands and allow flow across the bands.

Summary of Deformation Bands (S₃)

Deformation band formation is not ubiquitous across Tensleep Formation sandstones. They are aligned at specific locations but random in orientation relative to the larger structure. One style of documented deformation bands is bed-parallel and cross-bed parallel indicates shear along these surfaces. If this style of deformation was common it would significantly decrease flow across bed and cross-bed boundaries. However, relatively few deformation bands were formed suggesting the lithologic character of the sandstones was not ideal for this type of deformation process.

EXAMPLES OF FRACTURE VARIABILITY AS A FUNCTION OF STRUCTURAL POSITION AND LITHOLOGY

This section details some of the fracture variability as function of location around the anticline. This is a sampling of the data available in supporting data files available through EORI. The following figures, rose diagrams and associated descriptions are correlated by site number to the site map below.



Locations of data collection sites at Beer Mug Anticline, all of the following figures are keyed by site to this location map. Base map is the Difficulty Quadrangle from United States Geological Survey 7 ½ Minute Topographic Map Series.



Site 2: Minnekahta Limestone bedding plane, bedding strike 220 degrees dip 50 degrees. Two major through going extension fractures sets. One set (F_3) is parallel to the Indian Springs fault, the other is the early NW striking extension fracture set (F_1).



Site 6: Upper cross-bedded sandstone unit within the Tensleep Formation, bedding strike 205 degrees, dip 40 degrees. Combination of strike-parallel extension fractures (F_3), F_0 extension fractures and micrite-filled fractures (F_m).



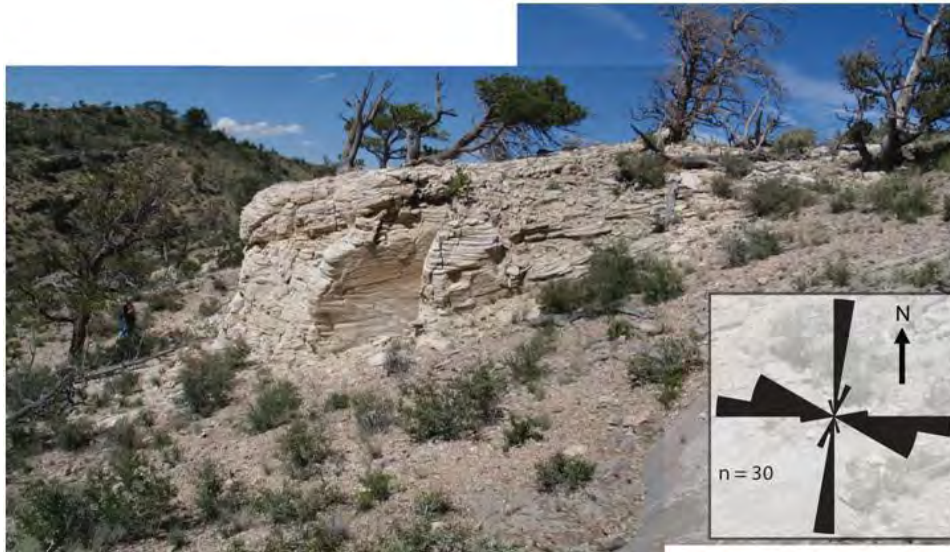
Site 9: Upper cross-bedded sandstone unit within the Tensleep Fm, bedding strike 206 degrees, dip 42 degrees. Combination of extension fractures (F_0 , F_1 , F_2), shear fractures (S_1) and micrite-filled (F_m) fractures.



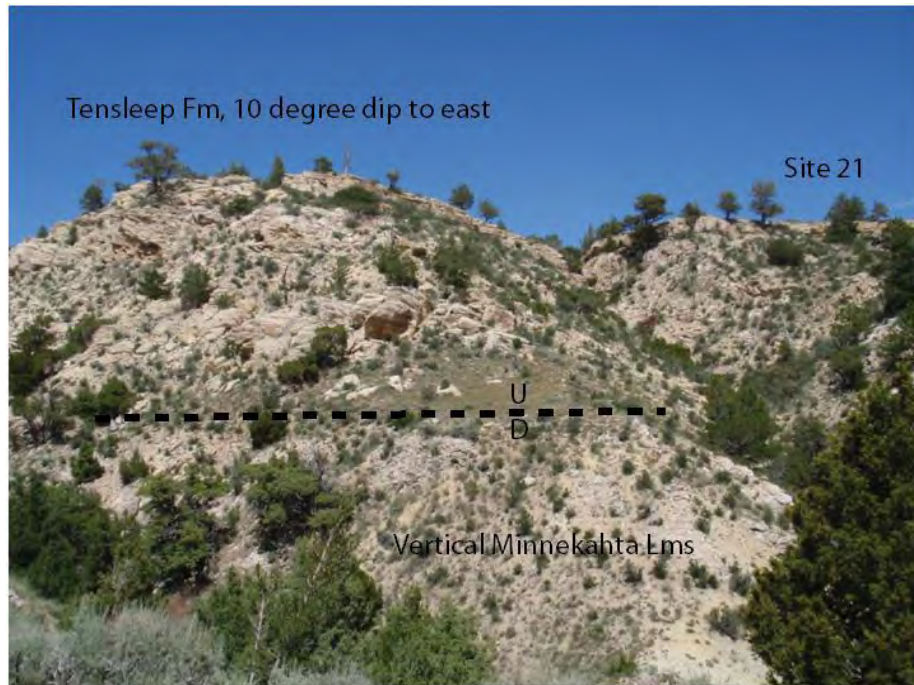
Site 10: View upper cross-bedded sandstone unit within the Tensleep Formation, bedding strike 198 degrees, dip 38 degrees. Combination of extension fractures (F_0 , F_1 , F_2), micrite-filled fractures (F_m), and deformation bands (S_3).



Site 13: Cross sectional view of upper sandstone unit within the Tensleep Formation, bedding strike 205 degrees, dip 48 degrees. Combination of extension fractures (F_0 , F_1 , F_2 , F_3), shear fractures (S_1), and deformation bands (S_3).



Site 18: View of near horizontal pavement of cross-bedded sandstone unit within the Tensleep Formation, bedding strike 160 degrees, dip 10 degrees. Combination of extension fractures (F_0 , F_1 , F_2).



Site 21: Left photograph is of the west vergent fault plane, measured Tensleep Fm outcrop is at top. Right photograph shows extension fractures in upper cross-bedded sandstone unit of the Tensleep Formation, bedding strike 350 degrees, dip 12 degrees. Combination of extension fractures (F_0 , F_1 , F_2), primarily F_0 .



Site 18: View of near horizontal pavement of cross-bedded sandstone unit within the Tensleep Formation, bedding strike 160 degrees, dip 10 degrees. Combination of extension fractures (F_0 , F_1 , F_2).

VARIATION AS A FUNCTION OF LITHOLOGY: THE ALCOVA LIMESTONE

Introduction

On the western limb of the anticline, small thrust faults were documented in the Alcova Limestone. These structures indicate that the maximum stress (σ_1) was in the horizontal plane and approximately ESE-WNW prior to tilting of the beds. This suggests that the Beer Mug Anticline was not passively draped over a basement thrust but was rather formed by folding due to high horizontal stresses in the thin-bedded sedimentary cover.

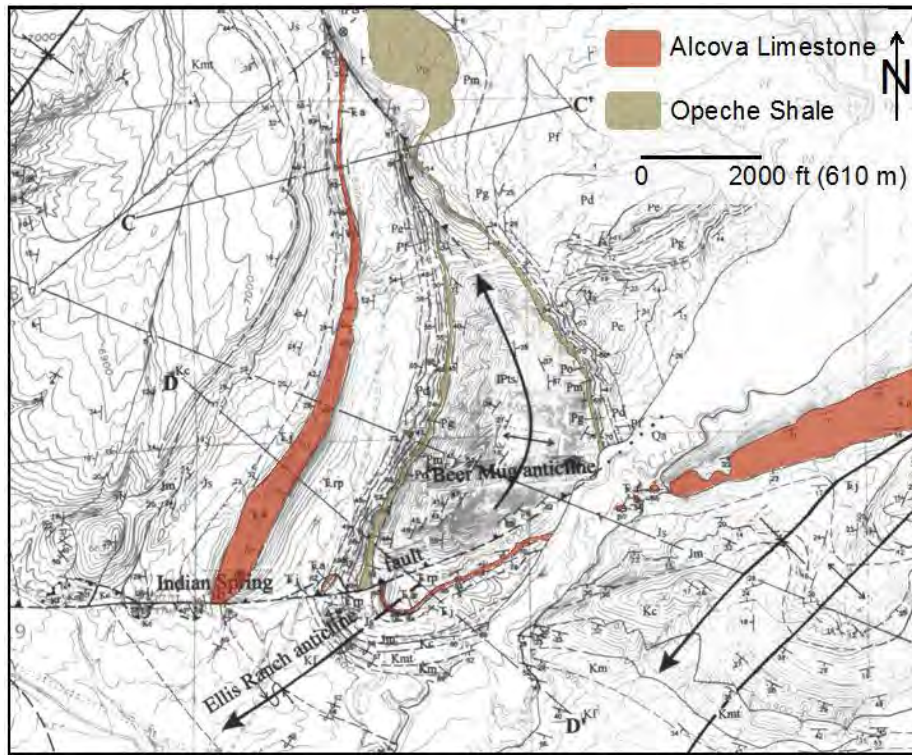
Alcova Thrust Faults/Fractures

The two-meter thick Triassic Alcova Limestone, a heterogeneous, thin-bedded carbonate, forms a stiff strut within a thicker shale sequence. Small, complex thrust faults in the Alcova Limestone near Beer Mug Anticline in southeastern Wyoming record a bedding-parallel compressive stress that exceeded the weight of the overburden.

Structures characteristic of the Alcova thrust system include standard thrust planes, back-thrusts, bedding-parallel decollement zones, bed-parallel shear in the folds, folds, and fold-core voids. Local stylolites suggest that dissolution also played a role. The main thrusts in the Alcova Limestone form meter-scale en echelon planes that step back at each offset when traced up section, and that have offsets of 1-20 centimeters. The thrusts cut ductile lithologies, where the beds thickened plastically, and brittle lithologies where the beds fractured. These thrust planes can be traced from down-dip initiation at bed-parallel slip planes up-dip to where they steepen and terminate blindly in folded duplex structures. Smaller, centimeter-scale synthetic and antithetic thrusts are also pervasive in the formation. Most of the main thrusts are relatively small, and none seems to have developed into a larger structure that localized meters or tens of meters of offset, suggesting a self-limiting feedback mechanism that locked each fault after at most a few tens of centimeters of displacement.

These thrusts allow a unique interpretation of the local stress system that produced the kilometer scale thrust faults in the area. Only horizontal compressive stresses in excess of the overburden could have produced the Alcova thrust system, and those stresses rather than drape over a basement fault likely produced the local dramatic and tightly folded Beer Mug Anticline and therefore analogous at a larger scale.

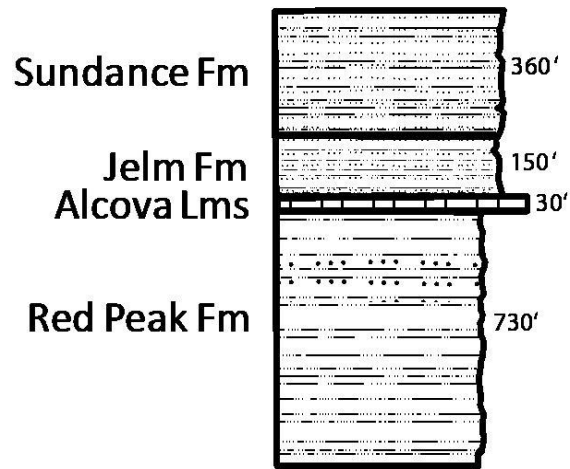
More importantly, the small Alcova thrusts mimic the geometry of kilometer-scale thrusts seen in seismic lines in thin-skinned fold and thrust belts, and can be used as analogs to study the characteristics of deformation in these systems.



Outcrops of the Alcova Limestone are highlighted on this geologic map of Beer Mug Anticline, modified from Taylor (1996).



The Alcova Limestone Member of the Chugwater Formation is two to three meters thick. It consists of a thin, hard, fine-bedded, pinkish to light-gray limestone with thinner interbedded shaley units. Fossils from the Alcova place it in Middle or Upper Triassic.



The Alcova Limestone currently forms a west-dipping hogback on the west side of Beer Mug Anticline; stratigraphic section after Taylor (1996). The limestone is essentially a stiff strut within a sequence of thick interbedded mudstones, siltstones and shales.



Alcova Limestone outcrop, western limb of BMA (view to the south).

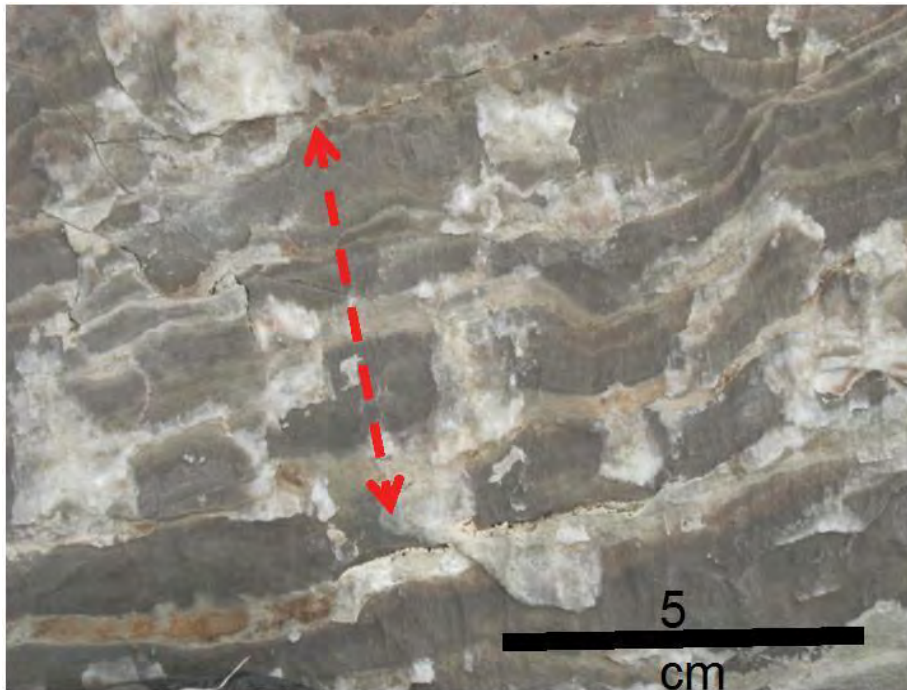


Aerial view of Alcova Limestone outcrop, western backlimb of BMA (view to the north).

West ← → East



The Alcova is cut by numerous oblique-to-bedding, strike-parallel, en echelon shear planes, most dipping to the west but also locally to the east.



Surfaces of the shear planes are marked by slickenlines, and by asymmetric calcite slickencrystals indicating dip-parallel, reverse offset.

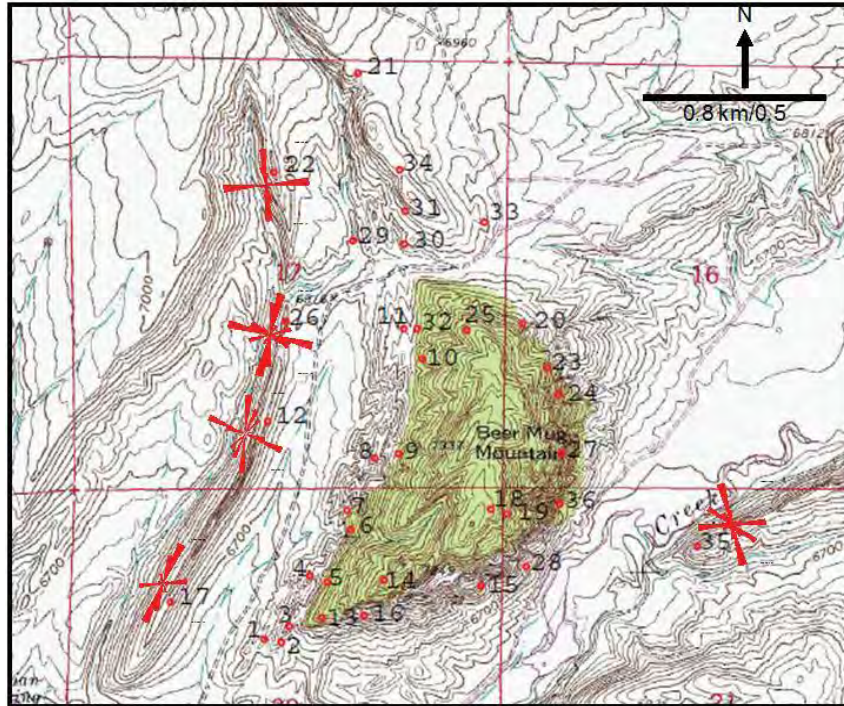
West ← → East



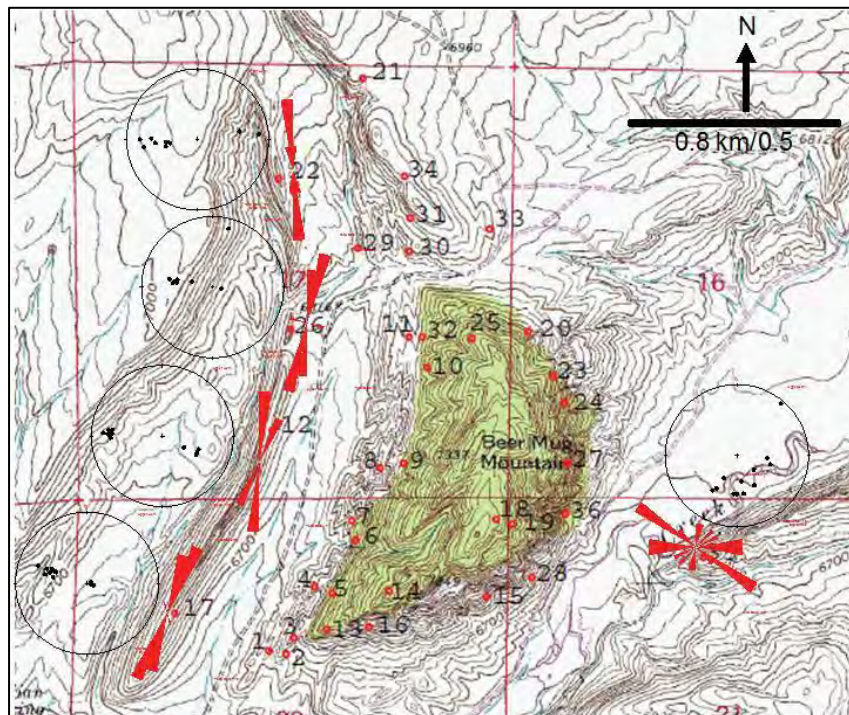
Offset bedding shows a reverse sense of motion on all shear planes. Calcite was deposited in the hollows formed between asperities.



Red arrow in top photograph points to shear plane surface shown in bottom photograph. This is one of the largest observed shear planes and extends across approximately four square meters.



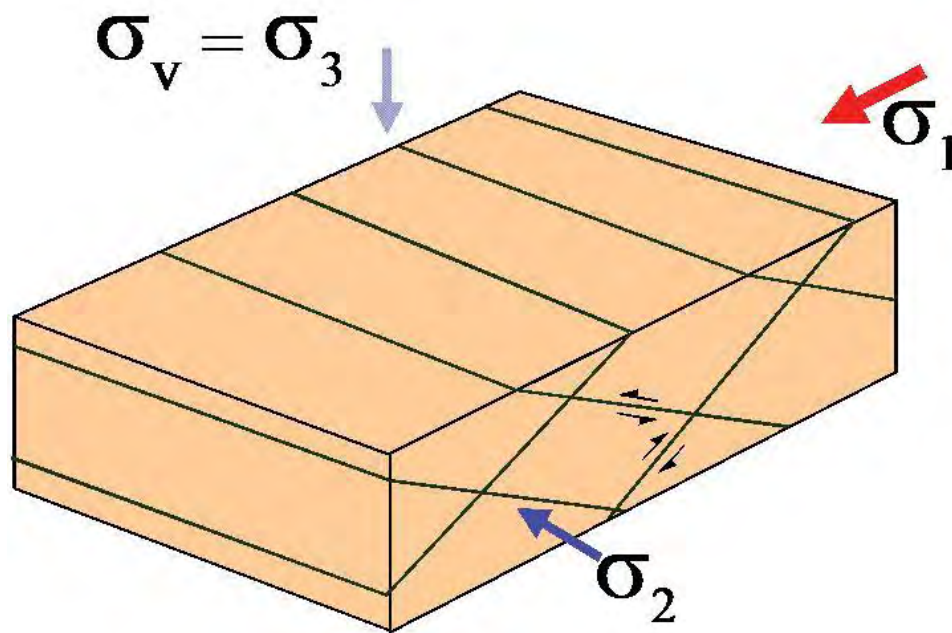
All fractures in the Alcova Limestone east and west of Beer Mug Anticline.



Strikes of the shear planes, parallel the strike of the Alcova bedding, indicate that the maximum compressive stress was generally east-west and parallel to bedding. Outcrops east of the Beer Mug Anticline show a more irregular thrust orientation pattern suggesting a more complex stress history.



Photographs of intersecting conjugate low-angle shear planes, these conjugate shears indicate that the maximum compressive stress was bed parallel.



Conjugate thrust faults/shear fractures indicate that the maximum compressive stress, bisecting the acute angle, was parallel to bedding and in the horizontal plane before folding of the strata.



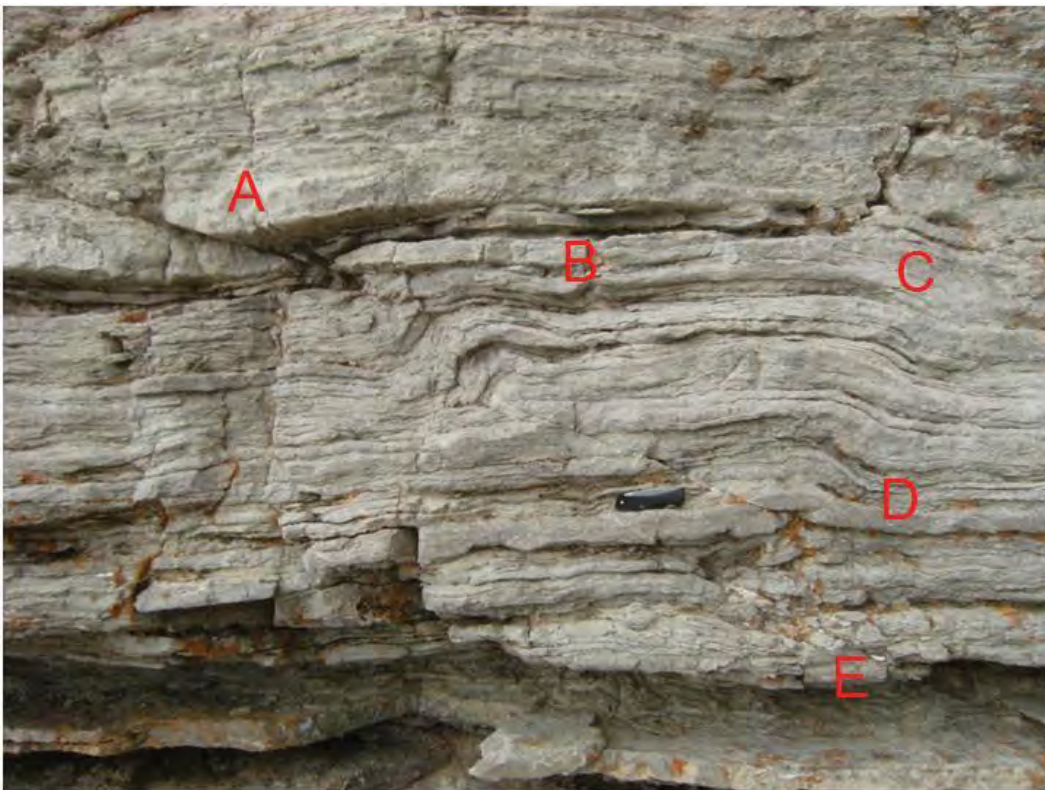
En echelon shear segments step back up-section (see close-up below).



Close-up of upper photo showing that en echelon offsets step back up section, and that they commonly step where propagation was interrupted by more ductile shaley beds.

Folds in the Alcova Limestone

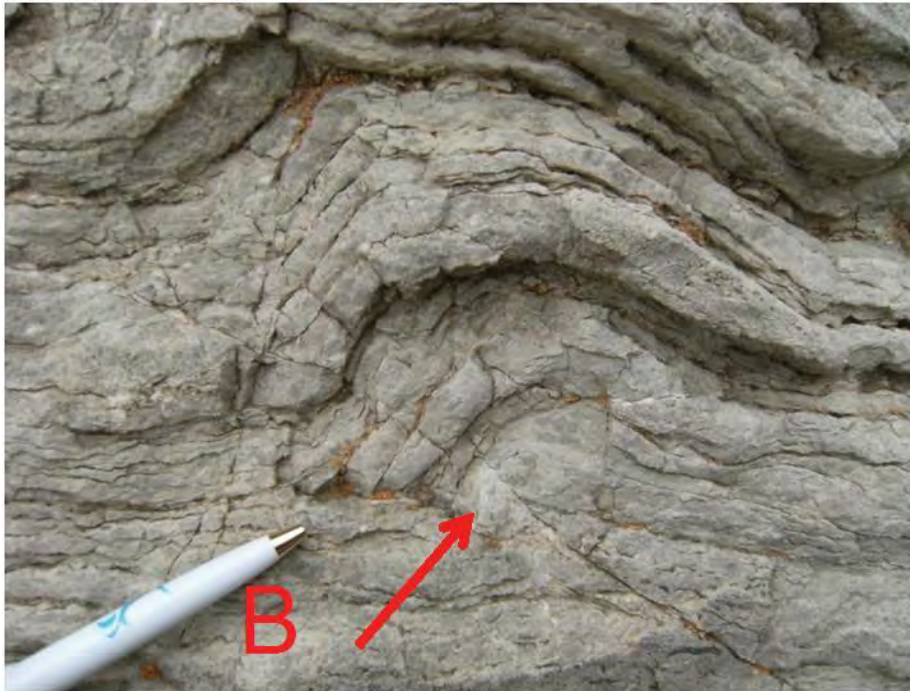
Numerous folds are also recorded in the Alcova limestone. These folds and associated faults are analogous to larger scale structures. The figure sequence below details the folds in just one site. Each close-up photograph is keyed by letter to the first large-scale outcrop photograph shown below. These structures are observed all along the western exposures of the Alcova Limestone.



Reverse-offset echelon shear planes with different characteristics in different lithologies, blind fold terminations, and back thrusts; pocket knife for scale. This and the associated photos of this outcrop have been rotated 20° ccw so that the inclined bedding appears horizontal.



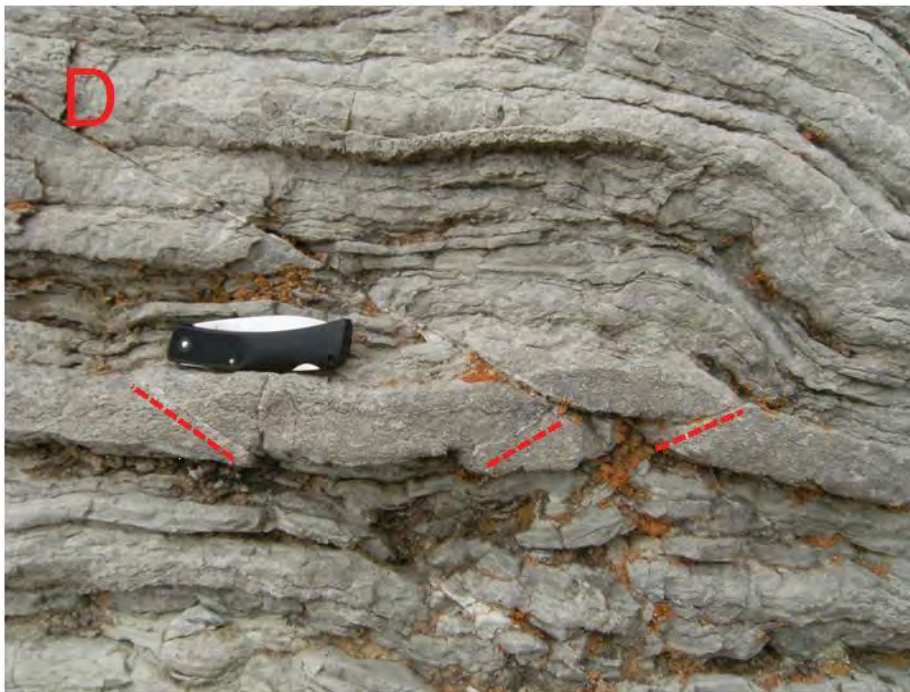
New thrust above the fold is back stepped and originates at volume constraints associated with the fold.



Thrust fault tips out upward in a splayed fault and overlying fold. Sparry calcite (arrow) fills a void under the fold. Beds thicken and thin due to pressure solution, overlap, and ductility.



Poorly defined back thrust is accommodated primarily by folding.



Back thrust (upward to the right) and associated fold lift a keystone wedge of rock in a more competent, grainstone unit (A) with several smaller subsidiary shears along the dotted lines. Less competent units above the wedge are folded, doubled, overlap, and locally dissolved.



Thrust initiated above a volume-constrained crush zone defined by breccia and irregular intersecting shears.

Interpretation

Implications for the kinematic origin of Beer Mug Anticline are; 1) the maximum horizontal compression was primarily E-W, 2) Beer Mug Anticline is likely a thin-skinned, crumpled-rug fold rather than a passive drape over a basement fault, and 3) bedding folded during and after formation of conjugate thrust faults

None of the thrust offsets in any of the lithologies are large but they are numerous and the cumulative effect is large.

Summary of Shear Fractures/Faults/Folds within the Alcova Limestone

The shear fractures in the Alcova Limestone are typically small-scale intersecting thrust faults that have mm to cm scale reverse offset. These faults back up section, in an echelon segments and commonly terminate upward as blind thrusts in folds.

Deformation depends in part on lithology with faults terminating within interbeds of shale. The thrust faults in the Alcova indicate that the maximum stress (σ_1) was parallel to bedding, and E-W during folding of the associated Beer Mug Anticline.

STRUCTURAL HYPOTHESIS FOR BEER MUG ANTICLINE

The Beer Mug Anticline is a tight fold: bedding dip changes from 40° to 55° on the western backlimb to 90° on the eastern forelimb. Fold-related fractures are intensely developed along the crest. The core of the anticline is a shattered zone. The initial folded arch may have been cut through by a thrust fault. The core has much void space and evidence for previous oil fill, may have been a good reservoir prior to breaching. The northern extension of the Beer Mug Anticline is a west vergent fold (vs. east vergent along the main southern extension). The northern extension is north of a cross-strike structural discontinuity. The tight structure leaves little room for a basement block in the middle, so this structure is probably a detachment and not a basement-cored thrust.

This hypothesis of the Beer Mug Anticline structure as a thin-skinned fault propagation fold vs. a basement-involved thrust is similar to the structure at Oil Mountain west of Casper Wyoming as described by Hennings et al. (2000). The extensive surface and subsurface data provided by Hennings et al. (2000) show that thin-skinned style thrust faulting can occur in an overall Laramide basement-involved structural setting.

Additionally the height of Beer Mug Anticline above the cross-strike structural discontinuity is approximately 750 feet and is on the same order of thickness as the stratigraphic thickness from the Goose Egg Formation/Tensleep Formation contact (where numerous bed-parallel shears were documented) to the basement suggesting possible duplication of the Tensleep section.

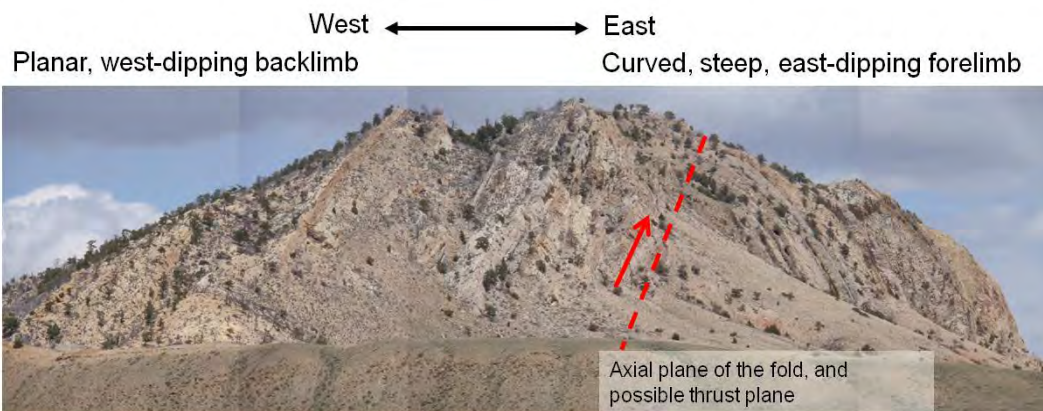
Evidence for this interpretation also includes bed-parallel shear in the interbedded limestones and shales of the Goose Egg Formation, the intraformational thrusts in the Alcova Limestone, the bed-parallel shears and faults in the Tensleep Formation, and that Beer Mug Anticline is thrust over the Ellis Ranch Anticline. Intersection of the north-trending basement continuity with the Indian Spring fault produced the “trapdoor style” structure at the southern end of Beer Mug Anticline as described by Stone (1993).



The core of the anticline is a shattered zone. The initial folded arch may have been cut through by a thrust fault. The core has much void space and evidence for previous oil fill and may have been a good reservoir prior to breaching.



Within the Alcova Limestone shear planes commonly die out in folds. This geometry is interpreted to mimic that of the larger-scale Beer Mug Anticline – compare photographs above and below.

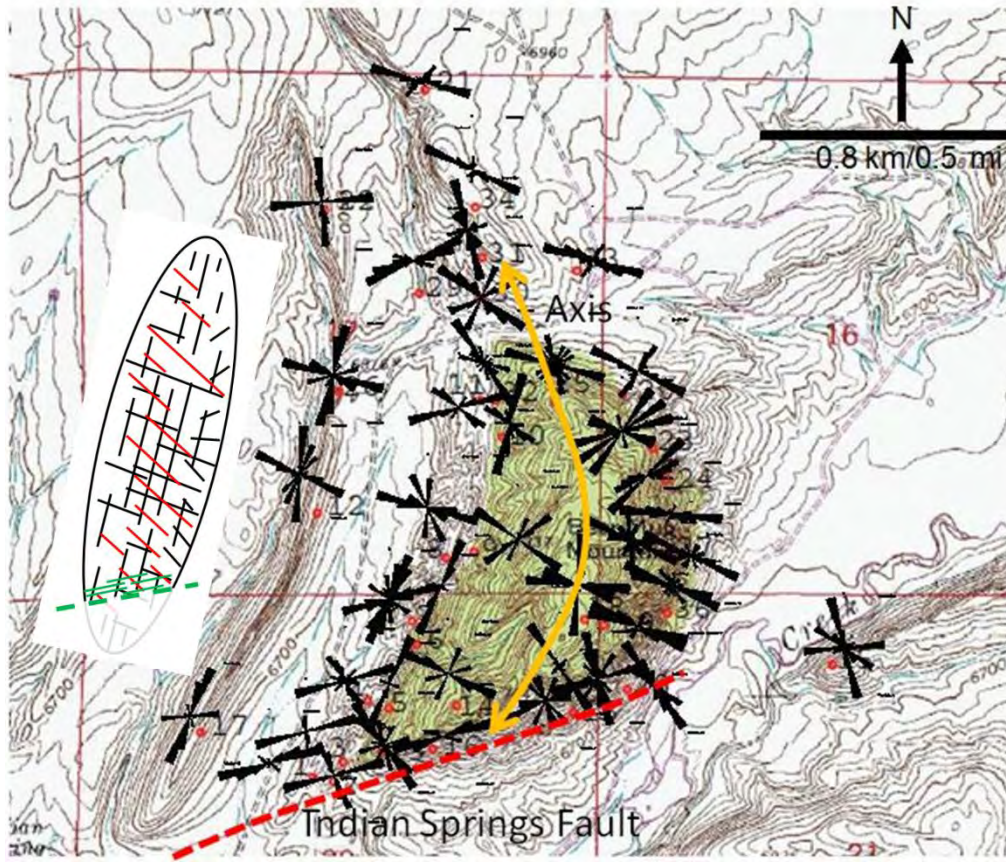


Shear fractures/thrust faults in the Alcova Limestone indicate that Beer Mug Anticline was formed primarily by E-W horizontal compressive stress as a detached fold.

SEQUENCE OF DEFORMATION

The most regular fracture sets are interpreted as follows. The oldest, NW to WNW striking fracture set (F_0) probably formed during the early stages of regional compression that eventually led to uplift of Beer Mug Anticline but pre-dated folding. This extension fracture set likely formed at the same time as small thrusts observed in the Alcova Limestone to the west (Lorenz and Cooper, 2010); both indicate a general NW-SE to WNW-ESE direction of shortening. The next fracture sets, dip-parallel (F_1) and strike-parallel (F_2) are related to folding and extension of beds across the anticline. Initial horizontal compression initiated the F_1 fracture set, continued compression started to fold the beds and the subsequent initiation of the F_2 fracture set. The S_1 shear fractures formed during folding and the related to bed-parallel slip. The S_2 shear fractures and deformation bands (S_2 ; parallel, normal and oblique to bedding), are also related to folding. The Indian Springs wrench-fault-parallel fractures (F_3), formed at the same time as wrench displacement which was late to penecontemporaneous with folding.

Many of these structures formed early in one mode and were reactivated in other modes, producing enigmatic compound structures with conflicting evidence for their origin.



Rose diagrams of fractures at select sites and a conceptualized model of fracture sets at Beer Mug anticline.

IMPLICATIONS FOR PRODUCTION

The Tensleep Formation contains interconnected, intensely developed fractures in most parts of the anticline but with internal variations due to both lithology and structural position. Fracture development (spacing, number and type of fracture sets) varies on different structural parts of an anticline.

Intersecting deformation bands with their associated reduction in porosity and permeability (Antonellini and Aydin, 1995) may create baffles that can compartmentalize a reservoir. However, the intersecting and closely spaced extension fractures likely counteract this compartmentalization effect.

Limestones are uniquely “whole/intact” re-cemented units that are likely vertical barriers and baffles relative to the more densely fractured dolomites, sandstones and sandy limestones.

The Tensleep Formation in the core of tightly-folded anticlines (bedding dip change greater than 30°) should be a great target.

An understanding of the origins of these fractures in differing structures (such as the tightly-folded Beer Mug Anticline) structural settings and lithologies provides a basis for predicting fracture characteristics and distributions between wells, and thus their effects on flow for various EOR techniques.

CONCLUSIONS

The suite of strain-accommodation structures at Beer Mug Anticline consists of early-formed regional compression-related extension fractures (F_0) and later-formed dip-parallel (F_1) and strike-parallel (F_2) extension fractures, both bedding-parallel shear planes (S_1), bedding-oblique shears (S_2) and additional shears such as deformation bands with a variety of strikes (S_3), and wrench fault related fractures (F_3). Most of these structures formed during anticline development, as the strata were extended parallel to and oblique to the anticlinal hinge.

Additional structures, some with similar orientations, formed at different times during structural development of the anticlines. As folding intensified and tightened many of these structures were reactivated with differing senses of offset, leaving a suite of compound features that do not record a simple, linear, progressive sequence of development for individual strain-accommodation structures.

Though complex the variability in the fracture patterns can be synthesized and captured in idealized fracture models constructed with the understanding that local variations are common. Development of a thorough understanding of fracture characteristics and distributions within the Tensleep Formation over a spectrum of anticlines, will allow operators to place wells in the optimum positions and design enhanced oil recovery (EOR) programs to maximize efficiency.

REFERENCES

- Ahlbrandt, T.S., and R.E. Harris, 1975, Clastic dikes in the Fountain and Casper formations (Permo-Pennsylvanian), southeastern Wyoming: *Rocky Mountain Geology*, v. 14, p. 51-54.
- Antonellini, M.A., and Aydin, A., 1995, Effect of faulting on fluid flow in porous sandstones: geometry and spatial distribution, *American Association of Petroleum Geologists Bulletin*, v. 79, p. 642-671.
- Antonellini, M.A., Aydin, A., and Pollard, D.D., 1994, Microstructure of deformation bands in porous sandstones at Arches National Park, Utah, *Journal of Structural Geology*, v. 16, p. 941-959.
- Aydin, A., 1978. Small faults formed as deformation bands in sandstone. *Pure and Applied Geophysics* v. 116, p. 913-930.
- Aydin, A., and Johnson, A.M., 1983, Analysis of faulting in porous sandstones, *Journal of Structural Geology*, v. 5, p. 19-31.
- Boyd, D.W., 1993, Paleozoic history of Wyoming, in Snoke, A.W., Steidtmann, J.R., and Roberts, S.M., eds., *Geology of Wyoming: Geological Survey of Wyoming Memoir no. 5*, p. 164-187.
- Blackstone, D.L. 1994, Oil Springs and Flat Top anticlines, Carbon County Wyoming: An unusual fold pair: *The Mountain Geologist*, v. 31, p. 53-60.
- Blevens, D.M., 1984, Computer assisted structural analysis of the western termination of the Flat Top anticline, Carbon County, Wyoming: Master's thesis, University of Wyoming, 119 p.
- Brown, O.P., 1939, The geology of Difficulty-Little Shirley Basin area, Carbon County, Wyoming: Master's thesis, University of Wyoming, 22p.
- Carey, B.D., 1950, Geology of the eastern part of the Flat Top anticline, Albany and Carbon Counties, Wyoming: Master's thesis, University of Wyoming, 62 p.
- Carr-Crabaugh, M., Dunn, T.L., 1996, Reservoir Heterogeneity as a function of accumulation and preservation dynamics, Tensleep sandstone, Bighorn and Wind River basins, Wyoming, *in* Longman, M.W. and Sonnenfeld, M.D., eds., 1996, *Paleozoic Systems of the Rocky Mountain Region*, Rocky Mountain Section SEPM (Society for Sedimentary Geology), p. 305-320.
- Cooper, S.P., 2000, Deformation within a basement-cored anticline: Teapot Dome, Wyoming, M.S. Thesis, New Mexico Institute of Mining and Technology, 274p.
- Cooper, S.P., and Lorenz, J.L., 2010, Fracture patterns associated with tightly folded Laramide structures: the example of Beer Mug Anticline, Wyoming: *American Association of Petroleum Geologists 2010 Annual Meeting, Abstract with Programs*.
- Cooper, S. P., Goodwin, L. B., and Lorenz, J. C., 2006, Fracture and fault patterns associated with basement-cored anticlines: The example of Teapot Dome, Wyoming: *American Association of Petroleum Geologists Bulletin*, v. 90, p. 1903-1920.
- Dunn, T.L. 1997, Anisotropy and spatial variation of relative permeability and lithologic character of Tensleep sandstone reservoirs in the Bighorn and Wind River basins, Wyoming: Department of Energy Contract No. DE-AC22-93BC14897: Final report, 187p.
- Duranti, D., and A. Hurst, 2004, Fluidization and injection in the deep-water sandstones of the Eocene Alba Formation (UK North Sea): *Sedimentology*, v. 51, p. 503-529.

- Emmett, W.R., K.W. Beaver, and J.A. McCaleb, 1971, Little Buffalo Basin Tensleep heterogeneity—its influence on drilling and secondary recovery: *Journal of Petroleum Technology*, February, 1971, p. 161-168.
- Glennie, K.W., 1970, Desert sedimentary environments, *in* *Developments in Sedimentology*, no. 15, New York, Elsevier Publishing Company, 222 p.
- Hart, B.S., 2006, Seismic expression of fracture-swarm sweet spots, Upper Cretaceous tight-gas reservoirs, San Juan Basin, *American Association of Petroleum Geologists Bulletin*, p. 1519-1534.
- Hennings, P.H., Olson, J.E., and Thompson, L.B., 2000, Combining outcrop data and three-dimensional structural models to characterize fractured reservoirs: an example from Wyoming, *American Association of Petroleum Geologists Bulletin*, v.84, p. 830-849.
- Johnson, S.A., and Huntoon, P.W., 1994, Permeability architecture and groundwater circulation along a fault-severed margin, northern Hanna Basin, Carbon County, Wyoming, Final Report WWRC-94-27, Wyoming Water Resources Center, University of Wyoming, 115p.
- Knight, W.C., 1900, Jurassic Rocks of southeastern Wyoming, *Geological Society of America Bulletin*, v. 2, p. 377-388.
- Knight, W.H., 1944, Geology of the western part of the Flat Top anticline, Albany and Carbon Counties, Wyoming: Master's thesis, University of Wyoming, 30p.
- Lee, W.T., 1927, Correlation of geological formations between east-central Colorado, central Wyoming, and southern Montana, U.S. Geological Survey Professional Paper 149, 80p.
- Lillegraven, J.A., and Snoke, A.W., 1996, A new look at the Laramide orogeny in the Seminoe and Shirley Mountains, Freezeout Hills, and Hanna Basin, south-central Wyoming: Wyoming State Geological Survey, Public Information Circular 36, 52p.
- Lillegraven, J.A., Snoke, A.W., and McKenna, M.C., 2004, Tectonic and paleogeographic implications of late Laramide geologic history in the northeastern corner of Wyoming's Hanna Basin: *Rocky Mountain Geology*, v. 39, p. 7-64.
- Logan, W.N., 1900, The stratigraphy and invertebrate faunas of the Jurassic Formations in the Freezeout Hills of Wyoming, *Kansas University Quarterly Bulletin*, v. 9, n. 2, p. 109-134.
- Long, J.C.S., Aydin, A., Brown, S.R., Einstein, H.H., Hestir, K., Hsieh, P.A., Myer, L.R., Nolte, K.G., Norton, D.L., Olsson, O.L., Paillet, F.L., Smith, J.L., and Thomsen, L., 1997, Rock fracture and fluid flow: National Academy Press, Washington, D.C., 551 p.
- Lorenz, J.C., 2007a, Summary of the published information on Tensleep fractures; report to the Enhanced Oil Recovery Institute, University of Wyoming, April 20, 2007, 36 p.
- Lorenz, J.C., 2007b, Fractures and strain accommodation in the Tensleep Formation at Flat Top Anticline, Carbon County, Wyoming: Implications for Analog Reservoir Systems; report to the Enhanced Oil Recovery Institute, University of Wyoming, November 13, 2007, 89p.
- Lorenz, J.C., and Cooper, S.P., 2010, Thrust Faults in the Alcova Limestone: Nature's Sand-Table Experiment, *American Association of Petroleum Geologists Rocky Mountain Section Meeting Official Program Book*, June 13-16, 2010, Durango, CO.
- Lorenz, J.C., Teufel, L.W., and Warpinski, N.R., 1991, Regional fractures I: A mechanism for the formation of regional fractures at depth in flat-lying reservoirs: *American Association of Petroleum Geologists Bulletin*, v. 75, p. 1714-1737.
- Love, J. D., and Christiansen, A. C., 1985, Geologic Map of Wyoming: U.S. Geological Survey, scale 1:500,000.

- Love, J.D., Christiansen, A.C., and Ver Pleog, A.J., 1993, Stratigraphic nomenclature chart of Wyoming: Geological Survey of Wyoming Map series 41.
- Mair, K., Main, I., Elphick, S., 2000, Sequential growth of deformation bands in the laboratory, *Journal of Structural Geology*, v. p. 22, p. 25–42.
- Maravich, M.D., 1941 Geology of Freezeout Mountain – Bald Mountain Area, Carbon County, Wyoming: *American Association of Petroleum Geologists Bulletin*, v. 25, p. 883-897.
- Olsson, W.A., 2000, Origin of Luders' bands in deformed rock, *Journal of Geophysical Research*, v. 105, p. 5931–5938.
- Olsson, W.A., Lorenz, J.C., and Cooper, S.P., 2004, A mechanical model for multiply-oriented conjugate deformation bands, *Journal of Structural Geology*, v. 26, p. 325 -338.
- Peng, S., and Johnson, A.M., 1972, Crack growth and faulting in cylindrical specimens of Chelmsford granite: *International Journal of Rock Mechanics and Mining Science*, v. 9, p. 37-86.
- Peterson, G.L., 1968, Flow structures in sandstone dikes: *Sedimentary Geology*, v. 2, p. 177-190.
- Pollard, D.D., and Aydin, A., 1988, Progress in understanding jointing over the past century: *Geological Society of America, Bulletin*, v. 100, no. 8, pp. 1181-1204.
- Rudnicki, J.W., and Rice, J.R., 1975, Conditions for the localization of deformation in pressure-sensitive dilatant materials: *Journal Mech. Phys. Solids*, v. 23, p. 371-394.
- Shebl, M.A., 1996, Geochemical and diagenetic investigations of the Tensleep Sandstone, Bighorn Basin, Wyoming: PhD dissertation, University of Wyoming, Laramie, Wyoming, 285p.
- Stone, D.S., 1993, Basement-involved thrust-generated folds as seismically imaged in the subsurface of the Rocky Mountain foreland, in Schimdt, C.J., Chase, R.B., and Erslev, E.A., eds., *Laramide Basement Deformation in the Rocky Mountain Foreland of the Western United States: Boulder, Colorado: Geological Society of America Special Paper 280*, p. 271-318.
- Taylor, D.A., 1996, Structural geology of the Difficulty Creek area, Carbon County, Wyoming (Master's Thesis): University of Wyoming, 119p.
- Weijermars, R., 1997, Principles of rock mechanics, Alboran Science Publishing, Lectures in Geoscience, 360p.
- Wong, T.-f., David, C., and Zhu, W., 1997, The transition from brittle faulting to cataclastic flow in porous sandstones: Mechanical deformation: *Journal of Geophysical Research*, v. 102, p. 3009-3025.
- Zahm, C.K., and Henning, P.H., 2009, Complex fracture development related to stratigraphic architecture: Challenges for structural deformation prediction, Tensleep Sandstone at the Alcova anticline, Wyoming, *American Association of Petroleum Geologists Bulletin*, v.93, n.11, p. 1427-1446.

APPENDIX

The following appendix contains 1) ground level and aerial views of the larger scale Beer Mug anticlinal structure, 2) a map of the site collection areas, 3) a map of rose diagrams showing all fractures in their present day orientation, 4) a list of lithologic units at each site location, and 5) a page for each site containing a rose diagram and outcrop photograph.

The full data set includes excel files of the data collected at each site and all available imagery for each site. These data are available through the Enhanced Oil Recovery Institute at the University of Wyoming.



Beer Mug Anticline view from Difficulty Ranch Road, view to the northwest.



Aerial view of Beer Mug Anticline view to the northwest.



Aerial view to the northwest across Beer Mug Anticline, red circle highlights the area of the next photograph.



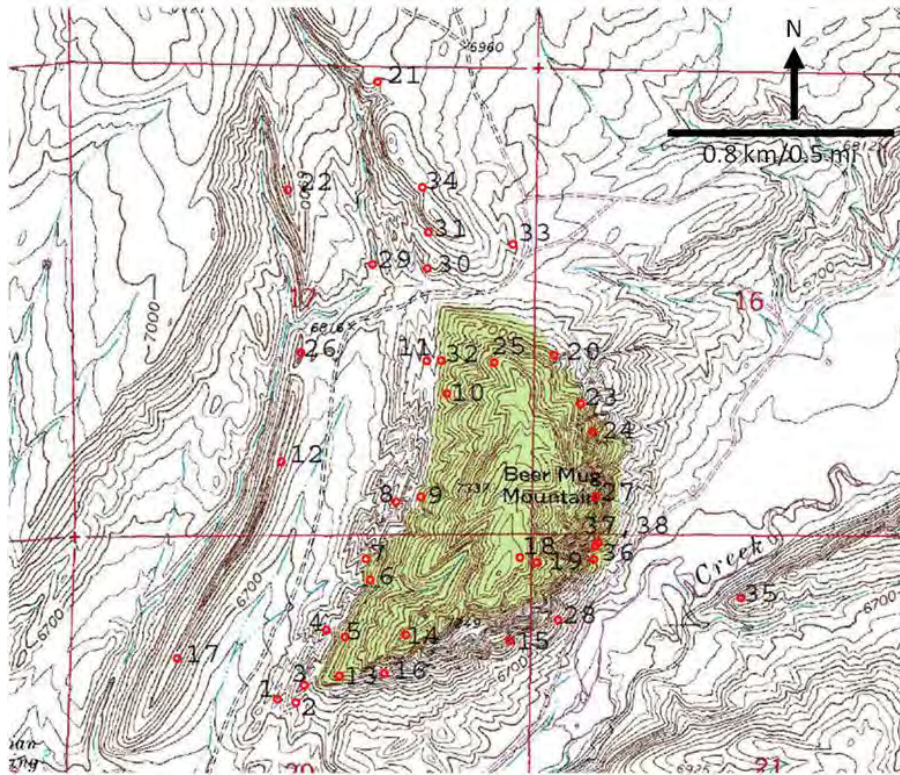
Close-up of the anticlinal core within the circle of the above photograph.



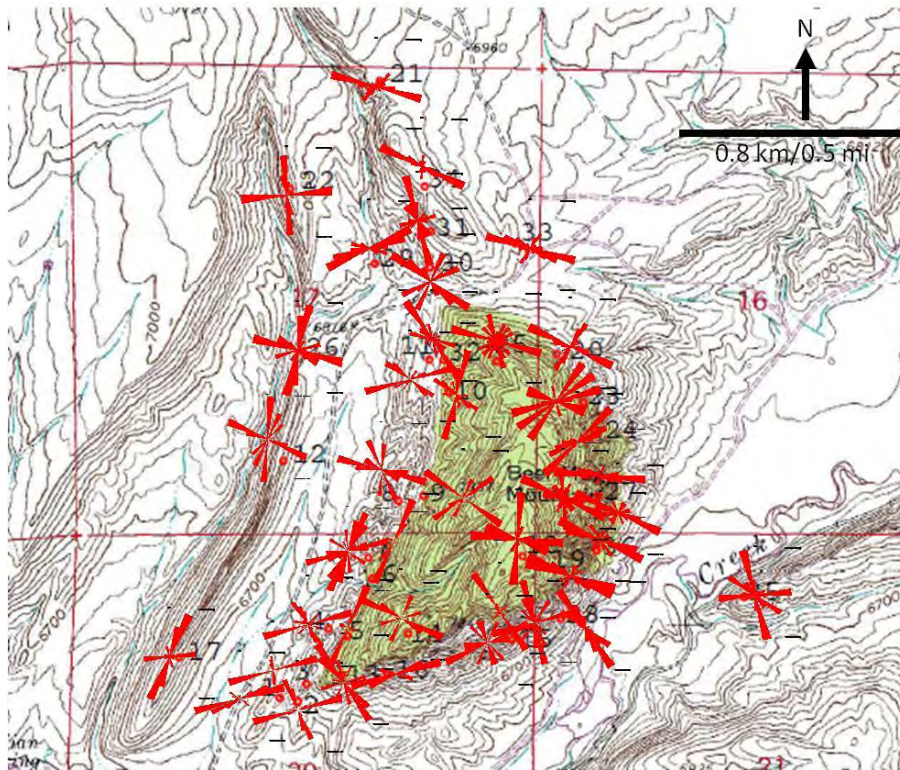
Aerial view to northeast, Ellis Ranch Anticline in the foreground, rim composed of Alcova Limestone.



View to the northeast, Alcova Limestone in the foreground Beer Mug anticline in the background.



Data collection site locations across Beer Mug Anticline.



Rose diagrams of each collection site showing orientation of all fractures in present day orientation.

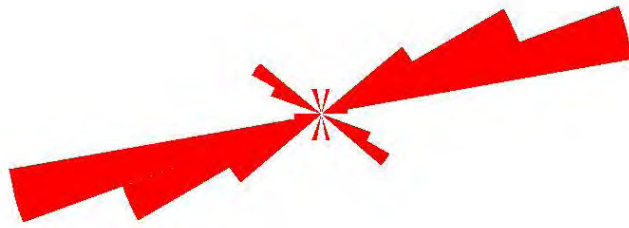
Site #	Formation	Lithology	Bedding strike	Bedding dip	Bed thickness	Mechanical thickness	Fracture
Site 1	Forelle	lms	207	57	45 cm	45 cm	ve
Site 2	Minnekahta	lms	220	50	2.5 m	2.5 m	ve
Site 3	Tensleep	ss	220	45	5m	5m	ve, if
Site 4	Minnekahta	lms	213	55	3m	1m	ve
Site 5	Tensleep	ss	205	55	5m	1-5m	ve, if
Site 6	Tensleep	ss	205	48	5m	5m	ve, if
Site 7	Minnekahta	lms	210	48	2m	1m	ve, faults
Site 8	Minnekahta	lms	206	50	2m	1m	ext, und
Site 9	Tensleep	lms	206	42	5m	5m	ve, if, sh
Site 10	Tensleep	ss	198	38	5m	5m	ve, db, if
Site 11	Minnekahta	lms	184	50	1m	1m	ve, sh
Site 12	Alcova	lms	205	45	1.8m	1 cm	ext, sh
Site 13	Tensleep	ss	205	48	6m	5m	ext, sh, c
Site 14	Tensleep	ss	207	45	3m	3m	ext
Site 15a	Tensleep	ss	33	75	4m	4m	db,ext, s
Site 15b	Tensleep	sandy lms	33	75	3m	3m	ext, sh
Site 15c	Tensleep	lms	33	75	3m	3m	ext, und
Site 15 adit. 1	Tensleep	ss	38	78	4m	4m	ext, sh
Site 15 adit. 2	Tensleep	sandy lms	38	78	3m	3m	ext, sh
Site 15 adit. 3	Tensleep	lms	38	78	3m	3m	ext, und
Site 16	Tensleep	ss	190	42	6m	6m	ext,sh, u
Site 17	Alcova	lms	201	28	2.8m	2cm-2.8m	ext,sh
Site 18	Tensleep	ss	160	10	4-5m	4-5m	und
Site 19	Tensleep	ss	18	75			ca multi-
Site 20	Tensleep	ss	342	44	5m	5m	if, ve
Site 21	Tensleep	zz	350	12	10m	10m	ext
Site 22	Alcova	lms	170	80	3 m	2-6cm	ext, sh
Site 23	Tensleep	ss	350	76	2 m	2 m	ext, nf
Site 24	Tensleep	ss	345	60	5 m	5 m	ext, if, sh
Site 25	Tensleep	ss	flat lying	0	2 m	~ 2 m	ext, db, s
Site 26	Alcova	lms	198	45	1 m	2 cm - 1 m	ext, sh
Site 27	Tensleep	ss	26	54	5 m	~ 5 m	ext, db,if
Site 28	Tensleep	ss	38	85	5 m	~ 5 m	ext, if, sh
Site 29	Minnekahta	lms	170	45	2 m	0.5 - 1 m	ext, sh
Site 30	Tensleep	ss	180	30	5 m	5 m	ve, if, sh
Site 31	Tensleep	ss	flat lying	0	5 m	5m	vcf, if, ve
Site 32	Tensleep	ss	180	35			ve, if
Site 33	Minnekahta	lms	350	30	1.5 m	1.5m	ext, sh
Site 34	Tensleep	ss	near hz	~ 10 to E	5m	5m	ve, sh
Site 35	Alcova	lms	62	30	1 m	1cm - 1m	ve, sh
Site 36	Red Peak	ss	80	25	170	170	ve
Site 37	Tensleep	ss	22	65	35-40 m		if, ve
Site 38	Tensleep	lms	10	75	1-2 m	1-2 m	if, ve, sh

Lithologic units at each data collection site.

SITE 1

N

Linear Scaling

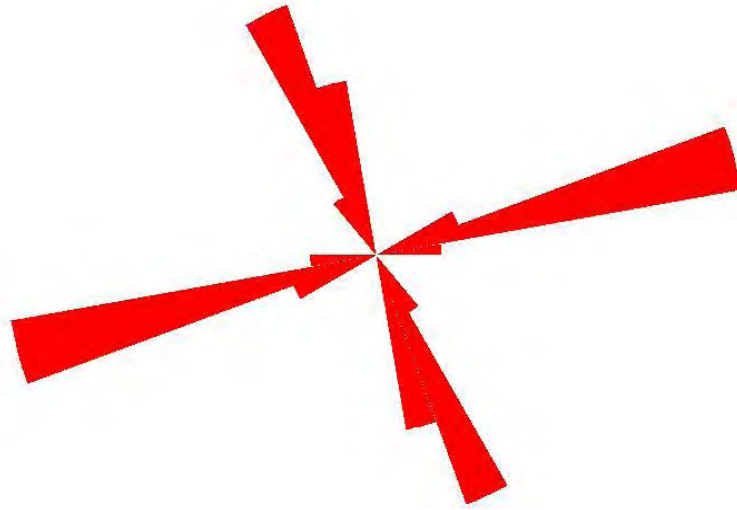


Site 1
n = 32

Total Data : 32



SITE 2



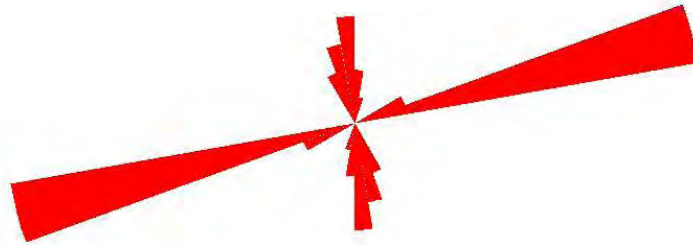
Site 2
n = 47



SITE 3

N

Linear Scaling



Site 3
n = 27

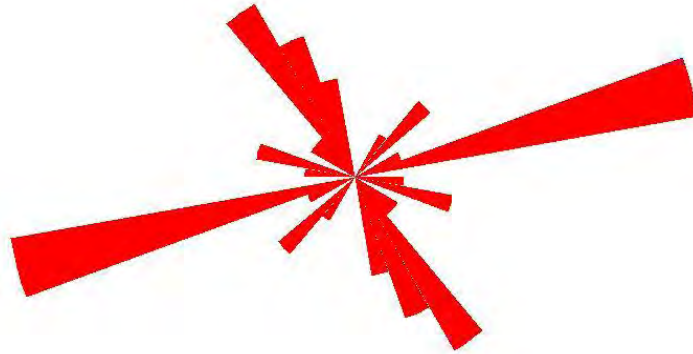
Total Data : 27



SITE 4

N

Linear Scaling

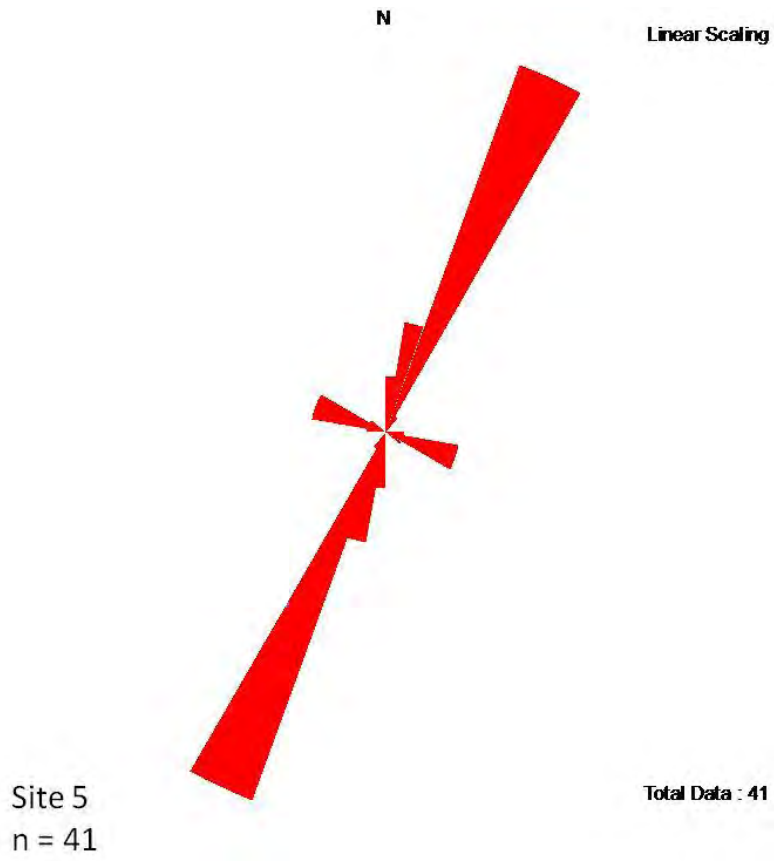


Site 4
n = 25

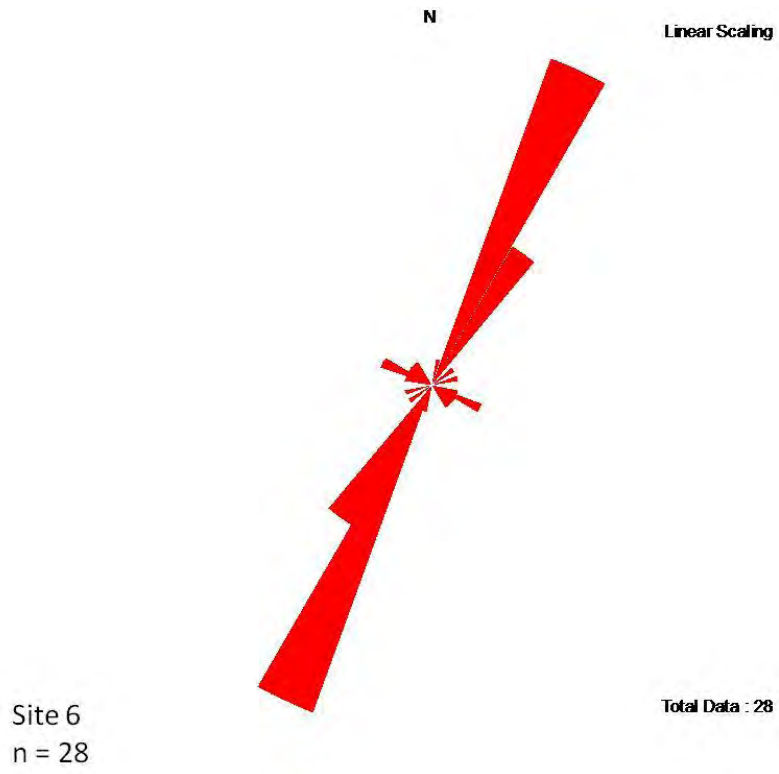
Total Data : 25



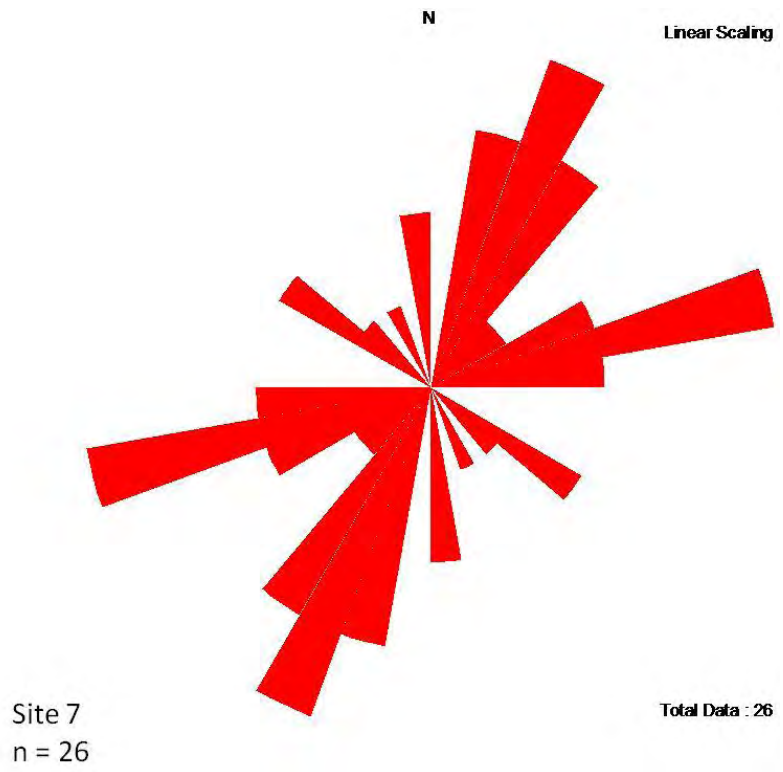
SITE 5



SITE 6



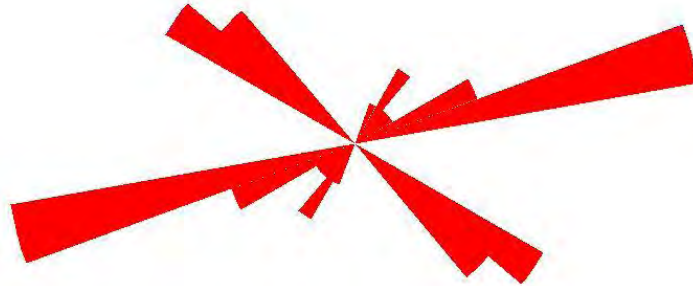
SITE 7



SITE 8

N

Linear Scaling



Site 8
n = 25

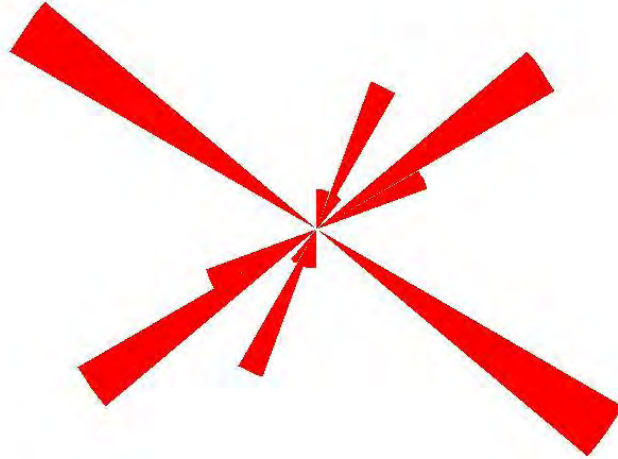
Total Data : 25



SITE 9

N

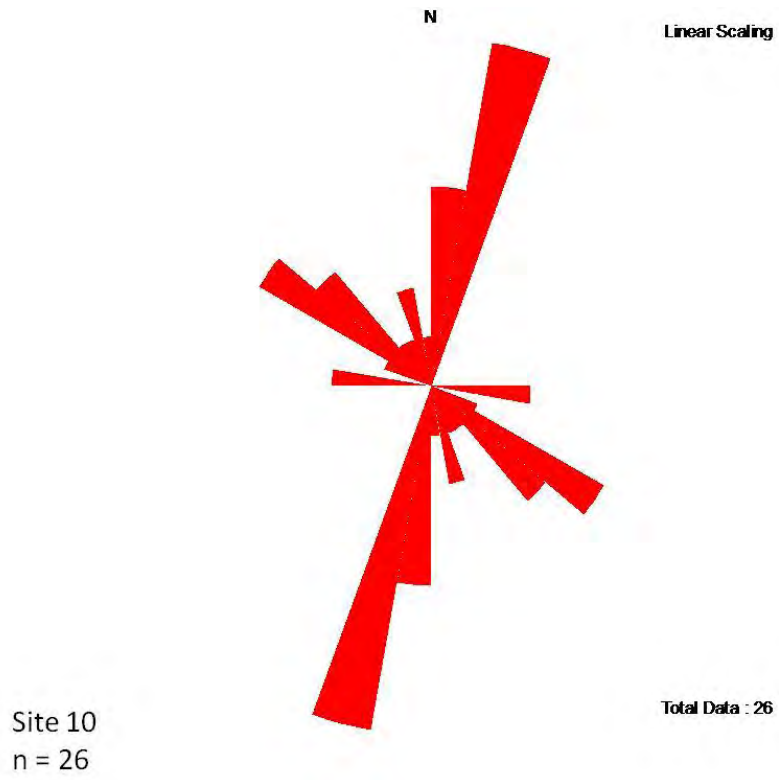
Linear Scaling



Site 9
n = 25



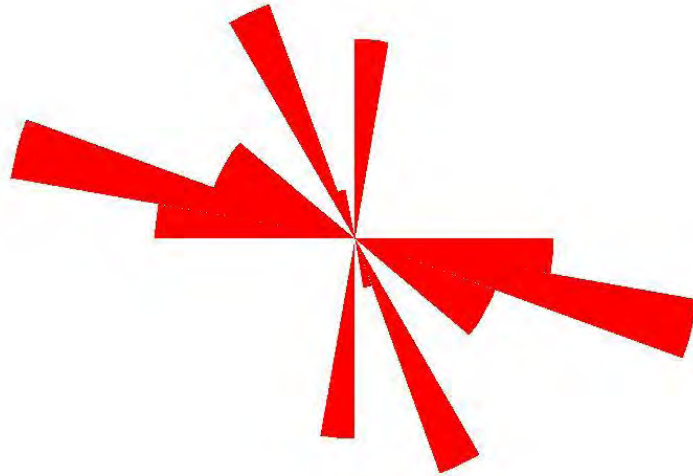
SITE 10



SITE 11

N

Linear Scaling

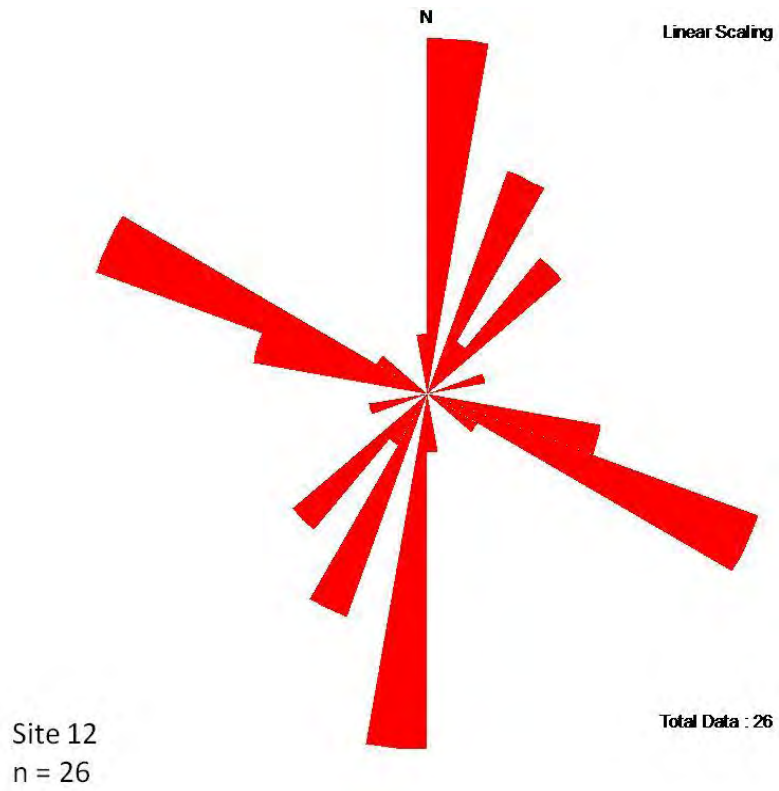


Site 11
n = 27

Total Data : 27



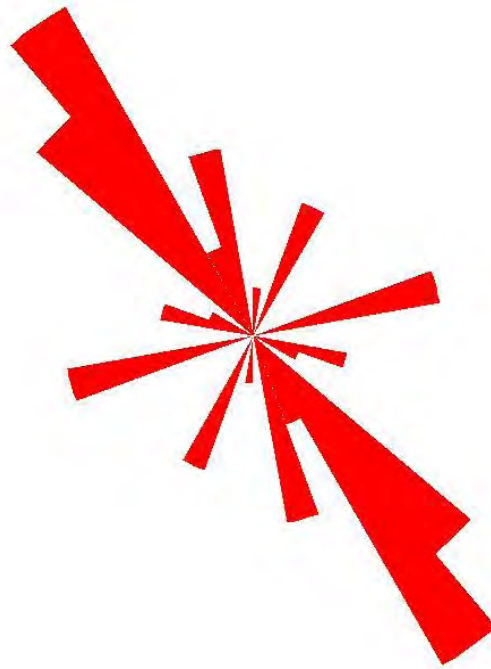
SITE 12



SITE 13

N

Linear Scaling



Site 13
n = 31

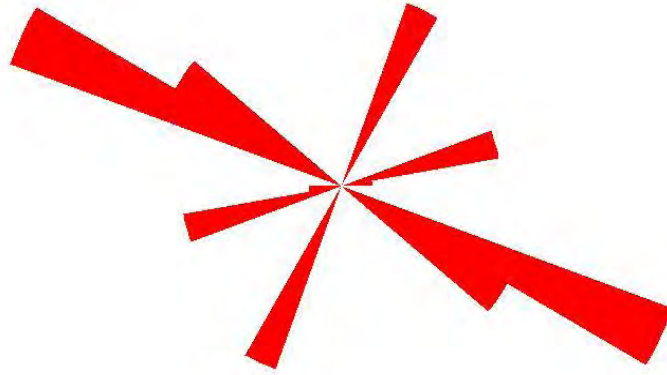
Total Data : 31



SITE 14

N

Linear Scaling

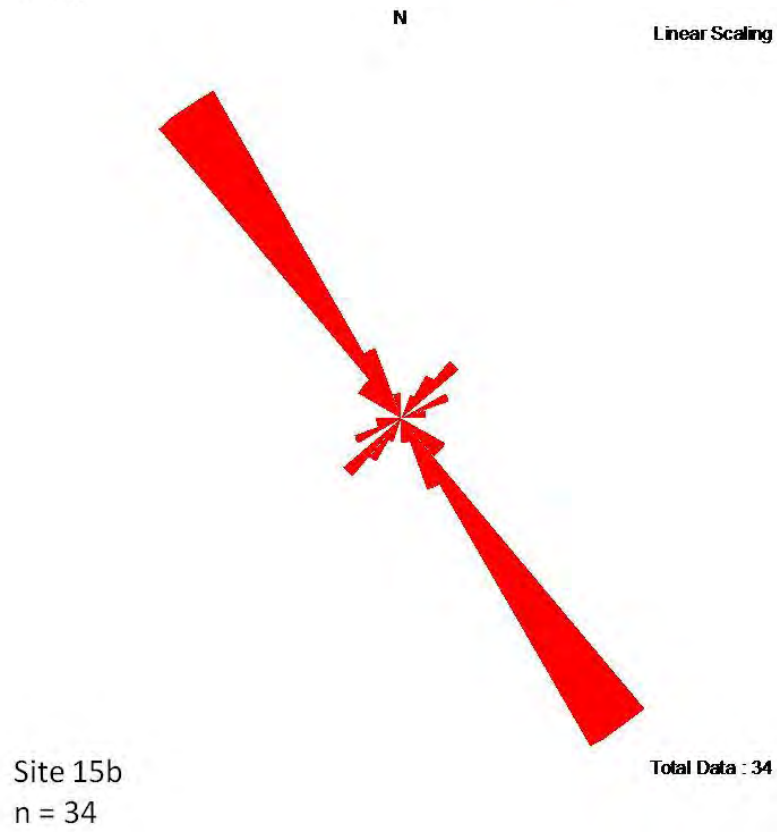
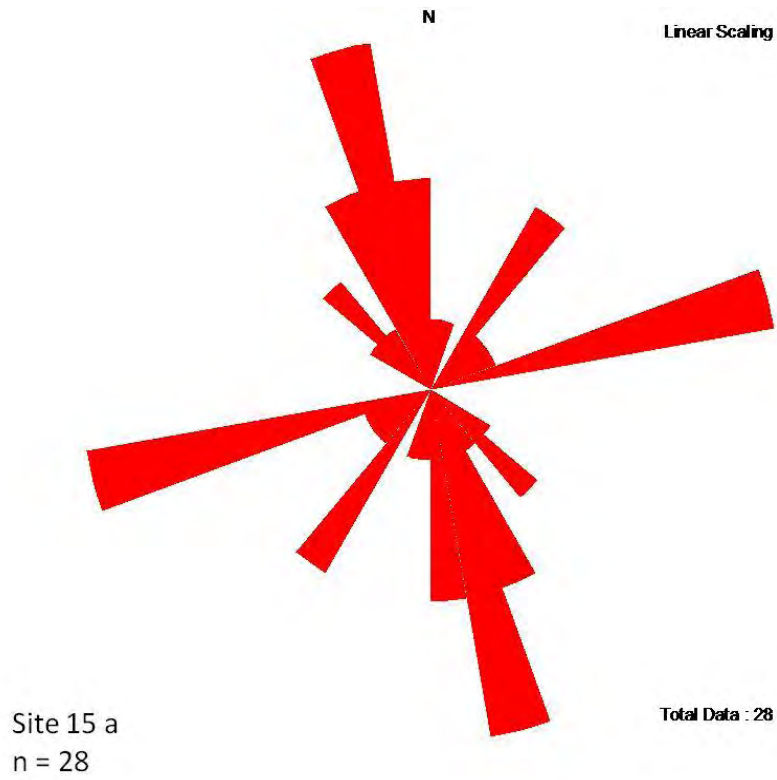


Site 14
n = 29

Total Data : 29

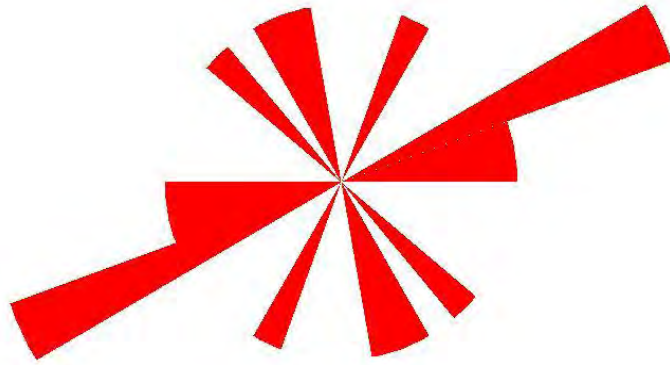


SITE 15



N

Linear Scaling



Site 15 c
n = 8

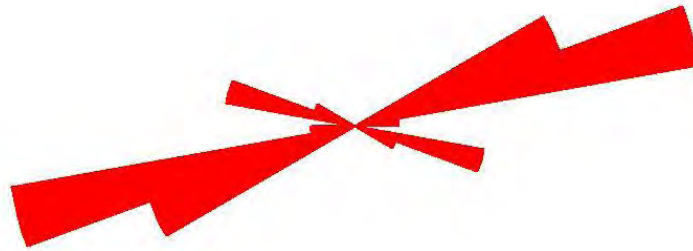
Total Data : 8



SITE 16

N

Linear Scaling

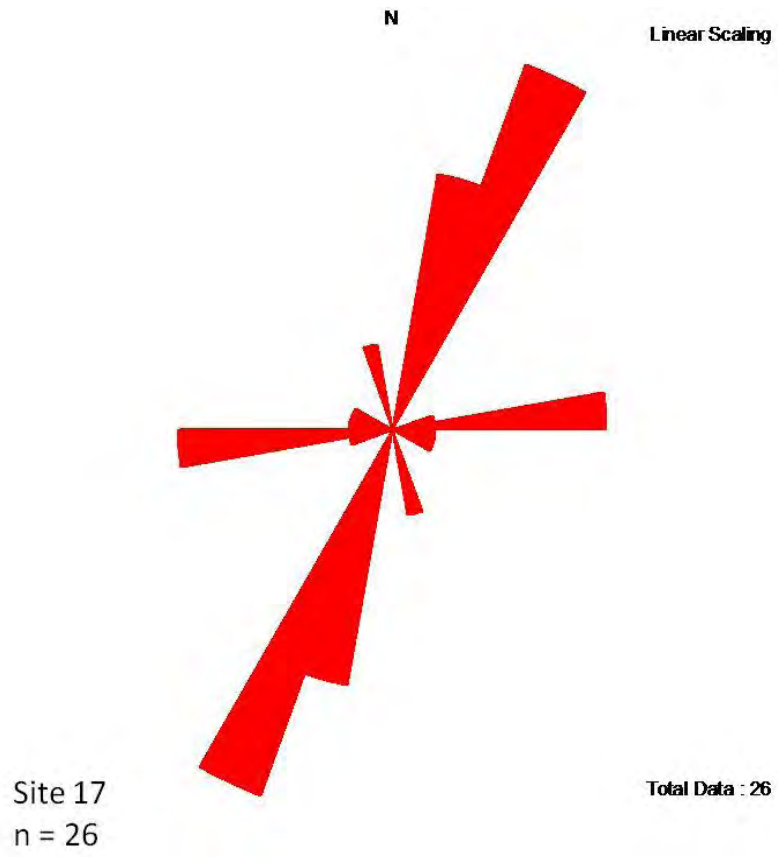


Site 16
n = 18

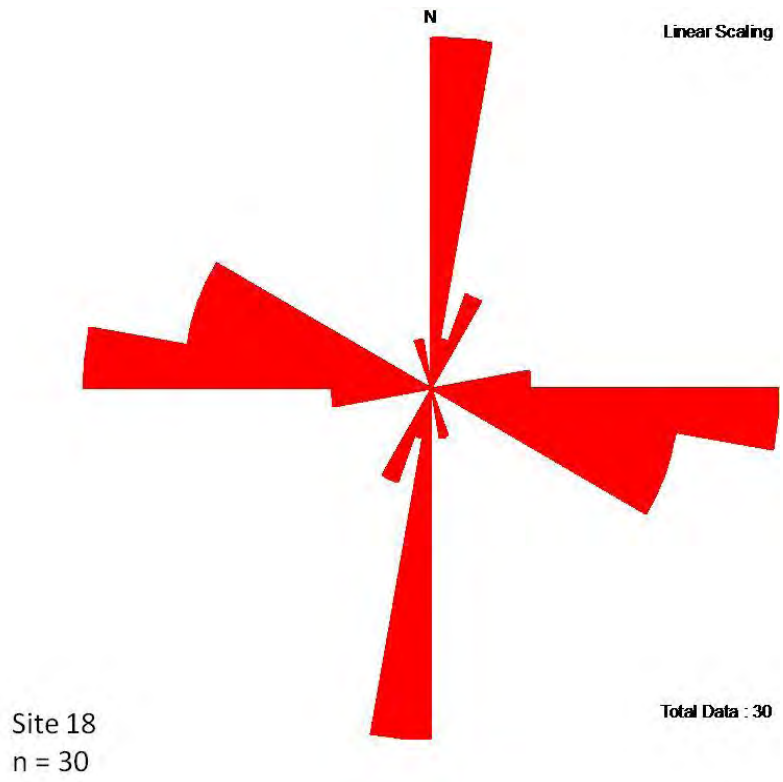
Total Data : 18



SITE 17



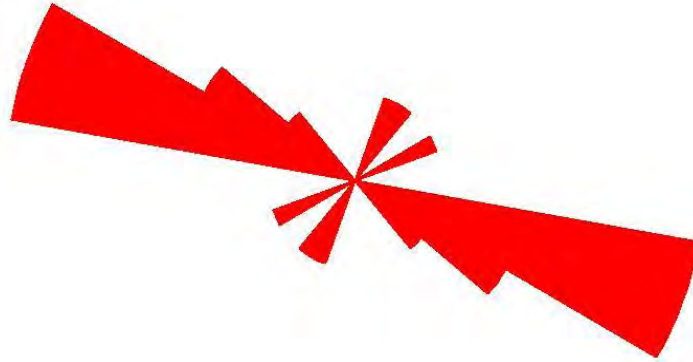
SITE 18



SITE 19

N

Linear Scaling



Site 19
n = 14

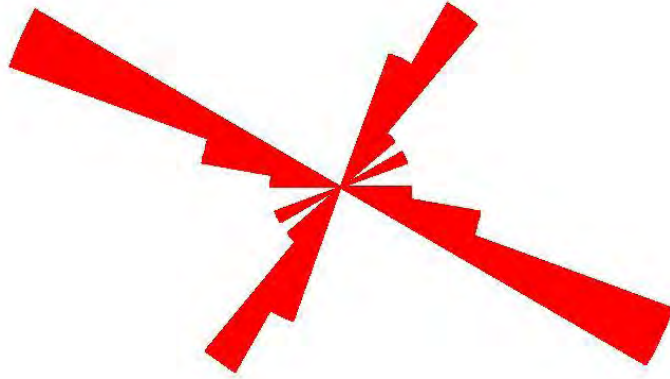
Total Data : 14



SITE 20

N

Linear Scaling



Site 20
n = 15

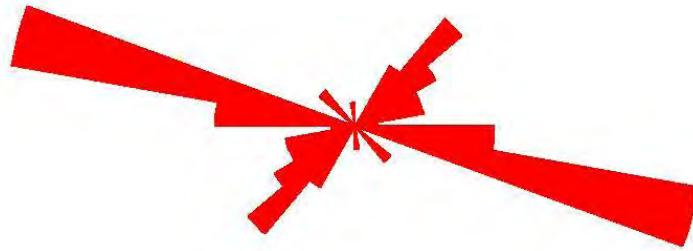
Total Data : 15



SITE 21

N

Linear Scaling

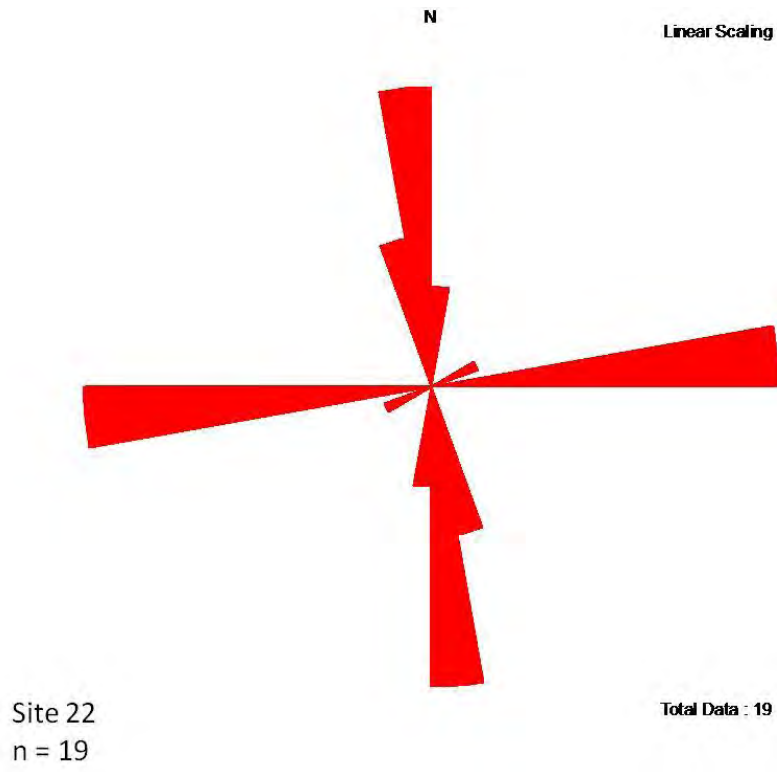


Site 21
n = 44

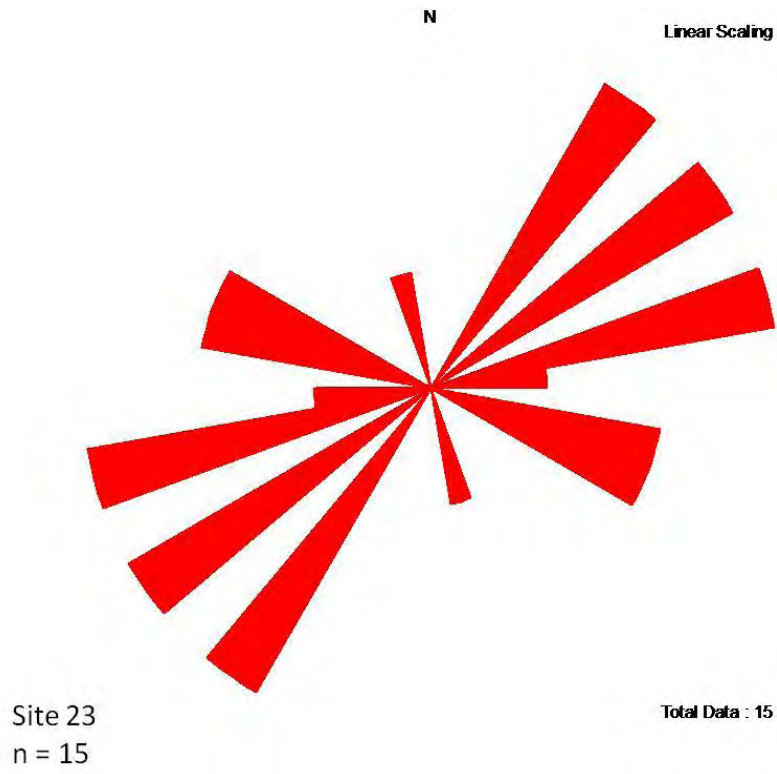
Total Data : 44



SITE 22



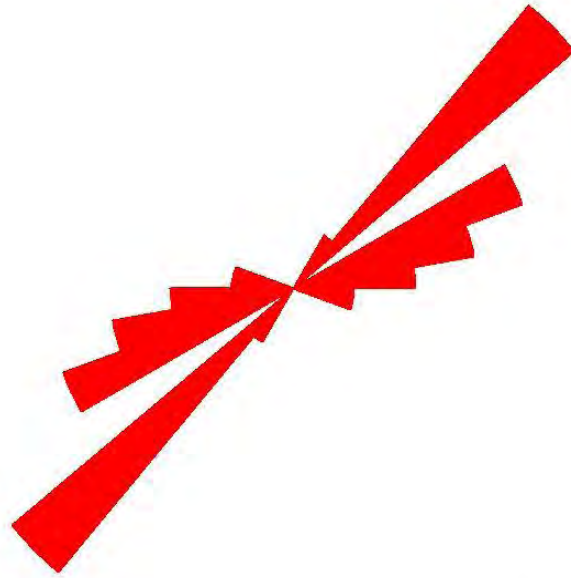
SITE 23



SITE 24

N

Linear Scaling



Site 24
n = 18

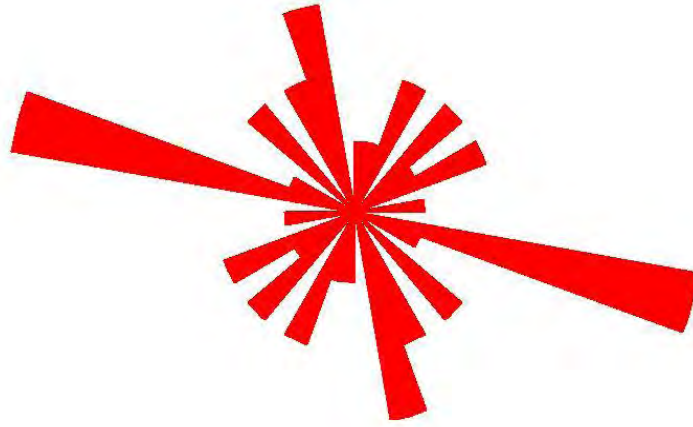
Total Data : 18



SITE 25

N

Linear Scaling

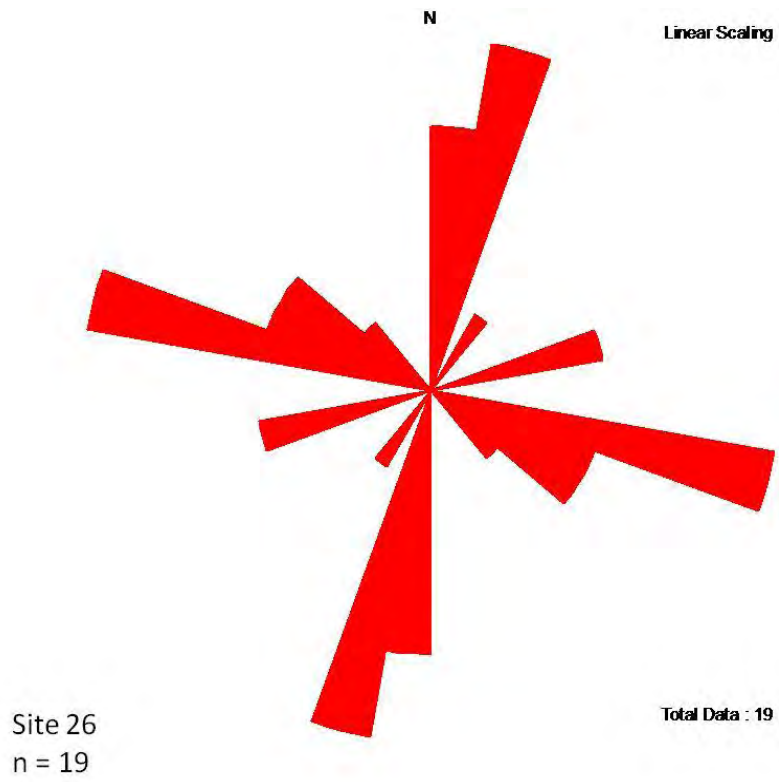


Site 25
n = 23

Total Data : 23



SITE 26



SITE 27

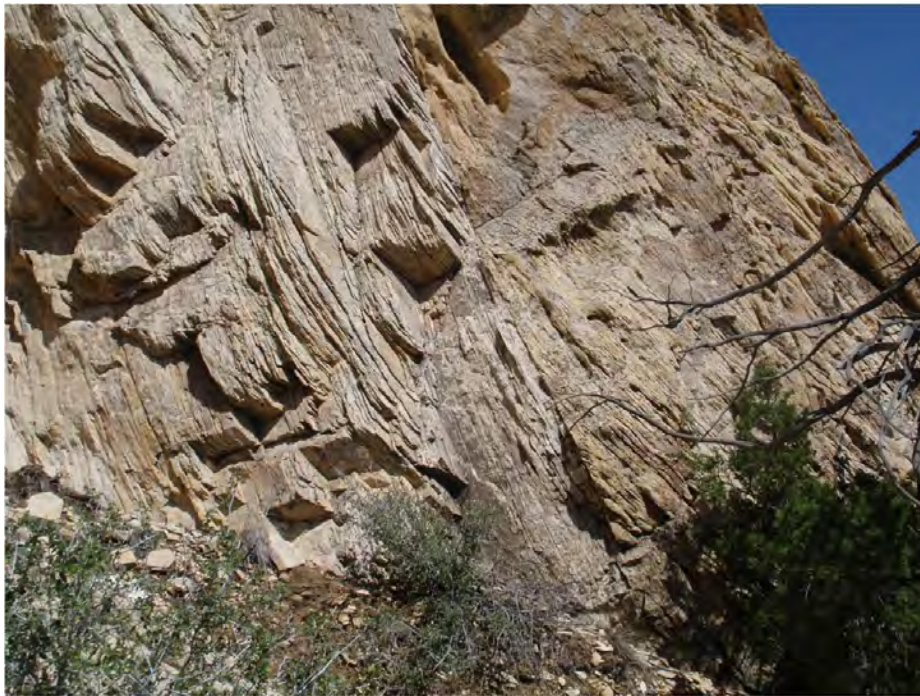
N

Linear Scaling



Site 27
n = 29

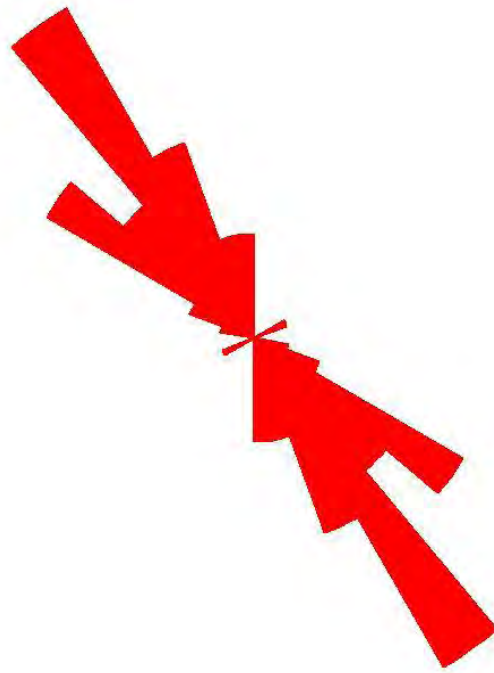
Total Data : 29



SITE 28

N

Linear Scaling



Site 28
n = 39

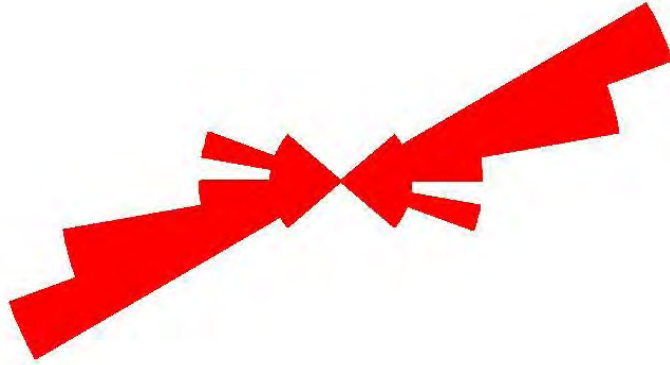
Total Data : 39



SITE 29

N

Linear Scaling



Site 29
n = 17

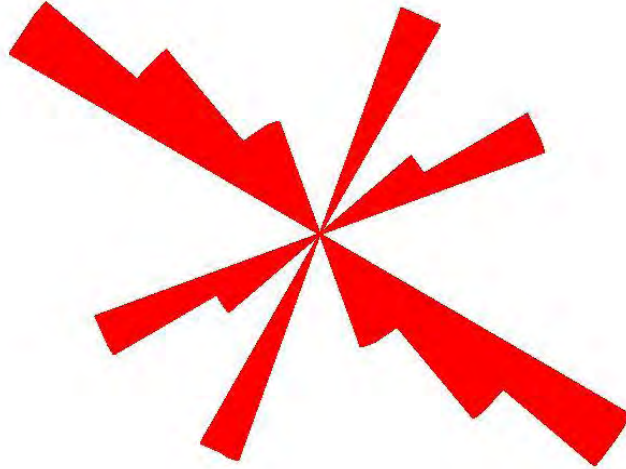
Total Data : 17



SITE 30

N

Linear Scaling

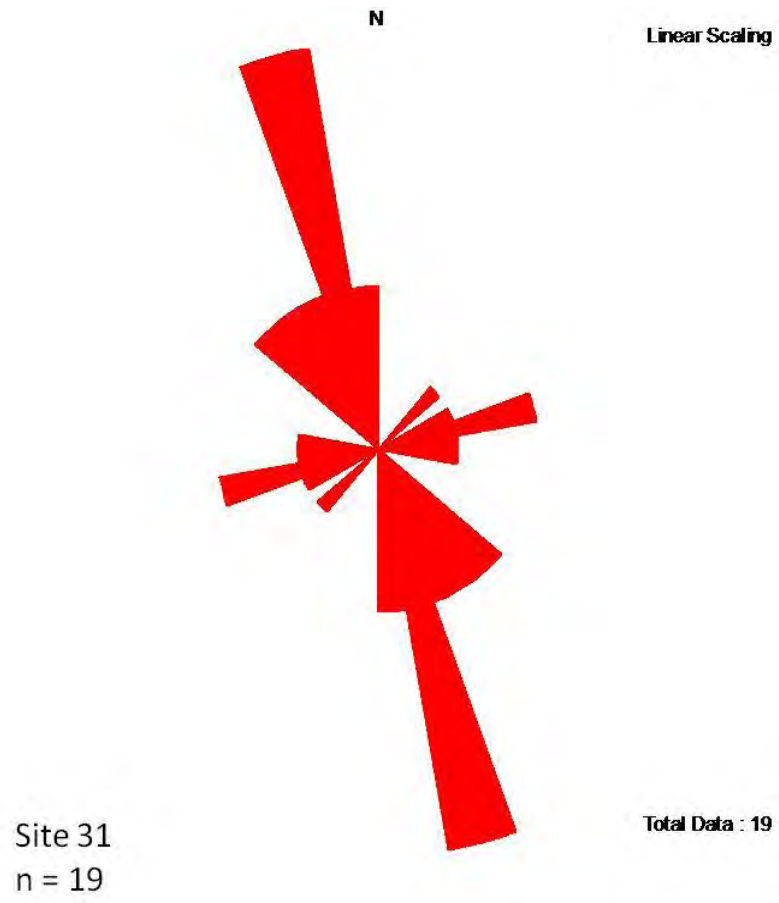


Site 30
n = 12

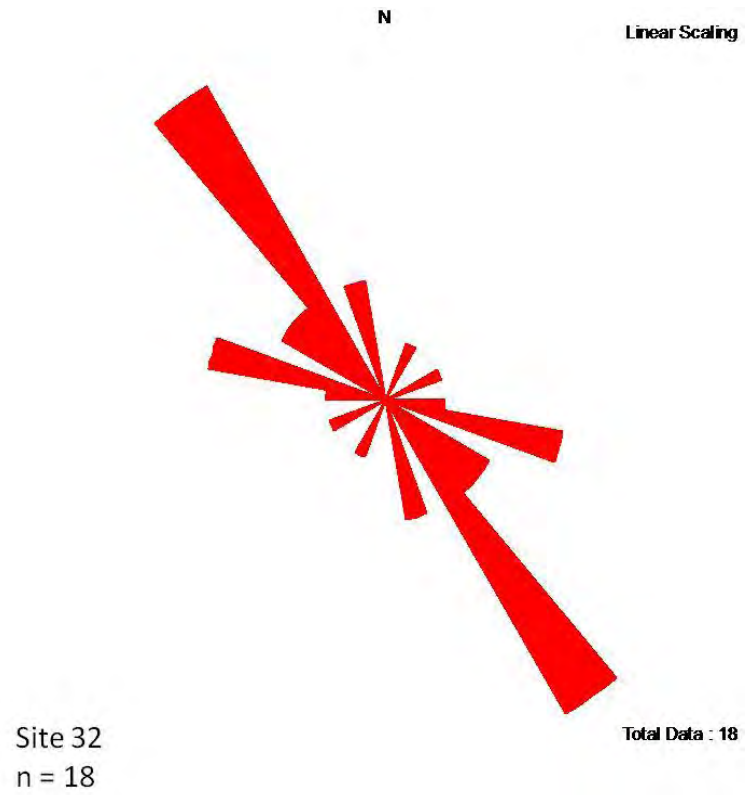
Total Data : 12



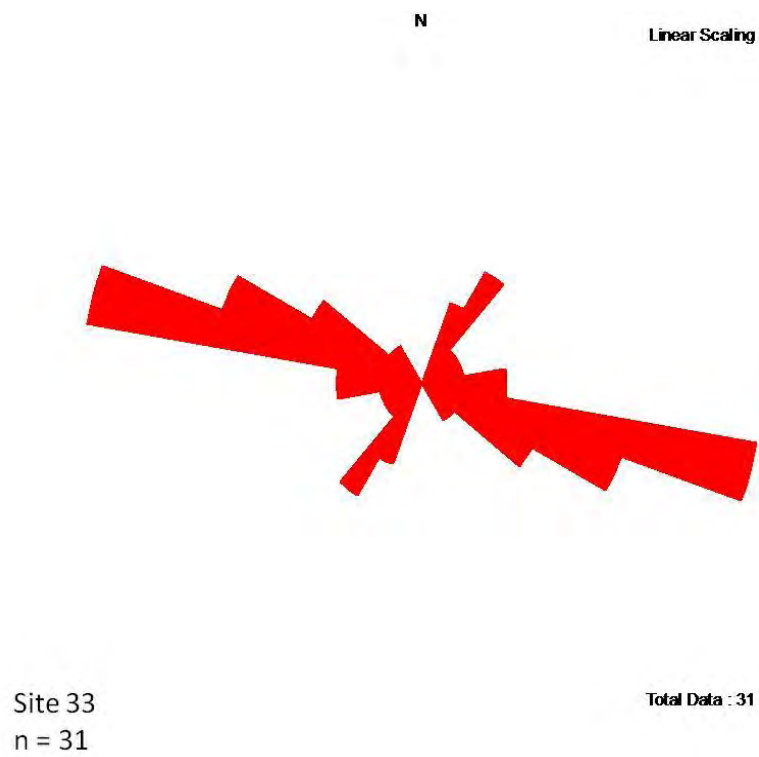
SITE 31



SITE 32



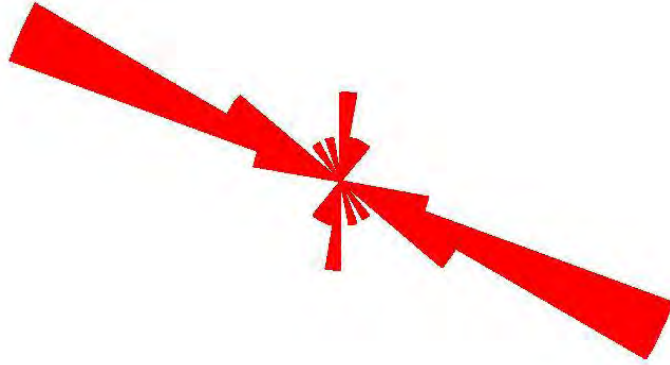
SITE 33



SITE 34

N

Linear Scaling

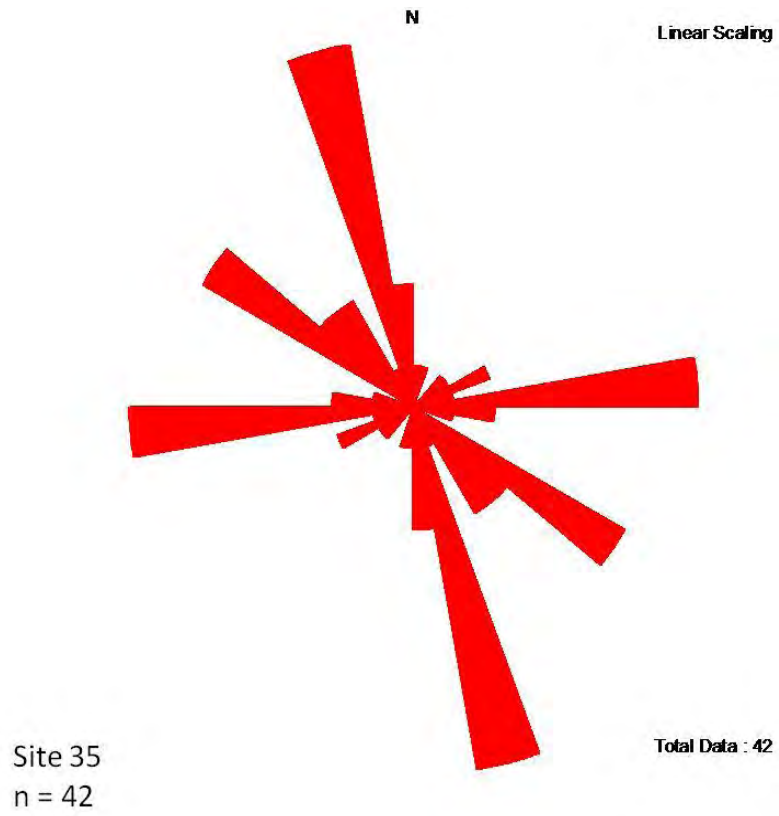


Site 34
n = 20

Total Data : 20



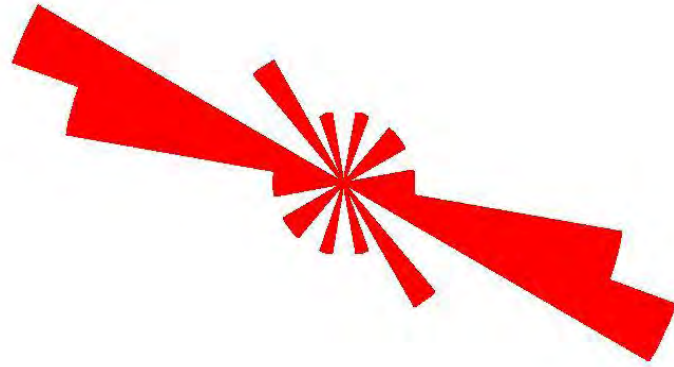
SITE 35



SITE 36

N

Linear Scaling



Site 36
n = 17

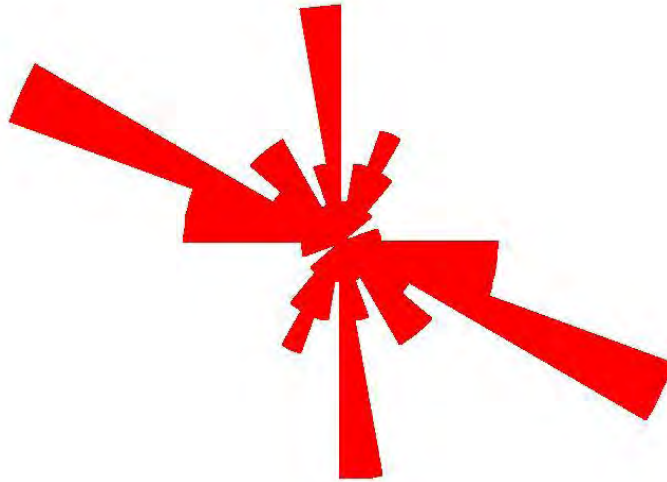
Total Data : 17



SITE 37

N

Linear Scaling



Site 37
n = 45

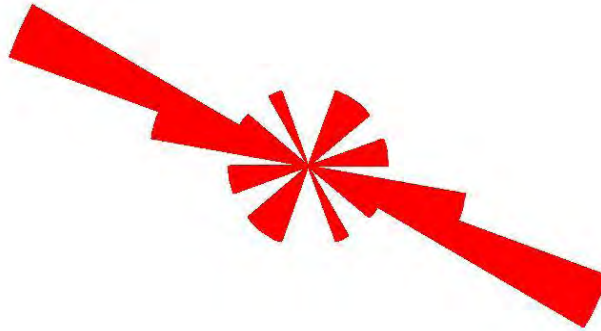
Total Data : 45



SITE 38

N

Linear Scaling



Site 38
n = 13

Total Data : 13



OUTCROP STUDIES

WYOMING GEOLOGICAL ASSOCIATION 2010 FIELD GUIDEBOOK PAPER

The authors would like to thank the WGA for allowing us to reprint this paper so it could be included in the full study report.

FRACTURE VARIABILITY WITHIN THE TENSLEEP FORMATION, SOUTHEASTERN WYOMING

AUTHORS

Scott P. Cooper

Enhanced Oil Recovery Institute, University of Wyoming, 1000 E. University Ave., Dept. 4068,
Laramie, WY 8207, Phone: (307) 766-2791, scott@fracturestudies.com

John C. Lorenz

Fracture Studies, Geoflight LLC, 61 Blanco Drive, Edgewood, NM 87015, Phone (505) 231-
6235, john@fracturestudies.com

ACKNOWLEDGEMENTS

The authors would like to thank the landowners across the miles and years of our projects in Wyoming. Without their help and support none of this work or previous work could have been accomplished. We also greatly benefited from interactions with the entire staff and contractors at the Enhanced Oil Recovery Institute at the University of Wyoming, including Lon Whitman, Glen Murrell, Brian Reyes, Mark Tomasso, Shaochang Wo, Gene R. George and Associates Inc., and past director Jim Steidtmann. Peigui Yin made the thin sections and photomicrographs presented here and helped formulate their interpretations. This study was funded by and conducted for the Enhanced Oil Recovery Institute, David Mohrbacher director.

ABSTRACT

The Pennsylvanian Tensleep Formation in south-central Wyoming is a complex package of repeated limestones and/or dolomites, and sandstones. Strata of these varied lithologic units are folded over Flat Top and Beer Mug anticlines and are cut by numerous intersecting fractures. These fracture patterns vary significantly by lithology, structural position and degree of folding.

The limestones within the Tensleep Formation accommodated much of the larger-scale bed-parallel shear through brecciation, although it is not always obvious due to weathering and secondary re-cementation. From a distance, many of the limestone beds in fact appear to be unfractured. Granulation, brecciation, pressure solution, internal thrust faulting, cementation and re-cementation likely occurred nearly simultaneously during deformation. The eolian sandstone facies accommodated strain by extension fractures, and by shear both parallel and oblique to the large-scale cross bed foresets and bedding.

The Tensleep Formation has been folded to different degrees over a variety of Laramide-age thrust faults. Most of these strata exhibit inherited F_0 fracture patterns that pre-date folding, as well as fold-related extension fractures that trend approximately normal (F_1) and parallel (F_2) to the axis of folding. The F_1 set can strike oblique to the hinge in anticlines where the stress orientation that caused both folding and fracturing was oblique to the inherited basement structure that dictated the hinge trend. Areas on anticlines that were not significantly folded, i.e., relatively planar backlimbs, contain only the early, F_1 fracture set and locally the F_0 set. Many of the earlier-formed fractures were reactivated in shear and/or extension, and additional fracture sets developed as the degree of folding increased.

INTRODUCTION

The two objectives of this extended abstract/paper are to detail the variability of extension and shear fractures in the Tensleep Formation at two anticlines (Flat Top and Beer Mug anticlines) near Medicine Bow, Wyoming, and to discuss how these may influence production. Fractures within the Pennsylvanian-age Tensleep Formation were found to vary as a function of lithology, structural position and degree of folding. These natural fractures dominate fluid flow in Tensleep reservoirs and are therefore a dominant control on the recovery of oil from the subsurface.

This paper is a short version of a report that will contain additional supporting data and analyses on all fracture types in the Tensleep Formation from anticlines, outcrops and cores from across Wyoming for the Enhanced Oil Recovery Institute (EORI) at the University of Wyoming. When completed, copies of the longer compilation report can be requested directly from the EORI at The University of Wyoming or from their website at www.eori.uwyo.edu.

BACKGROUND

Location and Structural Setting

Flat Top Anticline is located in southeastern Wyoming, about six miles north of the small town of Medicine Bow. Beer Mug Anticline is located approximately 15 miles northwest of Medicine Bow (Figure 1). Both are at the northern margin of the Hanna basin and just south of the Shirley Mountains. Flat Top Anticline is the northernmost of several ENE-WSW trending, asymmetric anticlines in the area, each overlying a north-vergent thrust fault a few tens of miles long (Blackstone, 1994; Lillegraven and Snoke, 1996; Lillegraven et al., 2004). Beer Mug

Anticline (Figure 2) has been previously interpreted as a basement involved Laramide structure by Maravich (1941), Stone (1993) and Taylor (1996). Beer Mug Anticline has a near vertical forelimb and a steeply dipping backlimb (40° or more; Figure 2) whereas the Flat Top Anticline has at most a 40° dip on the forelimb and backlimb dips of only 10° to 20° (Knight, 1944; Carey, 1950; Blackstone, 1994; Blevens, 1984; Figure 3).



Figure 1: Wyoming Department of Transportation map modified to show the general location of Flat Top and Beer Mug anticlines.



Figure 2: Aerial photograph (view to the northwest) showing the tightly folded and steeply dipping Tensleep Formation on Beer Mug Anticline (twenty foot wide gravel road in the foreground for scale).



Figure 3: Aerial photograph of one of the subanticlines that comprise Flat Top Anticline, view is to the northeast (ranch buildings in the lower left foreground for scale). Note this is a much broader, less tightly folded anticline relative to Beer Mug Anticline.

Tensleep Formation Sedimentology

The Tensleep Formation in south-central Wyoming is Middle to Upper Pennsylvanian in age, and consists of a complex package of repeated marine limestones and/or dolomites, and eolian sandstones formed in near-shore dune and interdune environments with both horizontal and large scale cross-bedding (Boyd, 1993; Love et al., 1993). The Tensleep Formation is laterally equivalent in part to the Minnelusa Formation to the north and east, to the Casper Sandstone to the east and south, and to the Weber Sandstone to the west (Love et al., 1993).

Fracture Terminology

Consistent with the terminology utilized in the fossil-energy industry, discontinuities in rock will be described as either extension or shear fractures. Extension fractures, also termed joints, tensile fractures, dilation fractures, or Mode I fractures (Pollard and Aydin, 1988), are characterized by displacement perpendicular to the fracture wall. Extension fractures form perpendicular to the least compressive stress and would bisect the acute angle between conjugate shear fracture pairs formed in the same stress regime (Peng and Johnson, 1972; Long et al., 1997). Tectonic fractures are extension fractures that are interpreted to have formed during a tectonic event such as the formation of Beer Mug and Flat Top anticlines.

Shear fractures are characterized by displacements parallel to the fracture wall, also termed Mode II or III fractures depending upon relative displacement to the fracture front (Pollard and Aydin, 1988). Deformation bands were also documented at Flat Top and Beer Mug anticlines. These structures are roughly planar features that record small amounts of displacement and typically form in high-porosity, poorly cemented sandstone. Deformation bands have been also referred to as coherent shear fractures or small-displacement faults

(millimeters to centimeters of displacement; Aydin, 1978; Antonellini et al., 1994; Mair et al., 2000; Olsson et al., 2004). Larger amounts of displacement can be accommodated by zones of multiple, composite deformation bands (Aydin, 1978; Aydin and Johnson, 1983; Antonellini et al., 1994).

CONTROLS ON FRACTURE TYPE AND VARIABILITY

Fracture Variability by Lithology

Where lithology is similar, fractures are also similar at Flat Top and Beer Mug anticlines. The extension fractures at both anticlines are relatively planar features that may have plumes on the fracture faces, and locally millimeter-scale calcite mineralization of the fracture aperture. However, other fractures consist of simple planar breaks in the rock. Plumose structures and arrest lines, indicative of extension fracturing, are in fact rare in the strata; because poor cementation, 1) did not leave the rock prone to plume formation, and 2) allowed plumes to be quickly destroyed by weathering. In better cemented units some plumes have been obscured or destroyed by shear reactivation of the original extension fracture sets. Regardless, hints of plume structures are present on some fracture faces, and, along with the absence of offset, suggest that most of the planar breaks in the Tensleep sandstones formed initially in extension. Two primary extension fracture sets are documented within different sedimentary facies at Flat Top Anticline (Figure 4).

Pervasive small-scale strain at both anticlines was accommodated in the sandstone dune facies both by subtle slip parallel to the large-scale cross bed foresets and by more prominent offsets oblique to bedding. Steps, slickenlines, slickencrysts (elongate calcite crystals) and

gouge indicative of shear fractures are present in many outcrops, as well as local deformation bands.

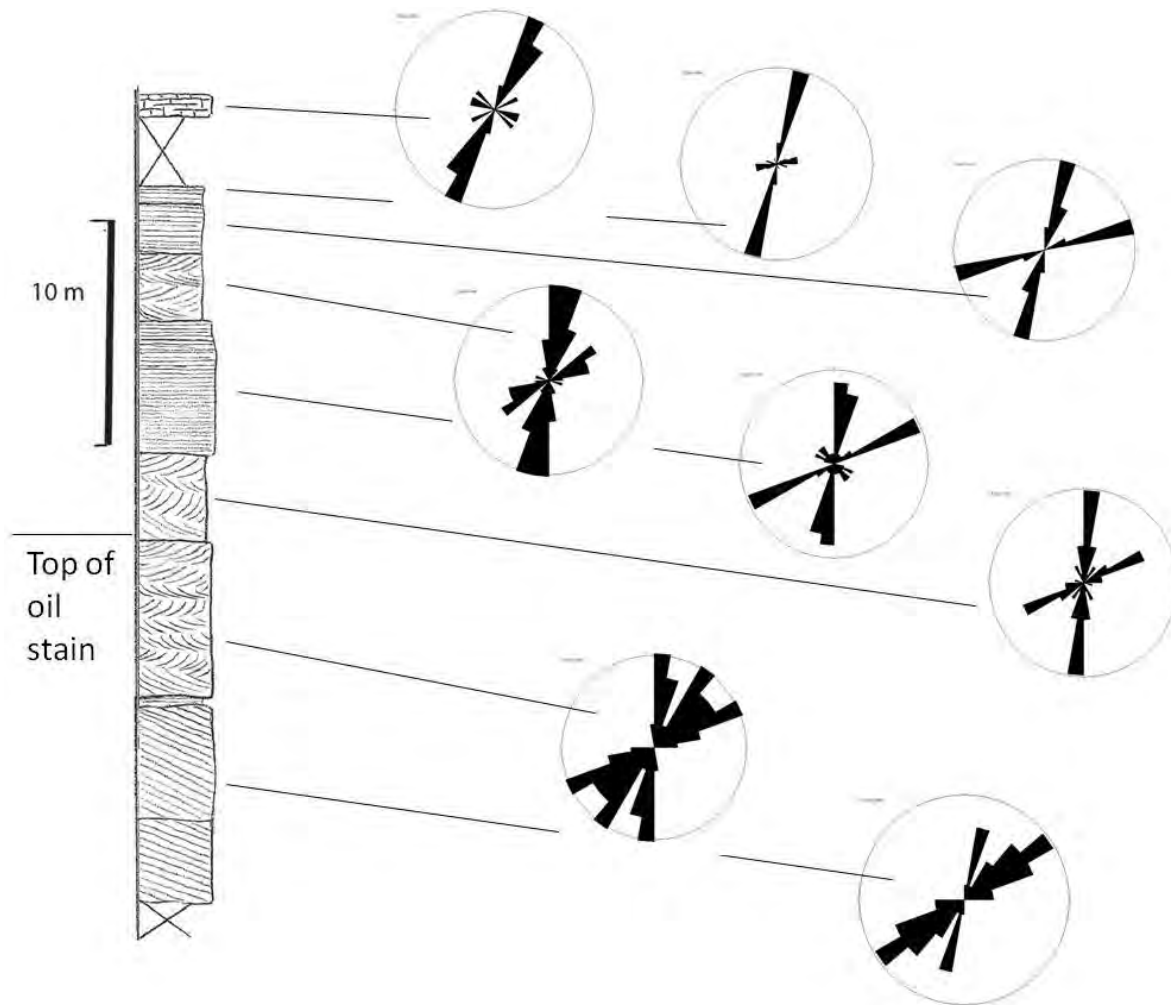


Figure 4: Summary of fracture orientations in the different sedimentary facies that crop out near the hinge on the south side of Flat Top Mountain. Most beds contain a set of older NNE-SSW, through-going F_1 fractures and a younger set of approximately ENE-WSW F_2 fractures. Between 12 and 40 fracture measurements were taken from each bed.

From a distance, many exposures of the limestone beds at Beer Bug Anticline appear to be unfractured relative to the interbedded sandy limestones and eolian sandstones (Figure 5). The limestones within the Tensleep Formation accommodated much of the larger-scale bed-parallel shear through granulation, brecciation and pressure solution although it is not always

obvious due to weathering and secondary re-cementation. Re-cementation likely occurred nearly simultaneously with deformation. The dolomites in contrast were either not recemented or were re-cemented to a much lesser degree. Extensive fracture patterns are recorded from the capping dolomite at Flat Top Anticline, as are unhealed fractures in Tensleep Formation dolomite cores from other locations.

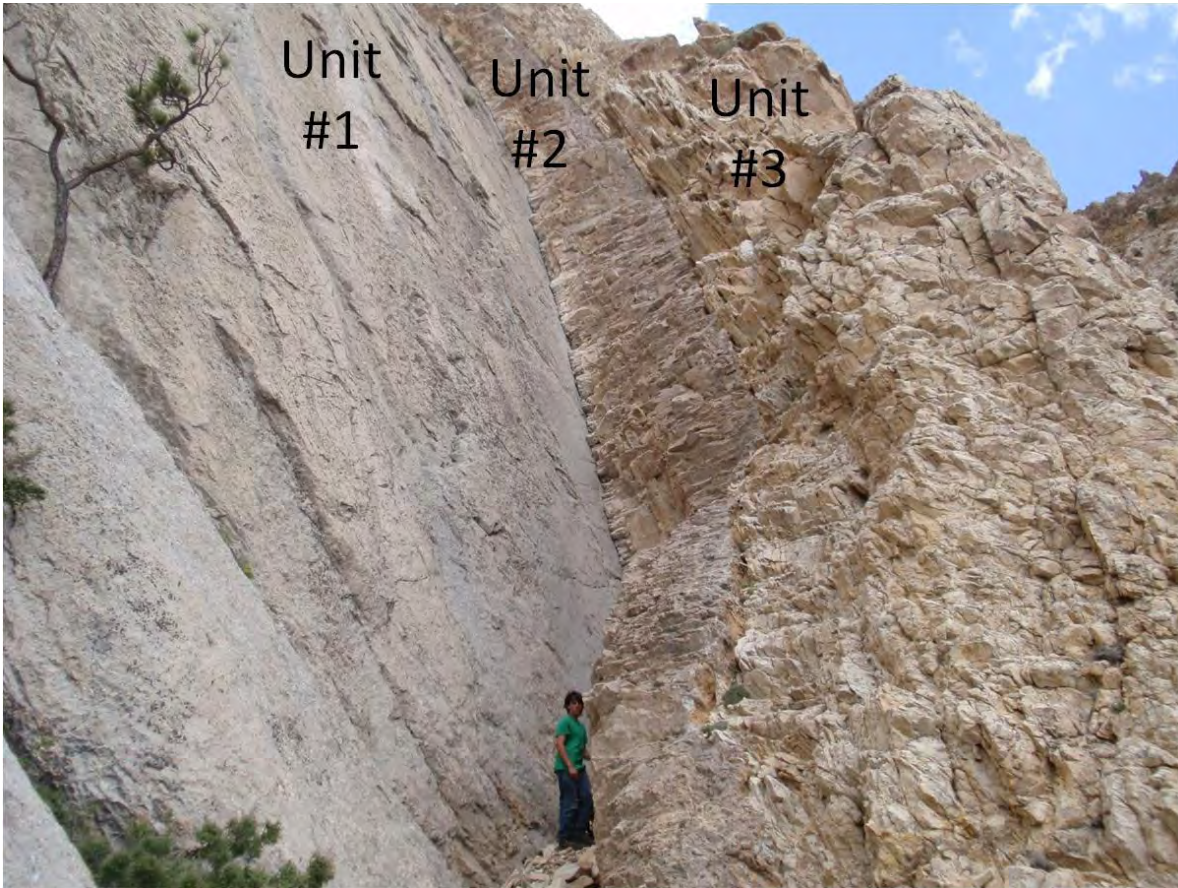


Figure 5A: Transition from marine limestone (unit #1 above, 5B), to near shore sandy limestone (unit #2 above, 5C), to beach sandstone (unit #3 above, 5D). Fracture intensity is different in the differing lithologies. At the macro scale there appear to be few fractures in the limestone (unit #1) a relatively uniform fracture pattern in the transitional sandy limestone (unit #2) and an almost brecciated appearance to the sandstones (unit #3). Close-up photo of the limestone (unit #1, 5E) shows that it is brecciated into centimeter scale pieces but that the limestone was self-healing by cementing the pieces with calcite penecontemporaneously with brecciation. When viewed on pavement surface rather than side view the sandstone exhibits an ordered fracture pattern.

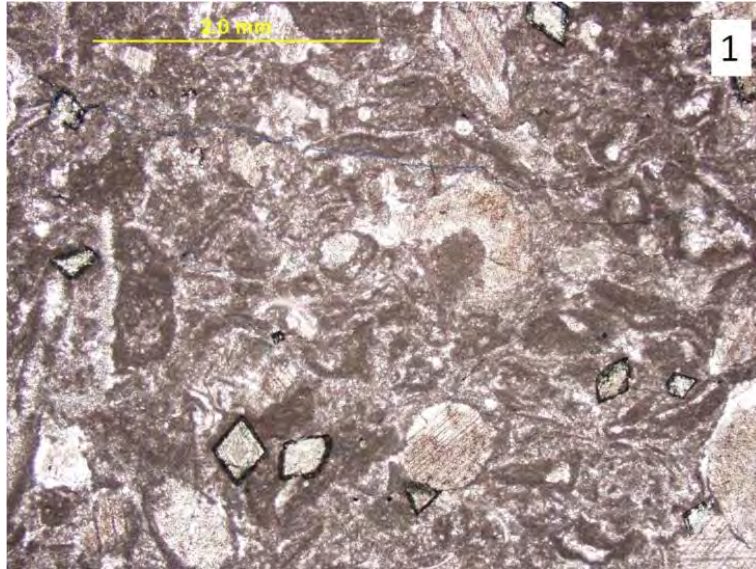


Figure 5B: Photomicrograph of the limestone (unit #1), it is primarily composed of calcite with a few secondary dolomite rhombohedrons (scale bar 2 mm).



Figure 5C: Photomicrograph of the sandy limestone (unit #2), it is fossiliferous and composed of silica sand grains floating in a calcite matrix (scale bar 2 mm).

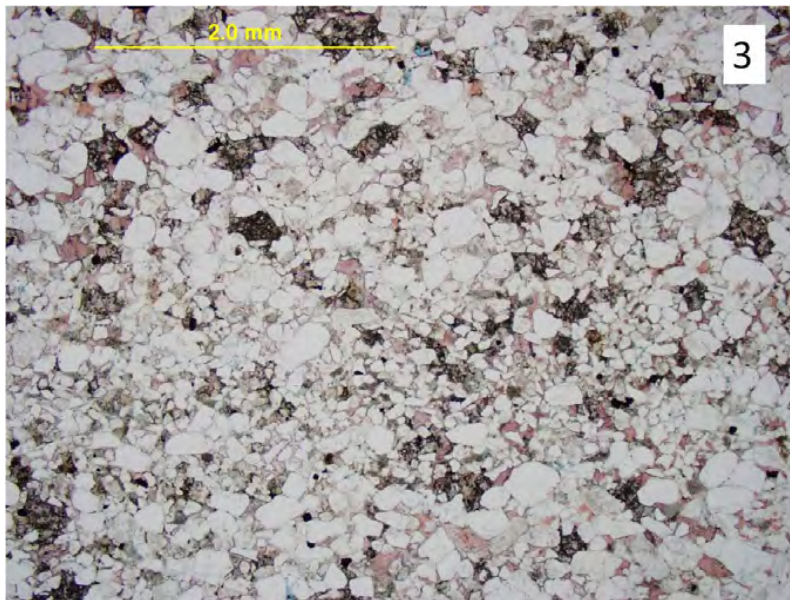


Figure 5D: Photomicrograph of the sandstone (unit #3), it is well-rounded, fine-grained and cemented with calcite (scale bar 2 mm).



Figure 5E: Close-up image of the limestone (1) surface, at this scale one can begin to see the granulation and clasts under the weathered and lichen covered surface.

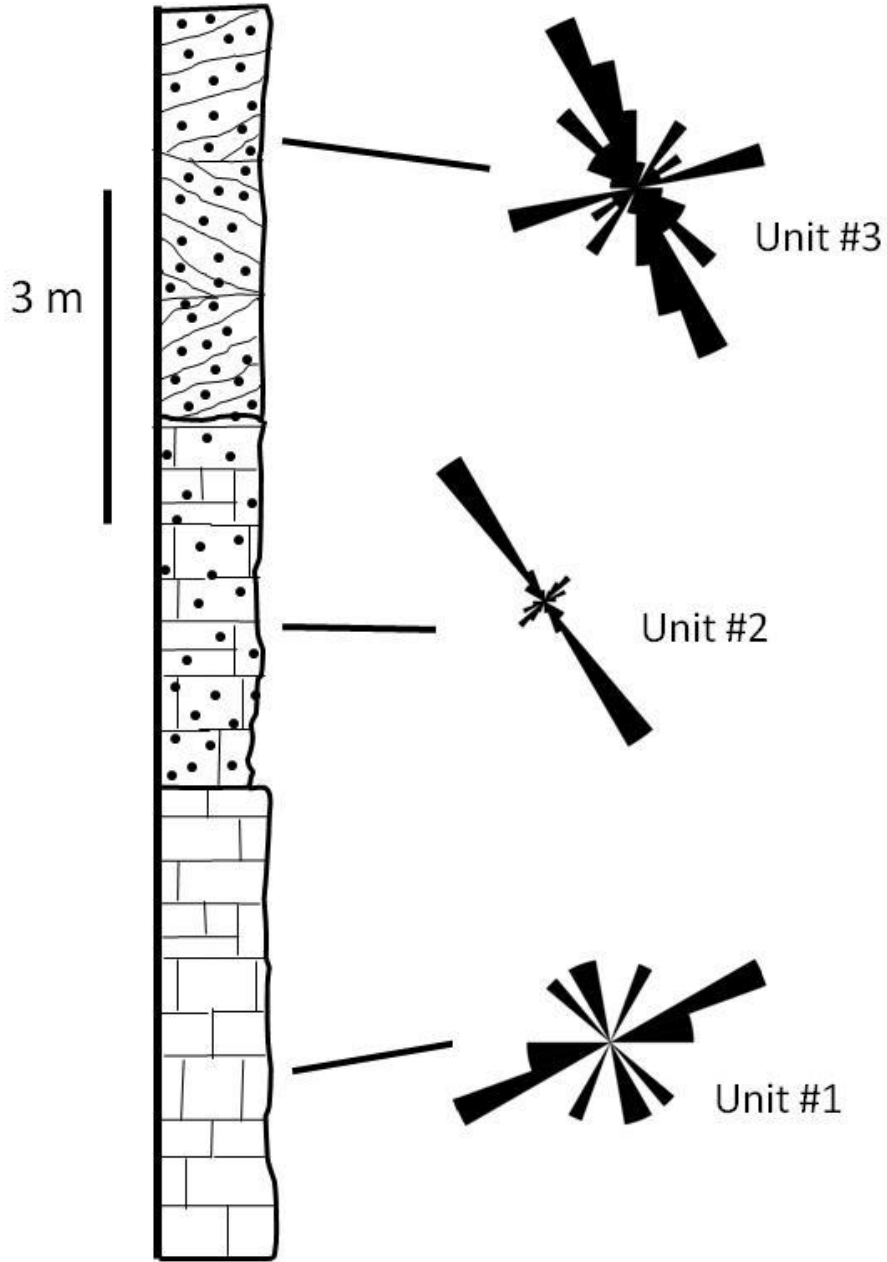


Figure 5F: Summary of orientations of the larger scale fractures within these three different sedimentary facies (unit #1 n = 9, unit #2 n = 34, unit #3 n = 41); at Beer Mug most beds contain the older NW-SE fracture (F_0) set.

Fracture Variability by Structural Position and Degree of Folding

The Tensleep Formation has been folded to different degrees over a variety of Laramide basement-cored thrusts. Many of these anticlines exhibit inherited F_0 fracture patterns that pre-date folding, as well as fold-related extension fractures that are approximately dip-parallel (F_1) and strike-parallel (F_2); normal and parallel to the axis of folding respectively. The F_1 set can strike oblique to the hinge in anticlines where the stress orientation that caused both folding and fracturing was oblique to the inherited basement structure that dictated the hinge trend, as at Flat Top Anticline. Areas on anticlines that were not significantly folded, i.e., relatively planar backlimbs, contain only the early, F_1 fractures caused by dilation perpendicular to thrusting during initial uplift, although locally it is superimposed on prethrust F_0 fractures. Intensified folding 1) reactivated earlier-formed fractures in shear and/or extension, 2) formed additional strike-parallel F_2 fractures caused by folding and the related hinge parallel extension, and 3) wrench-fault related F_3 fractures present at Beer Mug Anticline. Table 1 correlates these fracture sets and types to the two anticlines.

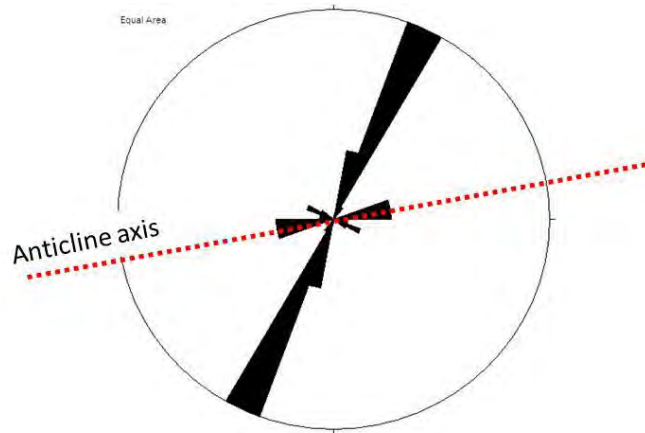
	Early regional	Dip-parallel	Strike-parallel	Wrench-parallel	Stress release	Bed-parallel shear	Deformation band shear
Flat Top	absent	F_1	F_2	absent	F_x	S_1	S_2
Beer Mug	F_0	F_1	F_2	F_3	F_x	S_1	S_2

Table 1: The table above cross references the type of extension and shear fractures by anticline as documented within this paper.

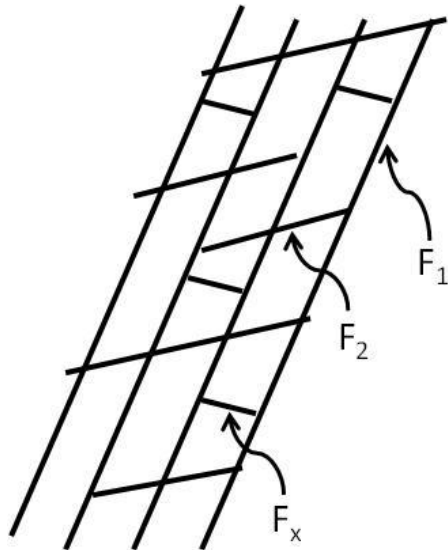
Flat Top Anticline

Fracture data were measured at numerous stations in the outward-dipping Tensleep Formation beds that define the perimeter of the North Flat Top Anticline. The fold is not tight: bedding dip changes only from 10° to the south on the backlimb to an estimated 40° to the north on the steepest parts of the forelimb. Fold-related fractures are poorly developed along the crest.

Tectonic fractures strike in two directions in most of the Tensleep sandstones at Flat Top Mountain, although those two basic strikes vary slightly with structure and stratigraphy; fracture patterns are both more regular and consistent in thin, well-cemented Tensleep Formation sandstones. The basic Tensleep Formation tectonic fracture pattern is well developed and well preserved in the calcareous, thinly and horizontally bedded, 1.2 meter (4 ft.) thick sandstone layer at the top of Flat Top Mountain (Figure 6). Three fracture sets are present in this bed: 1) F_1 an early, through-going set of tectonic fractures that strike NNE-SSW, 2) F_2 an intermediate-age set of strike-parallel fractures that strike ENE-WSW, parallel to the general axis of the anticline, and locally cut across and abut fractures of the F_1 set, and 3) F_x a youngest, irregularly developed set of short, non-tectonic fractures that are generally normal to the earliest set and that terminate against fractures of either of the older sets. Strike-parallel F_2 fractures are absent from much of the unfolded backlimb; although stress-release cross-fractures are present there (Figure 7), whereas an additional, possibly fault-related fracture set is present locally in the forelimb. Bed parallel shear (S_1) is recorded on the forelimb by slickenlines on a bedding plane separating a planar-bedded sandstone and a sandstone with large cross beds.



A



B

Figure 6: Rose diagram (A) and schematic drawing (B) showing the relatively simple strikes and geometric relationships of 42 fractures in the thinly bedded, well cemented calcareous sandstone at the top of Flat Top Mountain. This unit displays the three basic fracture sets observed at Flat Top Anticline and is the unit immediately below the covered interval near the top of the measured section shown in Figure 4. The three fracture sets are F_1 , nearly dip-parallel related to thrusting, F_2 strike-parallel related to folding, and F_x related to stress release. Only F_1 and F_2 fractures would be present in the subsurface.

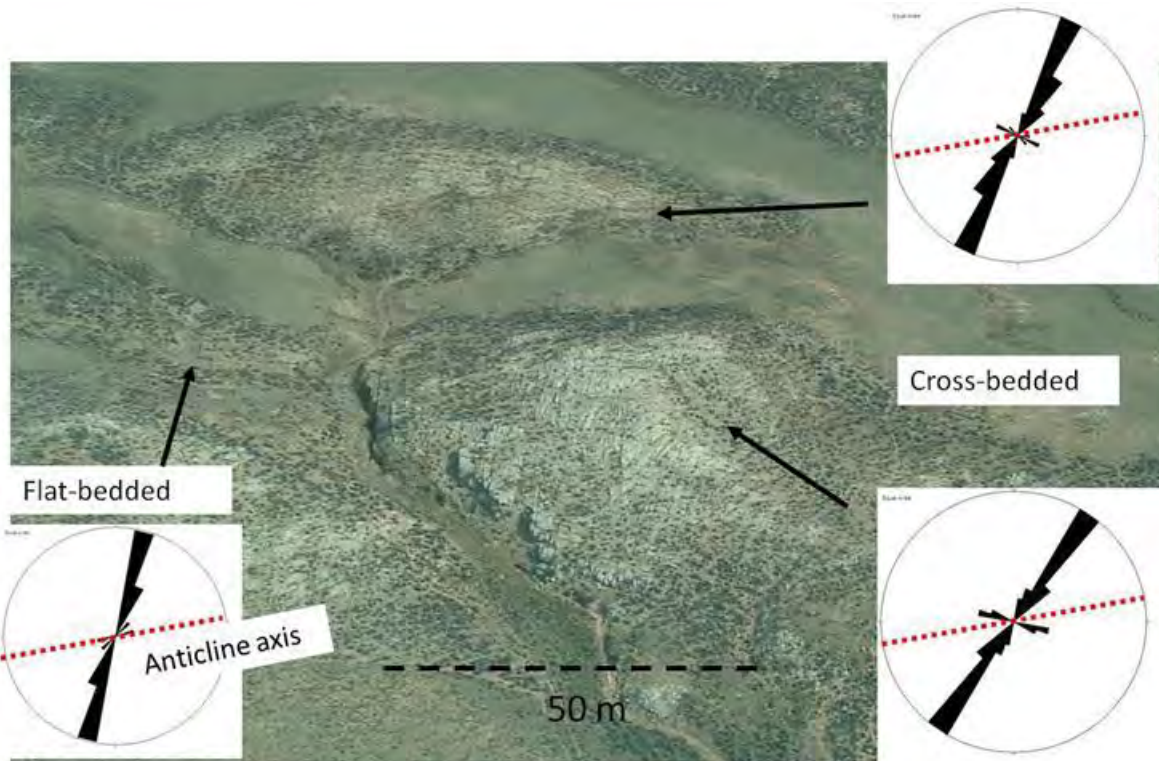


Figure 7: The aerial photograph and rose diagrams show that F_1 fractures and stress release fractures (F_x) are well developed in the unfolded backlimb sandstones on the south flank of Flat Top Anticline, but strike-parallel (F_2) fractures are absent.

Interpretation - Flat Top Anticline

This most regular of the observed fracture patterns is plausibly interpreted as follows. The oldest, NNE-SSW striking fractures (F_1) formed as load-parallel extension fractures (Lorenz et al., 1991) just prior to or contemporaneously with early stages of anticline development. These fractures do not strike normal to the trend of the anticline or to the map trace of the thrust fault, as might be expected if the direction of thrust translation is assumed to be normal to the thrust front. However, the fracture strikes *are* parallel to the probable direction of transport for the Flat Top Mountain thrust, as interpreted by Blevens (1984) and Carey (1950) from small-scale structures, which is oblique to the trace of the thrust fault, towards the NNE. Thus the

early set of Tensleep fractures strikes parallel to that interpreted direction of motion and the strikes are consistent with an interpretation of their formation as load-parallel extension fractures under same the stress conditions that initiated thrusting (Figure 8).

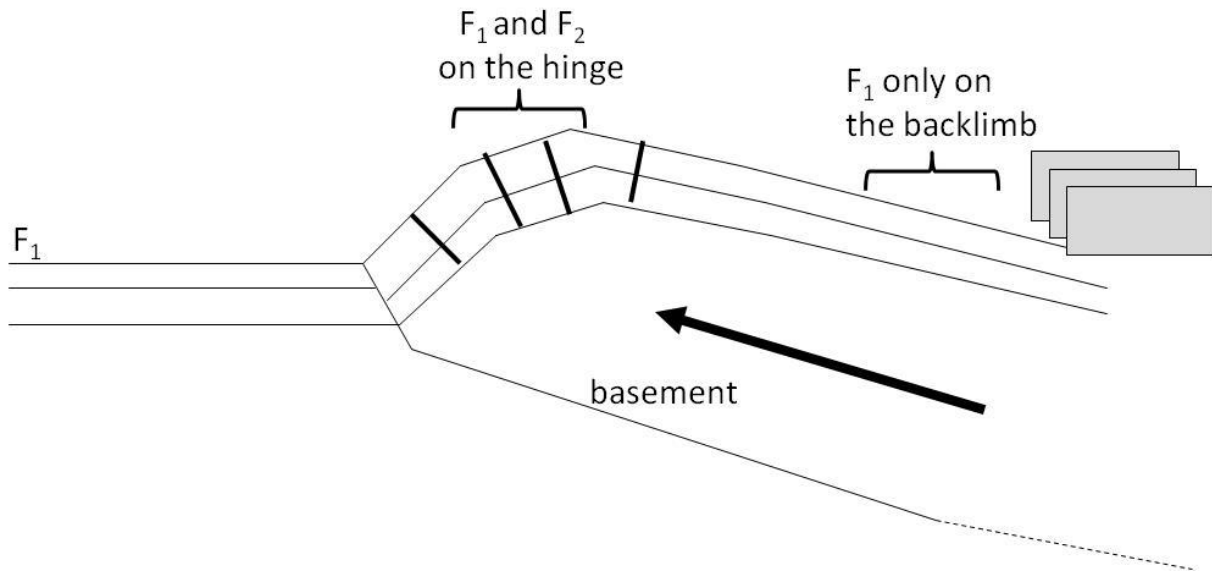


Figure 8: The F_1 set of fractures strikes parallel to the direction of thrust motion and nearly normal to the later-developed fold hinge and are nearly dip-parallel. F_2 fractures strike parallel to the fold axis, formed in extension caused by the flexure of the beds over the fold.

The intermediate-age, ENE-WSW striking fractures (F_2), striking parallel to the anticlinal hinge, can easily be interpreted as having formed slightly later, during fold-related extension across the developing anticline. Bed-parallel shear fractures (S_1) formed by bed-parallel slip during folding. Finally, the short youngest fractures (F_x) formed by stress release during uplift and exposure. These fractures would not be present in subsurface reservoirs, but the older F_1 and F_2 would be present.

Beer Mug Anticline

Fracture data were collected at numerous stations and transects across Beer Mug Anticline (Figure 9). The fold is tight: bedding dip changes from 40° to 55° on the western

backlimb to 90° on the eastern forelimb. Fold-related fractures are intensely developed along the crest. The core of Beer Mug Anticline is extensively fractured and brecciated with numerous void spaces and dead oil stain (Figure 10).

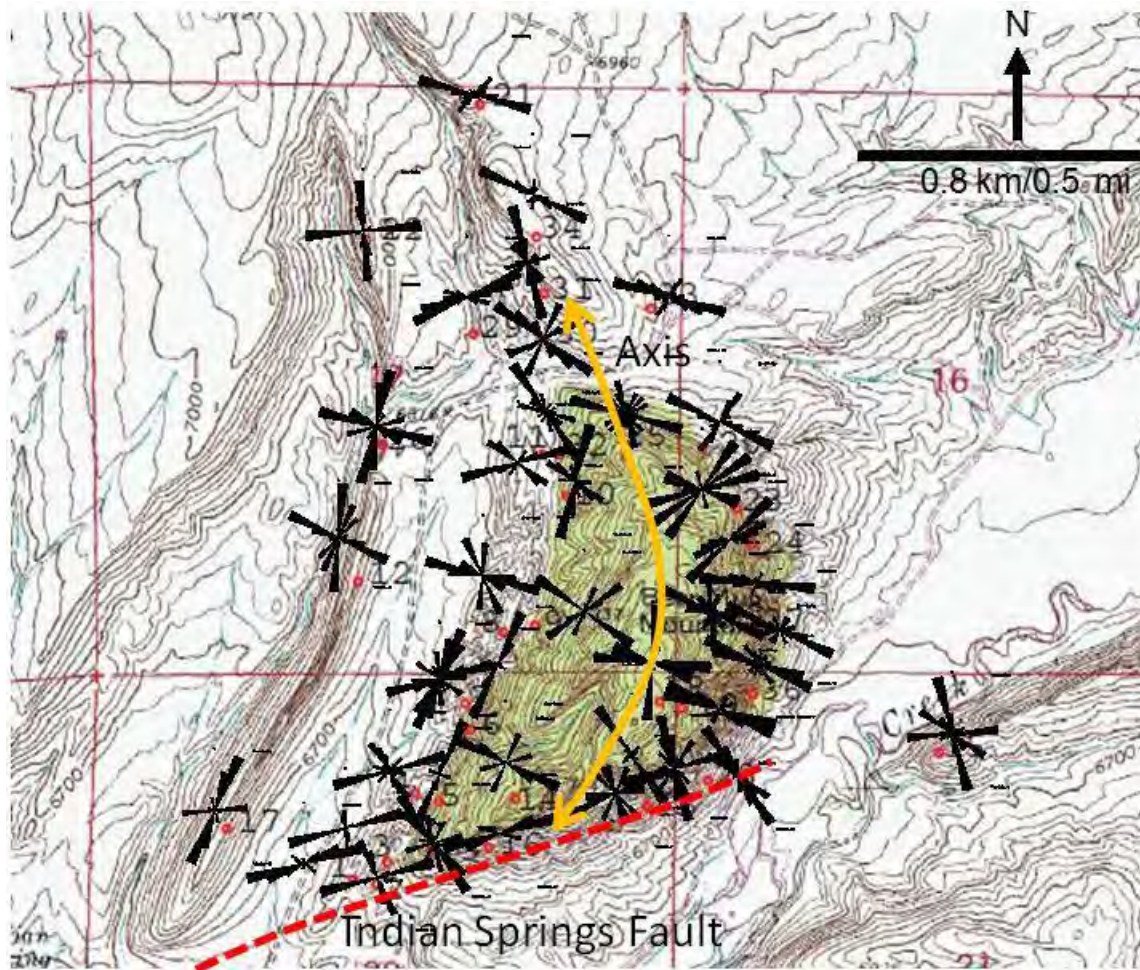


Figure 9: Rose diagrams of present-day fracture orientations at thirty-eight stations across Beer Mug Anticline. The axis of anticline is curved; it strikes NE in the south and rotates to a NW strike in the northern sections. The Indian Springs fault cuts the southeastern section of the anticline. Base map is the Difficulty Quadrangle from United States Geological Survey 7 ½ Minute Topographic Map Series.



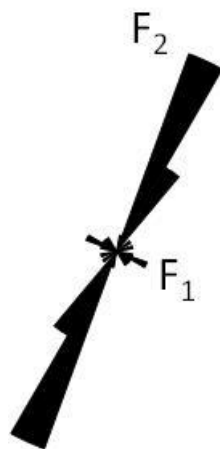
Figure 10: Outcrop of the shattered core of Beer Mug Anticline. The core has much void space and evidence for previous oil fill and was likely a good reservoir prior to breaching.

At Beer Mug Anticline a NW to WNW striking (F_0) set of fractures is recorded. The next extension fracture sets have orientations that are dip-parallel (F_1 : Figure 11) and strike-parallel (F_2). Shear fractures parallel to bedding are common at major lithologic discontinuities (S_1). Additional shear structures, such as deformation bands (S_2), are parallel, normal and oblique to bedding, including cross bedding (Figure 12). Another set of fractures (F_3), along the southeastern section of the anticline, strikes parallel to the Indian Springs wrench fault. This fracture set is localized within approximately 300 meters (1000 ft.) of the wrench fault (Figure 9). Only a few stress release (F_x) fractures are also recorded at Beer Mug Anticline, probably

because the numerous pre-existing fractures accommodated enough of the stress release to preclude the need for an entirely new fracture set.



A

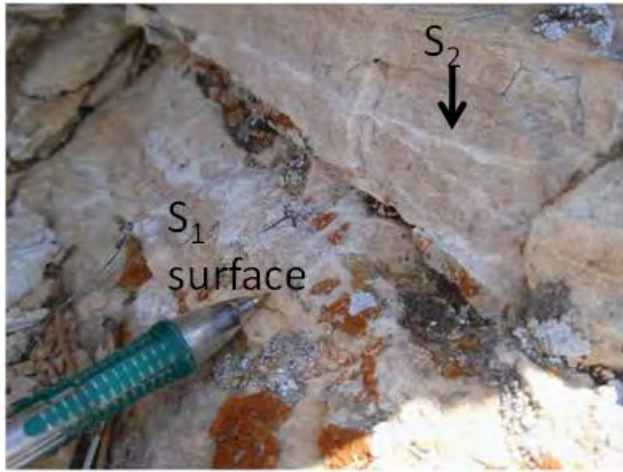


B

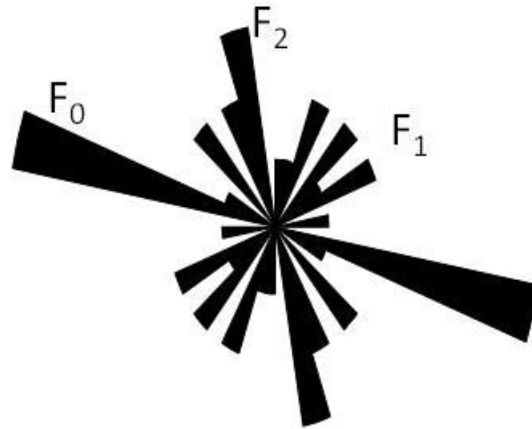
Figure 11: Outcrop on the southwestern back limb of Beer Mug Anticline. A) Cross-bedded sandstone unit within the Tensleep Formation, bedding strike N25°E, dip 40° SW. F₁ dip-parallel fractures are the exposed cliff face, F₂ strike-parallel fractures cut perpendicular to the cliff face. B) The rose diagram illustrates this combination of strike-parallel extension fractures (F₂), and dip-parallel extension fractures (F₁) (n = 28).



A



B



C

Figure 12: A) Photograph of cross bedded sandstone unit within the Tensleep Formation on the northwestern section back limb of Beer Mug Anticline. It contains a combination of F_0 , F_1 and F_2 extension fractures; F_1 and F_2 tend to terminate against F_0 at this location. B) Photograph of cross bed-parallel shears (S_1), and deformation bands (S_2) in the same outcrop. C) Rose diagram of present-day fracture orientations ($n = 24$).

Interpretation - Beer Mug Anticline

The most regular fracture sets are interpreted as follows. The oldest, NW to WNW striking fracture set (F_0) probably formed during the early stages of regional compression that eventually led to uplift of Beer Mug Anticline but pre-dated folding. This extension fracture set likely formed at the same time as small thrusts observed in the Alcova Limestone to the west (Lorenz and Cooper, 2010); both indicate a general NW-SE to WNW-ESE direction of shortening. The next fracture sets, dip-parallel (F_1) and strike-parallel (F_2) are related to folding and extension of beds across the anticline. The S_1 shear fractures formed during folding and are related to bed-parallel slip. The deformation bands (S_2 ; parallel, normal and oblique to bedding), are also related to folding. The Indian Springs wrench-fault-parallel fractures (F_3), formed at the same time as wrench displacement, which was late to penecontemporaneous with folding.

As at Flat Top Anticline, many of these structures formed early in one mode and were reactivated in other modes, producing enigmatic compound structures with conflicting evidence for their origin.

IMPLICATIONS FOR PRODUCTION

1. The Tensleep Formation contains interconnected, intensely developed fractures in most parts of the anticline but with internal variations due to both lithology and structural position.
2. Fracture development (spacing, number and type of fracture sets) varies on different structural parts of an anticline.
3. Intersecting deformation bands with their associated reduction in porosity and permeability (Antonellini and Aydin, 1995) may create baffles that can compartmentalize a reservoir. However, the intersecting and closely spaced extension fractures likely counteract this compartmentalization effect.
4. Limestones are uniquely “whole/intact” re-cemented units that are likely vertical barriers and baffles relative to the more densely fractured dolomites, sandstones and sandy limestones.
5. The Tensleep Formation in the core of tightly-folded anticlines (bedding dip change greater than 30°) should be a great target.

An understanding of the origins of these fractures in differing structures, structural settings and lithologies provides a basis for predicting fracture characteristics and distributions between wells, and thus their effects on flow for various EOR techniques.

CONCLUSIONS

The suite of strain-accommodation structures at Flat Top and Beer Mug anticlines consists of early-formed regional compression-related extension fractures (F_0) and later-formed dip-parallel (F_1) and strike-parallel (F_2) extension fractures, both bedding-parallel shear planes (S_1), additional shears such as deformation bands with a variety of strikes (S_2), and wrench fault related fractures (F_3). Most of these structures formed during anticline development, as the strata were extended parallel to and oblique to the anticlinal hinge. Additional structures, some with similar orientations, formed at different times during structural development of the anticlines. As folding intensified and tightened many of these structures were reactivated with differing senses of offset, leaving a suite of compound features that do not record a simple, linear, progressive sequence of development for individual strain-accommodation structures.

Though complex, the variability in the fracture patterns can be synthesized and captured in idealized fracture models constructed with the understanding that local variations are common. Development of a thorough understanding of fracture characteristics and distributions within the Tensleep Formation over a spectrum of anticlines, with Flat Top and Beer Mug Anticlines as end members, will allow operators to place wells in the optimum positions and design enhanced oil recovery (EOR) programs to maximize efficiency.

REFERENCES

- Antonellini, M.A., and Aydin, A., 1995, Effect of faulting on fluid flow in porous sandstones: geometry and spatial distribution, *American Association of Petroleum Geologists Bulletin*, v. 79, p. 642–671.
- Antonellini, M.A., Aydin, A., and Pollard, D.D., 1994, Microstructure of deformation bands in porous sandstones at Arches National Park, Utah, *Journal of Structural Geology*, v. 16, p. 941–959.
- Aydin, A., 1978. Small faults formed as deformation bands in sandstone. *Pure and Applied Geophysics* v. 116, p. 913–930.
- Aydin, A., and Johnson, A.M., 1983, Analysis of faulting in porous sandstones, *Journal of Structural Geology*, v. 5, p. 19–31.
- Boyd, D.W., 1993, Paleozoic history of Wyoming, in Snoke, A.W., Steidtmann, J.R., and Roberts, S.M., eds., *Geology of Wyoming: Geological Survey of Wyoming Memoir no. 5*, p. 164-187.
- Blackstone, D.L. 1994, Oil Springs and Flat Top anticlines, Carbon County Wyoming: An unusual fold pair: *The Mountain Geologist*, v. 31, p. 53-60.
- Blevens, D.M., 1984, Computer assisted structural analysis of the western termination of the Flat Top anticline, Carbon County, Wyoming: Master's thesis, University of Wyoming, 119 p.
- Carey, B.D., 1950, Geology of the eastern part of the Flat Top anticline, Albany and Carbon Counties, Wyoming: Master's thesis, University of Wyoming, 62 p.
- Knight, W.H., 1944, Geology of the western part of the Flat Top anticline, Albany and Carbon Counties, Wyoming: Master's thesis, University of Wyoming, 30 p.
- Lillegraven, J.A., and Snoke, A.W., 1996, A new look at the Laramide orogeny in the Seminoe and Shirley Mountains, Freezeout Hills, and Hanna Basin, south-central Wyoming: Wyoming State Geological Survey, Public Information Circular 36, 52p.
- Lillegraven, J.A., Snoke, A.W., and McKenna, M.C., 2004, Tectonic and paleogeographic implications of late Laramide geologic history in the northeastern corner of Wyoming's Hanna Basin: *Rocky Mountain Geology*, v. 39, p. 7-64.
- Long, J.C.S., Aydin, A., Brown, S.R., Einstein, H.H., Hestir, K., Hsieh, P.A., Myer, L.R., Nolte, K.G., Norton, D.L., Olsson, O.L., Paillet, F.L., Smith, J.L., and Thomsen, L., 1997, *Rock fracture and fluid flow*: National Academy Press, Washington, D.C., 551 p.
- Lorenz, J.C., and Cooper, S.P., 2010, Thrust Faults in the Alcova Limestone: Nature's Sand-Table Experiment, *American Association of Petroleum Geologists Rocky Mountain Section Meeting Official Program Book*, June 13-16, 2010, Durango, CO.
- Lorenz, J.C., Teufel, L.W., and Warpinski, N.R., 1991, Regional fractures I: A mechanism for the formation of regional fractures at depth in flat-lying reservoirs: *American Association of Petroleum Geologists Bulletin*, v. 75, p. 1714-1737.
- Love, J.D., Christiansen, A.C., and Ver Pleog, A.J., 1993, Stratigraphic nomenclature chart of Wyoming: Geological Survey of Wyoming Map series 41.
- Mair, K., Main, I., Elphick, S., 2000, Sequential growth of deformation bands in the laboratory, *Journal of Structural Geology*, v. p. 22, p. 25–42.
- Maravich, M.D., 1941 Geology of Freezeout Mountain – Bald Mountain Area, Carbon County, Wyoming: *American Association of Petroleum Geologists Bulletin*, v. 25, p. 883-897.

- Olsson, W.A., Lorenz, J.C., and Cooper, S.P., 2004, A mechanical model for multiply-oriented conjugate deformation bands, *Journal of Structural Geology*, v. 26, p. 325 -338.
- Peng, S., and Johnson, A.M., 1972, Crack growth and faulting in cylindrical specimens of Chelmsford granite: *International Journal of Rock Mechanics and Mining Science*, v. 9, pp.37-86.
- Pollard, D.D., and Aydin, A., 1988, Progress in understanding jointing over the past century: *Geological Society of America, Bulletin*, v. 100, no. 8, pp. 1181-1204.
- Stone, D.S., 1993, Basement-involved thrust-generated folds as seismically imaged in the subsurface of the Rocky Mountain foreland, in Schimdt, C.J., Chase, R.B., and Erslev, E.A., eds., *Laramide Basement Deformation in the Rocky Mountain Foreland of the Western United States: Boulder, Colorado: Geological Society of America Special Paper 280*, p. 271-318.
- Taylor, D.A., 1996, *Structural Geology of the Difficulty Creek area, Carbon County, Wyoming (Master's Thesis): University of Wyoming*, 119p.

APPENDIX

Abstracts

Presentations/posters associated with the abstracts are available through EORI

2008 - Natural hydraulic Injection Fractures, Lorenz and Yin

Natural Hydraulic Injection Fractures: Examples from the Tensleep Formation, Wyoming

John Lorenz and Peigui Yin, EORI, University of Wyoming

Several types of material, including bitumen, sand, and microcrystalline calcite, have been hydraulically injected into the dolomites and sandstones of the Tensleep Formation in Wyoming. The more irregular and branching injections, typically consisting of mm to cm-thick bands of sand and carbonate but locally consisting of zones of better-cemented rock suggesting injection of mineralizing fluids only, are interpreted to be early burial/early diagenesis features. These were probably created when pockets of water, liberated as the gypsum cements in the sandstones were converted to anhydrite, were injected along with entrained sediment into adjacent strata when pressurized by the overburden during burial. Poor planarity and branching suggest poor consolidation of the host sediment and low stress anisotropy at the time of injection. Multiple injections of sand and/or carbonate commonly used the same pathways, following planes of weakness in the rock created by an initial injection. A second, more planar type of injection appears to have formed later, possibly as late as the Laramide thrusting that resulted in local folding of the formation, as suggested by parallelism between hinge-parallel and hinge-normal strikes of the hydraulic injection planes and the fold-related extension fractures. Thrusting and folding are the probable sources of stress for these injections, but the sources of fluids and injected material are not obvious. A third type of injection consists of localized, vertical, bitumen-lined planes in dolomites, requires a separate mechanism. These injections overlie drained but oil-stained sandstones, suggesting that they formed by breaching of reservoir cap-rock seals during overpressuring during hydrocarbon maturation. Hydraulic injection fractures are common in parts of the Flat Top Anticline in southeastern Wyoming, and “sand- and silt-filled fractures” have been reported from cores of Tensleep sandstones, but studies of other cores across the state suggest that such hydraulic fractures are not abundant.

2008 - Tensleep Reservoir fractures, AAPG RMS, Lorenz

Fracture Characteristics in Core from Tensleep Reservoirs Across Wyoming

John Lorenz

Cores from 25 wells across Wyoming show that fractures are common in the anticlinal reservoirs of the Tensleep Formation, and that most of them are vertical extension fractures. The most intense fracturing is typically found along crests of the folds. Where orientation data are available, most of the fractures trend approximately normal and parallel to the hinge of the anticlines, although oblique fracture orientations have also been reported. Shear fractures are present in the more tightly folded anticlines. Tests on fractured plugs from core usually show that the fractures have less permeability than the associated matrix, and these test results are commonly used to erroneously suggest that fractures have little effect or may even degrade system permeability. This is because typically only the tightest fractures are tested since they are the only ones that will keep their integrity during plugging. Fracture populations typically include a range of sizes, and it is the more open fractures, those that don't remain intact during plugging and that get discarded, that control permeability. In fact, well tests suggest that fracture-enhanced permeability is present in most of the fields studied. Tensleep fractures are variously mineralized with anhydrite, quartz, calcite, dolomite bitumen, yet most fractures are not completely occluded, retaining up to 80% of the original aperture as remnant porosity. In contrast, although the tight dolomites between the Tensleep sandstone reservoirs commonly act as seals for pressure compartments even though they tend to be highly fractured, probably because the fractures in this facies are short and poorly interconnected.

**Fractures and Faults in an Eolian Sandstone in a
Non-Structural Setting: the Casper Sandstone**

John Lorenz

Exposures of the Casper Sandstone 25 miles southwest of Laramie, Wyoming, contain faults and fractures even though the local structure consists only of a gentle dip of several degrees northward into the basin. Equivalent Tensleep strata are intensely fractured and faulted where they have been folded on Laramide anticlines, and the Casper Sandstone exposure provides an opportunity to separate those fractures that may be present in flat-lying strata from those that are created by folding.

Systematic fractures in the Casper Sandstone are found in half-meter thick lenses of interbedded dolomite, where fracture spacing is on the order of centimeters to tens of centimeters and distinct sets of parallel fractures are present. Fractures of the same sets can be found in the associated, dune cross-bedded sandstones, but spacing is on the order of tens of meters and strikes are less regular since the sandstones are thicker and less brittle. Much of the deformation in the sandstones was probably accommodated by pervasive grain boundary slip, but fracture zones meters to a few tens of meters in height, length, and width are present locally. Many of these fracture zones form isolated pods within otherwise poorly fractured strata. Some fractures have coalesced into fault zones that consistently terminate at the whiter, crossbedded, sand-dune facies that caps the sequence. Larger fault zones can be inferred from the presence/absence of strata across linear trends and from apparent offsets of bedding across valleys. Some beds are marked by irregular, closely spaced, horizontal planes that may record a pervasive horizontal shear in the formation near the larger faults.

Thrust faults in the Alcova Limestone: Nature's sand-table experiment

John Lorenz and Scott Cooper

The two-meter thick Triassic Alcova Limestone, a heterogeneous, thin-bedded carbonate, forms a stiff strut within a thicker shale sequence. Small, complex thrust faults in the Alcova Limestone near Beer Mug Anticline in southeastern Wyoming record a horizontal compressive stress that exceeded the weight of the overburden.

Structures characteristic of the Alcova thrust system include standard thrust planes, back-thrusts, bedding-parallel decollement zones, bed-parallel shear in the folds, folds, and fold-core voids. Local stylolites suggest that dissolution also played a role. The main thrusts in the Alcova Limestone form meter-scale en echelon planes that step back at each offset when traced up section and have offsets of 1-20 centimeters. The thrusts cut ductile lithologies, where the beds thickened plastically, and brittle lithologies where the beds fractured. These thrust planes can be traced from down-dip initiation up-dip to where they steepen and terminate blindly in folded duplex structures. Smaller, centimeter-scale synthetic and antithetic thrusts are also pervasive in the formation. Given most of the main thrusts are relatively small, and none seems to have developed into a larger structure that localized meters or tens of meters of offset, suggests some sort of self-limiting feedback mechanism that locked each fault up after at most a few tens of centimeters of displacement.

These thrusts allow a unique interpretation of the local stress system that produced the kilometer scale thrust faults in the area. Only horizontal compressive stresses in excess of the overburden could have produced the Alcova thrust system, and those stresses rather than drape over a basement fault likely produced the local dramatic and tightly folded Beer Mug Anticline.

More importantly, the small Alcova thrusts mimic the geometry of kilometer-scale thrusts seen in seismic lines in thin-skinned fold and thrust belts, and can be used as analogs to study the characteristics of deformation in these systems.

2010 - Beer Mug AAPG Annual Meeting, Cooper and Lorenz

Fracture Patterns Associated with Tightly Folded Laramide Structures: The Example of Beer Mug Anticline, Wyoming

Scott P. Cooper and John C. Lorenz

Beer Mug anticline, with a near-vertical forelimb and backlimb dip up to 50 degrees provides an ideal analogue for fracture systems that will have a significant effect on fluid flow in tightly folded Laramide reservoirs. Outcrop data collected over the 2009 field season indicate that the entire exposed sedimentary package, Tensleep Formation through the Alcova Limestone, is cut by numerous intersecting fractures. Fracture type and degree of development vary systematically with lithology and structural position. Fracturing is most intense towards the core of the anticline, which consists of brecciated, oil-stained rock with large-scale vuggy porosity. The age relationships of the fracture sets are commonly ambiguous since offset is minimal and most intersections are mutually crosscutting, but pre-fold and fold-related fracture sets can be recognized. Many of the early-formed fractures were reactivated in shear and/or extension.

Within the Tensleep Formation, bedding-parallel slip, commonly along the large dune cross-bed foresets, accommodated much of the pervasive strain. Small offsets were also documented on irregular calcite-mineralized planes oblique to bedding. The meter-scale dolomite beds interbedded within the thicker Tensleep sandstone units accommodated much of the larger-scale bed-parallel shear through brecciation, but brecciation is not always obvious due to cementation and weathering. In fact, at a gross scale, many of the dolomite beds give the appearance of being massive and completely unfractured. Granulation, brecciation, pressure solution, and cementation likely occurred nearly simultaneously with deformation. Natural hydraulic or injection fractures with random strikes occur within both sandstone and dolomite strata. Some injection fractures are parallel to the ESE-WNW striking early-strain extension fractures, suggesting an age and/or mechanical relationship. Many injection fractures contain not only dolomitic mudstone fill but also euhedral calcite crystals suggesting extension and open aperture at depth.

Shales overlying the Tensleep Formation accommodated strain by localized bedding-parallel shear faulting. Small thrust faults and shear fractures in the overlying Alcova Limestone provide additional evidence that the maximum stress was in the horizontal plane and approximately ESE-WNW prior to tilting of the beds. This suggests that the Beer Mug anticline was not passively draped over an underlying basement thrust.

Fracture Patterns Associated with Laramide Anticlines

Scott P. Cooper and John C. Lorenz

Outcrop and core fracture data from formations that have been folded to different degrees above Laramide thrust structures in Wyoming suggests that idealized fracture models can be constructed but that local variations are common. Inherited F_0 fracture patterns unrelated to folding are present in some structures. Fold-related extension fractures trend approximately normal (F_1) and parallel (F_2) to the axis of folding. Hinge-normal F_1 extension fractures typically formed in response to horizontal stress prior to uplift and prior to the hinge-parallel F_2 fractures that formed during folding. Areas on anticlines that were not significantly folded, i.e., relatively planar backlimbs, contain only the early, F_1 fractures. This fracture set can strike oblique to the hinge in anticlines where the stress orientation that caused both folding and fracturing was oblique to the inherited basement structure that dictated the hinge trend of the anticline.

Outcrop data from tightly folded structures; such as Beer Mug anticline, with a near-vertical forelimb, and backlimb dips up to 50 degrees, indicate that the entire exposed sedimentary package is cut by numerous intersecting fractures. Fractures of all three sets (F_0 , F_1 , and F_2) were locally reactivated in both shear and extension as folding intensified. Some fractures also formed originally as shear fractures, F_s . Small, complex thrust faults and shear fractures in the Alcova Limestone on the backlimb and in front of the forelimb record a horizontal compressive stress that exceeded the weight of the overburden. Knowledge of the actual fracture patterns were used to reconstruct tectonic evolution, and knowledge of likely fracture patterns can be used to model fluid flow.

Fracture Variability within the Tensleep Formation

Scott P. Cooper and John C. Lorenz

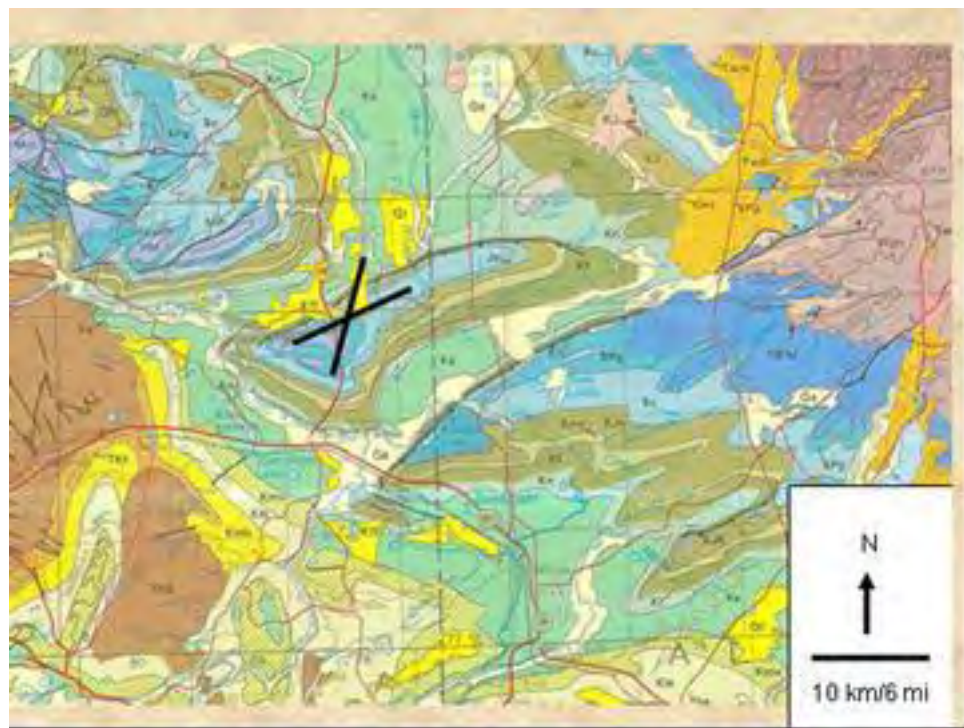
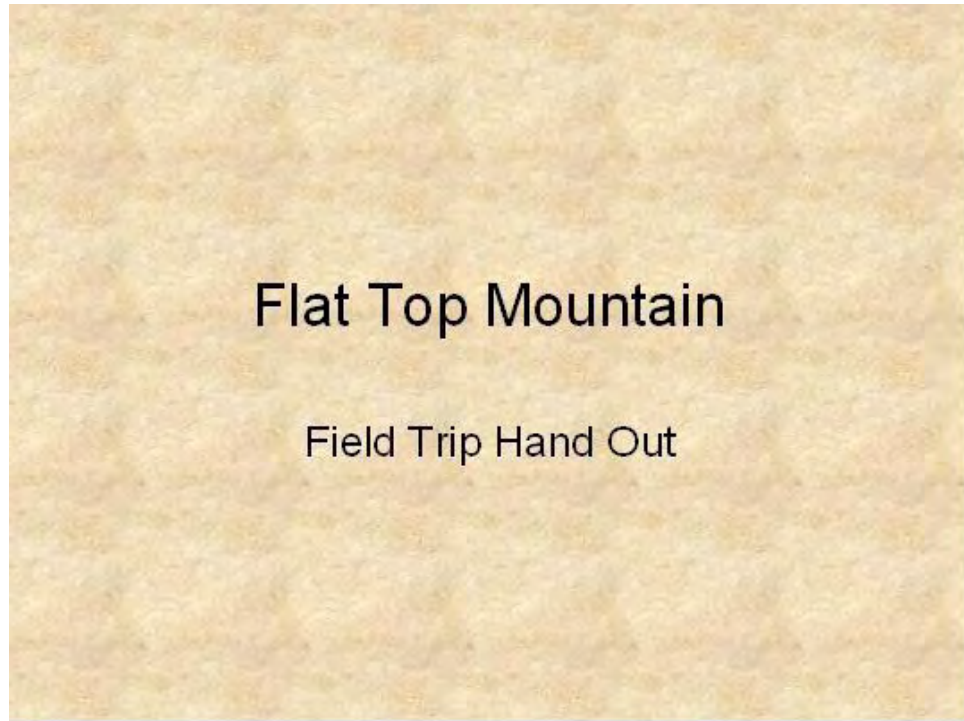
Outcrops of the Pennsylvanian Tensleep Formation over anticlines are cut by numerous intersecting fractures. The fractures patterns vary significantly by lithology, structural position and degree of folding.

The Tensleep Formation in south-central Wyoming is a complex package of repeated marine limestones and/or dolomites, and sandstones formed in near-shore, dunes, and interdune environments with both horizontal and large scale cross bedding. Pervasive small-scale strain, recorded by calcite-mineralized planes, was accommodated in the dune facies by both slip parallel to the large-scale cross bed foresets and by offsets oblique to bedding. The dolomites and limestones within the Tensleep Formation accommodated much of the larger-scale bed-parallel shear through brecciation although it is not always obvious due to weathering and secondary re-cementation. From a distance, many of the limestone beds in fact appear to be unfractured. Granulation, brecciation, pressure solution, cementation and re-cementation likely occurred nearly simultaneously during deformation.

The Tensleep Formation has been folded to different degrees over a variety of Laramide basement-cored thrusts. Most of these anticlines exhibit inherited F_0 fracture patterns that pre-date folding, as well as fold-related extension fractures that trend approximately normal (F_1) and parallel (F_2) to the axis of folding. The F_1 set can strike oblique to the hinge in anticlines where the stress orientation that caused both folding and fracturing was oblique to the inherited basement structure that dictated the hinge trend. Areas on anticlines that were not significantly folded, i.e., relatively planar backlimbs, contain only the early, F_1 fractures. Many of the earlier-formed fractures were reactivated in shear and/or extension during continued folding.

The variability in the fracture patterns can be synthesized and captured in an idealized fracture model constructed with the understanding that local variations are common.

FLAT TOP MOUNTAIN FIELD TRIP HANDOUT



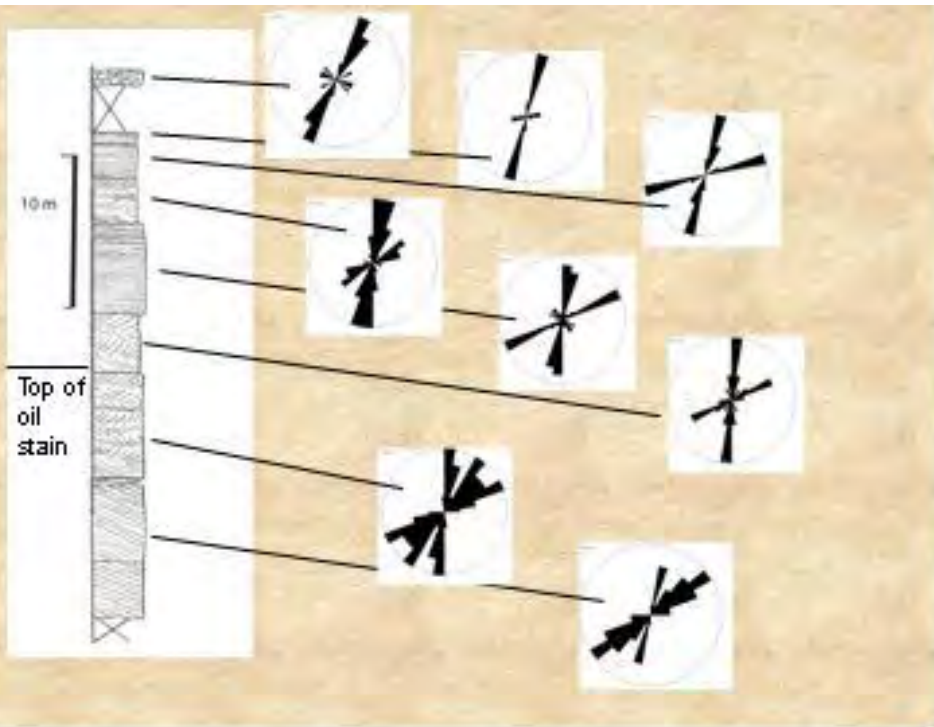
Thrust translation was *oblique* to the thrust front



N
↑
1 mi / 1.6 km



Blevins, 1984



Flat-bedded sandstone caprock



Bed thickness 1.2 m. Average spacing 0.7 m

Parallel-bedded sandstone

1.47 m average spacing
37.4° mean strike



Crossbedded sandstone directly underlying
1.65 m average spacing
37.6° mean strike



Minimal facies variations in fracturing, backlimb



Strike varies with structural position



TENSLEEP FRACTURE STUDY BIBLIOGRAPHY

- Agatston, R.S., 1952, Tensleep Formation of the Big Horn Basin: Wyoming Geological Association Guidebook, 7th Annual Field Conference, p. 44-48.
- Agatston, R.S., 1954, Pennsylvanian and lower Permian of northern and eastern Wyoming: AAPG Bulletin, v. 38, p. 508-583.
- Agatston, R.S., 1957, Pennsylvanian of the Wind River Basin: Wyoming Geological Association Guidebook, 12th Annual Field Conference, p. 29-33.
- Ahlbrandt, T.S., and R.E. Harris, 1975, Clastic dikes in the Fountain and Casper formations (Permo-Pennsylvanian), southeastern Wyoming: Rocky Mountain Geology, v. 14, p. 51-54.
- Andrew, D.A., W.G., Pierce, and D.H. Eargle, 1947, Geologic map of the Bighorn Basin, Wyoming and Montana, showing terrace deposits and physiographic features: U.S. Geological Survey Oil and Gas Investigations, Preliminary Map 71.
- Andrews, S., and L.S. Higgins, 1984, Influence of depositional facies on hydrocarbon production in the Tensleep Sandstone, Big Horn Basin, Wyoming: a working hypothesis: Wyoming Geological Association Guidebook, 35th Annual Field Conference, p. 183-197.
- Antonellini, M.A., and Aydin, A., 1995, Effect of faulting on fluid flow in porous sandstones: geometry and spatial distribution, American Association of Petroleum Geologists Bulletin, v. 79, p. 642-671.
- Antonellini, M.A., Aydin, A., and Pollard, D.D., 1994, Microstructure of deformation bands in porous sandstones at Arches National Park, Utah, Journal of Structural Geology, v. 16, p. 941-959.
- Aviantara, A., 1996, Facies and fracture architecture of the Tensleep sandstone, Bighorn Basin, Wyoming: preliminary result of outcrop and subsurface study (abstract): American Association of Petroleum Geologists Convention and Exhibition, 19-22 May 1996, San Diego, California, AAPG Search and Discover Article #91019.
- Aviantara, A., 1999, Facies architecture of the Tensleep Sandstone, Bighorn Basin, North-Central Wyoming: PhD Dissertation, University of Tulsa, 249 p.
- Aviantara, A.A., 1998, Facies architecture of the Tensleep Sandstone, Bighorn Basin, north-central Wyoming (abstract): AAPG Bulletin, v. 82, no. 13 (supplement).
- Aydin, A., 1978. Small faults formed as deformation bands in sandstone. Pure and Applied Geophysics v. 116, p. 913-930.
- Aydin, A., and Johnson, A.M., 1983, Analysis of faulting in porous sandstones, Journal of Structural Geology, v. 5, p. 19-31.
- Babcock, L.C., J.A. McCaleb, and B.D. Keith (in press as of 1984), Reservoir heterogeneity in the Pennsylvanian Tensleep Sandstone, Torchlight and Little Buffalo Basin Fields, *in*, Tillman, R.W. (ed.), Reservoir Sedimentology and Synergy: Society of Economic Paleontologists and Mineralogists, Special Publication.....
- Bellhasen, Nicholas, Patricia Fiore, and David D. Pollard, 2003, Fold-fracture relationships in the Sheep Mountain Anticline, Bighorn Basin, Wyoming (abstract): Geological Society of America, Abstracts with Programs, v. 35, no. 6, p. 177.
- Bellhasen, Nicholas, Patricia Fiore, and David D. Pollard, 2006, From spatial variation of fracture patterns to fold kinematics: a geomechanical approach: Geophysical Research Letters, v. 33, p. L02301, 4 p.

- Berg, R.R., 1976, Deformation of Mesozoic shales at Hamilton Dome, Bighorn Basin, Wyoming; AAPG Bulletin, v. 60, p. 1425-1433.
- Bird, Peter, 1998, Kinematic history of the Laramide orogeny in latitudes 35° -49° N, western United States: Tectonics, v. 17, p. 780-801.
- Bjoroy, M., J.A. Williams, D.L. Dolcater, M.K. Kemp, and J.C. Winters, 1996, Maturity assessment and characterization of Big Horn Basin Paleozoic oils: Marine and Petroleum Geology, v. 13, p. 3-13.
- Blackstone, D.L. 1994, Oil Springs and Flat Top anticlines, Carbon County Wyoming: An unusual fold pair: The Mountain Geologist, v. 31, p. 53-60.
- Blackstone, D.L., 1981, Compression as an agent in deformation of the east-central flank of the Bighorn Mountains, Sheridan and Johnson Counties, Wyoming: Contributions to Geology, University of Wyoming, v. 19, p. 105-122.
- Blevens, D.M., 1984, Computer assisted structural analysis of the western termination of the Flat Top anticline, Carbon County, Wyoming: Master's thesis, University of Wyoming, 119 p.
- Bowles, C.G., and W.A. Braddock, 1963, Solution breccias of the Minnelusa Formation in the Black Hills, South Dakota and Wyoming, in, Unsorted Papers in Geology and Hydrology: U.S Geological Survey Professional Paper 475-C, p. C91-C95.
- Boyd, D.W., 1993, Paleozoic history of Wyoming, in Snoke, A.W., Steidtmann, J.R., and Roberts, S.M., eds., Geology of Wyoming: Geological Survey of Wyoming Memoir no. 5, p. 164-187.
- Brown, O.P., 1939, The geology of Difficulty-Little Shirley Basin area, Carbon County, Wyoming: Master's thesis, University of Wyoming, 22p.
- Carey, B.D., 1950, Geology of the eastern part of the Flat Top anticline, Albany and Carbon Counties, Wyoming: Master's thesis, University of Wyoming, 62 p.
- Carr-Crabaugh, M., Dunn, T.L., 1996, Reservoir Heterogeneity as a function of accumulation and preservation dynamics, Tensleep sandstone, Bighorn and Wind River basins, Wyoming, in Longman, M.W. and Sonnenfeld, M.D., eds., 1996, Paleozoic Systems of the Rocky Mountain Region, Rocky Mountain Section SEPM (Society for Sedimentary Geology), p. 305-320.
- Carr-Crabaugh, M., Hurley, N.F., and Carlson, J., 1996, Interpreting eolian reservoir architecture using borehole images, GCSSEPM Foundation 17th Annual Research Conference Stratigraphic Analysis, December 8-11, 1996, p. 39-50.
- Ciftci, B.N., Aviantara, A.A., Hurley, N.F., and Kerr, D.R., 2004, Outcrop-based three-dimensional modeling of the Tensleep Sandstone at Alkali Creek, Bighorn basin, Wyoming, in Integration of Outcrop and Modern Analogs in Reservoir Modeling, p. 235-259.
- Chappell, W.M., and J.H. Spang, 1974, Significance of layer-parallel slip during folding of layered sedimentary rocks: Geological Society of America, Bulletin, v. 85, p. 1523-1534.
- Claypool, G.E., A.H. Love, and E.K. Maughan, 1978, Organic geochemistry, incipient metamorphism, and oil generation in black shale members of the Phosphoria Formation, western interior United States: AAPG Bulletin, v. 62, p. 98-120.
- Cole, R.D., and C.E. Mullen, 1992, Sedimentologic reservoir characterization of Tensleep Sandstone, South Casper Creek Field, Wyoming: Wyoming Geological Association, 43rd Annual Field Conference Guidebook, p. 121-137.

- Cooper, S.P., 2000, Deformation within a basement-cored anticline: Teapot Dome, Wyoming, M.S. Thesis, New Mexico Institute of Mining and Technology, 274p.
- Cooper, S. P., Goodwin, L. B., and Lorenz, J. C., 2006, Fracture and fault patterns associated with basement-cored anticlines: The example of Teapot Dome, Wyoming: American Association of Petroleum Geologists Bulletin, v. 90, p. 1903-1920.
- Cooper, S.P., and Lorenz, J.C., 2010, Fracture Variability within the Tensleep Formation, Southeastern Wyoming in Fletcher, L., ed., Unconventional Energy Resources, 2010 Wyoming Geological Association Symposium, p. 39-50.
- Cooper, S.P., and Lorenz, J.L., 2010, Fracture patterns associated with tightly folded Laramide structures: the example of Beer Mug Anticline, Wyoming: American Association of Petroleum Geologists 2010 Annual Meeting, Abstract with Programs.
- Curry, W.H. III, 1984, Paleotopography at the top of the Tensleep Formation, Bighorn Basin, Wyoming: Wyoming Geological Association Guidebook, 35th Annual Field Conference, p. 199-211.
- Darton, N.H., 1906, Geology of the Bighorn Mountains: U.S. Geological Survey Professional Paper 51, 129 p.
- DeBruin, 2002, Wyoming oil and gas map, series 55,
- Desmond, R.J., J.R. Steidtmann, and D.F. Cardinal, 1984, Stratigraphy and depositional environments of the middle member of the Minnelusa Formation, central Powder River Basin, Wyoming: Wyoming Geological Association Guidebook, 35th Annual Field Conference, p. 213-239.
- Dunn, T.L., 1994, Anisotropy and spatial variation of relative permeability and lithologic character of Tensleep sandstone reservoirs in the Bighorn and Wind River basins, Wyoming: Department of Energy Contract No. DE-AC22-93BC14897: Annual report, 76p.
- Dunn, T.L., 1995, Anisotropy and spatial variation of relative permeability and lithologic character of Tensleep sandstone reservoirs in the Bighorn and Wind River basins, Wyoming: Department of Energy Contract No. DE-AC22-93BC14897: Second Annual report, 114p.
- Dunn, T.L., 1996, Anisotropy and spatial variation of relative permeability and lithologic character of Tensleep Sandstone reservoirs in the Bighorn and Wind River basin, Wyoming: Quarterly Report, DOE Contract no. DE-AC22-93BC14897, 8p.
- Dunn, T.L. 1997, Anisotropy and spatial variation of relative permeability and lithologic character of Tensleep sandstone reservoirs in the Bighorn and Wind River basins, Wyoming: Department of Energy Contract No. DE-AC22-93BC14897: Final report, 187p.
- Duranti, D., and A. Hurst, 2004, Fluidization and injection in the deep-water sandstones of the Eocene Alba Formation (UK North Sea): Sedimentology, v. 51, p. 503-529.
- Emmett, W.R., K.W. Beaver, and J.A. McCaleb, 1971, Little Buffalo Basin Tensleep heterogeneity—its influence on drilling and secondary recovery: Journal of Petroleum Technology, February, 1971, p. 161-168.
- Engelder, T., M.R. Gross, and P. Pinkerton, 1997, An analysis of joint development in thick sandstone beds of Elk Anticline, Montana-Wyoming: Rocky Mountain Association of Geologists 1997 Field Conference Guidebook, p. 1-18.
- Fanshaw, J.R., 1971, Structural evolution of the Bighorn Basin: Wyoming Geological Association Guidebook, 23rd Annual Field Conference, p. 35-37.

- Fischer, M.P., and Christensen, R.D., 2004, Insights into the growth of basement uplifts deduced from a study of fracture systems in the San Rafael Monocline, east central Utah: *Tectonics*, v. 23, p. 1018. doi:10.1029/2002TC001470.
- Fox, J.E., and G.L. Dolton, 1989, *Petroleum Geology of the Wind River and Bighorn Basins, Wyoming and Montana: United States Geological Survey, Open-File Report 87-450*, 43 p. [I 19.76]
- Fox, J.E., P.W. Lambert, R.F. Mast, N.W. Nuss, and R.D. Rein, 1975, Porosity variation in the Tensleep and its equivalent the Weber Sandstone, western Wyoming: a log and petrographic analysis, *in*, *Deep Drilling Frontiers of the Central Rocky Mountains: Rocky Mountain Association of Geologists Field Conference Guidebook*, p. 185-216.
- Fryberger, S.G., et al., 1983, Eolian dune, interdune, sand sheet, and siliciclastic sabkha sediments of an offshore prograding sand sea, Dhahran area, Saudi Arabia: *AAPG Bulletin*, v. 67, p. 280-311.
- Fryberger, S.G., 1984, The Permian Upper Minnelusa Formation, Wyoming, ancient example of an offshore-prograding eolian sand sea with geomorphic facies, and system-boundary traps for petroleum: *Wyoming Geological Association Guidebook, 35th Annual Field Conference*, p. 241-272.
- Gilbertson, N. J., 2004, 3D geologic modeling and fracture interpretation of the Tensleep Sandstone, Alcova Anticline, Wyoming: (abstract), American Association of Petroleum Geologists, Annual Convention,
- Gilbertson, Nathaniel J., 2005, 3D geologic modeling and fracture interpretation of the Tensleep Sandstone, Alcova Anticline, Wyoming: (abstract), American Association of Petroleum Geologists, Annual Convention,
- Gilbertson, N.J., 2006, 3D geologic modeling and fracture interpretation of the Tensleep Sandstone, Alcova Anticline, Wyoming, Colorado School of Mines, PhD dissertation, 265 p.
- Glennie, K.W., 1970, Desert sedimentary environments, *in* *Developments in Sedimentology*, no. 15, New York, Elsevier Publishing Company, 222 p.
- Gray, David, and Dragana Todorovic-Marinic, 2004, Fracture detection using 3D azimuthal AVO: *CESG Recorder*, December 2004, p. 5-8.
- Guiton, M., W. Sassi, Y. Leroy, and B Gauthier, 2003, Mechanical constraints on the chronology of fracture activation in the folded Devonian Sandstone of the western Moroccan Anti-Atlas: *Journal of Structural Geology*, v. 25, p. 1317-1330.
- Guiton, M., Y Leroy, and W. Sassi, 2003, Activation of diffuse discontinuities and folding of the sedimentary layers: *Journal of Geophysical Research*, v. 108, p. 2183
- Hanley, J.H., and J.R. Steidtmann, 1973, Petrology of limestone lenses in the Casper Formation, southernmost Laramie Basin, Wyoming and Colorado: *Journal of Sedimentary Petrology*, v. 43, p. 428-434.
- Hart, B.S., 2006, Seismic expression of fracture-swarm sweet spots, Upper Cretaceous tight-gas reservoirs, San Juan Basin, American Association of Petroleum Geologists Bulletin, p. 1519-1534.
- He, Hongzhan, Leigh Royden, Clark Burchfiel, and Martin Schuepach, 1996, Late Paleozoic deformation of interior North America: the greater Ancestral Rocky Mountains: *AAPG Bulletin*, v. 80, p. 1397-1432.

- Hennier, J., and Spang, J.H., 1983, Mechanisms for deformation of sedimentary strata at Sheep Mountain Anticline, Bighorn Basin, Wyoming: 34th Annual Field Conference, Wyoming Geological Association guidebook, p 97-111.
- Hennings, P.H., Olson, J.E., and Thompson, L.B., 2000, Combining outcrop data and three-dimensional structural models to characterize fractured reservoirs: an example from Wyoming, American Association of Petroleum Geologists Bulletin, v.84, p. 830-849.
- Hurley, N.F., 2001, Structural and stratigraphic compartments determined from horizontal drilling in an eolian reservoir, Tensleep Sandstone, Wyoming (abstract): AAPG Bulletin (supplement), v. 85, p.
- Hurst, A., and Cartwright, J., 2007, Sand injectites: implications for hydrocarbon exploration and production: American Association of Petroleum Geologists, Memoir 87, 274p.
- Jamison, W.R., and Spang, J.H., 1976, Use of calcite twin lamellae to infer differential stress, Geological Society of America Bulletin, p. 868-872.
- Johnson, S.A., and Huntoon, P.W., 1994, Permeability architecture and groundwater circulation along a fault-severed margin, northern Hanna Basin, Carbon County, Wyoming, Final Report WWRC-94-27, Wyoming Water Resources Center, University of Wyoming, 115p.
- Keith, B.D., and McCaleb, J.A., 1978, A geologic model for improved oil recovery project—Tensleep Sandstone, Torchlight Field, Big Horn Basin, Wyoming: Reg. Gas Technology Symposium, Society of Petroleum Engineers SPE 7178, 7 p.
- Kelly, A.O., 1984, Significance of interdune deposits in the upper Casper Formation: Wyoming Geological Association Guidebook, 35th Annual Field Conference, p. 97-110..
- Kerr D., and A. Aviantara, 1999, Facies architecture of the Tensleep Sandstone, Bighorn Basin Wyoming: outcrop analogs to subsurface reservoirs (abstract): AAPG Bulletin, v. 83, no. 7., p. 1179-1180.
- Kerr, D.R., A. Aviantara, and B. Tapp, 1996, Facies and fracture architecture of the Tensleep Sandstone, north-central Wyoming, Phase I, Outcrop and subsurface characterization, an applied research proposal from the University of Tulsa (unpublished): University of Tulsa, 43 p. [As referenced in 1996 AAPG extended Aviantara abstract. Is this the field guide Kerr promised?]
- Kerr, D.R., and B. Tapp, 1998, Facies and fracture architecture of the Tensleep Sandstone, north-central Wyoming (unpublished), abbreviated field guide [for Marathon-supported research], University of Tulsa. [As referenced in McGinty thesis; Is this the field guide Kerr promised?]
- Kilic, A.T., 2002, Fracture quantification and modeling in the Tensleep Sandstone near the Alkali Fault, Bighorn Basin, Wyoming: Colorado School of Mines 169 p.
- Knight, W.C., 1900, Jurassic Rocks of southeastern Wyoming, Geological Society of America Bulletin, v. 2, p. 377-388.
- Knight, W.H., 1944, Geology of the western part of the Flat Top anticline, Albany and Carbon Counties, Wyoming: Master's thesis, University of Wyoming, 30p.
- Ladd, E.Z., 1979, The geology of the Sheep Canyon Quadrangle: Wyoming: PhD dissertation, Ames, Iowa State University, 124 p.
- LaPointe, P.R., Robert Parney, Thorsten Eiben, Mike Dunleavey, John Whitney, and Darrel Eubanks, 2002, 3-D reservoir and stochastic fracture network modeling for enhanced oil recovery, Circle Ridge Phosphoria/Tensleep reservoir, Wind River Reservation, Arapaho and Shoshone tribes, Wyoming: National Energy Technology Laboratory, National

- Petroleum Technology Office, U.S. Department of Energy, Tulsa, Oklahoma, DOE/BC/15190-3 (OSTI ID: 800797), 63 p.
- Larson, T.C., 1975, Geological considerations of the Weber Sandstone reservoir, Rangely field, Colorado, *in* Deep Drilling Frontiers of the Central Rocky Mountains: Rocky Mountain Association of Geologists Field Conference Guidebook, p. 275-279.
- Laubach, S.E., T.F. Hentz, M.K. Johns, H. Baek, and S.J. Clift, 1995, Using diagenesis information to augment fracture analysis: Topical Report for the Bureau of Economic Geology and the Gas Research Institute, 189 p. [cited in McGinty thesis]
- Lawson, D.E., and J.R. Smith, 1966, Pennsylvanian and Permian influence on Tensleep oil accumulation, Bighorn Basin, Wyoming: AAPG Bulletin, v. 50, p. 2197-2220.
- Lee, W.T., 1927, Correlation of geological formations between east-central Colorado, central Wyoming, and southern Montana, U.S. Geological Survey Professional Paper 149, 80p.
- Lillegraven, J.A., and Snoke, A.W., 1996, A new look at the Laramide orogeny in the Seminoe and Shirley Mountains, Freezeout Hills, and Hanna Basin, south-central Wyoming: Wyoming State Geological Survey, Public Information Circular 36, 52p.
- Lillegraven, J.A., Snoke, A.W., and McKenna, M.C., 2004, Tectonic and paleogeographic implications of late Laramide geologic history in the northeastern corner of Wyoming's Hanna Basin: Rocky Mountain Geology, v. 39, p. 7-64.
- Logan, W.N., 1900, The stratigraphy and invertebrate faunas of the Jurassic Formations in the Freezeout Hills of Wyoming, Kansas University Quarterly Bulletin, v. 9, n. 2, p. 109-134.
- Long, J.C.S., Aydin, A., Brown, S.R., Einstein, H.H., Hestir, K., Hsieh, P.A., Myer, L.R., Nolte, K.G., Norton, D.L., Olsson, O.L., Paillet, F.L., Smith, J.L., and Thomsen, L., 1997, Rock fracture and fluid flow: National Academy Press, Washington, D.C., 551 p.
- Lorenz, J.C., 2007a, Summary of the published information on Tensleep fractures; report to the Enhanced Oil Recovery Institute, University of Wyoming, April 20, 2007, 36 p.
- Lorenz, J.C., 2007b, Fractures and strain accommodation in the Tensleep Formation at Flat Top Anticline, Carbon County, Wyoming: Implications for Analog Reservoir Systems; report to the Enhanced Oil Recovery Institute, University of Wyoming, November 13, 2007, 89p.
- Lorenz, J.C., and Cooper, S.P., 2010, Thrust Faults in the Alcova Limestone: Nature's Sand-Table Experiment, American Association of Petroleum Geologists Rocky Mountain Section Meeting Official Program Book, June 13-16, 2010, Durango, CO.
- Lorenz, J.C., Teufel, L.W., and Warpinski, N.R., 1991, Regional fractures I: A mechanism for the formation of regional fractures at depth in flat-lying reservoirs: American Association of Petroleum Geologists Bulletin, v. 75, p. 1714-1737.
- Love, J. D., and Christiansen, A. C., 1985, Geologic Map of Wyoming: U.S. Geological Survey, scale 1:500,000.
- Love, J.D., Christiansen, A.C., and Ver Pleog, A.J., 1993, Stratigraphic nomenclature chart of Wyoming: Geological Survey of Wyoming Map series 41.
- Love, J.D., Christiansen, A.C., and Ver Pleog, A.J., 1993, Stratigraphic nomenclature chart of Wyoming: Geological Survey of Wyoming Map series 41.
- Mair, K., Main, I., Elphick, S., 2000, Sequential growth of deformation bands in the laboratory, Journal of Structural Geology, v. p. 22, p. 25-42.
- Mankiewicz, David, and J.R. Steidtmann, 1979, Depositional environments and diagenesis of the Tensleep Sandstone, eastern Big Horn Basin, Wyoming: SEPM Special Publication no. 26, p. 319-336.

- Maravich, M.D., 1941 Geology of Freezeout Mountain – Bald Mountain Area, Carbon County, Wyoming: American Association of Petroleum Geologists Bulletin, v. 25, p. 883-897.
- McConnell, D.A., 1994, Fixed-hinge, basement-involved fault-propagation folds, Wyoming: Geological Society of America Bulletin, v. 106, p. 1583-1593.
- McGinty, Sheila R., 2002, Fracture architecture of the Tensleep Sandstone at Zeisman Dome and Brokenback Anticline, Wyoming: PhD dissertation for the University of Tulsa, 170 pages plus appendices.
- McGinty, Sheila R., 2003, Fracture architecture of the Tensleep Sandstone at Zeisman Dome and Brokenback Anticline, Wyoming (abstract): American Association of Petroleum Geologists, Annual Meeting, June 3-6, Denver, Colorado.
- McGinty-Davis, S.R., 1998, Fracture geometry in a forced fold; an FEM case study of Zeisman Dome: MSc thesis, University of Tulsa, 72 p. [cited in Aviantara thesis].
- Mitra, S., and V.S. Mount, 1998, Foreland basement-involved structures: American Association of Petroleum Geologists Bulletin, v. 82, p. 70-109.
- Montgomery, S., 1992, Reservoir characterization in older fields: benefits for secondary recovery—a case history in the Tensleep Sandstone, South Casper Creek field, Littleton, Petroleum Information Corporation, v. 8, no. 3, 61p. [cited by Cole and Mullen 1992 as giving additional fracture info]
- Montgomery, Scott L., 1996, South Casper Creek Field: a study in reservoir heterogeneity: American Association of Petroleum Geologists Bulletin, v. 80, p. 1161-1176.
- Moore, D.A., The Tensleep Formation of the Southeastern Big Horn Basin, Wyoming: Wyoming Geological Association Guidebook, 35th Annual Field Conference, p. 271-279.
- Morgan, J.T., F.S. Cordiner, and A.R. Livingston, 1976, Tensleep reservoir study, Oregon Basin Field, Wyoming—reservoir characteristics: Society of Petroleum Engineers of AIME, paper number SPE 6141, 7 p.
- Morgan, J.T., F.S. Cordiner, and A.R. Livingston, 1978, Tensleep reservoir, Oregon Basin Field, Wyoming: American Association of Petroleum Geologists Bulletin, v. 62, p. 609-632.
- Mou, D.C., and R.L. Brenner, 1982, Control of Reservoir properties of the Tensleep sandstone by depositional and diagenetic facies Lost Soldier Field, Wyoming: Journal of Sedimentary Petrology, v. 52, p. 367-381.
- Narr, Wayne, 1998, Quantifying subsurface fracture sets: collecting and analyzing data with simulation in mind: (abstract), EXTIP 98 conference, Mexico City, 8 pages.
- Olsson, W.A., 2000, Origin of Luders' bands in deformed rock, Journal of Geophysical Research, v. 105, p. 5931–5938.
- Olsson, W.A., Lorenz, J.C., and Cooper, S.P., 2004, A mechanical model for multiply-oriented conjugate deformation bands, Journal of Structural Geology, v. 26, p. 325 -338.
- Pederson, S.L., 1953, Stratigraphy of the Fountain and Casper Formations of southeastern Wyoming and north-central Colorado: Wyoming Geological Association Guidebook, 8th Annual Field Conference, p. 18-25.
- Pedry, J.J., 1975, Tensleep sandstone stratigraphic-hydrodynamic traps, northeast Big Horn Basin, Wyoming: Wyoming Geological Association Guidebook, 27th Annual Field Conference, p. 117-127.
- Peng, S., and Johnson, A.M., 1972, Crack growth and faulting in cylindrical specimens of Chelmsford granite: International Journal of Rock Mechanics and Mining Science, v. 9, p. 37-86.

- Peng, S., and Johnson, A.M., 1972, Crack growth and faulting in cylindrical specimens of Chelmsford granite: *International Journal of Rock Mechanics and Mining Science*, v. 9, pp.37-86.
- Peterson, G.L., 1968, Flow structures in sandstone dikes: *Sedimentary Geology*, v. 2, p. 177-190.
- Pollard, D.D., and Aydin, A., 1988, Progress in understanding jointing over the past century: *Geological Society of America, Bulletin*, v. 100, no. 8, pp. 1181-1204.
- Rawnsley, K.D., T. Rives, J.-P. Petit, S.R. Hencher, and A.C. Lumsden, 1992, Joint development in perturbed stress fields near faults: *Journal of Structural Geology*, v. 14, p. 939-951.
- Rioux, R.L., 1994, Geologic map of the Sheep Mountain-Little Sheep Mountain area, Big Horn County, Wyoming: 1:31,680, U.S. Geological Survey Open-File Report 94-191. [I19.76]
- Rives, T., and J.-P. Petit, 1990, Experimental study of jointing during cylindrical and non-cylindrical folding, *in*, *Mechanics of Jointed and Faulted Rock*, Rossmanith, H.P. (ed.), p. 205-211, Balkema, Brookfield, VT.
- Rives, T., K.D. Rawnsley, and J.-P. Petit, 1999, Analog simulation of natural orthogonal joint set formation in brittle varnish, *Journal of Structural Geology*, v. 16(3), p. 419-429
- Rudnicki, J.W., and Rice, J.R., 1975, Conditions for the localization of deformation in pressure-sensitive dilatant materials: *Journal Mech. Phys. Solids*, v. 23, p. 371-394.
- Savage, H.M., and M.L. Cooke, 2004, The effect of non-parallel thrust fault interaction on fold pattern: *Journal of Structural Geology*, v. 26, p. 905-917.
- Schlagel, Michael, in progress as of 1999-2000, Tensleep fracture characterizations, University of Tulsa [cited as —in progress” in Aviantara thesis]
- Shebl, M.A., 1996, Geochemical and diagenetic investigations of the Tensleep Sandstone, Bighorn Basin, Wyoming: PhD dissertation, University of Wyoming, Laramie, Wyoming, 285p.
- Sheldon, R.P., 1967, Long-distance migration of oil in Wyoming: *Mountain Geologist*, v. 4, p. 53-65.
- Siguaw, S.G., J.E. Estes-Jackson, S.E. Ingraham, and D.W. Shoemaker, 2001, An integrated 3-E reservoir characterization at Riverton Dome Field, Wyoming: *The Leading Edge*, v. 11. p. 1226-1238.
- Simmons, S.P., and P.A. Scholle, 1990, Late Paleozoic uplift and sedimentation, northeast Bighorn Basin, Wyoming: *Wyoming Geological Association Guidebook, 41st Annual Field Conference*, p. 39-56.
- Steidtmann, J.R., 1974, Evidence for eolian origin of cross-stratification in sandstone of the Casper Formation, southernmost Laramie basin, Wyoming: *Geological Society of America, Bulletin*, v. 85, p. 1835-1842.
- Stevenson, V.M., and C.E. Mullen, 1991, Evolution of a successful steam drive in a geologically complex steeply dipping reservoir at South Casper Creek Field, Wyoming: *Society of Petroleum Engineers, paper number SPE 21528, International Thermal Operations Symposium, Bakersfield, California, Feb 7-8, 1991*, p. 61-72.
- Stone, D.L., 1993, Basement-involved thrust generated folds as seismically imaged in subsurface of the central Rocky Mountain foreland, in Schmidt, C.J., R.B., Chase, and E.A. Erslev (eds.), *Laramide Basement Deformation in the Rocky Mountain Foreland of the Western United States: Geological Society of America Special Paper 280*, p. 271-318.
- Stone, D.S., 1967, Theory of Paleozoic oil and gas accumulation in Bighorn Basin, Wyoming: *AAPG Bulletin*, v. 51, p. 2056-2114.

- Stone, D.S., 1993, Basement-involved thrust-generated folds as seismically imaged in the subsurface of the Rocky Mountain foreland, in Schimdt, C.J., Chase, R.B., and Erslev, E.A., eds., *Laramide Basement Deformation in the Rocky Mountain Foreland of the Western United States*: Boulder, Colorado: Geological Society of America Special Paper 280, p. 271-318.
- Taylor, D.A., 1996, *Structural Geology of the Difficulty Creek area, Carbon County, Wyoming* (Master's Thesis): University of Wyoming, 119p.
- Thomas, A.L., and D.D. Pollard, 1993, The geometry of echelon fractures in rock; implications from laboratory and numerical experiments, *in* Casey, M., D. Dietrich, M. Ford, J. Watkinson, and P.J. Huddleston (eds.), *The geometry of naturally deformed rocks*: Oxford, Pergamon, p. 323-334.
- Todd, T.W., 1963, Post-depositional history of Tensleep Sandstone (Pennsylvanian), Bighorn Basin, Wyoming: *AAPG Bulletin*, v. 47, p. 599-616.
- Treagus, S.H., 1988, Strain refraction in layered systems: *Journal of Structural Geology*, v. 10, p. 517-527.
- Trotter, J.F., 1984, *The Minnelusa Revisited 1984*: Wyoming Geological Association Guidebook, 35th Annual Field Conference, p. 127-151.
- Varga, R.J., 1993, Rocky Mountain foreland uplifts: Products of a rotating stress field or strain partitioning?: *Geology*, v. 21, p. 1115-1118.
- Walsh, J.J., A. Nichol, and C. Childs, 2002, An alternative model for the growth of faults: *Journal of Structural Geology*, v. 24, p. 1669-1675.
- Weijermars, R., 1997, *Principles of rock mechanics*, Alboran Science Publishing, Lectures in Geoscience, 360p.
- Wicks, J.L., S.L. Dean, and B.R. Kulander, 2000, Regional tectonics and fracture patterns in the Fall River Formation (Lower Cretaceous) around the Black Hills Foreland uplifts, western South Dakota, *in*, Cosgrove, J.W., and M.S. Ameen (eds.), *Forced Folds and Fractures*: Geological Society of London Special Publication 169, p. 145-165.
- Wong, T.-f., David, C., and Zhu, W., 1997, The transition from brittle faulting to cataclastic flow in porous sandstones: Mechanical deformation: *Journal of Geophysical Research*, v. 102, p. 3009-3025.
- Yin, Peigui, 2005, *Characterization of Tensleep Sandstone reservoirs* (abstract): AAPG Search and Discovery article #50024.
- Yin, Peigui, Dag Nummedal, and Quigsheng Zhang, 2005, *Reservoir heterogeneity caused by diagenesis in Tensleep sandstones, Teapot Dome, Wyoming* (abstract): AAPG Search and Discovery Article #50016.
- Zahm, C.K., 2002, *3D Strain and basement-involved folding, Thermopolis anticline, Wyoming*, PhD. Dissertation, Colorado School of Mines, 242p.
- Zahm, C.K., and Henning, P.H., 2009, Complex fracture development related to stratigraphic architecture: Challenges for structural deformation prediction, Tensleep Sandstone at the Alcova anticline, Wyoming, *American Association of Petroleum Geologists Bulletin*, v.93, n.11, p. 1427-1446.